NUMERICAL SIMULATION OF UNSATURATED FLOW USING MODIFIED TRANSFORMATION METHODS

CHENG YONGGANG

NATIONAL UNIVERSITY OF SINGAPORE
2008

NUMERICAL SIMULATION OF UNSATURATED FLOW USING MODIFIED TRANSFORMATION METHODS

CHENG YONGGANG

(*B.Eng., M.Eng., Tsinghua University*)

A THESIS SUBMITTED
FOR THE DEGREE OF DOCTOR OF PHILOSOPHY
DEPARTMENT OF CIVIL ENGINEERING
NATIONAL UNIVERSITY OF SINGAPORE
2008

Dedicated to my family
for their unconditional support all the time ...

Acknowledgements

I would like to express my sincere appreciation to my supervisor, Associate Professor Phoon Kok Kwang, for his continuous encouragement and guidance given to me throughout the whole Ph.D period. Without his patient and strict instruction, I will not understand the correct way of "research". I also would like to thank my co-supervisor, Professor Tan Thiam Soon, for sharing with me his vast knowledge in academic research and also real life. The members of my thesis committee, Associate Professor Tan Siew Ann and Professor Leung Chun Fai, deserve my appreciation for their helpful suggestions on my research work.

Grateful acknowledgements should be also given to my research colleagues and technical staffs in the geotechnical group for their assistance and warm-hearted help, especially during the days when I stayed in hospital. Special thanks are given to Dr. Chen Xi, Dr. Zhou Xiaoxian, Dr. Zhang Xiying, Mr. Yang Haibo, Dr. Muthusamy Karthikeyan, Ms. Zhang Rongrong and Mr. Li Liangbo for their help and encouragement during my most difficult time. Though some could be left unmentioned, other friends must be named are: Ms. Teh Kar Lu, Ms. Bui Thi Yen, Dr. Phoon Hung Leong, Mr. Xie Yi, Mr. Liu Dongming, Mr. Ong Chee Wee, Dr. Ma Rui, Ms. Zhou Yuqian, Mr. He Xuefei, Mr. Zhang Sheng and Mr. Wang Lei.

A particular gratefulness is owned to my best friend Mr. Feng Shuhong and his wife Ms. Wang Chunneng. My stay in Singapore has been less struggling with their friendship.

Table of Contents

Summary

The accurate prediction of the propagating wetting front arising from infiltration into an unsaturated soil is of considerable importance to geotechnical and geoenvironmental problems. As the relevant soil properties are highly nonlinear, numerical methods such as the finite element method are often used for solving this problem. These numerical methods work effectively in boundary and initial value problems with complex geometry. However, it has been shown in previous studies that numerical problems like oscillation and slow convergence rate affect the calculation of pore-water pressures in a finite element analysis. These results can lead to great errors in the calculation of other design variables such as safety factor of slopes. Furthermore, highly nonlinear soil-water characteristic curves are commonly encountered in sandy soils. Numerical simulations of unsaturated flow problem with such soils are still plagued with difficulties and not completely solved yet. Practical solution methods are thus of great practical importance.

This thesis presents a new combination approach TUR1 consisting of a rational function transformation method and a common under-relaxation technique to solve the h-based form of Richards equation. Detailed investigation shows that the proposed TUR1 method appeared to be a practical choice for unsaturated flow simulations, because it can produce accurate solutions at reasonable computing

costs; only one ad-hoc parameter is introduced and a robust recommendation on the choice of such parameter value is available. However, TUR1 would also break down when the soil hydraulic property curves are rather steep and relatively large time-step is used.

The combination of proposed TUR1 approach and the automatic adaptive scheme (referred as ATUR1 hereafter) is shown to be a more practical numerical method for unsaturated flow simulations, as it provides the most efficient solution at minimal computational cost; its performance is rather robust with moderate changes of several parameters introduced; and it is conceptually and computationally simple which can be easily incorporated into existing software codes based on the backward Euler scheme.

A number of multi-dimensional examples with both homogeneous or heterogenous materials are analyzed to show the robustness and efficiency of the proposed TUR1 and ATUR1 methods. It is shown that these improved approaches are efficient in complex problems with both very dry and variably saturated condition in homogenous or heterogeneous soils.

In the last, two typical numerical errors which are sometimes not well emphasized in unsaturated flow simulations due to rainfall infiltration are investigated. Numerical results show that such numerical errors could be a result of inappropriate mesh size or time-step size adopted in simulations. These errors in unsaturated flow analysis, including the overprediction of the wetting fronts and artificial positive pore-water pressure values above the infiltration fronts, have serious influence on the slope stability calculations. The proposed TUR1 method could be an attractive choice to produce more accurate solutions.

List of Tables

List of Figures

List of Symbols

a	shape parameter in van Genuchten model
$[B]$	gradient matrix
c'	the effective cohesion of the soil
d	element thickness
EPS	machine constant
$F_{decrease}$	time-step deceleration factor
$F_{increase}$	time-step acceleration factor
H	total head
$\{H\}$	vector of total head
$\{H\}, t$	vector of time derivative of H at nodal points
h	pressure head
K	hydraulic conductivity
K_s	saturated hydraulic conductivity
$[K]$	conductivity matrix
$[K]^*$	transformed conductivity matrix
$[k]$	element conductivity matrix
$[k]^*$	transformed element conductivity matrix
L	boundary of element
$[M]$	mass matrix

$[M]^*$	transformed mass matrix
m	shape parameter in van Genuchten model
m_w	slope of the soil-water characteristic curve
$\{N\}$	vector of interpolating function
N_{iter}^i	number of iterations required by the nonlinear solver to converge for time-step i
N_{min}	lower iteration limit
N_{max}	upper iteration limit
n	shape parameter in van Genuchten model
nn	number of nodes
p	transformed head
$\{p\}$	vector of transformed head
$\{p\}, t$	vector of time derivative of p at nodal points
Q	applied boundary flux
$\{Q\}$	vector of applied boundary flux
q	unit flux across the side of an element
$r_{\max}$	maximum multiplier constraints
$r_{\min}$	minimum multiplier constraints
S	saturation
s	safety factor
t	time
u_a	the pore-air pressure
$u_a - u_w$	the matric suction
u_w	the pore-water pressure

z	elevation
β	transformation parameter
γ_w	unit weight of water
Δt	time-step
Δt_{min}	minimum allowable time-step size
Δt_{max}	maximum allowable time-step size
ϵ	L_2 error
λ	specific moisture capacity
λ^*	transformed specific moisture capacity
Θ	effective saturation
θ	volumetric water content
θ_r	residual volumetric water content
θ_s	saturated volumetric water content
σ	the total stress
$\sigma - u_a$	net stress
σ'	effective normal stress
τ_R	absolute error tolerance
τ_A	relative error tolerance
ϕ'	effective angle of internal friction with respect to changes of the net stress
ϕ^b	angle of internal friction with respect to changes of the matric suction
χ	factor related to the degree of saturation of the soil

Chapter 1

Introduction

1.1 Background

Accurate prediction of the propagating wetting front arising from infiltration into an unsaturated soil is of considerable importance to geotechnical and geo-environmental problems such as slope stability, contaminant transport and design of capillary barrier. As the relevant soil properties (soil-water characteristic curve and the conductivity function) are highly non-linear, numerical methods such as the finite element and finite difference methods are often used for solving this problem. These numerical methods work effectively in boundary and initial value problems with complex geometry. These complicated scenarios are commonly encountered in practice, but analytical solutions are rarely available. However, numerical solution of this unsaturated seepage problem is known to be plagued by a number of difficulties such as efficiency and robustness. Advancements in the solution of these problems is an important and active topic of research in many areas.

1.2 Numerical Modeling for Richards Equation

The finite element method is an attractive method for modeling water flow in both saturated and unsaturated soils. It works effectively in boundary and initial value problems with complex geometry. These problems are usually complicated, and in which analytical solutions are generally not available. Many finite element programs are available for such soil seepage analyses. Among them, the software program, SEEP/W, developed by GEO-SLOPE (2004) is one of the more popular programs among practicing engineers. This program can be linked with its associate slope stability program, SLOPE/W and allows for a more realistic prediction of slope stability under different external hydraulic influences such as rainfall infiltration with time. Fredlund and Rahardjo (1993) and Karthikeyan (2000) have made use of both SEEP/W and SLOPE/W to investigate the influence of rainfall infiltration and soil hydraulic properties on the stability of unsaturated soil slopes.

In any time dependent finite element analysis, the first step is to discretize the spatial domain and time duration. In principle, a comprehensive convergence study is necessary for each problem to arrive at an acceptable discretization scheme. In practice, it is computationally expensive to conduct such studies over the full range of mesh sizes and time-steps. In particular, existing desktop computers cannot provide sufficient computational resources to study complex two-dimensional and three-dimensional problems with very dense spatial grids and at very small time-steps.

For such problems, an approximate solution, obtained by using a reasonable element size and time-step, is often deemed satisfactory for "practical" engineering

problems based on a fairly limited convergence study. However, in such analyses, numerical solution is known to be plagued by a number of problems. Firstly, it was observed that oscillations occur near the wetting front as water seeps through the partially saturated soil. Secondly, the convergence of solutions to the final "correct" value was found to take place slowly with decreasing spatial and temporal discretization. Given limited computational resources, numerical analyses are usually carried out using a coarse mesh and a relatively large time-step size. This will thus lead to a solution that might not converge to the correct value. These numerical artifacts have an adverse influence on the calculation of pore-water pressure, leading to errors in the computation of other important design variables, such as the factor of safety of an embankment slope against translational and/or rotational failure. With the limitations often exhibited by analytical solutions and the practical limitations of convergence studies, the correctness of numerical solutions obtained by reasonable discretization schemes based on limited convergence studies is a serious issue of practical concern.

1.3 Convergence Problems

Because of the high nonlinearity of soil hydraulic properties, convergence problems exist in numerical simulations of unsaturated flow analyses. It is necessary to distinguish between different convergence problems.

Firstly, very steep hydraulic conductivity functions create difficulties for non-linear equations that have to be solved iteratively at each time-step. The iterations tend to oscillate between two extreme solutions represented by the extremities of

the hydraulic conductivity function, leading to slow convergence to a stable solution within each time-step. In order to prevent this from happening, some form of relaxation is often used to enhance the performance of nonlinear iterative schemes. In programs such as SEEP/W, a typical under-relaxation technique is applied such that the new iterate is calculated from the head at the mid-point of the time interval. In this way, the tendency for h to oscillate around its limits will be dampened and a smaller number of iterations will be needed.

While the under-relaxation technique discussed above helps to accelerate convergence in the iterative solution of highly nonlinear equations within each time-step, such technique may lead to a slow convergence to the correct solution with respect to increasing refinement in mesh size and time-step. This is another form of convergence and should not be confused with the one discussed previously. Chong (2001) and Tan et al. (2004) studied the influence of different under-relaxation techniques on the rate of such convergence. They demonstrated that the slow convergence with respect to refinement of the time-step was an indirect result of the under-relaxation technique used to update the hydraulic conductivity during the iterative solution of the discretized nonlinear transient seepage equations at each time-step. The under-relaxation technique used by standard programs such as SEEP/W seems to optimize the number of iterations per time-step, but comes with a hidden cost of requiring an extreme refinement of time-step to arrive at a solution of acceptable accuracy, which is rarely appreciated. They recommended an alternative under-relaxation technique that the material properties for the new iteration are defined as the average of the pressure heads computed from the two most recent iterations of the current time-step. It is shown that this form of under

relaxation does not require very small time-steps to produce reasonably accurate results, but does so at a price of increasing the number of iterations within each time-step, and even diverges instead of converging to a stable solution when dealing with soils with highly nonlinear hydraulic properties. Clearly, this limits its application. Tan et al. (2004) did not study highly nonlinear soil parameter curves as well. For example, Figures 1.1 and 1.2 show the soil-water characteristic curves and the relative hydraulic conductivity curves for four typical type of soils and the sandy clay loam used in the study of Tan et al. (2004). We can see that the sandy clay loam is far from extreme cases. Sandy soils, such as loamy sand and sand, are shown to be have much steeper soil parameter curves than the sandy clay loam. Simulations with such soils are still of great difficulties and the problems have not been solved completely.

Previous studies have already shown that the slow convergence problem exists in unsaturated seepage analysis using SEEP/W. It is found that the calculated pressure heads converge to a correct solution very slowly with progressive refinement of the element size and time-step. However, coarse meshes and big time-steps were usually used by practising engineers. Few of them discussed whether the solutions generated with such meshes and time-steps were accurate or not. For slope stability problems in unsaturated residual soils, errors made in the position of the wetting front seriously affect the location of the failure surface and the eventual factor of safety. For example, Figure 1.3 shows a slope stability problem which will be studied in more detail in Chapter 6. The pore-water pressure profiles at the crest of the slope during three days of rainfall from SEEP/W with different mesh sizes are shown in Figure 1.4. It clearly shows that with a coarse

mesh of 0.5 × 0.5 m, elevations of the wetting fronts are largely over predicted compared to the dense mesh of 0.1 × 0.1 m. And this overprediction has serious influence on the slope stability calculations, which can be seen in Figure 1.5. The factor of safety for the coarse mesh is significantly unconservative! Note that the "coarse" mesh - 0.5 × 0.5 m - is already fine for most analyses undertaken by practising engineers. The error in prediction of the wetting front can be viewed as an optimistic estimate. Thus, the correctness of numerical solutions obtained using reasonable spatial and temporal discretization schemes based on limited convergence studies is of direct practical concern.

1.4 Motivation and Objectives

The accurate prediction of the propagation of a wetting front in an unsaturated soil subjected to surficial infiltration is of practical importance to many geotechnical and geoenvironmental problems. As the soil hydraulic properties are highly nonlinear, the finite element method is the most commonly used tool for modeling such problems with complex geometry. However, it has been shown in previous studies that numerical problems like oscillation and slow convergence rate affect the calculation of pore-water pressures in a finite element analysis. These results can lead to significant errors in the calculation of other design variables such as safety factor of slopes. Furthermore, highly nonlinear soil-water characteristic curves are commonly encountered in sandy soils. Numerical simulations of unsaturated flow problem with such soils are still plagued with difficulties and not completely solved in terms of achieving accurate solutions at reasonable costs. Workable solution

methods are thus of great practical importance.

The goal of this research is to develop robust numerical methods for solving the highly nonlinear partial differential equation describing unsaturated flow in porous media. This is motivated by the inability of current numerical methods to provide accurate and efficient solutions to such difficult problems. The key focus of this research is to develop methods that are **practical**, i.e. reasonably easy to implement into existing computing codes and easy to use, with a minimized number of *ad-hoc* parameters that need "expert" judgement, able to solve a broad range of soil hydraulic properties, accurate and robust, and suitable for running on ordinary personal computer.

The objectives of this study can be summarized as follows:

1. To develop a new combination approach (hereafter referred to as TUR1) of transformation method and under-relaxation technique to solve the finite element formulation of the h-based form of Richards equation. The performance of this combination approach is to be examined in the sense of convergence rate of the pore-water pressures distribution to the correct solution with mesh and time-step refinement. To assure the robustness of this new approach, the selection of the only *ad-hoc* transformation parameter value will also be investigated;

2. To investigate the numerical performance of the proposed TUR1 method with several popular temporal adaptive schemes. Since the TUR1 method is expected to be able to produce more accurate results with larger time-step and coarser mesh, and the adaptive schemes could have the ability to control

temporal errors, it is reasonable to conjecture that the combination of TUR1 with a proper temporal adaptive scheme will produce a more efficient and robust solution strategy for unsaturated flow analysis, rather than TUR1 or adaptive schemes on their own.

3. To carry out a series of application studies on different one-dimensional and two-dimensional infiltration problems as well as the rainfall-induced slope stability analysis. The robustness and efficiency of the developed numerical methods are to be investigated.

1.5 Organization

The organization of this report is listed as follows:

Chapter 2 presents a review of the literature, which covers the general introduction to the rainfall-induced slope stability analysis and the theory of water flow in unsaturated soils. Some common numerical methods and difficulties frequently encountered in solving the governing partial differential flow equation are discussed.

Chapter 3 presents the numerical formulations to be adopted in the proposed TUR1 method. These include the standard finite element formulation adopted by SEEP/W and the combination of rational function transformation (RFT) approach and under-relaxation technique. A detailed study is then carried out to investigate the performance of the proposed combination approach.

Chapter 4 investigates the numerical performance of the proposed TUR1 method with several different time stepping schemes.

Chapter 5 presents a number of more examples appeared in multi-dimensions and with homogeneous or heterogenous materials to show the robustness and efficiency of proposed methods.

Chapter 6 investigates the influence of different kind of numerical errors in unsaturated flow simulations on the slope stability analysis. The superiority of proposed TUR1 method is expected to be shown.

Chapter 7 presents the summary of valuable conclusions. In addition, some suggestions on future research work are mapped out.

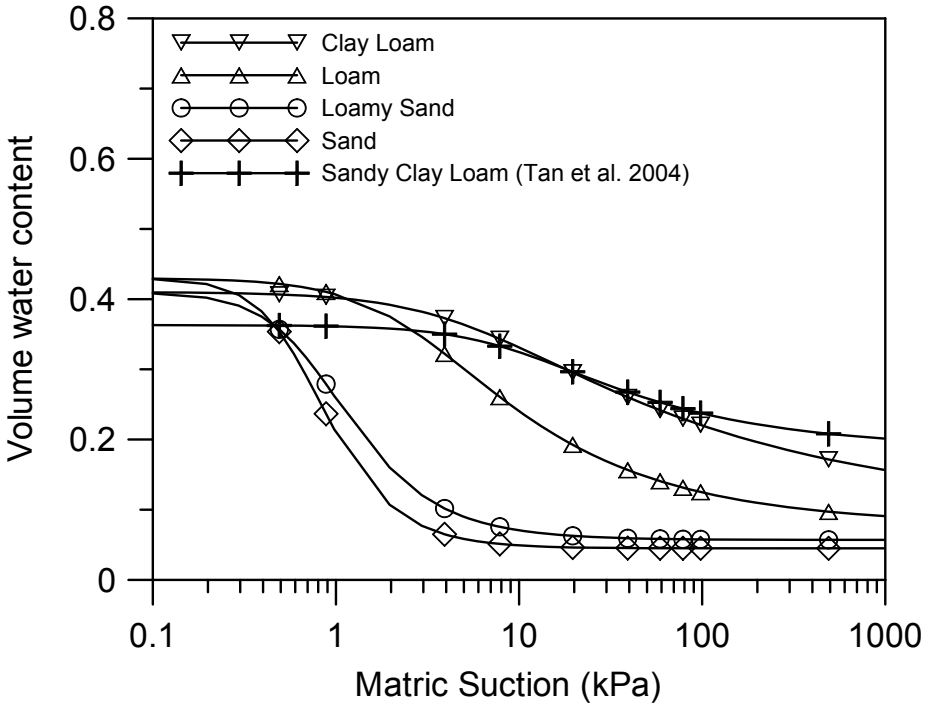

Figure 1.1: Soil-water characteristic curves

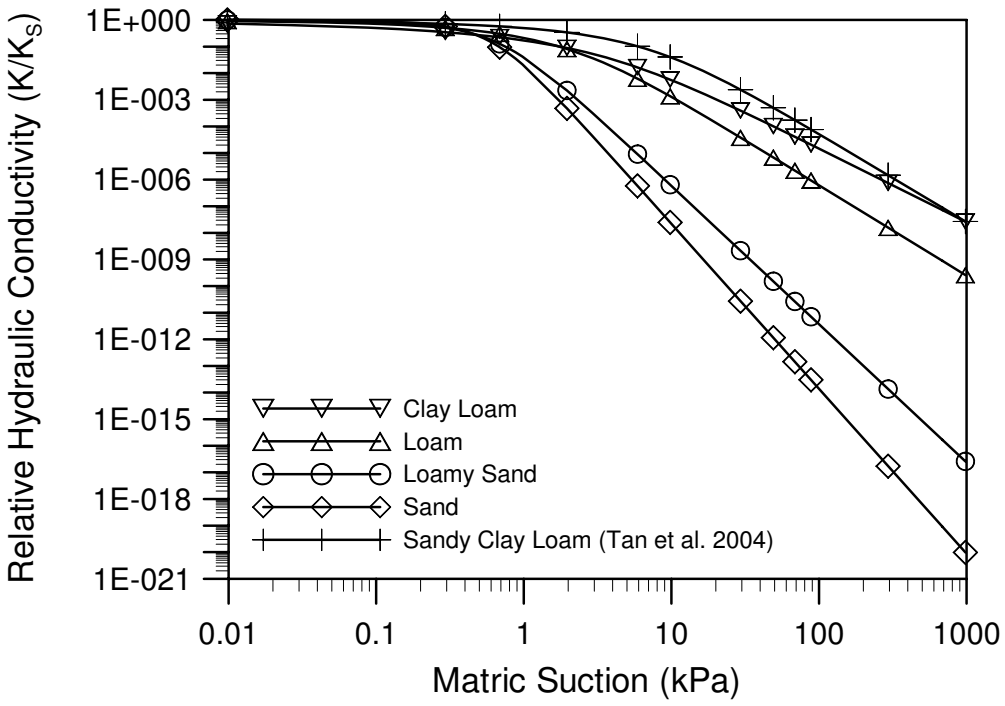

Figure 1.2: Relative hydraulic conductivity functions

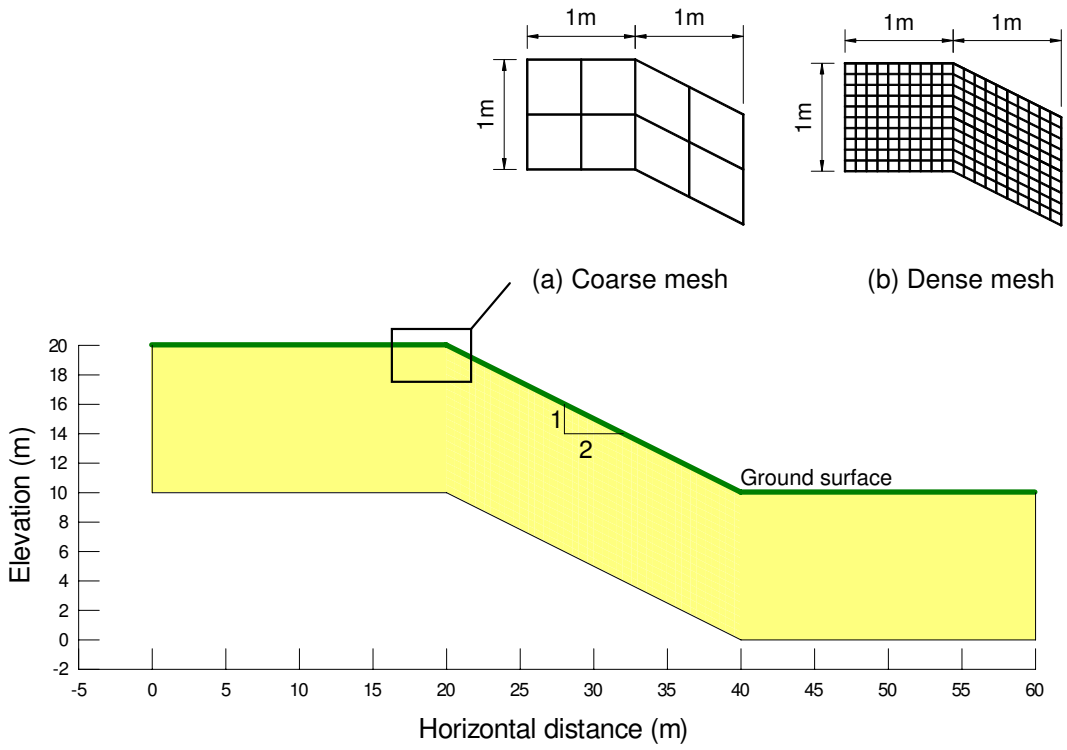

Figure 1.3: Geometry and finite element mesh of the slope used for stability analysis

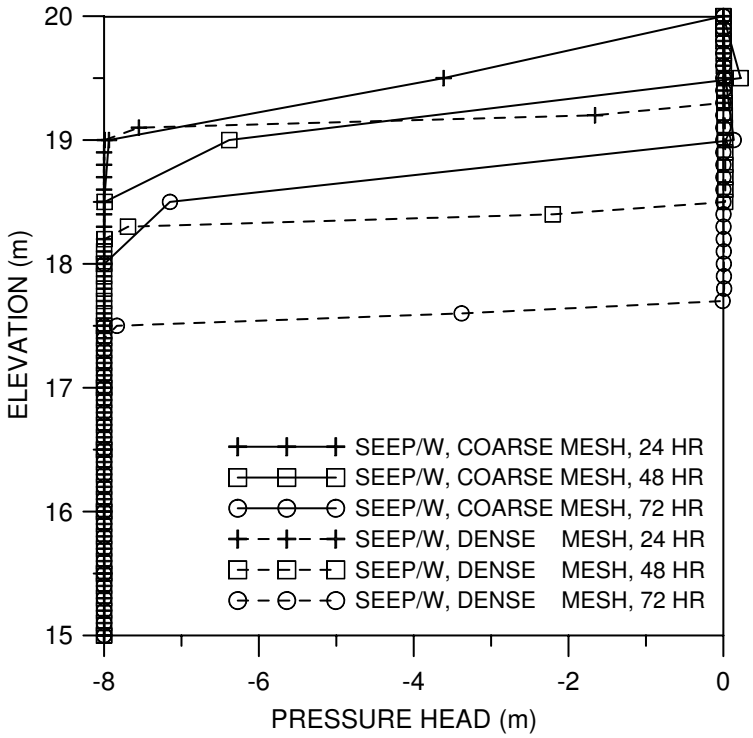

Figure 1.4: Pore-water pressure profiles at the crest of the slope from SEEP/W with different mesh sizes

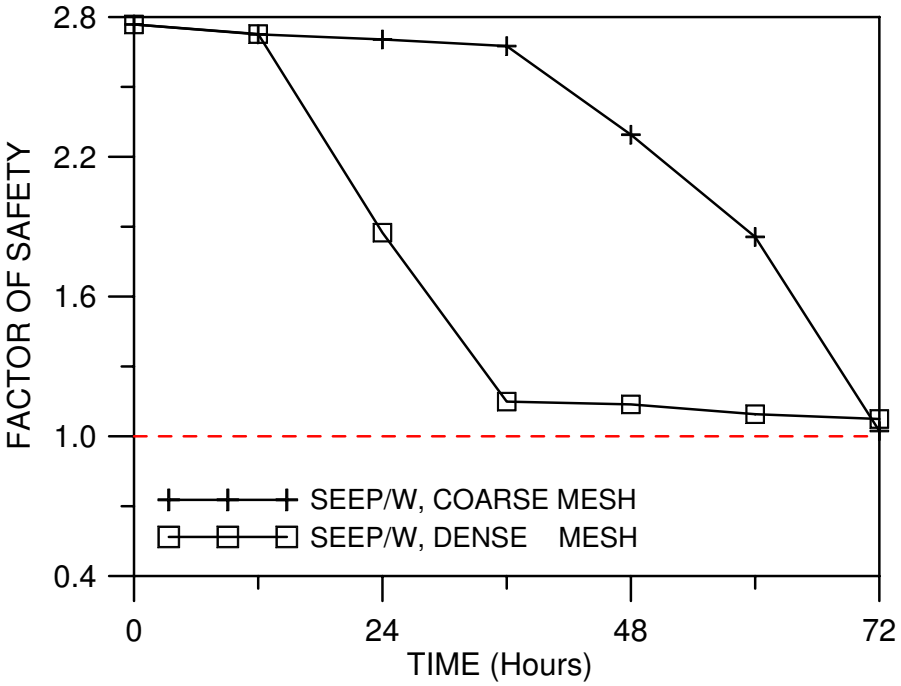

Figure 1.5: Change of slope factor of safety with time

Chapter 2

Literature Review

2.1 Introduction

In many tropical countries, slope failures in residual soils are common, particularly during periods of intense rainfall. The groundwater table in these slopes may be located deep below the ground surface and the pore-water pressures in the soil above the groundwater table are negative to atmospheric conditions. This negative pore-water pressure, referred to as matric suction when referenced to the pore-air pressure, is now recognized to contribute towards the stability of unsaturated soil slopes (Fredlund and Rahardjo, 1993; Rahardjo et al., 1995; Griffiths and Lu, 2005).

Under an external hydraulic influence, such as rainfall infiltration, seepage of water can cause a gradual loss of matric suction in an unsaturated soil slope. As the hydraulic properties of the soil with respect to matric suction are often highly nonlinear, rapid changes in pore-water pressure have a significant effect on the soil strength, and therefore the stability of the slope. Thus, the accurate prediction of the propagating wetting front arising from infiltration into an unsaturated soil is of considerable importance.

2.2 Rainfall-induced Slope Failures

Slope failures due to rainfall infiltration are quite usual in tropical areas such as Singapore, whereas these slopes remain stable for a long time before the rainstorms (Brand, 1984; Toll, 2001). During the rainfall, a wetting front goes deeper into the slope, which results in a gradual increase of the water content and a decrease of the negative pore-water pressure. As this negative pore-water pressure, referred to as matric suction when referenced to the pore air pressure, is recognized to contribute towards the stability of unsaturated soil slopes, the loss of suction causes a decrease in shear strength of the soil on the potential failure surface and finally triggers the failure (Rahardjo et al., 1995; Ng and Shi, 1998). These rainfall-induced landslides are usually shallow, as the rainfall infiltration alters the pore-water pressures only for shallow depths (Au, 1993; Tsaparas, 2002).

There is a considerable volume of literature that has discussed the correlation between total rainfall and probability of landslides for various geographical areas. For Hong Kong, Brand (1984) concluded that a rainfall intensity of 70 mm/h and above can be an indication of landslides, and a 24-hour rainfall of less than 100 mm is unlikely to produce any slope failures. For Singapore, Toll (2001) concluded based on the available data of slope failures that major slope failures may occur after a 24-hour rainfall of larger than 110 mm.

Although rainfall has been well recognized to have a major effect on the stability of unsaturated slopes, there are on-going debates on the effect of the antecedent rainfall, i.e. the rainfall that falls on the slope over a certain period prior to the major rainfall event. Wolle and Hachichi (1989) reviewed landslides

caused by rainfall in Brazil and concluded that intense rainfall does not cause slope failure by itself and the antecedent rainfall must be considered in the analysis as it increases the initial moisture of the soil. Lumb (1975) studied the slope failures in Hong Kong between 1950 to 1973 and concluded that a 15 days of antecedent rainfall plays an important role in the probability of slope failure occurring. However, Brand (1984) showed that the antecedent rainfall is not a significant factor in slope failures as long as the major rainfall is of a high intensity, and that the controlling parameters for rainfall-induced landslides are the peak intensity and the 24-hour rainfall. For Singapore, Pitts (1985) came to a similar conclusion that the antecedent rainfall was not important. However, Rahardjo et al. (1998), Toll (2001) and Rahardjo et al. (2001) showed that antecedent rainfall plays a major role in rainfall-induced landslides in Singapore. Toll (2001) states that minor landslides may occur after significant amounts of antecedent rainfall. Observations of past landslides suggest that a total rainfall of 100 mm within a six-day period would be sufficient for minor landslides to take place. Chatterjea (1989) studied the effect of antecedent rainfall on slope failures in Singapore and concluded that a period of 5 days should be enough for analysis of rainfall-induced landslides.

2.3 Strength of Unsaturated Soil

Bishop (1959) firstly developed a framework to describe unsaturated soil strength using the effective stress concept. The relationship between the effective normal

stress and the matric suction is given by

$$\sigma' = (\sigma - u_a) + \chi(u_a - u_w) \tag{2.1}$$

where

σ' = the effective normal stress;

σ = the total stress;

u_a = the pore-air pressure;

u_w = the pore-water pressure;

$\sigma - u_a$ = the net stress;

$u_a - u_w$ = the matric suction; and

χ = factor related to the degree of saturation of the soil.

Fredlund et al. (1978) proposed a constitutive equation which described the relationship between the shear strength and the two stress state variables, the net normal stress $(\sigma - u_a)$ and the matric suction $(u_a - u_w)$, given as

$$\tau = c' + (\sigma - u_a) \cdot \tan\phi' + (u_a - u_w) \cdot \tan\phi^b \tag{2.2}$$

where

c' = the effective cohesion of the soil;

ϕ' = the effective angle of internal friction with respect to changes of the net stress;

ϕ^b = the angle of internal friction with respect to changes of the matric suction.

The equation above is also referred to as the extended Mohr-Coulomb failure criterion for unsaturated soils (Fredlund and Rahardjo, 1993), because

the behavior of saturated soils can be described by this failure criterion as a special case when the matric suction is zero. The graphical presentation of this extended Mohr-Coulomb failure criterion can be seen in Figure 2.1. In the three dimensional graph, the classical Mohr circles defined by the shear stress axis, and the effective normal stress are extended to the third axis of matric suction. The failure envelope, which defines the shear strength of the unsaturated soil, is the surface tangent to the Mohr circles.

2.4 Governing Equation for Seepage through Unsaturated Soil

It can be seen from Equation 2.1 and Equation 2.2 that the matric suction is very important in calculation of unsaturated soil strength. For most practical problems, seepage in unsaturated media must be modeled appropriately to estimate this quantity. Several models have been proposed to simulate such problem. These include the models of Horton (Horton, 1933), and Green-Ampt (Green and Ampt, 1911). According to their concepts and assumptions, the Horton formula can be seen as a conceptual model and the Green-Ampt formula is a physically approximative and mathematical exact solution. However, in virtually all studies of the unsaturated zone, the fluid motion is assumed to obey the classical Richards equation, which is obtained by applying the mass conservative law and the Darcy's flow law. It may be written in several forms with either the pressure head, h or the volumetric water content, θ as the dependent variable. The three standard forms of the Richards equation can be identified as the "h-based" form, the "θ-based"

form and the "mixed" form as follows:

$$C(h)\frac{\partial h}{\partial t} = \nabla \cdot K(h)\nabla h + \frac{\partial K(h)}{\partial z} \qquad \textit{h-based} \tag{2.3a}$$

$$\frac{\partial \theta}{\partial t} = \nabla \cdot D(\theta)\nabla \theta + \frac{\partial K(\theta)}{\partial z} \qquad \textit{θ-based} \tag{2.3b}$$

$$\frac{\partial \theta}{\partial t} = \nabla \cdot K(h)\nabla h + \frac{\partial K(h)}{\partial z} \qquad \textit{mixed} \tag{2.3c}$$

where

$K(h \text{ or } \theta)$ = the unsaturated hydraulic conductivity, ms^{-1};

$C(h) = \mathrm{d}\theta/\mathrm{d}h$ = specific moisture capacity, m^{-1};

$D(\theta) = K(\theta)/C(\theta)$ = unsaturated diffusivity, $\mathrm{m}^2\mathrm{s}^{-1}$;

z = vertical coordinate, assumed positive upward, m;

t = time, sec.

Other forms that are not widely used also exist such as the mixed-hybrid form proposed by Bergamaschi and Putti (1999) which is expressed using the pressure head and the Darcy's velocity vector as independent variables.

The h-based formulation is considered to be more useful for practical problems involving flow in layered or spatially heterogeneous soils, as well as for partially saturated flow problems because the pressure head profiles generated are always continuous across the spatial domain. Models of this type have been extensively used in various applications (Haverkamp et al., 1977; Neuman, 1973; Paniconi and Putti, 1994; Rathfelder and Abriola, 1994; Guarracino and Quintana, 2004). But, it has been shown that the h-based form can produce significant global mass balance errors unless very small time-steps are used. The h-based approach can be improved if the derivation of the moisture capacity term is performed by suited chord

slope approximations in replacing analytical derivatives as proposed by Rathfelder and Abriola (1994). However, the numerical differentiation must be prevented if the pressure head difference falls below a specific range and a proper treatment of the derivative term is then required (for instance, resorting to an analytical evaluation). Accordingly, chord slope approximation does not appear as a general and sufficiently robust technique. It would fail under drastic parameters and initial conditions. Difficulties of this kind were reported by Paniconi and Putti (1994).

On the other hand, θ-based schemes may be written in a mass-conservative form and therefore should in most cases ensure mass conservation within the computation domain regardless of time-step size and grid spacing (Huyakorn and Pinder, 1983; Hill et al., 1989). They showed that it is advantageous to use such schemes for initially dry homogeneous soils, since the water content varies less across a wetting front than does the pressure head. A severe limitation of θ-based formulations is that this form cannot be used to describe flow in the saturated zone, and flow in layered soils is also not easily simulated because of its discontinuity. Furthermore, θ-based algorithms may suffer from mass balance errors at the boundaries even when this formulation accurately conserves mass in the interior of the flow system.

Perceiving the drawbacks of existing h-based and θ-based solutions of the Richards equation, many have tried to combine the advantages of the two methods. The mixed form of Richards equation was thought to be able to maintain the mass conservative property inherent in the θ-based equation, while providing solutions in terms of the pressure head. Brutsaert (1971) was one of the first to use the mixed-form Richards equation for solving saturated-unsaturated flow. He

combined a finite difference approximation of the mixed-form equation with an iteration scheme to deal with the steep wetting fronts effectively. Allen and Murphy (1986), Celia et al. (1987, 1990) and Williams et al. (2000) also used a mixed form of Richards equation to derive numerical solution algorithms. Hao et al. (2005) found that when simulating irrigation cases with the bottom boundary as a free drainage condition, which means large amount of water moving through, large mass balance errors still can be encountered. To solve this problem, a switching method between the modified Picard iteration (Celia et al., 1990) and standard h-based Picard iteration method was then proposed.

As in saturated soil, the flow of water in unsaturated soils is assumed to follow Darcy's flow law. In this case, the coefficient of hydraulic conductivity is not a constant, but a function of the degree of saturation or negative pore-water pressure in the soil. Constitutive relationships between θ and h, and K and θ (or K and h) are almost always nonlinear in nature. These two relations are referred to as the Soil-water Characteristic Curve and the Conductivity Function, respectively.

2.5 Constitutive Relations of Unsaturated Soil

During a transient process, even if the soil matrix is not deforming but is unsaturated, a certain amount of water may either be retained in or released from an elemental volume of soil due to the difference in the flow of water in and out in a given time increment. The ability of the soil to store water is defined by the Soil-water Characteristic Curve, which relates the volumetric water content to the negative pore-water pressure of the soil. This negative pore-water pressure is also

known as matric suction when referred to the pore-air pressure. Over the years, many equations have been suggested to fit and extrapolate soil-water data obtained from field or laboratory measurements (Gardner, 1958; Brooks and Corey, 1964; van Genuchten, 1980; Fredlund and Xing, 1994). Reviews of the more popular soil-water characteristic models can be found in Leij et al. (1996) and Leong and Rahardjo (1997a).

On the other hand, the conductivity function, which relates the unsaturated hydraulic conductivity of the soil to matric suction, is usually associated indirectly with the soil-water characteristic curve. The prediction of the conductivity function from the soil-water characteristic curve is more attractive in comparison with direct measurements in the field or laboratory, which are difficult and costly to conduct. As with the soil-water characteristic curve, no single relationship for the conductivity function is valid for all types of soils. Many models have been proposed to predict the conductivity function. Some formulations are empirical in nature (Gardner, 1958; Brooks and Corey, 1964) while others are based on macroscopic models (Averjanov, 1950; Mualem, 1978) or statistical models (Childs and Collis-George, 1950; Burdine, 1953; Mualem, 1976a,b). Mualem (1986), Yates et al. (1992), Fredlund et al. (1994), Leong and Rahardjo (1997b) present reviews on the various formulations available for predicting conductivity functions.

2.6 Analytical Solutions to Richards Equation

Due to the nonlinearity often exhibited by these two soil hydraulic relationships, analytical solution to the Richards equation is limited to simple initial and bound-

ary conditions. In these solutions, calculations often involve tedious steps, which must be repeated for each particular case (Warrick et al., 1985). In addition, the solutions are often formulated for solving one-dimensional problems only (Srivastava and Yeh, 1991). For two-dimensional problems such as slope stability analyses involving unsaturated infiltration or evaporation, analytical solutions are only available with various simplifications and assumptions (Serrano, 2004; Griffiths and Lu, 2005). Thus the scope of application is highly restricted.

Many infiltration relationships have been derived in terms of soil hydraulic properties for simple initial and boundary conditions. The simplest condition is that of uniform soil-water conditions and the soil is effectively infinitely deep. Philip's solution (Philip, 1957a,b) of Richards equation is for such a condition with soil surface maintained at zero pore-water pressure after zero time, assuming no ponding. In addition, there are also other classical infiltration solutions, which involve constant surface flux condition and redistribution of soil-water into infinite soil depth. These are discussed by Youngs (1995), who presents a review of the developments in the physics of infiltration.

Utilizing the procedure of Philip (1957a,b), generalized solutions have been developed for infiltration problems (Warrick and Amoozegar-Fard, 1979; Warrick et al., 1985). In Warrick and Amoozegar-Fard (1979), infiltration and drainage calculations are developed using spatially scaled hydraulic properties. The approach adopted by Warrick et al. (1985) is analogous but more general than the former. In the latter, the equation is expressed in terms of dimensionless time, depth and water content. And, it uses the hydraulic functions of van Genuchten (1980) or of Brooks and Corey (1964) to describe the soil constitutive relations. The solutions

then can be presented in concise tables, which allow for finding moisture profiles, wetting front, intake rate and cumulative intake for a variety of soils and varying initial water contents. However, it is noted that such analytical solutions are applicable only with certain boundary conditions. They are valid only for homogeneous soil, with initial uniform moisture content. Moreover, it solves one-dimensional vertical flow problems only.

Due to the limitations often exhibited by analytical solutions, numerical approximations using the finite element approach or the finite difference approach have become more popular for solving unsaturated seepage flow problems with complex geometry, especially in the light of the advancement made in computational hardware. However, in such numerical analyses, the accuracy of the solution has to be tested and calibrated. The contribution made by the analytical solutions is that they can provide the correct benchmark for such testing and calibration.

2.7 Numerical Solutions to Richards Equation

Due to the limitations often exhibited by analytical solutions, numerical methods are often used for estimating and predicting variably saturated flow problems. These numerical methods work effectively in boundary and initial value problems with complex geometry. These complicated scenarios are commonly encountered in practice, but analytical solutions are rarely available.

The standard approximations that are applied to the spatial domain are the finite difference method and finite element method. For a time-dependent problem, this is usually coupled with a time-marching algorithm such as the backward

Euler scheme or the Crank-Nicholson scheme, which is used to perform the time integration. For any time scheme other than the fully explicit forward method, nonlinear algebraic equations can result and some linearization and/or iteration procedure must be used to solve the discrete equations. The common iterative schemes include the Newton-Raphson method, the Picard method and the repeated substitution method.

Examples of finite difference models used for seepage analysis in unsaturated soils include those presented by Brandt et al. (1971), Dane and Mathis (1981), Freeze (1971), Haverkamp et al. (1977), Vauclin et al. (1979), Haverkamp and Vauclin (1979), Huyakorn and Pinder (1983), Samani et al. (1985), Celia et al. (1990), Kirkland et al. (1992), Pan and Wierenga (1995), Williams and Miller (1999) and Williams et al. (2000). In recent years, studies have shifted towards the finite element method for its greater advantages in versatility and efficiency in solving problems with complex geometry (Neuman, 1973; Cooley, 1983; Milly, 1985; Allen and Murphy, 1986; Celia et al., 1990; Forsyth et al., 1995; Ju and Kung, 1997; Diersch and Perrochet, 1999; Guarracino and Quintana, 2004). Windows-based finite element software program with graphical user interface (GUI) such as SEEP/W have also been developed (GEO-SLOPE, 2004). SEEP/W is available commercially and has been used widely in many fields of engineering.

In a finite element formulation, the Galerkin method of weighted residuals is often applied to the governing partial differential equation. This form of formulation is also adopted by Neuman (1973), Milly (1985), Celia et al. (1990), Ju and Kung (1997) and Guarracino and Quintana (2004) in their studies and it is also the formulation adopted by SEEP/W. Furthermore, the backward difference approach

is more stable numerically and is often used in most finite element analyses (Celia et al., 1990; Ju and Kung, 1997). SEEP/W also uses this algorithm in its time integration process. Higher order temporal schemes also can be used (Guarracino and Quintana, 2004). However, in practical applications where accuracy of the order of few percent is desired, low order schemes are usually found to be superior to the higher order solvers (Wood, 1990). For example, numerical examples (Wood, 1990) showed that the second-order Crank-Nicolson scheme outperformed the first-order backward Euler scheme only when relative errors of less than 0.005% were required. Other time stepping schemes appeared in the literature for the solution of Richards equation include the three level Lees' scheme (Paniconi et al., 1991), the Douglas-Jones predictor-corrector method (Hornung and Messing, 1980; Babajimopoulos, 1991, 2000) and implicit Runge-Kutta schemes (Baker, 1995). Finally, to solve the nonlinear equations, some linearization and/or iteration procedure must be used. Paniconi et al. (1991) introduced several non-iterative procedures for solving the nonlinear Richards equation. However, there are concerns regarding the stability behavior of these schemes which need to be resolved. More commonly, iterative schemes include the Newton-Raphson method and the Picard method are often employed. Paniconi and Putti (1994) and Lehmann and Ackerer (1998) compared these two most popular schemes. It is shown that the advantages of the Picard method include its relative simplicity and low cost per iteration, whereas the Newton method achieves a higher rate of convergence and can be more robust for certain types of problems. SEEP/W (GEO-SLOPE, 2004) used a simple iteration technique, which involves repeated substitutions using the average of heads computed at the previous time-step level and the most recent iteration of the current

time-step level, to solve the nonlinear equations.

Linearizing the nonlinear problem by adopting the Newton-Raphson or Picard method always produce a system of linear equations that need to be solved. The traditional way to solve such linear systems is to employ direct solution methods or its variants which are based on the classical Gaussian elimination scheme. These direct methods can lead to the exact solution in the absence of round-off errors. However, especially for large sparse linear systems arising from multi-dimensional problems, direct solution methods may incur a large number of floating point operations (additions, subtractions and multiplications), which makes it significantly expensive to solve such a large linear system. On the contrary, iterative solution methods are more attractive for such large scale linear equations because only matrix-vector products and inner-products are required in the iteration process. Preconditioned Krylov subspace iterative methods, such as Bi-CG or GMRES, are commonly used in the simulation of unsaturated flow problems (Tocci et al., 1998; Jones and Woodward, 2001; GEO-SLOPE, 2004).

2.8 Numerical Problems

Numerical modeling provides a convenient and effective means for solving problems of seepage in unsaturated soils with complex geometry. However, numerical solution is known to be plagued by a number of difficulties, such as oscillations near the wetting fronts and slow convergence rate.

2.8.1 Numerical Oscillation

In time-dependent field problems, oscillatory results in the finite element solution are quite common. They are found to occur when certain criteria on the ratios of element size to time-step size are not met, even in cases where the material properties are constant. This phenomenon has already been noticed by many researchers in consolidation, heat diffusion and seepage flow problems (Sandhu et al., 1977; Vermeer and Verruijt, 1981; Segerlind, 1984; Celia et al., 1990; Pan et al., 1996; Ju and Kung, 1997; Thomas and Zhou, 1997). The common point about the governing equations adopted in these problems is that they belong to the same class of parabolic partial differential equations.

Sandhu et al. (1977) and Vermeer and Verruijt (1981) observed oscillations of pore-water pressures in consolidation problems. The authors suggested a minimum time-step size in terms of mesh size and the coefficient of consolidation, which is shown to be useful in eliminating oscillation in one dimensional problems. Thomas and Zhou (1997) derived two minimum time-step criteria to avoid numerical oscillations in heat diffusion problems, which involves only one dependent variable, that is temperature. The criteria are formulated in terms of thermal conductivity, specific heat capacity and element size, and they apply strictly for constant material properties. The authors hypothesized that oscillation is purely due to time-step size and element size and it is not affected by the oscillatory result obtained from the previous time-step. From a theoretical verification of a one-dimensional two-noded element case, they developed an approach to further derive minimum time-step sizes for other types of elements, such as two-dimensional eight-noded element, which is useful in more complex problems.

Karthikeyan et al. (2001) made use of the minimum time-step criteria proposed by Thomas and Zhou (1997) in typical two-dimensional unsaturated seepage problems. Due to an analogy between the h-based form of Richards equation and the heat diffusion equation, the criteria, which have been re-interpreted in terms of hydraulic conductivity and specific storage capacity, can be shown to be adequate in controlling oscillation in seepage flow problems. They are applicable for both constant and highly nonlinear soil hydraulic properties. To account for material nonlinearity, the criteria are calculated based on the most critical state, in which the material properties correspond to the highest negative pore-water pressure under the initial condition. These simple criteria are of considerable practical value as they allow the engineer to remove numerical oscillations using their existing software without any modifications.

On the other hand, in a finite element formulation, the mass matrix can be consistent or lumped. Pan et al. (1996) compared the consistent (mass-distributed) formulation with the lumped (mass-lumped) formulation for an unsaturated seepage flow analysis. It is found that the mass-distributed scheme generates numerical oscillation at the sharp wetting fronts due to the highly nonlinear properties of water flow when linear elements are used. Whereas oscillation was observed to be eliminated in mass-lumped approach. This can be explained by the fact that only in the lumped case does the numerical solution satisfies the maximum principle of the partial differential equation (Bouloutas, 1989), which states that the maximum value of the numerical solution is dictated by either the boundary conditions or the initial data. It implies that the maximum value at current time-step level is less than or equal to the maximum value at the previous one. Similarly, the

minimum value at current time-step is greater than or equal to the minimum value at the previous time-step level. However, they also found that the assumption of the mass-lumped scheme that the neighboring node response is always positive may be physically incorrect in a dry medium and may cause smearing of the wetting front. Finally, Pan et al. (1996) developed two new mass-distributed schemes which can be shown to be always oscillation free. However, they are not popular, in part because they are difficult to use. Ju and Kung (1997) also discussed similar oscillatory phenomena. They found that quadratic/cubic elements could cause oscillation with both consistent mass and lumped mass schemes.

2.8.2 Rate of Convergence

In numerical simulation of unsaturated seepage flow problems, the accuracy of the solution depends on the spatial and temporal discretization adopted. In view of the fact that analytical solutions are not generally available, convergence is a necessary criterion for any numerical solution to be meaningful. It is important to determine whether the results for different element and time-step sizes converge to the true solution when the soil hydraulic properties are highly nonlinear with respect to the pore-water pressure. In this case, the rate of convergence will affect the acceptability of a solution, since it is not feasible to always use a refined spatial and temporal discretization to generate the correct value, especially when computational resources are limited.

However, slow convergence has been observed by numerous researchers. Celia et al. (1990) showed that the results of computed wetting fronts converge to the

correct solution slowly with reducing time-step sizes over a fixed element size. The authors attributed the cause of the slow convergence to a mass imbalance across the element domain when the h-based Richards equation is used. They attributed significant under-prediction of the depth of wetting front for larger element and time-step sizes to an improper evaluation of the capacity coefficient, which creates the mass balance error. To maintain mass conservation, they recommended that the mixed form of the Richards equation be used instead of the more frequently used h-based form. Rathfelder and Abriola (1994) and Ju and Kung (1997) also argued that attention should be given to the proper evaluation of the capacity coefficient and its time derivative.

On the other hand, Paniconi and Putti (1994) believed that the rate of convergence is dependent on the iterative and under-relaxation strategy used to solve the nonlinear Richards equation. Recently, Chong (2001) and Tan et al. (2004) studied the influence of mass balance and different under-relaxation techniques on the rate of such convergence. They showed that even with mass balance, slow convergence could still be observed. They demonstrated that the slow convergence with respect to refinement of the time-step is an indirect result of the under-relaxation technique used to update the hydraulic conductivity during the iterative solution of the discretized nonlinear transient seepage equations at each time-step. The under-relaxation technique used by standard programs such as SEEP/W seems to optimize the number of iterations per time-step, but comes with a hidden cost of requiring an extreme refinement of time-step to arrive at a solution of acceptable accuracy, which is not well appreciated. They recommended an alternative under-relaxation technique that the material properties for the

new iteration are defined as the average of the pressure heads computed from the two most recent iterations of the current time-step. It is shown that this form of under-relaxation does not require very small time-steps to produce reasonably accurate results, but does so at a price of increasing the number of iterations within each time-step, and even diverges instead of converging to a stable solution when dealing with soils with highly nonlinear hydraulic properties.

2.9 Transformation Approach

Transformation methods for solving Richards equation have existed for several decades (Haverkamp et al., 1977; Vauclin et al., 1979). The general objective of these methods is to overcome inefficiencies in the numerical solution process caused by the strong nonlinearity of the media hydraulic properties, especially in the case of infiltration into a media that is initially relatively dry. These types of infiltration problems can generate very sharp wetting fronts and lead to computationally inefficient solutions when using standard numerical techniques. Unacceptable fine discretizations in space and time are often required to achieve convergence to the accurate solution. Transformation methods can reduce the nonlinearity of the solution profiles through the identification and application of an appropriate change of variable applied to the dependent variable in the governing equations. The solution of the original problem may then be retrieved by applying an inverse transformation. Current transformation approaches include the use of water content (θ) (Kirkland et al., 1992), integral (Haverkamp et al., 1977; Williams and Miller, 1999; Williams et al., 2000), hyperbolic (Ross, 1990), and rational (Pan and Wierenga,

1995) transform functions, as well as variable switching methods (Forsyth et al., 1995; Diersch and Perrochet, 1999; Wu and Forsyth, 2001).

Early attempts of transformation methods used an integral transform commonly referred to as the Kirchhoff integral transform (Haverkamp et al., 1977; Vauclin et al., 1979). It directly reduces the nonlinearity of the conductivity terms in Richards equation and, as a result, can optimize the number of nonlinear iterations required for a solution. However, it depends on media hydraulic properties and will therefore vary spatially with different soil types. Thus, simple application of the Kirchhoff integral transform is limited to homogeneous media. Ross and Bristow (1990) added a flux balancing correction term to the formula and made it applicable to layered and gradational soils. Williams and Miller (1999) and Williams et al. (2000) proposed a new integral transform based on the Kirchhoff integral transform. Their study showed that this new transform is in general more efficient. Integral transforms are more complex to implement, because an analytic function of the inverse transform is generally not available.

Hill et al. (1989) have shown that the θ-based form of Richards equation can result in significantly improved performances compared to h-based methods, especially when applied to very dry heterogeneous soils. This is due to the fact that the media hydraulic functions are not as highly nonlinear when expressed in terms of θ rather than h. However, it is restricted to unsaturated flow conditions. To benefit from the good convergence properties of the θ-based form for both saturated and unsaturated conditions, Kirkland et al. (1992) suggested using a transform defined in terms of θ (THT). It is defined as an affine transformation of θ, resulting in a dependent variable that has the characteristics of θ in the unsaturated zone and of

the pressure head in the saturated zone. The variable switching technique (Forsyth et al., 1995; Diersch and Perrochet, 1999; Wu and Forsyth, 2001) is similar to THT in that it is based on switching between variables θ and h, yet it does not define a new continuous dependent variable. Since THT is defined from the volumetric water content, it will vary with the media type. Therefore, simple application of THT is also restricted to homogeneous media.

Considering the limitation of transform approaches above to heterogeneous media, an alternate class of transforms was developed that are defined strictly in terms of h. Since h is continuous across the whole domain with different media types, these transform functions will also be continuous in heterogeneous media. Ross (1990) introduced an efficient transform defined in terms of the hyperbolic sine function. However, it introduces two arbitrary parameters requiring determination to get optimal performance. Pan and Wierenga (1995) proposed another transform defined in terms of a rational function (referred as RFT hereafter) of h. It provides performance improvements and introduces only one arbitrary parameter.

Previous studies have shown that transformation approaches have the potential to lead to more efficient and robust solutions of Richards equation than traditional approaches. And the potential advantage of transformation approaches increases as the difficulty of the problem increases, which can be measured by the average number of nonlinear iterations within each time-step that are required to get a stable solution. Thus it is conjectured that the combination of the transformation method and the under-relaxation technique will lead to a more robust and efficient solution strategy. This combination of approaches has not been examined in the literature to the author's knowledge.

2.10 Temporal Adaptive Method

In most unsaturated flow simulation methods, usually fixed spatial grids and fixed time-steps are used. Although virtually all modern ordinary differential equation (ODE) software employ highly sophisticated step size adjustment procedures, relatively few Richards equation solvers use these adaptive schemes. Instead, most of them use uniform time-steps (e.g. Celia et al., 1990). Such a strategy may be inadequate if the behavior of the solution changes within the simulation because the step size may become either too large (annihilating accuracy) or too small (wasting computational time).

A common temporal adaptive strategy is to adjust the step size according to the number of iterations required for convergence of the non-linear solver (Yeh, 1987; Celia and Binning, 1992; Simunek and van Genuchten, 1994; Rathfelder and Abriola, 1994). This heuristic method is cheap to implement into existing programs. However, there is no clear general relation between the temporal discretization errors and solver performance, requiring purely empirical fine-tuning of the parameters without any apparent guidelines. And, it is unclear now how to accommodate such a method to non-iterative solvers.

Recently, Tocci et al. (1997), Miller et al. (1998) and Williams and Miller (1999) showed that DASPK, which is a variable-order variable-stepsize differential algebraic equation integrator, could outperform standard fixed time-step schemes. This approach approximates the spatial derivatives using standard schemes like finite difference or finite element methods and then integrated in time using a differential algebraic equation (DAE) code. Thus, the Richards equation is reduced

to a system of ordinary differential equations (ODEs). Unlike the heuristic method, DASPK adjusts the time-step size and order based on temporal truncation error checking. However, in practical seepage flow simulations, the uncertainty in the soil hydraulic properties and boundary conditions is usually large, which makes it unnecessary to use stringent error tolerance. When medium accuracy requirements are applied, high-order does not necessarily lead to high performance.

Another group of temporal adaptive methods are based on different kind of local truncation error monitoring strategy. For example, a predictor-corrector time integrator was originally introduced by Gresho et al. (1979) and subsequently improved by Bixler (1989), and employed for groundwater flow problems by Diersch (1988); Diersch and Perrochet (1999). In this integrator, the local truncation error is evaluated by comparing a predictor solution and a subsequent corrector solution, and then the time-step size is varied in accordance with temporal accuracy requirements. More recently, Sloan and Abbo (1999) proposed a new approach for quality-controlled automatic time stepping for elasto-plastic consolidation analysis in geomechanics. The algorithm uses a numerical estimate of the local temporal truncation error and an efficient time-step selector to constrain the temporal error near a user prescribed tolerance. Based on the solution of first-order backward Euler scheme, a solution of the second-order Thomas-Gladwell approximation (Thomas and Gladwell, 1988) can be obtained at virtually no extra cost. Thus, the local truncation error can be monitored by comparing these two solutions of adjacent order of accuracy. Kavetski et al. (2001) and Kavetski et al. (2002) applied the principles of the adaptive scheme of Sloan and Abbo (1999) to the solution of Richards equation. The studies showed

that this method was superior to existing uniform and heuristic time stepping approaches, and also conceptually and computationally simple. It can be directly incorporated into any software based on the backward Euler scheme which is prevalent in unsaturated flow modeling.

2.11 Concluding Remarks

It is often necessary to study the effect of rainfall infiltration on the stability of slopes using numerical methods. Considerable attention has been focused on numerical modeling of such unsaturated flow problem. This chapter gives a broad, but not in-depth, introduction to some popular numerical methods and related topics on solutions of the governing differential equations. Especially, numerical difficulties in these methods and possible causes are highlighted and discussed in detail. It has been shown in previous studies that numerical problems like oscillation and slow convergence rate affect the calculation of pore-water pressures in a finite element analysis, due to the highly nonlinearity of soil hydraulic properties. These results can lead to errors in the calculation of other design variables. On the other hand, transformation methods are shown to be able to reduce the sharpness of the wetting front in unsaturated flow problems and can overcome inefficiencies in the numerical solution process which are caused by the strong nonlinearity of the soil hydraulic properties. It suggests that transformation methods might be able to improve the convergence difficulties. Hence, a combination approach is proposed in this thesis and a detailed investigation is implemented to look into its effect on the slow convergence problems.

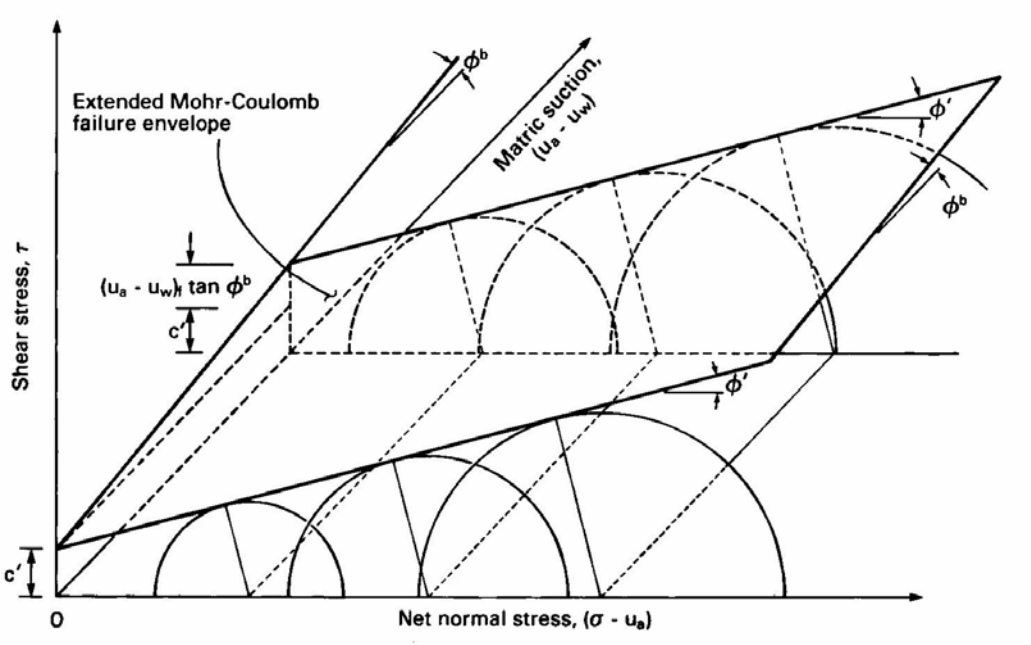

Figure 2.1: Extended Mohr-Coulomb failure envelope for unsaturated soils (from Fredlund and Rahardjo, 1993)

Chapter 3

Rational Transformation Method with Under-Relaxation

3.1 Introduction

Numerical modeling of transient unsaturated seepage flow is gaining importance due to a growing recognition that matric suction contributes towards the shear strength of partially saturated soils. Usually, the fluid motion in the unsaturated zone can be described by the classical Richards equation. Valid solutions for different forms of Richards equation are difficult to obtain because of the strong nonlinearity often exhibited by the soil-water characteristic curve and the soil hydraulic conductivity function. By using different methods of discretization in the numerical resolution of these equations, a different level of accuracy can be obtained. Generally, the standard approximations that are applied to the spatial domain are the finite element method and the finite difference method. Among them, the finite element method is the more popular. These are usually coupled with a simple one-step Euler time-marching algorithm for transient problems. For any Euler method other than the fully explicit forward method, nonlinear algebraic equations result and some linearization and/or iteration procedure must be used

to solve the discrete equations.

However, very steep hydraulic conductivity functions create difficulties for the convergence of solution. The solution will tend to diverge instead of converge and oscillate between two extreme solutions represented by the extremities of the hydraulic conductivity function, leading to slow convergence to a stable solution within each time-step. In these cases, under-relaxation techniques are often necessary to curb the tendency of the calculated head from oscillating about its extreme values and improve the rate of convergence within a time-step, especially for steep hydraulic conductivity functions. Yet, it is found that a typical under-relaxation technique adopted by SEEP/W optimizes the number of iterations per time-step, but comes with a slow convergence to the correct solution with refinement of the time-step and element size. An alternative form of under-relaxation recommended by Chong (2001) and Tan et al. (2004) was shown to bring significant improvements to the rate of convergence to the true solution, but does so at a price of increasing the number of iterations within each time-step, and even diverges instead of converging to a stable solution when dealing with soils with highly nonlinear hydraulic properties.

On the other hand, a review of the literature in Chapter 2 has shown that transformation methods can reduce the sharpness of the wetting front in unsaturated flow problems and can overcome inefficiencies in the numerical solution process caused by the strong nonlinearity of the soil hydraulic properties. It suggests that transformation methods might be able to improve the convergence rate of the solution, but without dramatically increasing the number of iterations within each time-step.

In the following sections, numerical formulations for solving the h-based form of Richards equation will be described using a finite element approach. For simplicity, the formulations will be written for one-dimensional flow problems, in which only seepage in the vertical direction is looked into. Two dimensional flow problems are also studied, which will be shown in Chapter 5. A backward implicit time-stepping method is used and an iterative scheme is required to solve the nonlinear equations. A new approach TUR1 is then proposed, in which the RFT transformation method is applied to the finite element method, and then combined with a typical under relaxation technique to solve the Richards equation. To the best of the author's knowledge, there has insofar not been any published work found, which discusses the combination of the transformation method and under-relaxation techniques. A detailed investigation was then undertaken to look into its effect on the slow convergence problems. The minimum time-step criterion presented by Karthikeyan et al. (2001) or the lumped-mass formulation is applied to suppress oscillations so that the convergence issue can be studied without being encumbered by extraneous complications. In addition, because almost all transforms involve arbitrary parameters, selecting their values is important to determine the efficiency of a particular transformation. Yet few rigorous studies of the parameter selection have been done. In this chapter, the selection of such parameter values will be investigated. Note that a trial and error tuning process is self-defeating because the cost of previous tuning runs may beat the purported efficiency of the optimized parameter. The sensitivity of efficiency to choice of parameter value is of practical interest as well.

3.2 Numerical Formulations

3.2.1 Finite Element Formulation in h-based form

The governing partial differential equation for the flow of water through a one-dimensional unsaturated soil element is given as follows (GEO-SLOPE, 2004):

$$\frac{\partial}{\partial z}\left(K\frac{\partial H}{\partial z}\right)+Q=\frac{\partial \theta}{\partial t} \tag{3.1}$$

where

K = the hydraulic conductivity in the vertical direction, ms^{-1};

H = the total head, the sum of pressure head h and elevation head z;

Q = the applied boundary flux;

θ = the volumetric water content; and;

t = the time, sec.

Equation (3.1) can be expressed in terms of total head H by relating the volumetric water content θ to the change of H by the equation:

$$\mathrm{d}\theta=\lambda\,\mathrm{d}(H-z) \tag{3.2}$$

where

λ = the specific storage capacity which is equal to $m_w\gamma_w$;

m_w = the slope of the soil-water characteristic curve, $\mathrm{m}^2\mathrm{kN}^{-1}$;

γ_w = the unit weight of water, $\mathrm{kN}\cdot\mathrm{m}^{-3}$; and

z = the elevation, assumed positive upwards, m.

Substitute equation (3.2) into equation (3.1), leading to the following expression:

$$\frac{\partial}{\partial z}\left(K\frac{\partial H}{\partial z}\right)+Q=\lambda\frac{\partial H}{\partial t} \tag{3.3}$$

If the applied boundary flux Q is not present, equation (3.3) is equivalent to the h-based form of Richards equation, shown in equation (2.3a). It is now expressed in terms of total head, H rather than pressure head h. The parameter, λ thus corresponds to the specific moisture capacity function, C defined in equation (2.3a).

After applying the Galerkin weighted residual method to the governing differential equation (3.3), the corresponding finite element equation can then be expressed as follows:

$$[M]\{H\},t + [K]\{H\} = \{Q\} \tag{3.4a}$$

where

$$[M] = d\int_A (\lambda \{N\}^T \{N\})\,\mathrm{d}A \tag{3.4b}$$

$$[K] = d\int_A ([B]^T [k] [B])\,\mathrm{d}A \tag{3.4c}$$

and

$$\{Q\} = qd\int (\{N\}^T)\,\mathrm{d}L \tag{3.4d}$$

In the above equation,

$\{H\}$ = vector of total head;

$\{H\},t$ = vector of time derivative, $\partial H/\partial t$, at nodal points;

$[B]$ = gradient matrix;

$[k]$ = element hydraulic conductivity matrix;

$\{N\}$ = vector of interpolating function;

q = unit flux across the side of an element;

L = boundary of element;

A = area of element; and

d = element thickness.

To perform the time integration, a backward finite difference approximation scheme is adopted leading to the following equation:

$$(\Delta t\,[K] + [M])\,\{H_{n+1}\} = \Delta t\,\{Q_{n+1}\} + [M]\,\{H_n\} \tag{3.5}$$

where

$\{H_n\}$ = vector of total head at time-step n;

$\{Q_n\}$ = vector of nodal flux at time-step n; and

Δt = time-step.

To solve the finite element equations, a technique like the direct Gaussian elimination can be used. Since the material hydraulic conductivity and storage properties are the functions of head, the finite element equations are nonlinear and an iterative scheme is required for the solution process. A repeated substitution method named the Picard method is often used. And, some form of relaxation technique is often used to enhance the performance of the nonlinear iterative schemes. This will be discussed later in Section (3.2.3).

The iterative process will continue until the iteration number reaches a prescribed maximum or until the results satisfy the convergence criterion. As a measure of convergence, the Euclidean norm of the pressure head vector in SEEP/W is used. The pressure head vector norm is defined as:

$$\parallel h \parallel = \left(\sum_{i=1}^{nn} \left| h^i \right|^2 \right)^{1/2} + 1.0 \tag{3.6}$$

where nn = number of nodes; and h^i = pressure head at node i. The vector norm is a measure of the size of the pressure head vector. A constant value of 1.0 is added to the vector norm to prevent it from being equal to zero. The solution is deemed to have converged when the percentage difference in the pressure head vector norm between two consecutive iterations is less than a user specified tolerance value.

3.2.2 Constitutive Relations

There are many constitutive equations to describe the relationships between θ and h, and K and h, as reviewed in Section (2.5). Using appropriate parameters, most soil-water characteristic models can fit the experimental data well. Among the more popular choices to describe the soil-water characteristic curve, the four-parameter van Genuchten model (van Genuchten, 1980) is used here for its flexibility in fitting fine-textured soil data, given by

$$\Theta(h) = \frac{\theta(h) - \theta_r}{\theta_s - \theta_r} = \begin{cases} (1 + |ah|^n)^{-m}, & h < 0 \\ 1, & h \geq 0 \end{cases} \tag{3.7}$$

where

Θ = the effective saturation;

θ = volumetric water content;

θ_r and θ_s = the residual and saturated volumetric water contents, respectively;

a = shape parameter, m^{-1};

n and m = shape parameters, where $m = 1 - 1/n$; and

h = the pressure head.

The Mualem (1976) model can be coupled with the van Genuchten soil-water characteristic curve to provide an estimate for the conductivity function (van Genuchten 1980). The equation can be expressed by

$$K(\Theta) = K_s \Theta^{1/2} \left[1 - \left(1 - \Theta^{1/m}\right)^m\right]^2 \tag{3.8}$$

where

K_s = saturated hydraulic conductivity; and

$\Theta = \Theta(h)$ from Equation (3.7).

The other parameters are as defined in Equation (3.7).

3.2.3 Under-Relaxation Technique

As a result of the nonlinearity of the soil-water characteristic curve and conductivity function, the finite element equations are nonlinear and an iterative scheme is required for the solution process in each time-step. However, very steep hydraulic conductivity functions create convergence difficulties. The solution will tend to diverge instead of converge and oscillate between two extreme solutions represented by the extremities of the hydraulic conductivity function, leading to slow convergence to a stable solution within each time-step.

During the iterative process, under-relaxation techniques are often employed to curb the tendency of the calculated head from oscillating about its extreme values. This will improve the rate of convergence within a time-step, especially for steep hydraulic conductivity functions.

One form of under-relaxation uses the head at the mid-point of the time interval

to define the material properties in each time-step (hereafter referred to as UR1). That is, the material properties used for the next iteration $m+1$ at the current time-step $n+1$ is defined at the average of heads computed from the previous time-step n and the most recent iteration m of the current time-step $n+1$. The definition of this head can be expressed mathematically as follows:

$$\overline{H}^{i}_{n+1,m+1} = \frac{H^{i}_{n+1,m} + H^{i}_{n}}{2} \tag{3.9}$$

where

$H^{i}_{n+1,m}$ = total head at spatial node i, current time-step $n+1$ and iteration m; and

H^{i}_{n} = previously computed total head at spatial node i and time-step n.

In this way, the tendency for h to oscillate around its limits will be dampened and a smaller number of iterations will be needed for the convergence to a stable solution within each time-step. This is a commonly used under-relaxation approach and has been adopted by standard programs such as SEEP/W. However, previous studies (Chong, 2001; Tan et al., 2004) have shown that this form of under relaxation technique seems to optimize the number of iterations per time-step, but comes with a hidden cost of requiring an extreme refinement of time-step to arrive at a solution of acceptable accuracy, which is rarely appreciated.

Another variation of under-relaxation commonly used is Gauss-Seidel iteration (hereafter referred to as UR2). In this case, the material properties for the new iteration are defined at the average of heads computed from the two most recent iterations of the current time-step (Paniconi and Putti, 1994):

$$\overline{H}^{i}_{n+1,m+1} = \frac{H^{i}_{n+1,m} + H^{i}_{n+1,m-1}}{2} \tag{3.10}$$

This approach can also restrain the tendency of h from oscillating around its extreme values, thus improving the rate of convergence during the iterative process. Chong (2001) and Tan et al. (2004) recommended this form of under-relaxation in their study. They showed that it improves the rate of convergence of solutions with respect to increasing refinement in mesh size and time-step, but does so at a price of increasing the number of iterations within each time-step, and even diverge instead of converge to a stable solution when dealing with soils with highly nonlinear hydraulic properties.

Note that the under-relaxation technique is usually not strictly applied to determine λ or m_w. A purportedly more robust chord slope approximation approach is used whereby the slope of the soil-water characteristic curve (m_w) is evaluated from a straight line connecting the volumetric water content at H_n^i with that at H_{n+1}^i. When these two heads are nearly identical, then m_w is computed from the tangent of the soil-water characteristic curve at the average of these two heads.

In this study, a Fortran 90 program, named HFE, has been specifically written so as to explore different linearization and iterative techniques. The formulation adopted in HFE follows closely as that discussed previously, including the h-based form finite element formulation, under-relaxation technique (UR1), chord slope method for linearization and so on, which can be found in a typical finite element program like SEEP/W. Furthermore, HFE can be shown to generate essentially the same results as SEEP/W and this verification is included in Appendix C. The development of the program HFE is necessary to include modifications to the finite element formulation to be carried out easily for testing different methods such as UR2 technique.

3.2.4 Transformation Method

The basic idea behind the transformation approach is to define a function $p(h)$ that will result in a more efficient and robust solution to the Richards equation. Several transformations have been developed as discussed previously. In the following studies, the RFT transform approach will be adopted due to its efficiency in homogeneous and heterogeneous soils and easy implementation.

The RFT transform is defined in terms of a rational function of pressure head h (Pan and Wierenga, 1995), given by

$$p = \begin{cases} \dfrac{h}{1+\beta h}, & h < 0 \\ h, & h \geq 0 \end{cases} \tag{3.11}$$

where p is the transformed head; h is pressure head and β is a transform parameter.

With this transformation, the sharpness of the wetting front appearing in the spatial domain in unsaturated flow problems can be reduced, which can be seen in Figure 3.1 using a one-dimensional infiltration example. It also leads to a more gradual change of dependent variables in temporal domain, which is shown in Figure 3.2. Thus, more efficient and robust solutions are expected with the application of such transformation than traditional approaches.

With (3.11), equation (3.3) becomes

$$\frac{\partial}{\partial z}\left(K^* \frac{\partial p}{\partial z}\right) + \frac{\partial K}{\partial z} + Q = \lambda^* \frac{\partial p}{\partial t} \tag{3.12a}$$

where

$$K^* = K\frac{\partial h}{\partial p} \tag{3.12b}$$

$$\lambda^* = \lambda\frac{\partial h}{\partial p} \tag{3.12c}$$

$$\frac{\partial h}{\partial p} = \begin{cases} \dfrac{1}{(1-\beta p)^2}, & h < 0 \\ 1, & h \geq 0 \end{cases} \tag{3.12d}$$

The corresponding finite element equation for (3.12a) can then be expressed as follows:

$$[M]^* \{p\}, t + [K]^* \{p\} + [K] \{z\} = \{Q\} \tag{3.13a}$$

where

$$[M]^* = d \int_A (\lambda^* \{N\}^T \{N\}) \, \mathrm{d}A \tag{3.13b}$$

$$[K]^* = d \int_A ([B]^T [k]^* [B]) \, \mathrm{d}A \tag{3.13c}$$

$$[K] = d \int_A ([B]^T [k] [B]) \, \mathrm{d}A \tag{3.13d}$$

and

$$\{Q\} = qd \int (\{N\}^T) \, \mathrm{d}L \tag{3.13e}$$

In the above equations,

$\{p\}$ = vector of transformed head;

$\{p\}, t$ = vector of time derivative of $\{p\}$ at nodal points;

$[k]^*$ = transformed element hydraulic conductivity matrix.

To perform the time integration, a backward finite difference approximation scheme is adopted leading to the following equation:

$$(\Delta t \, [K]^* + [M]^*) \{p_{n+1}\} = \Delta t \, \{Q_{n+1}\} + [M]^* \{p_n\} - \Delta t \, [K] \{z\} \tag{3.14}$$

where $\{p_n\}$ = transformed head at time-step n.

Although the transformation method can reduce the sharpness of the wetting front significantly, an under-relaxation technique is still needed to solve the nonlinear finite element equations after transformation. Otherwise, in some cases with relatively large time-steps, stable solution cannot be achieved even after a large number of iterations. In the proposed new approach TUR1, the UR1 under-relaxation technique discussed above will be adopted. Studies show that the transformation method alone without any under-relaxation (hereafter referred as TUR0) or combined with the UR2 under-relaxation technique (hereafter referred as TUR2) gives less efficient solutions than TUR1, which will be shown in Section 3.3.8. The key difference is now the under-relaxation will be applied to the transformed heads instead of the pressure heads. It can be expressed mathematically as follows:

$$\overline{p}^{i}_{n+1,m+1} = \frac{p^{i}_{n+1,m} + p^{i}_{n}}{2} \tag{3.15}$$

where

$p^{i}_{n+1,m}$ = transformed head at spatial node i, time-step $n+1$ and iteration m; and

p^{i}_{n} = previously computed transformed head at spatial node i and time-step n.

In TUR2, the under-relaxation can be expressed as:

$$\overline{p}^{i}_{n+1,m+1} = \frac{p^{i}_{n+1,m} + p^{i}_{n+1,m-1}}{2} \tag{3.16}$$

where

$p^{i}_{n+1,m}$ = transformed head at spatial node i, time-step $n+1$ and iteration m; and

$p^i_{n+1,m-1}$ = transformed head at spatial node i, time-step $n+1$ and previous iteration $m-1$.

Note that the chord slope approach is still used here to determine λ or m_w. The under-relaxation is only applied to K and $\partial h/\partial p$. Thus,

$$K^* = K\frac{\partial h}{\partial p} = K(\overline{p}) \cdot \frac{1}{(1-\beta\overline{p})^2} \tag{3.17a}$$

$$\lambda^* = \lambda\frac{\partial h}{\partial p} = \lambda \cdot \frac{1}{(1-\beta\overline{p})^2} \tag{3.17b}$$

where $\overline{p}$ is the transformed heads after under relaxation.

3.3 Convergence Study of TUR1 method

3.3.1 Problem Descriptions

The one-dimensional test problem is similar to those used by Chong (2001) and Tan et al. (2004) for vertical infiltration under constant surface pressure heads. The geometry of the finite element mesh is shown schematically in Figure 3.3. In this problem, a typical sandy clay loam soil (Case A) and a typical loam soil with steeper hydraulic characteristic curves (Case B) are adopted. Hydraulic properties of the former soil (Case A) are obtained from the International UNsaturated SOil hydraulic DAtabase, UNSODA (Leij et al., 1996). The related soil parameters are computed by curve fitting laboratory data (Soil Type 1132) using van Genuchten (1980) soil-water characteristic model and Mualem (1976a) conductivity model simultaneously. The latter is taken from SoilVision (2003).

To define the boundary conditions, a uniform pressure head of -8 m is first generated throughout the soil column using a steady state analysis. This starts

the problem from an initial dry state, with a volumetric water content close to the residual value. The asymptotic behavior of the soil-water characteristic curve in this region creates computational difficulties for the numerical simulations, and thus should provide a rigorous test for all solution approaches. For subsequent transient analyses, a zero pressure head is imposed at the top of the column, while the pressure head is maintained at -8 m at the bottom. This simulates an infiltration condition, whereby the negative pore-water pressure at the top is reduced to zero as soon as infiltration starts.

The porous medium properties, initial conditions and boundary conditions are summarized in Table 3.2. The nonlinear soil hydraulic characteristics for these chosen soil types are illustrated in Figures 3.4 and 3.5.

3.3.2 Benchmark Solution

Chong (2001) and Tan et al. (2004) has showed that the solution of HFE with UR1 do converged to some values when extreme refinement of time-steps and corresponding extreme spatial discretization (hereafter referred to as the dense grid mesh) are used. In order to verify that the converged solution produced by the program HFE are correct, the generalized solution derived by Warrick et al. (1985) for the infiltration problem is computed and compared with the solution generated from such dense grid mesh for three different pressure heads as shown in Figure 3.6. A close agreement is observed between this dense mesh finite element solution and Warrick et al.'s (1985) generalized semi-analytical solution. Therefore, the converged solution generated by HFE, with an element size of 0.001

m and a corresponding time-step of 5.52 s, can be assumed correct. As Warrick et al.'s (1985) solution is only restricted to the three pressure heads shown in Figure 3.6, the dense mesh solution will be used as the benchmark solution in the following study for comparison and will appear as a bold line in all figures plotted subsequently.

3.3.3 Transformation Parameter β

Because the transformation in Equation (3.11) involves an arbitrary parameter β, selecting its value is important to determine the efficiency of this method. The absolute value of the transformation parameter β should not be too small in order to keep the benefits of the transformation. It also should not be too large, which would reduce the gradient too much and cause big errors. Pan and Wierenga (1995) recommended that in practice, one may calculate the transformed hydraulic conductivity K^*, and plot it versus the pressure head for the soil involved. The recommended value of β can be chosen as the largest value for which the curves remains monotonic. But this recommendation was not studied in detail. In particular, the difference in efficiency between this *a prior* choice and the most optimized parameter is unknown. The range of soils in which this recommendation is feasible is also unknown. These practical questions are important and are studied below.

The transformed hydraulic conductivity K^* curves are plotted in Figures 3.7 and 3.8 for Case A and Case B, respectively. For Case A, the biggest β allowed as long as the K^* curve is still monotonic is around -2.72 m^{-1} (previous recommendation). Figure 3.9 shows a comparison of results with different β

values. It shows that both a very small β value (-0.01 m^{-1}) and the biggest β allowed (-2.72 m^{-1}) generate unsatisfactory results, whereas an intermediate value (-1.4 m^{-1}) produce the most accurate solution. It suggests a tentative way to choose a more optimum β value. In the following studies, the average value of the biggest β and zero, that is, half of the biggest β is used. For Case A, the biggest β allowed is around -2.72 m^{-1}, thus, -1.4 m^{-1} will be used as the β value. For Case B, the biggest β allowed is around -24 m^{-1}, thus, -12 m^{-1} will be used as the β value. The choice of the optimal transformation parameter value will be explored further in the following sections.

3.3.4 Convergence for a General Case

Chong (2001) and Tan et al. (2004) have studied the convergence pattern of UR1 and UR2. When UR1 is adopted, it is shown that, apparent "convergence" of pressure head profiles was observed when the element size was reduced over a fixed time-step size. However, the wetting front was observed to migrate deeper as the time-step size was reduced, indicating that convergence to the "true" solution is actually not achieved. When the time-step size was reduced over a fixed element size, slow convergence resulted leading to a severe under-prediction of the wetting fronts. On the other hand, when UR2 is adopted, it is shown that, the calculated pressure head profiles converge to a solution closed to the correct one when the element size was reduced over a fixed time-step size. In addition, the converged profiles approached the correct solution as the time-step size reduced, with smaller discretization errors appear as reduced diffusion about this sharp profile.

In the following analysis, the convergence of TUR1 for a general case is studied. For the first analysis, the effect of element size is studied by keeping the time-step size fixed at 55200 sec. Figure 3.10(a) shows the variation of pressure head with elevation for this analysis. It can be observed that the calculated pressure heads of TUR1 converge to a sharp profile, close to the dense grid mesh solution. Similar convergence trends can be seen when the time-step size is further reduced to 13800 s, and subsequently 3450 s, as illustrated by Figures 3.10(b) and 3.10(c), respectively. In addition, the converged depth of infiltration approaches the correct solution as the time-step size reduces, generating correspondingly less diffusion in each case.

Next, to investigate the influence of temporal discretization, the time-step sizes are now reduced while keeping the element size fixed at 0.1 m. Figure 3.11(a) shows that for a fixed element size, the computed pressure heads begin to oscillate when the time-step is reduced below a certain threshold. The results converge to a sharp profile as shown by the dense grid mesh solution with refinement of the time-step, with the larger discretization errors appearing as increased diffusion about this sharp profile. Similarly, the same observations can be made from Figures 3.11(b) and 3.11(c), which show the calculated results for two other smaller element sizes.

3.3.5 Convergence with Minimum Time-step Criteria

3.3.5.1 Application of Minimum Time-step Criteria

Thomas and Zhou (1997) developed two minimum time-step criteria to avoid nu-

merical oscillations in heat diffusion problems. These criteria are formulated in terms of thermal conductivity, specific head capacity and element size, and they apply strictly for constant material properties. Karthikeyan et al. (2001) applied similar criteria to unsaturated seepage flow problems in SEEP/W, in which the same formulation was used in the solution process. These criteria were found to be applicable to seepage flow in unsaturated soil with nonlinear hydraulic properties to control oscillations.

Table 3.1 gives a summary of the minimum time-step sizes for different element types. It shows that the minimum time-step size is related to the element length, L, which is perpendicular to the direction of flow and material properties, K and λ.

To calculate the minimum time-step, it is necessary to determine the ratio of λ to K, which is not a constant when the soil-water characteristic curve and conductivity function are nonlinear. This ratio is observed to increase as the pore-water pressure becomes more negative. Since an imposed infiltration boundary condition is not expected to result in the further drying of the soil, the most critical case will correspond to the initial state where the negative pore-water pressure is the highest. This initial state is used to calculate the ratio of λ to K. In this case, the value of m_w is calculated from the tangential slope of the soil-water characteristic curve. This approach is found to be adequate in removing oscillations from the pore-water pressure profiles generated (Karthikeyan et al., 2001).

To illustrate the problem with the oscillation-free case, different sets of element sizes and corresponding time-step sizes that satisfy the Thomas and Zhou (1997) criteria are used.

From Table 3.1, there is only one minimum time-step criteria required by one-dimensional element to be satisfied for a non-oscillatory solution. For an initial pressure head of -8 m, the values of λ and K are found to be 3.70×10^{-3} m^{-1} and 1.12×10^{-10} ms^{-1}, respectively. Applying the criterion in Table 3.1, a minimum time-step of around 55200 s is required for an element size of 0.1 m. Other combinations are summarized in Table 3.3.

Figure 3.10 and Figure 3.11 show that the minimum time-step criteria developed by Thomas and Zhou (1997) is still applicable to TUR1 to curb oscillation. Further studies with other soils also validate this finding. To the author's knowledge, this observation is first demonstrated in this study. Note that the minimum time-step criteria are computed based on the original λ and K.

3.3.5.2 Stability of Solution within a Time-step

An analysis adopting an element size of 0.05 m and a time-step of 13800 s was carried out for the 1D unsaturated seepage flow problem. Figure 3.12 shows the variation in the normalized elevation corresponding to a pressure head of -6 m with the iteration number at four elapsed times. The normalized elevation is defined as the ratio of the computed elevation to the correct elevation from the dense grid mesh solution. The solution is considered to be "stable" when the percentage difference in the pressure head vector norm between two successive iterations is less than 0.001.

Figure 3.12 shows that during the iterative process in each time-step, calculations generated with UR1 converges to a stable solution very rapidly (less than

10 iterations) without oscillation. However, this stable solution differs significantly from the correct solution. It was found that the normalized elevation for the time of 55200 s can be as high as 2.5. This problem was also reported by Tan et al. (2004). In contrast, although the stable solutions for UR2 attained in each time-step are shown to be within 80% of the correct dense grid solution, it requires around 100 iterations to converge to stable solutions. It is also worth mentioning that the solution generated by UR2 converges to a stable solution in a different way from UR1. It appears to oscillate around the correct solution and converge slowly. On the other hand, TUR1 is able to produce stable solutions in each time-step that are within 90% of the correct dense grid solution with less than 20 iterations. Its convergence pattern within a time-step is like UR1. That is, the calculation converges to the stable solution monotonically without oscillation. This is possibly because relaxation technique in UR1 form is still used in TUR1. In addition, the nonlinearity of the problem will be alleviated by transformation method, which may greatly reduces the error that appeared in UR1.

Figure 3.13 shows the different convergence procedures of UR1, UR2 and TUR1 demonstrated on the hydraulic conductivity curve for a gauss point near the wetting front. It is observed that for the UR1 method, the calculated permeability have little changes during iterations, thus a stable solution can be obtained very quickly (6 iterations). However, these permeability values are far from accurate (about 1×10^{-10} m/s compared to the accurate value of 3.3×10^{-7} m/s), which makes the converged solution differs significantly from the correct one. For the UR2 method, the calculated permeability approaches the correct value gradually and converges slowly in an oscillatory pattern. Therefore, the converged solution of UR2 is more

accurate than UR1, but with the price of using much more iterations. While for the TUR1 method, the calculated permeability approaches the correct value monotonically without oscillation, hence a much more accurate solution compared to that using UR1 can be obtained quickly within less than 20 iterations.

Overall, the above results indicate the relatively significant advantages of the proposed TUR1 method compared to existing UR1 and UR2 schemes. The under-relaxation technique adopted by SEEP/W, UR1, requires fewer iterations per time-step but requires a significantly more refined time-step size to produce accurate solutions at a given elapsed time. At the same time, to suppress oscillation, the corresponding element size would also need to be refined significantly. The alternative under-relaxation technique, UR2, can produce more accurate solutions at the same elapsed time using a much coarser mesh and therefore a larger time-step but requires considerably more iterations per time-step. On the other hand, the proposed combination of transformation method and UR1 (TUR1) can improve its accuracy quite significantly but only with a marginal increase in cost in terms of iterations per time-step. But does this mean that TUR1 can reach a solution of specified accuracy at a give elapsed time with the least computer run time using different mesh sizes and time-steps? The following section will clarify this question.

3.3.5.3 Convergence of Solution with Mesh and Time-step Refinement

The computational effort required to calculate the wetting front at the elapsed time of 55200 s is studied using six combinations of element size and time-step, shown in Table 3.3. Figures 3.14, 3.15 and 3.16 show the wetting front plots

for reducing spatial and temporal discretization simultaneously of UR1, UR2 and TUR1, respectively. It is observed that the convergence patterns of UR1, UR2 and TUR1 are quite different. For UR1, the wetting fronts traversed slowly down the soil depth with decreasing time-step sizes, and large temporal discretization is found to under-predict the infiltration depth significantly. On the contrary, for UR2 and TUR1, the pressure heads are observed to converge to a sharp profile and larger discretization errors appear as increased diffusion about this sharp profile.

A comparison among UR1, UR2 and TUR1 on the basis of accuracy and total run time is shown in Figures 3.17 and 3.18. In the former plot, the accuracy of the computed wetting front is measured using the normalized elevations corresponding to two representative pressure heads of -6 m and -2 m. In the latter, the accuracy is measured using the L_2 error norm which is defined as

$$\| \epsilon \|_2 = \left[\frac{1}{nn} \sum_{i=1}^{nn} \left| \widehat{h^i} - h^i \right|^2 \right]^{1/2} \tag{3.18}$$

where $\widehat{h^i}$ is an accurate approximation of the true solution based on a dense grid mesh. Run time is obtained by executing the code (compiled using Microsoft Fortran^{TM} PowerStation 4.0) on a Pentium IV, 2.4 GHz machine. It appears that UR1 executes the fastest among these three approaches for each combination of element size and time-step, but approaches the correct solution slowly with mesh and time-step refinement. On the other hand, UR2 and TUR1 are able to approach the correct solution much more rapidly with the refinement of mesh and time-step. Between them, TUR1 is observed to be faster than UR2. For example, to maintain an error of around 5%, which is acceptable in practice, UR1 requires 200 elements and 400 time-steps, while both UR2 and TUR1 requires 40 elements and 16 time-steps. The corresponding run times are 14.72 s, 1.37 s and 0.33 s, respectively.

With a reasonable element size in practice to be used, such as 0.1 m, UR2 and TUR1 can get a solution with maximum error around 45%, while the solution from UR1 has a maximum error as high as 170% in terms of differences between the calculated wetting fronts and the correct solutions. Furthermore, TUR1 uses much less time than UR2. Hence, TUR1 is the most efficient from a computational viewpoint for any prescribed level of accuracy. It is also reassuring to note that with the refinement of the element size and time-step size, TUR1 approaches the same limit as UR1, which has been shown to produce the correct solutions at the extreme mesh and time-step refinement.

The total number of iterations and the average number of iterations per time-step are shown in Figure 3.19. At each combination of element size and time-step, it can be seen that UR2 requires the most iterations than UR1 and TUR1, while TUR1 requires a little more iterations than UR1. However, the total number of iterations needed to stay within a prescribed error band, say $\pm 5\%$, is 1261, 611 and 123 for UR1, UR2 and TUR1 respectively. The first reason for this difference is that both UR2 and TUR1 can use bigger time-steps thus require much less number of time-steps than UR1 to obtain such solutions. Between these two, TUR1 requires less iterations to converge within each time-step than UR2. Another reason is that a coarser time-step permits larger element sizes to be used if oscillations are to be suppressed using the minimum time-step criterion. This results in a smaller set of finite element equations to solve, which further implies that every iteration in every time-step is cheaper to perform for UR2 and TUR1 than UR1. For large 2D and 3D problems involving global matrices with significant bandwidth, the number of operations required for direct matrix solvers will approach $O(N^3)$ and this penalty

should be even heavier for UR1, where N is the number of degrees of freedom.

From the aspect of convergence to a correct solution with progressive refinement of the element size and time-step, the above results show the superiority of TUR1 over UR1 and UR2. UR1 is able to reach a stable solution very rapidly in each time-step, but requires significantly more refinement of the time-step to arrive at a solution of acceptable accuracy. At the same time, to suppress oscillation, element size needs to be correspondingly reduced, thus imposing even greater demands on computational resources. Adopting UR2 would mean that a large time-step which permits a much coarser mesh under the Thomas and Zhou (1997) criterion for oscillation control can produce reasonably accurate results, but at a price that within each time-step, much more iterations are needed. On the other hand, TUR1 has the advantages of both UR1 and UR2. Firstly, like UR2, TUR1 can use larger time-steps to produce acceptable results and thus corresponding coarser meshes to suppress oscillation. Secondly, like UR1, TUR1 can converge to a stable solution quickly in each time-step.

3.3.6 Convergence with Lumped Mass Scheme

3.3.6.1 Lumped Mass Scheme

In previous sections, numerical oscillations in the pressure head profiles are controlled by employing the minimum time-step criteria developed by Thomas and Zhou (1997). However in some cases, it is found that the oscillation-free time-step for a reasonable mesh size according to the minimum time-step criteria is too big to be used. Alternatively, oscillation was observed to be eliminated in lumped mass

formulation in which the mass matrix is diagonal (van Genuchten, 1982; Celia et al., 1990; Pan et al., 1996). Although it is reported that solutions with lumped mass formulation are less accurate than those with consistent mass formulation as it may cause smearing of the wetting front, and quadratic or cubic elements could cause oscillation with both consistent and lumped mass schemes, this lumped mass approach is very popular in the modeling of unsaturated flow problems and included in many commercial softwares such as SEEP/W (GEO-SLOPE, 2004). Thus, in the following sections, the performance of proposed TUR1 method with lumped mass formulation is examined.

Several lumping schemes have been developed in the context of finite element publications, e.g., Zienkiewicz and Taylor (2000) and Pan et al. (1996). Here, the mass matrix is diagonalized by simply adding the off-diagonal elements onto the main diagonal, which is often called a "row sum" method:

$$[M]^e_{i,j} = \begin{cases} \sum_k \int_{A^e} \left(\lambda\, N_i^T\, N_k\right) \mathrm{d}A, & i = j \\ 0, & i \neq j \end{cases} \tag{3.19}$$

This simplifies to

$$[M]^e_{i,j} = \begin{cases} \int_{A^e} \left(\lambda\, N_i^T\right) \mathrm{d}A, & i = j \\ 0, & i \neq j \end{cases} \tag{3.20}$$

since the sum of the shape functions is unity.

3.3.6.2 Convergence of Solution with Lumped Mass Scheme

The computational effort required to calculate the wetting front at the elapsed time of 55200 s is studied using four different element sizes with refinement in time-steps. A comparison among UR1, UR2 and TUR1 on the basis of accuracy

and total run time is shown in Figure 3.20. It can be seen that for all four element sizes, when a same large time-step is used, UR2 and TUR1 are able to produce much more accurate solutions than UR1, although UR1 uses the least run time to get a stable solution among these three approaches. And between UR2 and TUR1, the latter runs much faster than the former. For example, when 40 elements (element size of 0.025 m) and 16 time-steps (time-step size of 3450 s) are adopted, UR1 uses 0.24 s to get a solution with L_2 error of 3.53 m, while UR2 and TUR1 can get much more accurate solutions with L_2 error around just 0.3 m. However, UR2 uses 1.44 s to get such solution, which is 5 times more compared to UR1, while TUR1 runs almost as fast as UR1 (0.34 s). Thus, the superiority of TUR1 in efficiency over UR1 and UR2 is demonstrated again that for a fixed element size, TUR1 can use larger time-steps to produce much more accurate results than UR1, but without dramatically increasing the total run time as UR2.

3.3.7 Parameter Estimation

Firstly, the influence of transformation parameter on the performance of TUR1 method is studied when the minimum time-step criteria are used to control the oscillation problem. A comparison of performance on the basis of accuracy and total run time with different transformation parameter values is shown in Figure 3.21. The tentative observation in Section 3.3.3 that the intermediate value (-1.4 m^{-1}) is the optimal choice of the transformation parameter is validated. It appears to be the most efficient among 5 different values with the refinement of element size and time-step. It can be seen that for the same element size and time-step size,

total run times for different β values are similar. However, the intermediate value of -1.4 m^{-1} achieves the most accurate solution. Actually, when a very small β value such as -0.5 m^{-1} is used, the solution underpredicted the depth of the wetting front as UR1 method did. When the biggest β value for which the K^* curve remains monotonic such as -2.72 m^{-1} is adopted, which is recommended previously by Pan and Wierenga (1995), the solution is also quite erroneous as it overpredicts the depth of the wetting front.

For the case when lumped mass scheme is adopted to curb the oscillation problem, the choice of transformation parameter value is examined below. Figure 3.22 shows the effect of different transformation parameter values on the L_2 error of the solution with refinement in time-steps for different element sizes. The same observation can be seen that for almost all combinations of element sizes and time-steps, the intermediate value of -1.4 m^{-1} produces the most accurate solutions. The general trend of the curves is that the L_2 error decreases when the absolute β value increases from a very small value, say 0.01 m^{-1}; and the smallest L_2 error is obtained when the absolute β value increases to be around the intermediate value of 1.4 m^{-1}. Then the error begins to increase as the absolute β value increases further. Note that the previous recommendation by Pan and Wierenga (1995) of choosing the β value as -2.72 m^{-1} does not give satisfactory results.

The above results show that choosing an intermediate value which equals to half of the biggest β value allowed as long as the K^* curve is still monotonic for the transformation parameter in TUR1 method is a reasonable choice to produce near optimal results.

3.3.8 Performance of TUR1 versus TUR0 and TUR2

In previous studies, a new approach TUR1, which combines the RFT transformation method with the UR1 under-relaxation technique, is shown to outperform the original UR1 and UR2 methods without transformation. Obviously, the transformation in TUR1 improves the performance of original UR1 method dramatically. While it is interesting to ask whether the UR1 under-relaxation in TUR1 method is a necessity. Does the UR1 under-relaxation technique also improve the performance of the original transformation method? Thus, in this section, the performance of TUR1 method is examined versus the original transformation method alone without any under-relaxation (TUR0) or combined with the UR2 under-relaxation technique (TUR2). The effect of the UR1 under-relaxation then can be demonstrated.

A performance comparison among TUR1, TUR0 and TUR2 for four combinations of element size and corresponding oscillation-free time-step is shown in Table 3.4 for Case A example. Note that two transformation parameter values are adopted, which include the proposed value in this study (β = -1.4 m^{-1}), and the previous recommendation (β = -2.72 m^{-1}) by Pan and Wierenga (1995).

It can be seen that the transformation method alone without any under-relaxation (TUR0) does not guarantee an efficient solution. It fails to get a stable solution for most cases. Even when it gets a stable solution with a dense mesh and a small time-step, it is much less accurate than the TUR1 method. When the transformation method is combined with the UR2 under-relaxation technique (TUR2), the convergence becomes even worse. Much more iterations are needed

to complete the calculation. It also shows that the inefficiency of TUR0 and TUR2 methods is not because inappropriate transformation parameter value is adopted. Actually, the performances of TUR0 and TUR2 are almost the same with these two recommended β values.

The studies above show that the UR1 under-relaxation technique is a necessary part to assure the efficiency of the TUR1 combination approach. It dramatically improves the convergence ability of the original transformation method.

3.3.9 More Difficult Type of Soil

In this section, a different soil (Case B) with steeper soil-water characteristic curve and hydraulic conductivity curve is studied. The more severe nonlinearity of hydraulic properties combined with the extreme initial conditions make it a much more difficult problem to be solved, although the material type is not uncommon. To get the correct solution, very dense mesh and time-step must be used. Figure 3.23 shows the comparison between a dense grid mesh solution (element size of 0.00005 m and time-step size of 4.428 s) with the generalized solution of Warrick et al. (1985) for three different pressure heads. A close agreement is observed between this dense mesh finite element solution and Warrick et al.'s (1985) generalized semi-analytical solution. Therefore, this converged solution generated by HFE, with an element size of 0.00005 m and a corresponding time-step of 4.428 s, can be assumed correct.

3.3.9.1 With the Application of Minimum Time-step Criteria

For a elapsed time of 88560 s, the maximum element size that can be used is 0.005 m under the minimum time-step criteria. A performance comparison among UR1, UR2 and TUR1 for four combinations of element size and corresponding oscillation-free time-step is shown in Table 3.6. It can be seen that, for coarser material soil with more nonlinear hydraulic properties, UR2 needs a more refined time-step and corresponding element size to generate stable and oscillation-free solutions. TUR1 can get such a solution with a coarser mesh and a bigger time-step. UR1 can produce stable solutions for all cases, but large errors are found except when very small element size and time-steps are adopted. It is also noteworthy that TUR1 would also break down when the soil hydraulic property curves are steep (such as Case B soil) and relatively large time-step is used.

3.3.9.2 With the Application of Lumped Mass Scheme

In practice, the element size that engineers used in their simulations cannot be very small. For example, for a 2D infiltration problem of 10 m $\times$ 10 m, if quadrilateral elements with element size of 0.01 m $\times$ 0.01 m is used, then there will be one million elements in total. This is an exceptionally large number of elements which is impractical for most practical analysis. For a reasonable element size of 0.1 m, Table 3.5 shows that the minimum time-step to generate oscillation-free solutions is 17712000 s, which is obviously too big to use. Indeed, the resolution should be small enough to capture variations in hourly or daily rainfalls. Thus, the minimum time-step criteria is not applicable any more. The lumped mass scheme will be

used to control the oscillation instead.

In the following studies, a practical element size of 0.1 m is used. Table 3.7 shows the convergence of solutions with refinement in time-step with fixed element size of 0.1 m. It is showed that for a relatively coarse mesh, even with very small time-step, large errors are still observed in the results of UR1 and UR2. On the other hand, TUR1 can get a solution with an error of less than 10% with a large time-step size of 3542.4 s (approximately 1 hour resolution).

The above results show that when a relatively coarse mesh is used in practical simulations, TUR1 is still better than UR1 and UR2. It can use bigger time-steps to get "acceptable" results with a reasonable element size. Considering large 2D and 3D problems involving matrices with significant bandwidth, the run time for each time-step will be very long. Bigger time-step size means less number of time-step needed, thus, less computation time. Several 2D examples are discussed in Chapter 5.

3.4 Concluding Remarks

In this chapter, a combination approach of RFT transformation method (Pan and Wierenga, 1995) and a typical under-relaxation technique was applied to solve the finite element formulation of the h-based form of Richards equation. A detailed investigation was then implemented to look into its effect on the slow convergence problems. In addition, the minimum time-step criterion presented by Karthikeyan et al. (2001) or the lumped-mass formulation was applied to suppress oscillations so that the convergence issue can be studied without being encumbered by extraneous

complications.

Comparison of this proposed combination approach (TUR1) and two under-relaxation techniques without transformation (UR1 and UR2) were carried out. From the aspect of convergence to a correct solution with progressive refinement of the element size and time-step, numerical results showed the superiority of TUR1 over UR1 and UR2. UR1 is able to reach a stable solution very rapidly in each time-step, but requires significantly more refinement of the time-step to arrive at a solution of acceptable accuracy. At the same time, to suppress oscillation, element size needs to be correspondingly reduced, thus imposing even greater demands on computational resources. Adopting UR2 would mean that a large time-step which permits a much coarser mesh under the Thomas and Zhou (1997) criterion for oscillation control can produce reasonably accurate results, but at a price that within each time-step, much more iterations are needed and even diverges instead of converging to a stable solution when dealing with soils with highly nonlinear hydraulic properties. On the other hand, TUR1 has the advantages of both UR1 and UR2. Firstly, like UR2, TUR1 can use larger time-steps to produce acceptable results and thus corresponding coarser meshes to suppress oscillation. Secondly, like UR1, TUR1 converges to a stable solution quickly in each time-step. Above all, TUR1 appears superior than UR1 and UR2 in the sense that a more realistic solution can be obtained using a practically reasonable spatial and temporal discretization eventually.

The transformation methods often involve arbitrary parameters. A robust approach that does not resort to time-consuming trial and error "tuning" runs and does not compromise the efficiency significantly is of practical importance.

In this new approach TUR1, only one *ad-hoc* parameter is introduced. Pan and Wierenga (1995) recommended a practical way to choose this parameter value in RFT transform. But they did not explore it in detail. Williams et al. (2000) showed that the optimal transform parameters depend upon media properties, boundary conditions and spatial and temporal discretization. For the proposed combination method, numerical studies showed that choosing an intermediate value which equals to half of the biggest β value allowed as long as the K^* curve is still monotonic for the transformation parameter in TUR1 method is a reasonable choice to produce near optimal results.

This study also showed that the minimum time-step criteria can be applied to the transformed flow equation by using the original λ and K to curb the oscillations. However, when steep soil parameter curves are encountered, the minimum oscillation-free time-step is sometimes too large in comparison to hourly or daily varieties in rainfall intensity.

In conclusion, the proposed TUR1 method appears to be a more practical choice than existing methods, because it can produce accurate solutions at reasonable computing cost; only one *ad-hoc* parameter is introduced and a robust recommendation on the choice of such parameter value is given; and finally it is workable for difficult problems with highly nonlinear soil hydraulic parameters.

Table 3.1: Minimum time-step sizes for different types of elements (Karthikeyan et al., 2001)

Oscillation	One-dimensional element		Two-dimensional element	
Type	2-noded	3-noded	4-noded	8-noded
Type 1	$\Delta t \geq L^2\lambda/6K$	$\Delta t \geq L^2\lambda/40K$	$\Delta t \geq L^2\lambda/2K$	$\Delta t \geq L^2\lambda/40K$
Type 2	-	$\Delta t \geq L^2\lambda/20K$	-	$\Delta t \geq L^2\lambda/20K$

where Δt = time-step size;

λ = specific moisture capacity function, m^{-1};

K = hydraulic conductivity, ms^{-1}; and

L = element length or width perpendicular to the direction of flow.

Table 3.2: One-dimensional test problems

Variable			Case A	Case B
Medium Properties	θ_r		0.186	0.20
	θ_s		0.363	0.58
	a	m^{-1}	1.000	8.000
	n		1.53	1.412
	K_s	ms^{-1}	1.0×10^{-6}	1.1574×10^{-6}
Initial Conditions	$h(z, t = 0)$	m	-8	-8
Boundary Conditions	$h(z = 1, t)$	m	0	0
	$h(z = 0, t)$	m	-8	-8

Table 3.3: Minimum time-step size for different element sizes of Case A

Element Size (m)	Minimum Time-step (s)
0.1	55200
0.05	13800
0.025	3450
0.01	552
0.005	138
0.0025	34.50

Table 3.4: Comparison of efficiency between the proposed TUR1 method and the transformation method without under-relaxation (TUR0) and with UR2 under-relaxation (TUR2) under the minimum time-step criterion

Approaches	Element Size (m)	Time Step (s)	$\beta = -1.4$		$\beta = -2.72$	
			L_2 Error (m)	Total Iterations	L_2 Error (m)	Total Iterations
TUR1	0.1	55200	1.874	14		
	0.05	13800	0.577	55		
	0.025	3450	0.247	123		
	0.01	552	0.068	463		
TUR0	0.1	55200	-	Fail	4.075	28
	0.05	13800	-	Fail	-	Fail
	0.025	3450	-	Fail	-	Fail
	0.01	552	1.806	642	1.998	655
TUR2	0.1	55200	4.086	18	4.075	39
	0.05	13800	-	Fail	-	Fail
	0.025	3450	-	Fail	-	Fail
	0.01	552	1.801	918	1.991	951

Notes: "Fail" means "does not converge in 1000 iterations".

Table 3.5: Minimum time-step size for different element sizes of Case B

Element size (m)	Minimum Time-step (s)
0.1	17712000
0.05	4428000
0.025	1107000
0.01	177120
0.005	44280
0.0025	11070
0.001	1771.2
0.0005	442.8
0.0002	70.848

Table 3.6: Convergence of the solution with refinement in mesh size and time-step satisfying Thomas and Zhou's (1997) criterion of Case B (elapsed time 88560 s)

Approaches	Element size (m)	Time-step (s)	Normalized elevation of $h = -6$ m	L_2 error (m)	Runtime (s)
UR1	0.005	44280	1.481	4.56	0.1
	0.001	1771.2	1.418	4.26	10
	0.0005	442.8	1.338	3.85	75
	0.0002	70.848	1.095	2.11	1188
UR2	0.005	44280	-	-	Fail
	0.001	1771.2	-	-	Fail
	0.0005	442.8	-	-	Fail
	0.0002	70.848	1.011	0.75	2640
TUR1	0.005	44280	-	-	Fail
	0.001	1771.2	-	-	Fail
	0.0005	442.8	0.845	0.77	212
	0.0002	70.848	0.983	0.61	1975

Notes: "Fail" means "does not converge in 1000 iterations".

Table 3.7: Convergence of the solution with refinement in time-step with fixed element size of 0.1 m of Case B (elapsed time 88560 s)

Approaches	Time-step (s)	Number of Time-steps	Normalized elevation of $h = -6$ m	L_2 error (m)
UR1	88560	1	1.42	4.76
	44280	2	1.41	4.50
	17712	5	1.40	4.33
	8856	10	1.40	4.27
	3542.4	25	1.39	4.24
	1771.2	50	1.39	4.23
	885.6	100	1.39	4.22
	354.24	250	1.39	4.22
	141.696	625	1.39	4.22
	70.848	1250	1.39	4.22
UR2	88560	1	-	Fail
	44280	2	1.38	4.10
	17712	5	1.39	4.18
	8856	10	1.39	4.20
	3542.4	25	1.39	4.21
	1771.2	50	1.39	4.22
	885.6	100	1.39	4.22
	354.24	250	1.39	4.22
	141.696	625	1.39	4.21
	70.848	1250	1.39	4.21
TUR1	88560	1	1.39	3.85
	44280	2	1.24	3.00
	17712	5	1.24	2.87
	8856	10	1.10	2.48
	3542.4	25	1.09	2.55
	1771.2	50	1.09	2.58
	885.6	100	1.09	2.60
	354.24	250	1.09	2.60
	141.696	625	1.09	2.61
	70.848	1250	1.09	2.61

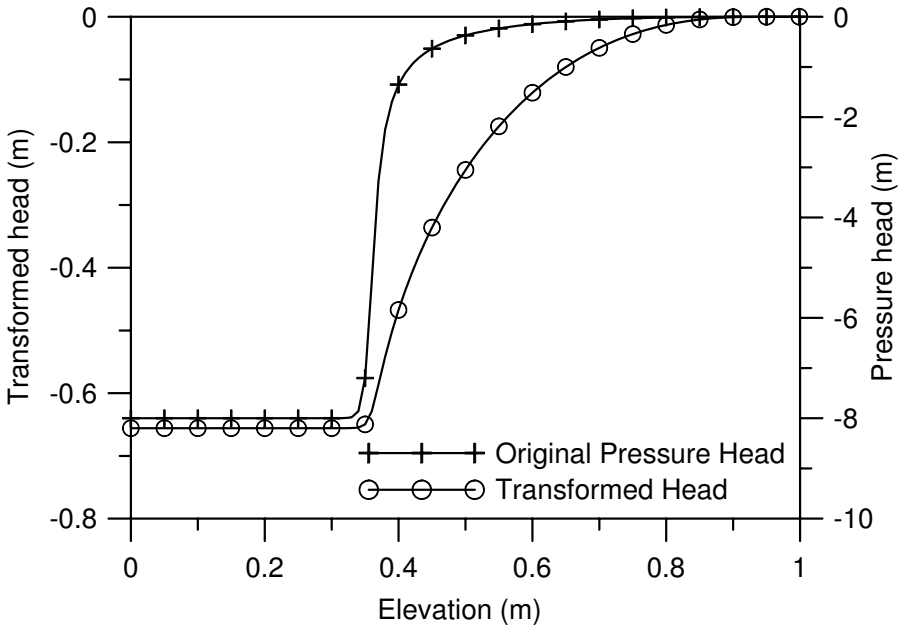

Figure 3.1: Spatial linearization by transformation ($t = 50000$ s)

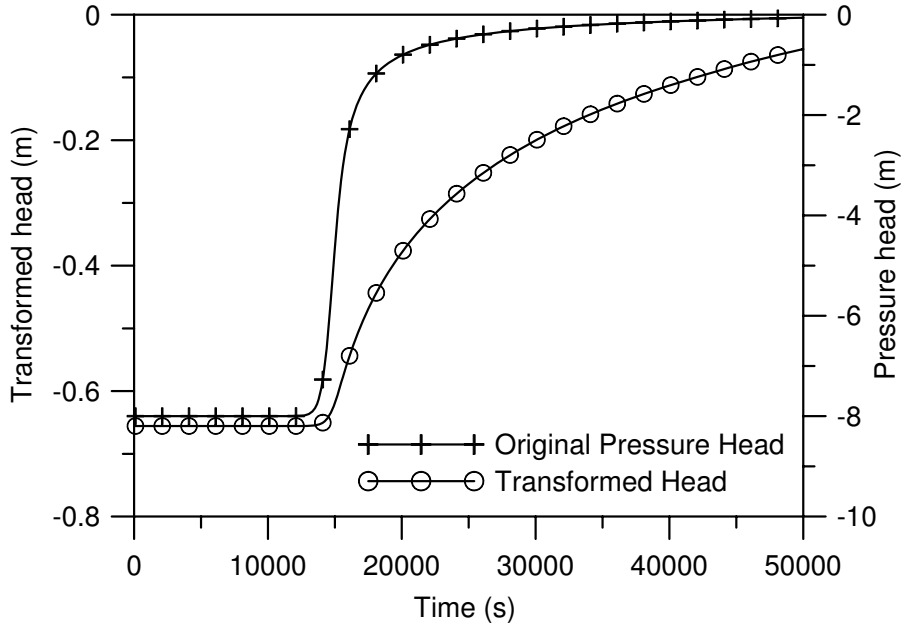

Figure 3.2: Temporal linearization by transformation ($z = 0.7$ m)

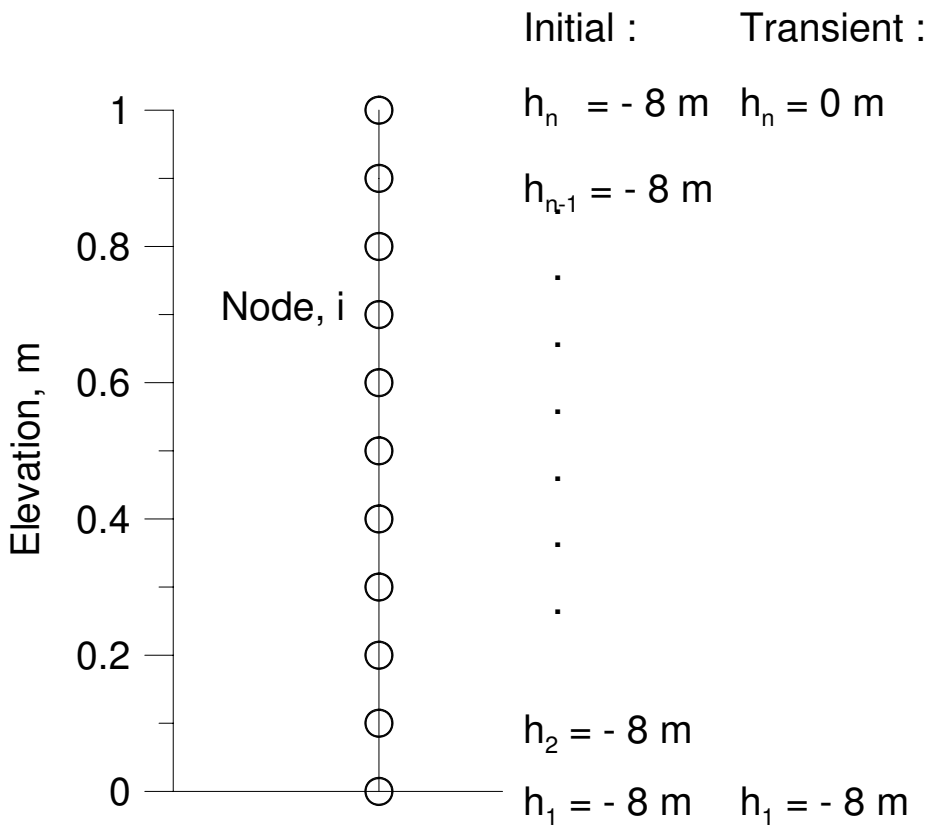

Figure 3.3: One-dimensional infiltration problem

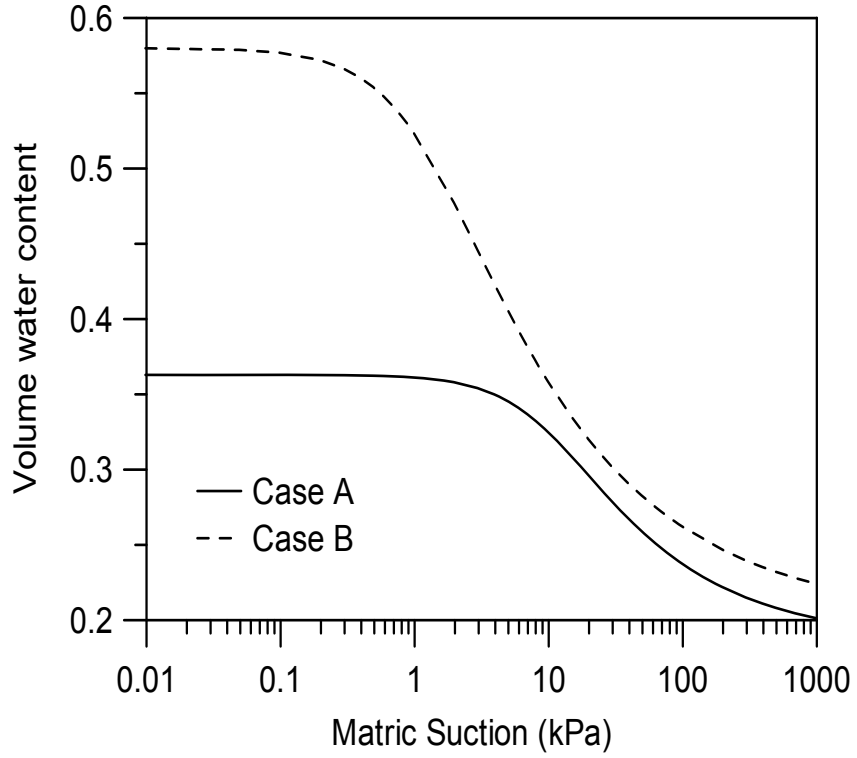

Figure 3.4: Soil-water characteristic curve

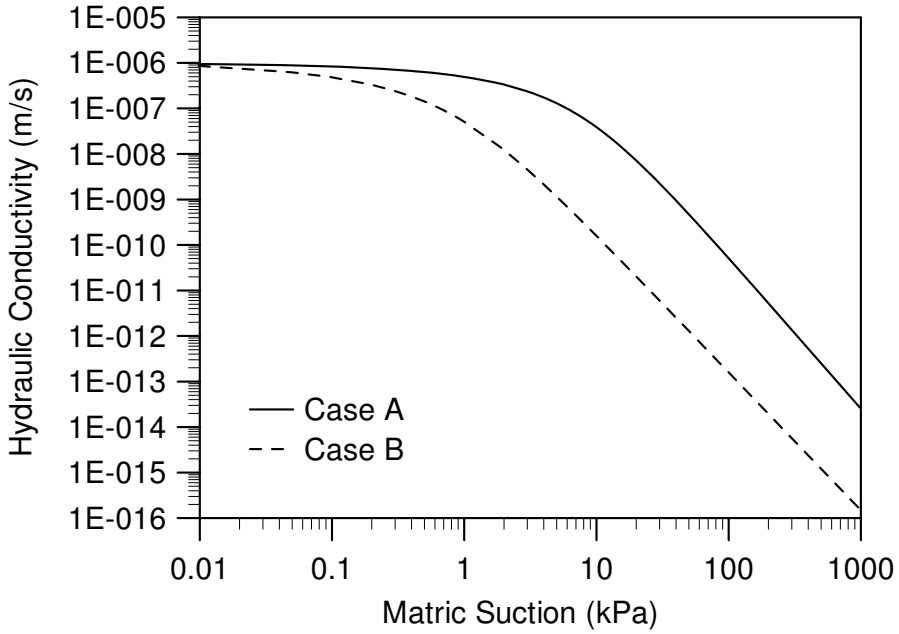

Figure 3.5: Conductivity function

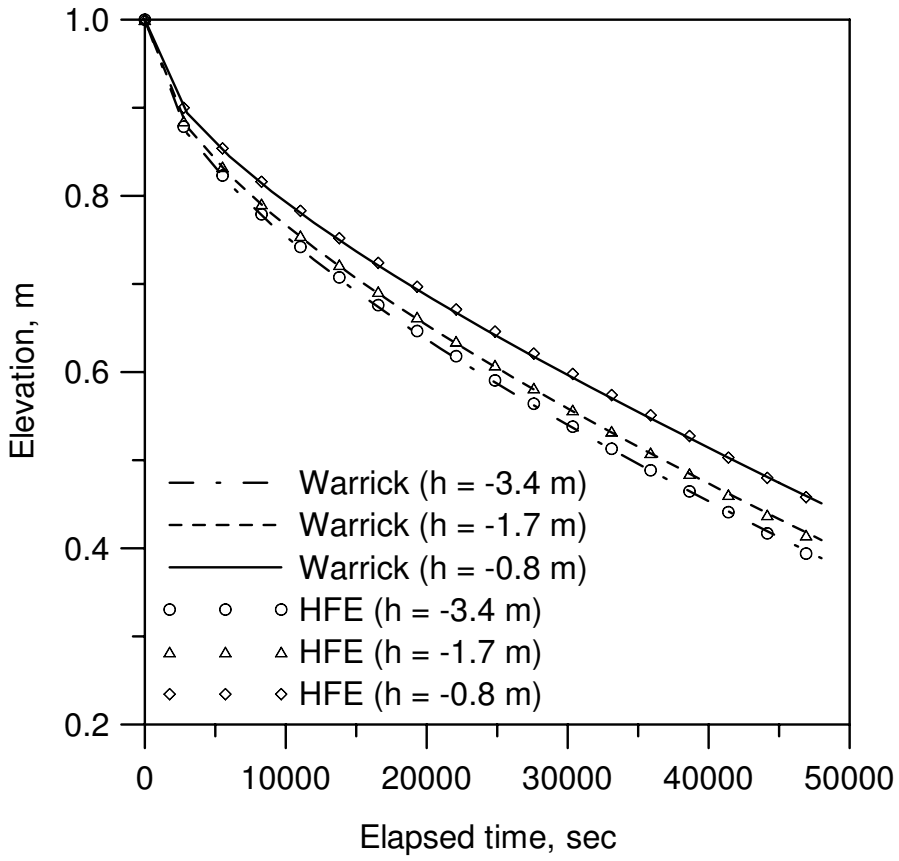

Figure 3.6: Comparison between dense grid HFE solution (element size = 0.001 m, time-step = 5.52 s) and Warrick et al.'s (1985) solution for Case A

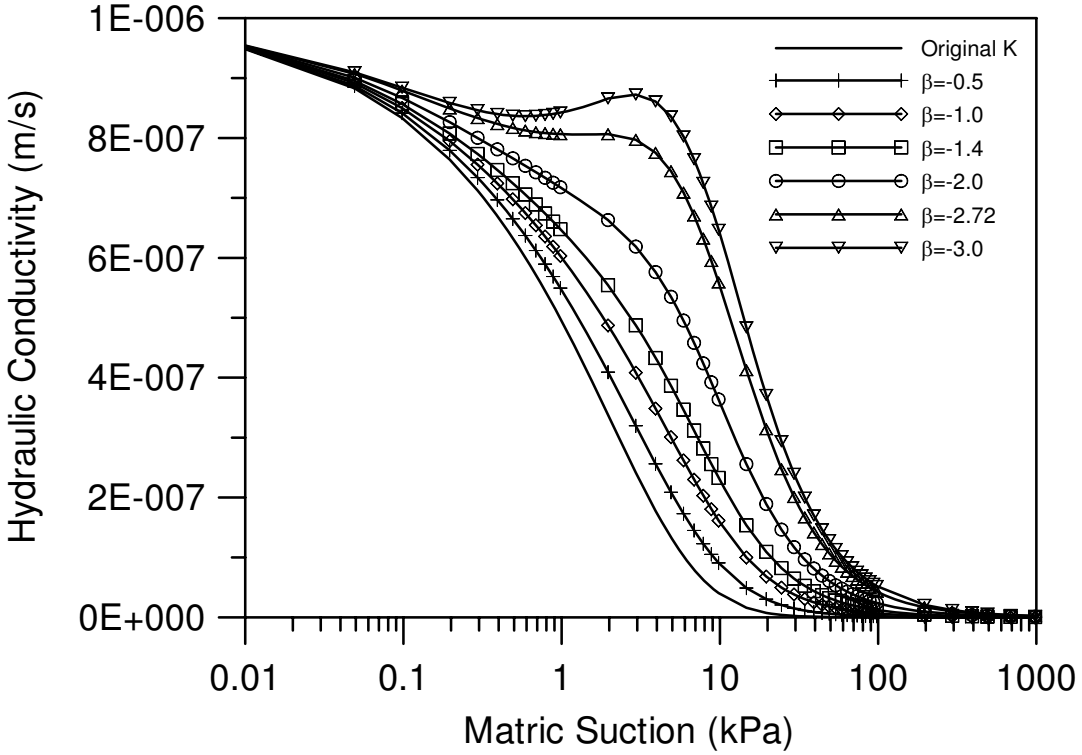

Figure 3.7: K^* function of Case A

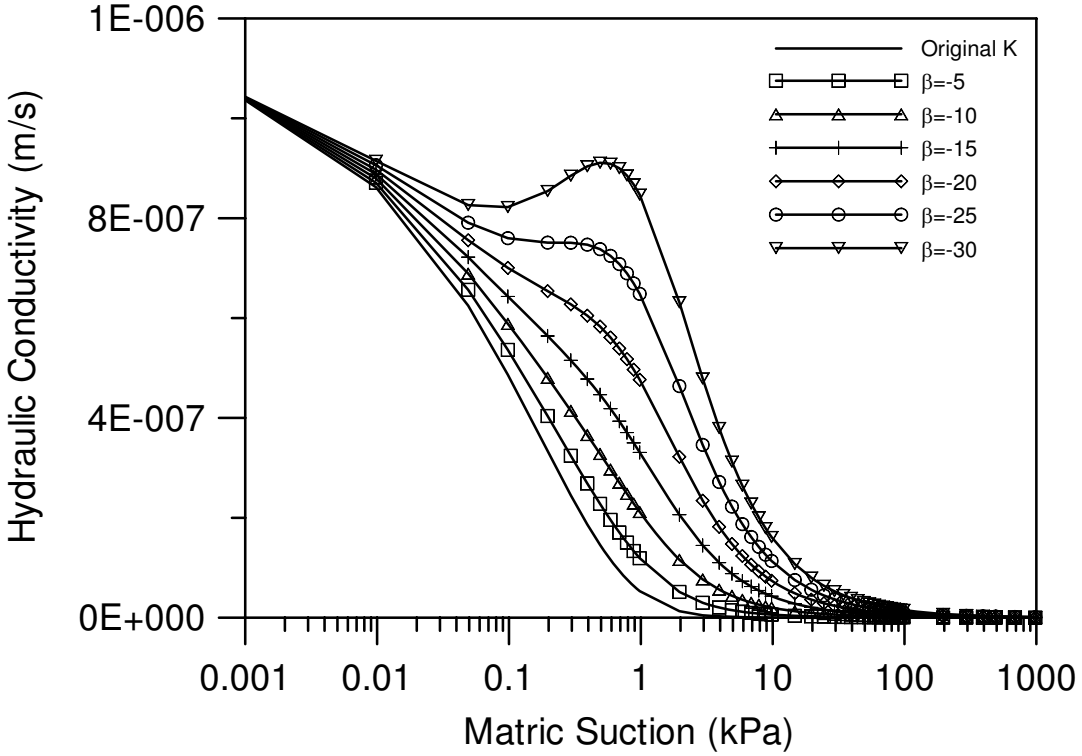

Figure 3.8: K^* function of Case B

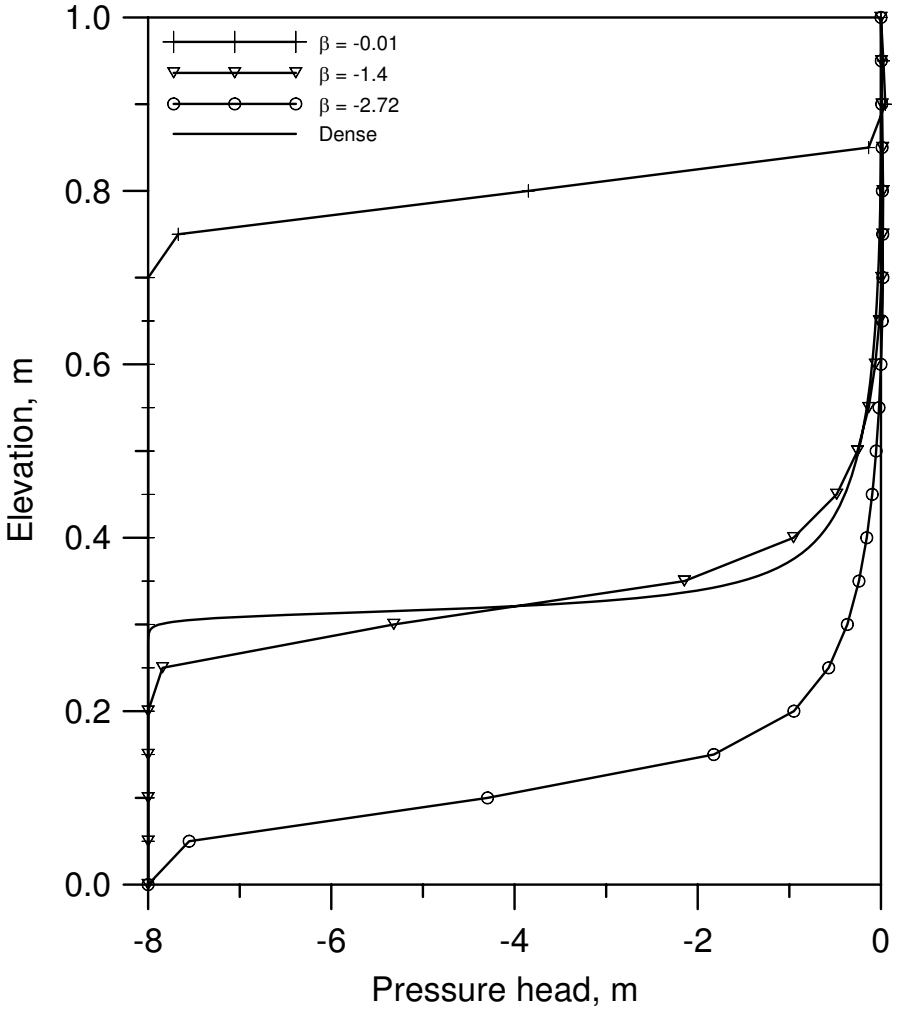

Figure 3.9: Variation of the pressure head with elevation of Case A from TUR1 for different β when time-step of 13800 s and element size of 0.05 m (elapsed time 55200 s)

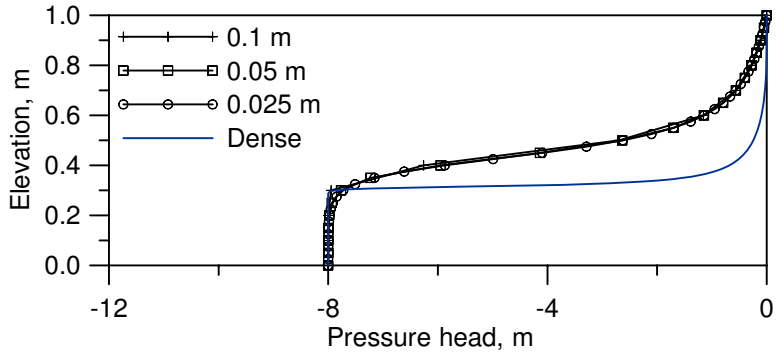

(a) Time-step size = 55200 s

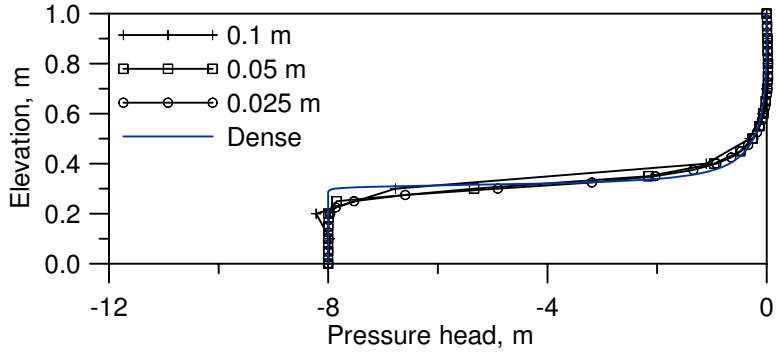

(b) Time-step size = 13800 s

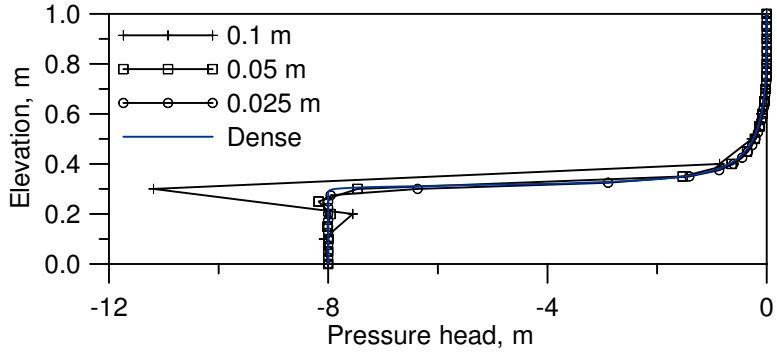

(c) Time-step size = 3450 s

Figure 3.10: Variation of pressure head with elevation at time = 55200 s for different element sizes at time-step sizes of (a) 55200 s, (b) 13800 s, (c) 3450 s

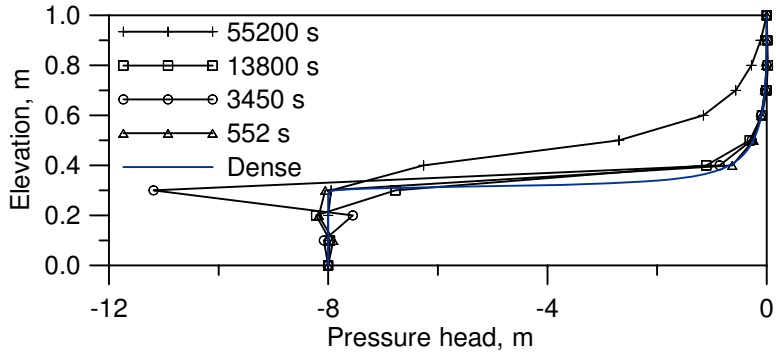

(a) Element size = 0.1 m

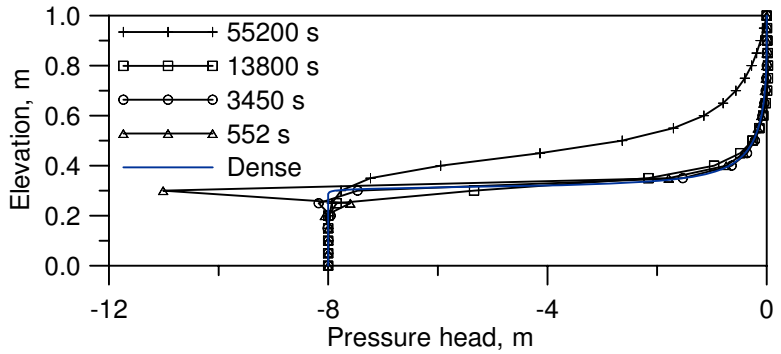

(b) Element size = 0.05 m

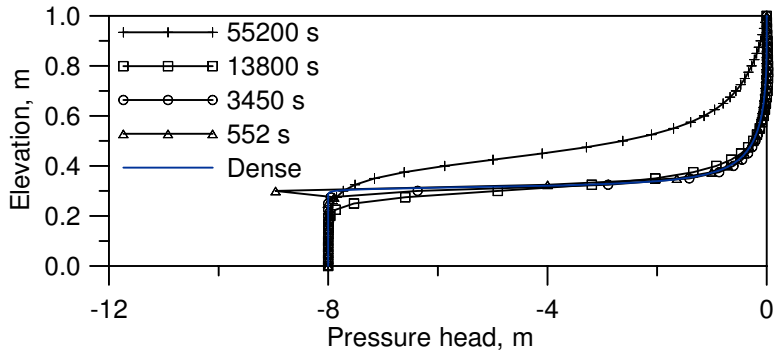

(c) Element size = 0.025 m

Figure 3.11: Variation of pressure head with elevation at time = 55200 s for different time-step sizes at element sizes of (a) 0.1 m, (b) 0.05 m, (c) 0.025 m

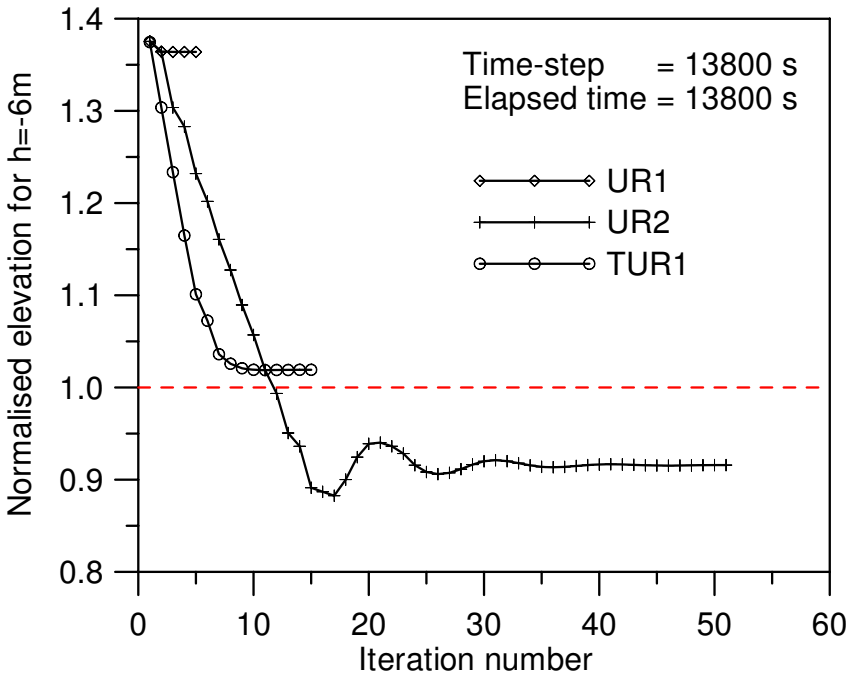

(a) Elapsed time = 13800 s

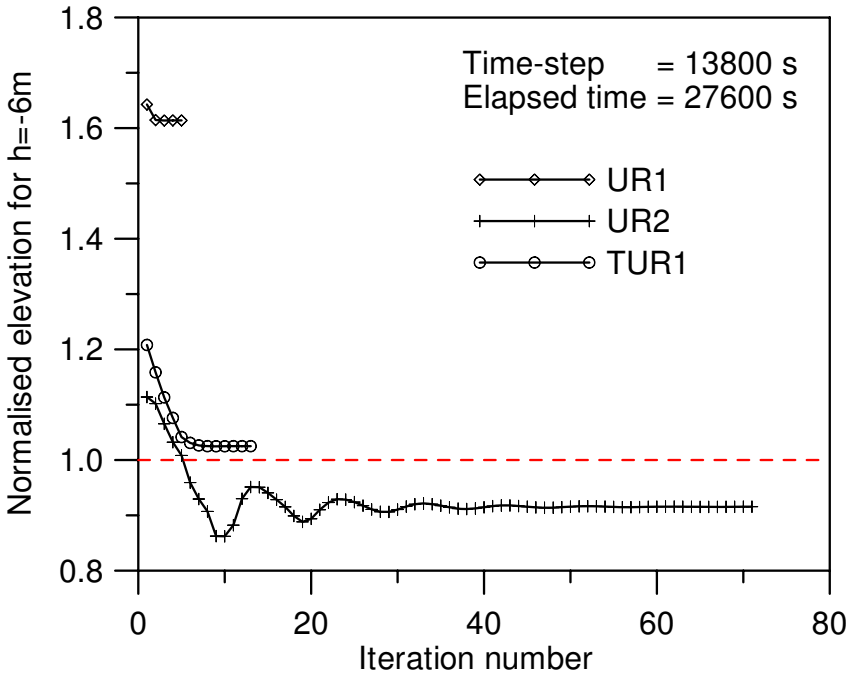

(b) Elapsed time = 27600 s

Figure 3.12: Convergence of the solution within a time-step at different elapse times

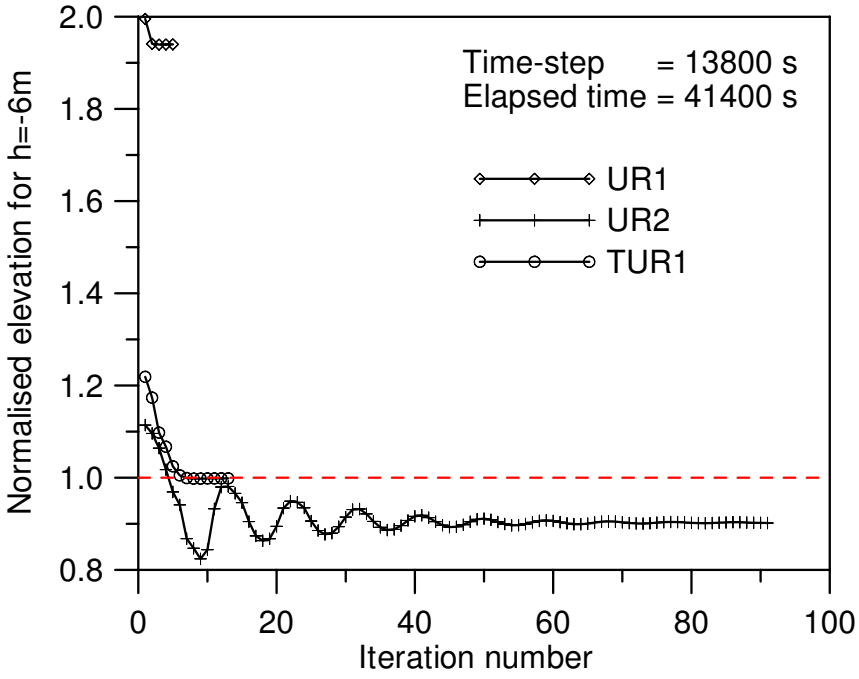

(c) Elapsed time = 41400 s

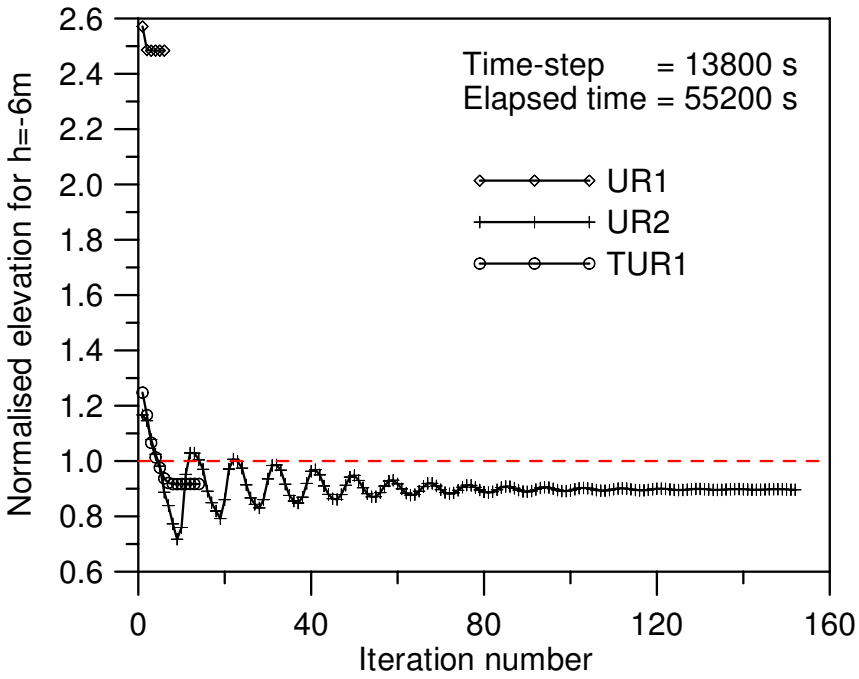

(d) Elapsed time = 55200 s

Figure 3.12: Convergence of the solution within a time-step at different elapse times (Cont'd)

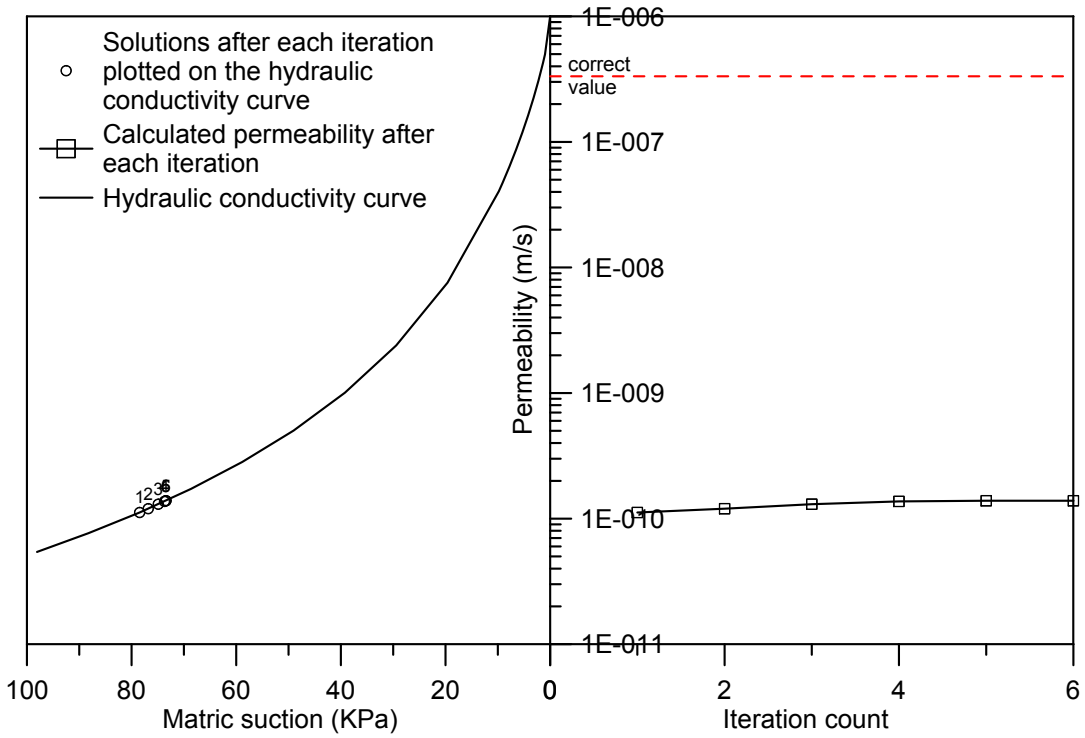

(a) UR1

Figure 3.13: Convergence of the solution for a gauss point near the wetting front plotted on the hydraulic conductivity curve

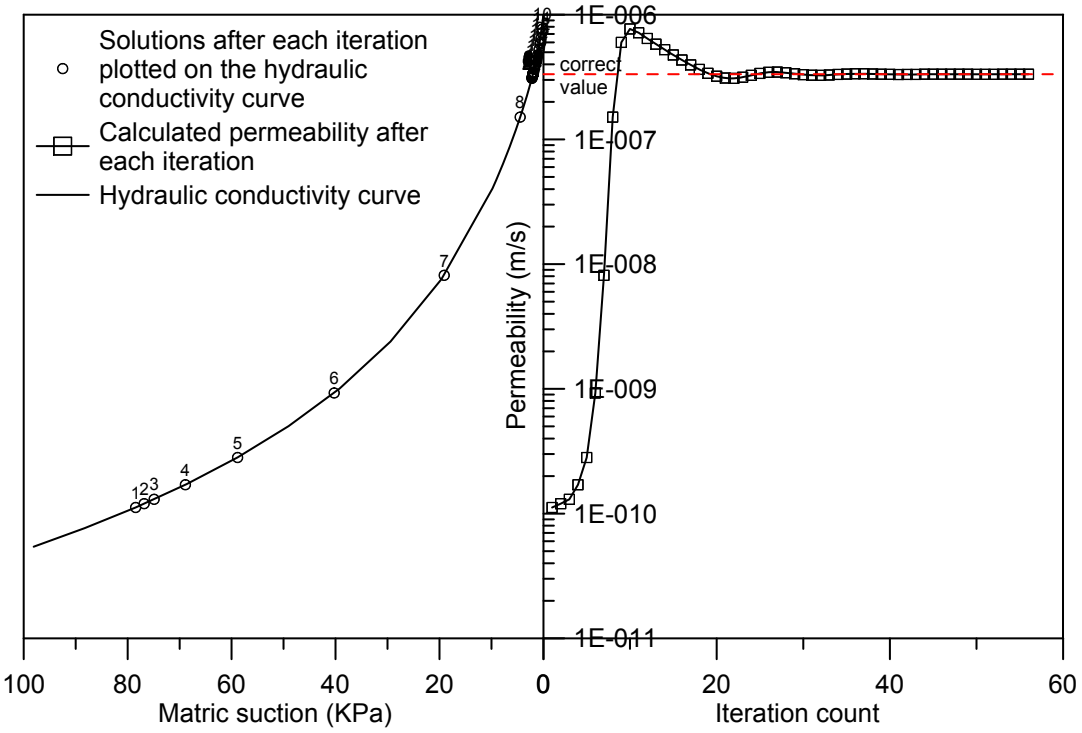

(b) UR2

Figure 3.13: Convergence of the solution for a gauss point near the wetting front plotted on the hydraulic conductivity curve (Cont'd)

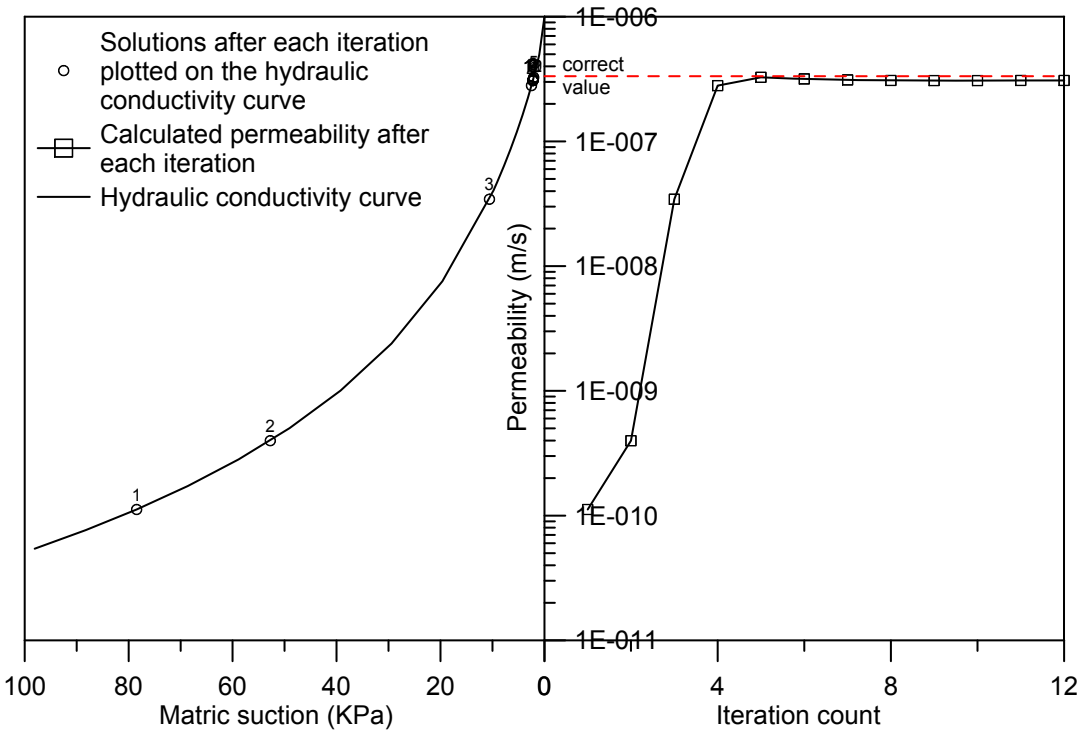

(c) TUR1

Figure 3.13: Convergence of the solution for a gauss point near the wetting front plotted on the hydraulic conductivity curve (Cont'd)

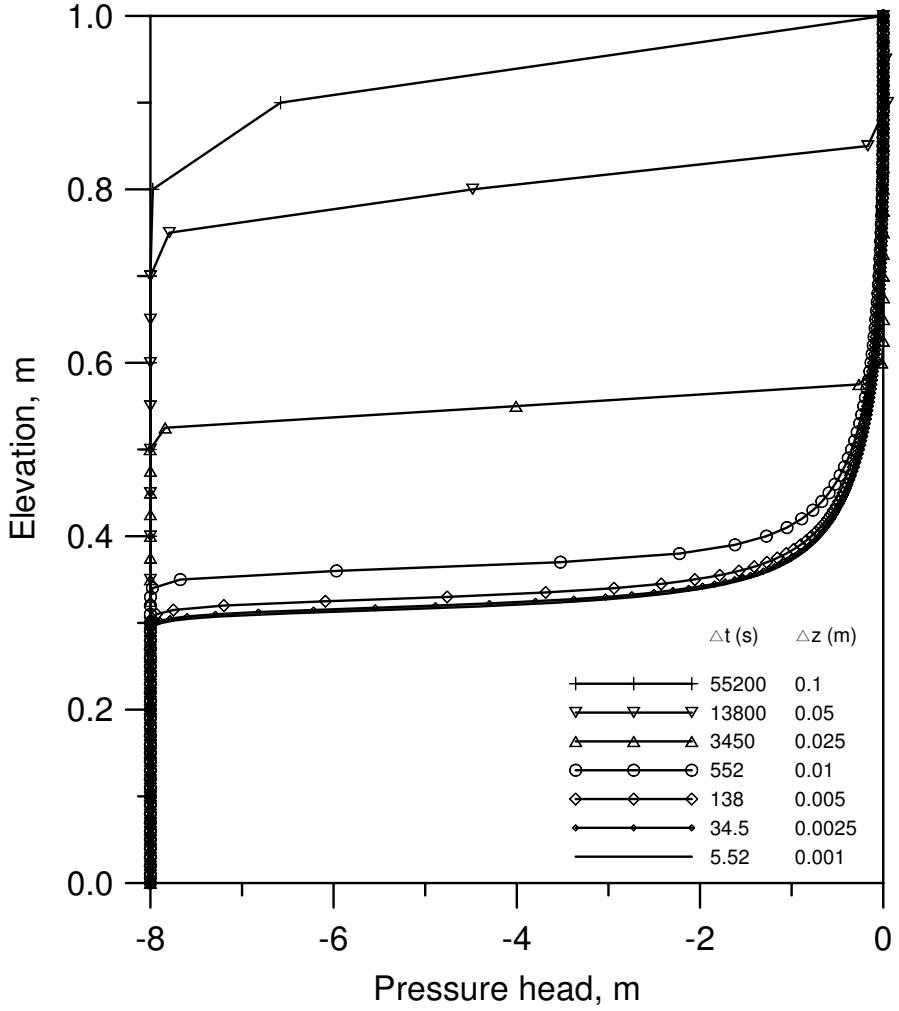

Figure 3.14: Variation of the pressure head with elevation from UR1 for nonoscillatory combinations of time-step and element size satisfying Thomas and Zhou's (1997) criterion (elapsed time 55200s)

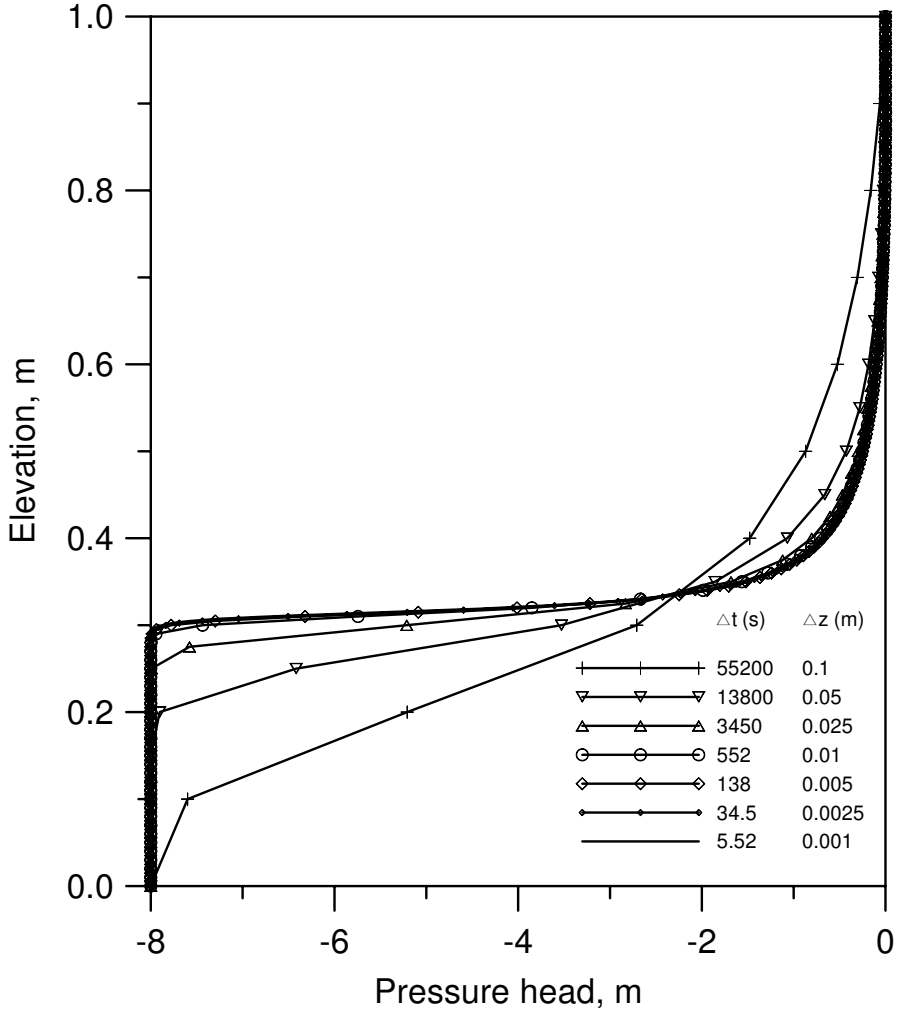

Figure 3.15: Variation of the pressure head with elevation from UR2 for nonoscillatory combinations of time-step and element size satisfying Thomas and Zhou's (1997) criterion (elapsed time 55200s)

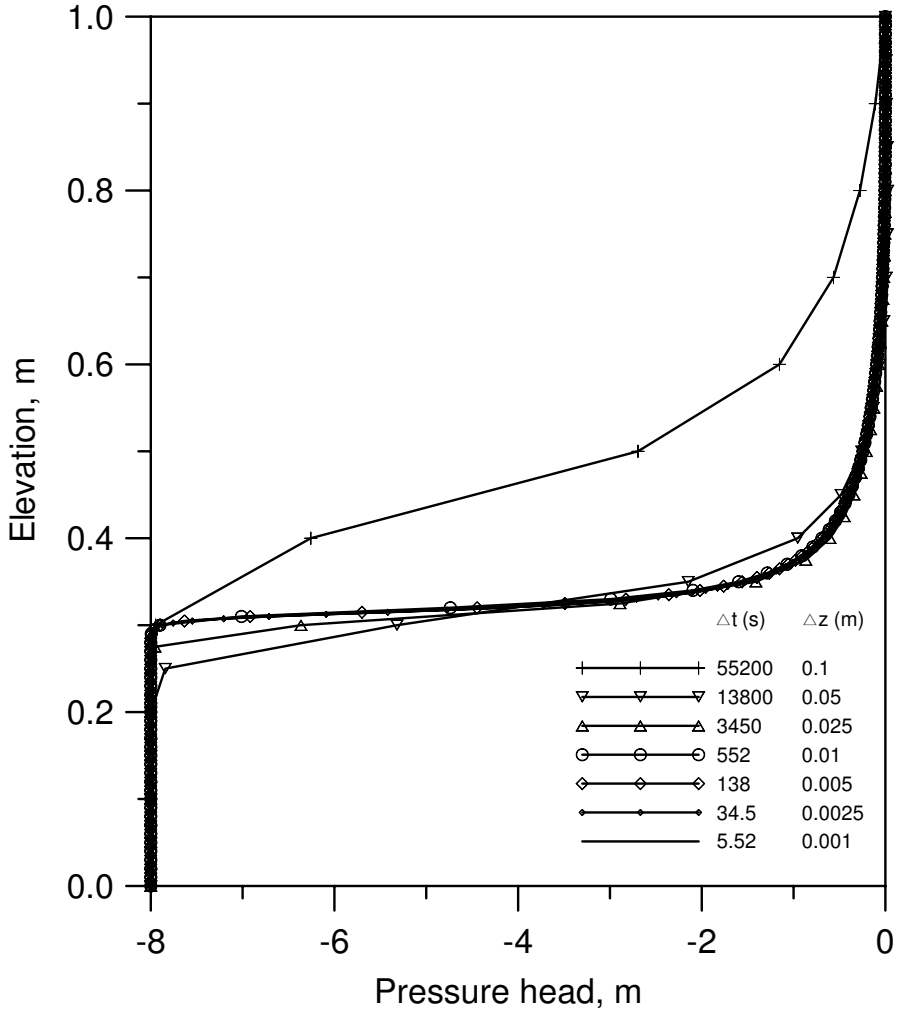

Figure 3.16: Variation of the pressure head with elevation from TUR1 for nonoscillatory combinations of time-step and element size satisfying Thomas and Zhou's (1997) criterion (elapsed time 55200s)

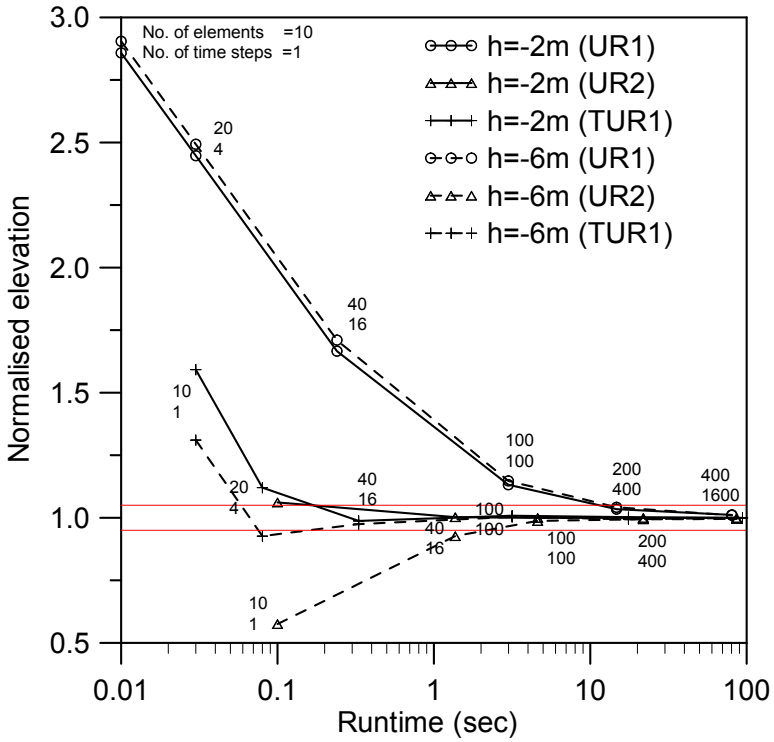

Figure 3.17: Convergence of the solution with refinement in mesh size and time-step satisfying Thomas and Zhou's (1997) criterion versus total run time

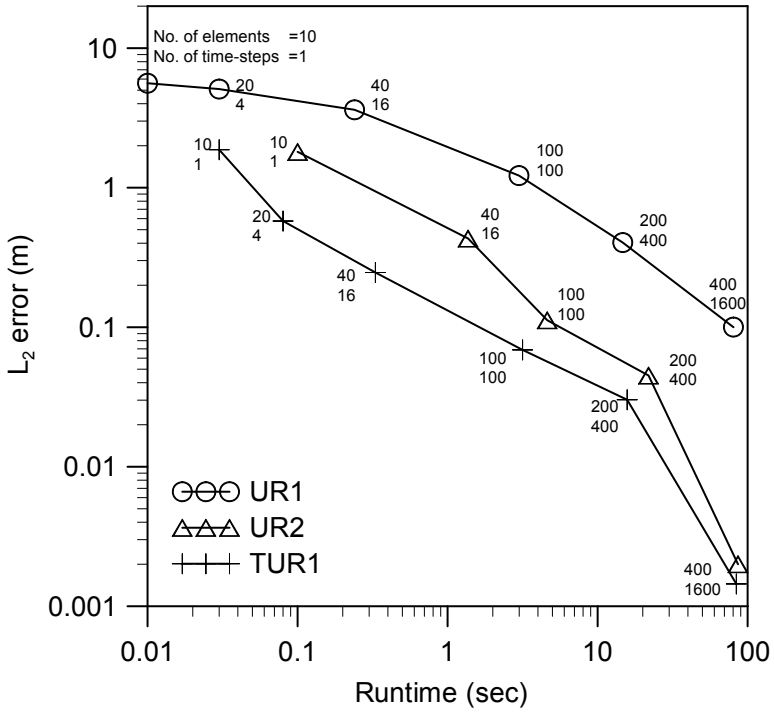

Figure 3.18: Convergence of the L_2 error of the solution with refinement in mesh size and time-step satisfying Thomas and Zhou's (1997) criterion versus total run time

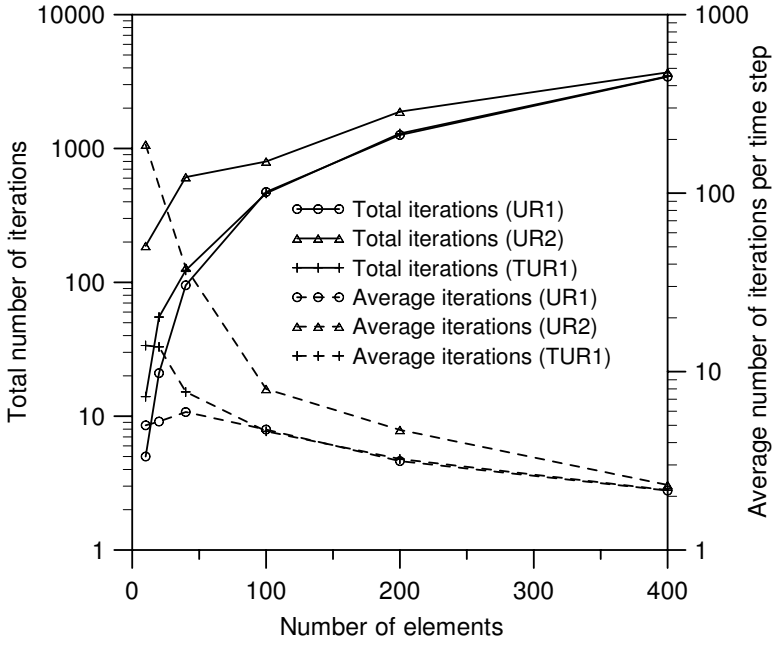

Figure 3.19: Total number of iterations and average number of iterations per time-step for various combination of element size and time-step

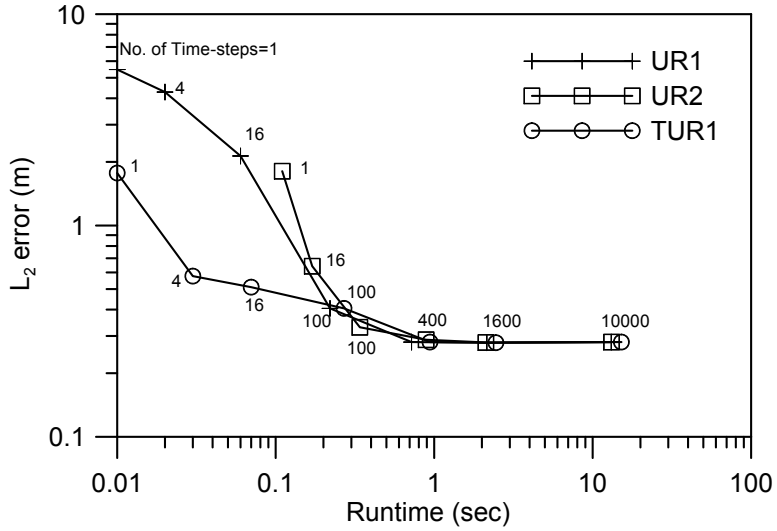

(a) Element size = 0.1 m

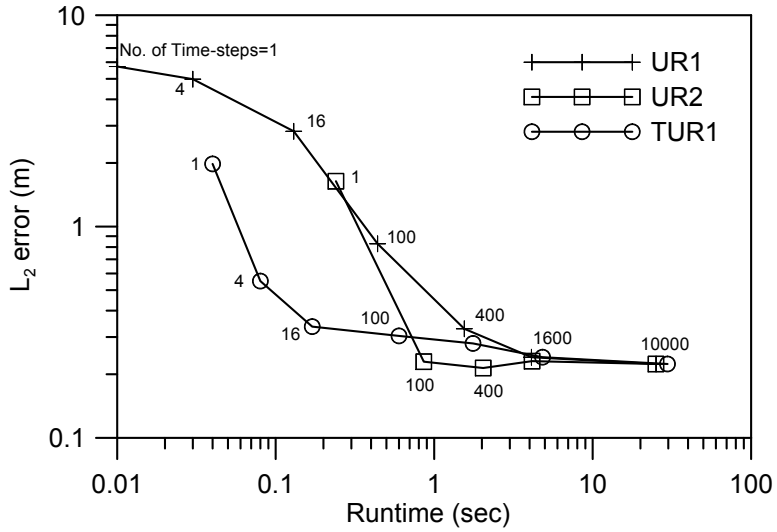

(b) Element size = 0.05 m

Figure 3.20: Convergence of the L_2 error of the solution with refinement in time-step for different element sizes with the application of lumped mass scheme

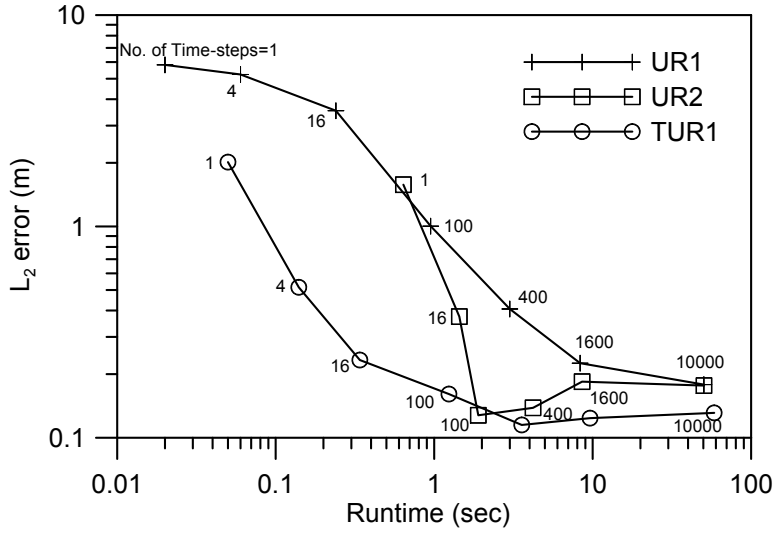

(c) Element size = 0.025 m

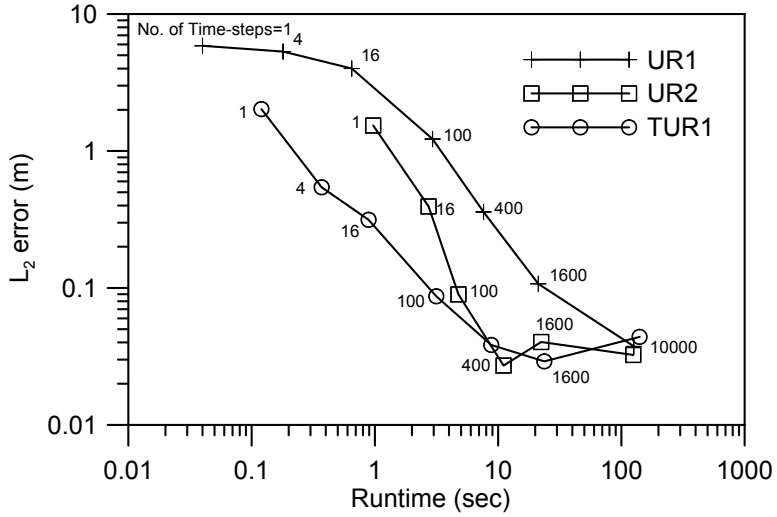

(d) Element size = 0.01 m

Figure 3.20: Convergence of the L_2 error of the solution with refinement in time-step for different element sizes with the application of lumped mass scheme (Cont'd)

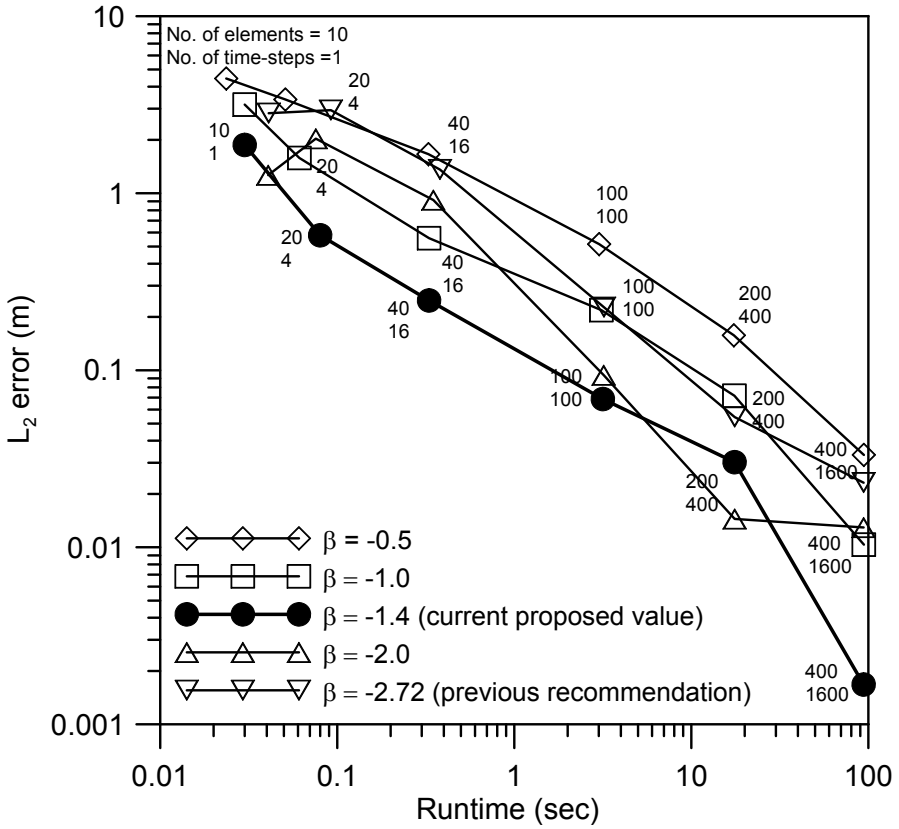

Figure 3.21: Convergence of the L_2 error of the solution with refinement in mesh size and time-step satisfying Thomas and Zhou's (1997) criterion versus total run time for different transformation parameter values

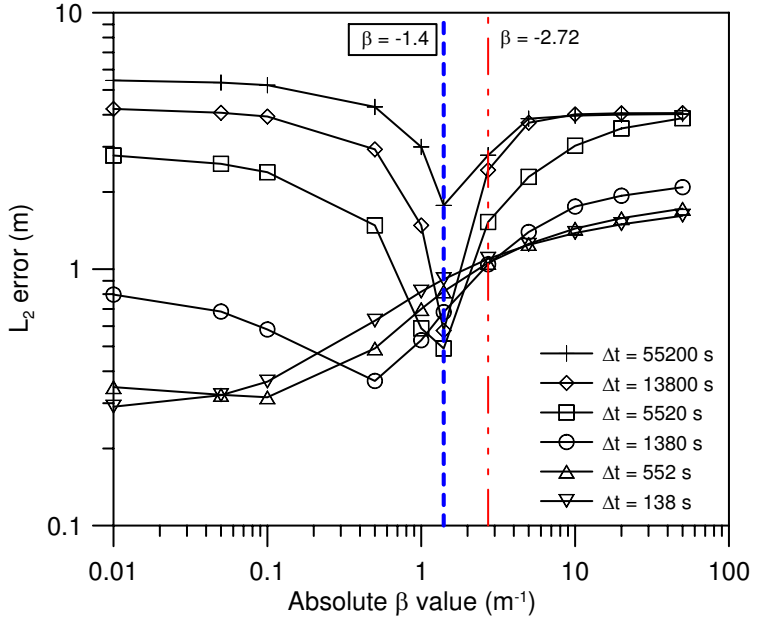

(a) Element size = 0.1 m

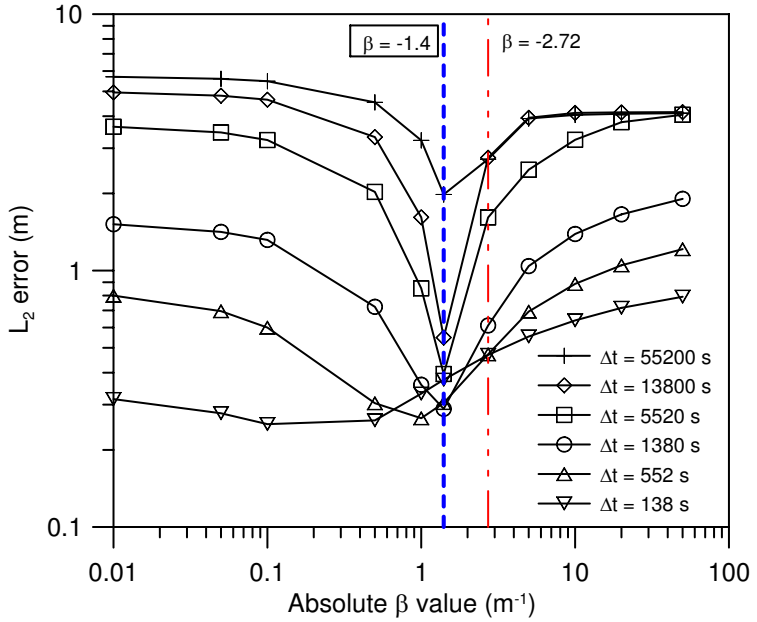

(b) Element size = 0.05 m

Figure 3.22: Effect of different transformation parameter values on the L_2 error of the solution with refinement in time-step for different element sizes

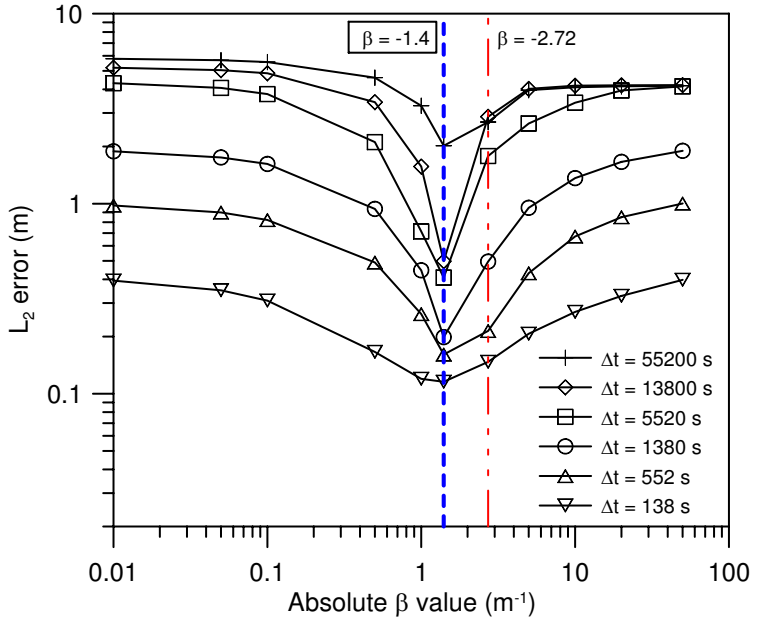

(c) Element size = 0.025 m

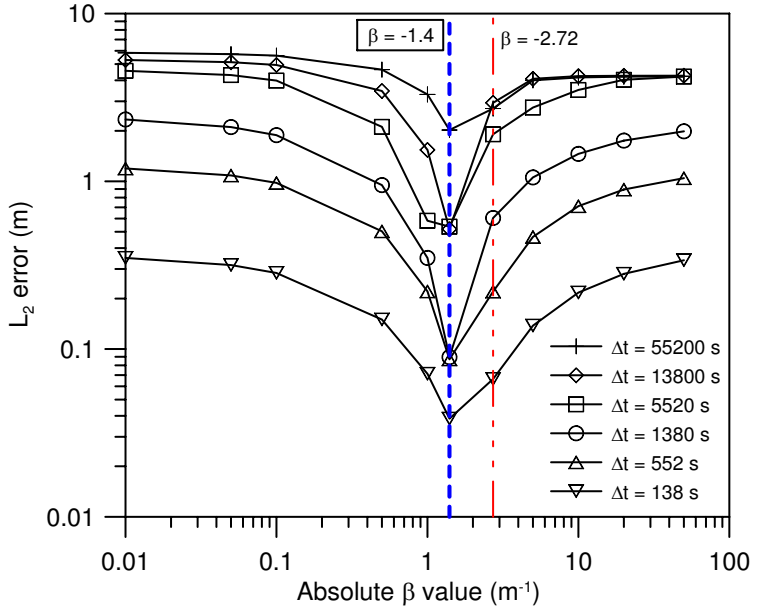

(d) Element size = 0.01 m

Figure 3.22: Effect of different transformation parameter values on the L_2 error of the solution with refinement in time-step for different element sizes (Cont'd)

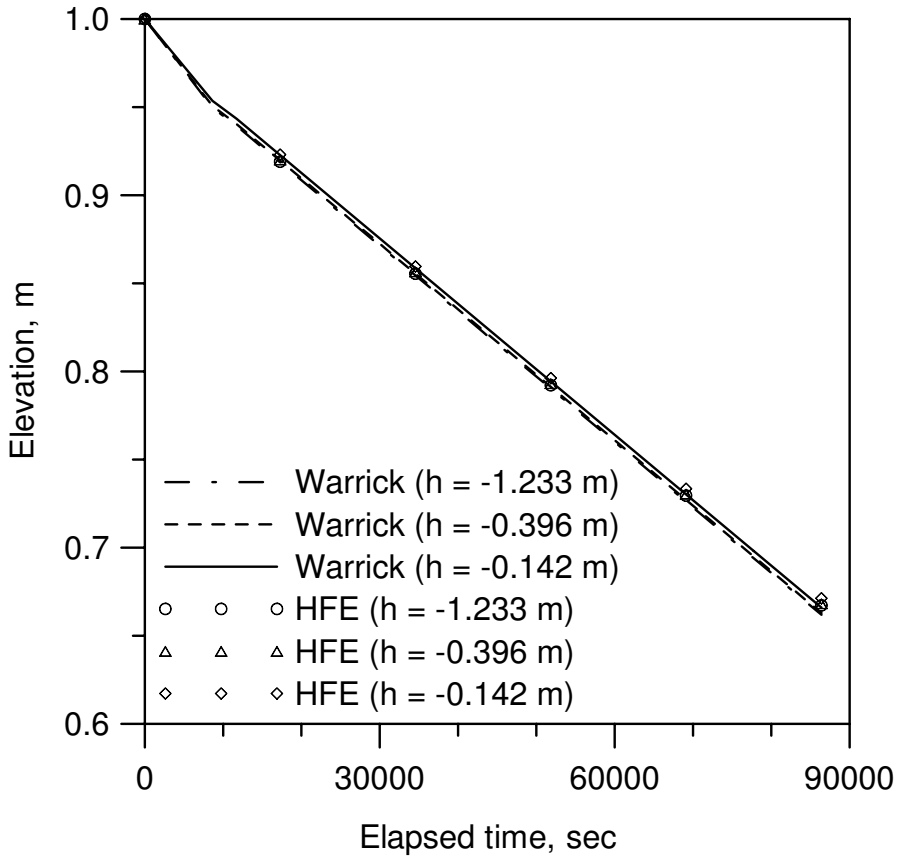

Figure 3.23: Comparison between dense grid HFE solution (element size = 0.00005 m, time-step = 4.428 s) and Warrick et al.'s (1985) solution for Case B

Chapter 4

Temporal Adaptive TUR1 Method

4.1 Introduction

In Chapter 3, a combination approach TUR1 of RFT transformation method (Pan and Wierenga, 1995) and a typical under-relaxation technique was applied to solve the finite element formulation of the h-based form of Richards equation for unsaturated flow analyses, where numerical difficulties such as slow convergence often exist because of the highly nonlinear soil hydraulic properties. In this approach, the inherent nonlinearity of the problem is reduced through application of the transformation on the dependent variable, thus the big error usually appearing in the original UR1 approach is dramatically alleviated, while the advantage of UR1 approach that it can converge to a stable solution very quickly in each time-step is retained. Numerical studies on several examples have demonstrated that TUR1 can use larger time-steps to produce acceptable results and also converge to a stable solution quickly in each time-step. The practical bottomline is that TUR1 can achieve a more accurate solution than UR1 and UR2 more quickly using a practically reasonable spatial and temporal discretization eventually.

However, numerical studies on TUR1 in Chapter 3 are based upon a fixed time-step method. In view of recent developments on temporal adaptive methods, especially the most recent automatic time stepping scheme developed by Kavetski et al. (2001) and Kavetski et al. (2002), it is worthwhile to investigate the numerical performance of the proposed TUR1 method with such adaptive schemes. Since the TUR1 method is shown to be able to produce more accurate results with larger time-steps and coarser meshes, and the adaptive schemes could have the ability to control temporal errors, it is reasonable to conjecture that the combination of TUR1 with a proper temporal adaptive scheme will produce a more efficient and robust solution strategy for unsaturated flow analysis, rather than TUR1 or adaptive schemes on their own.

Naturally, similar improvements in efficiency are also expected for spatial adaptive schemes with the application of proposed TUR1 method. However, a number of computational limitations are found in existing mesh adaption techniques (Mansell et al., 2002), such as

- The cost for development, implementation, and testing of those spatial adaptive algorithms may be substantial;
- Solution-based (*a posteriori*) error estimators are still limited to model problems (Bern et al., 1999);
- Optimal adaptive strategies remain largely under development, especially for complex problems with spatial heterogeneity of soils;
- Effectiveness of an adaptive mesh scheme often requires implementation of an efficient data management scheme. However, the complexity of data struc-

tures can be substantial (Oden and Demkowicz, 1987); etc.

Because of these difficulties, mesh adaption techniques are not commonly adopted by popular commercial softwares such as SEEP/W or PlaxFlow. Therefore, further studies are still needed to overcome these difficulties and to make spatial adaptive schemes more practical for engineering simulations.

The following studies are to illustrate the usefulness of the combination of adaptive schemes and the proposed TUR1 method. The major objectives of this chapter are to: (1) compare the performance of different time stepping schemes in the global temporal accuracy; (2) assess if combinations of the proposed TUR1 method and temporal adaptive schemes lead to more robust and efficient solutions, which means more efficient than TUR1 without adaptivity or adaptive schemes without under-relaxation and transformation.

4.2 Heuristic Temporal Adaptive Method

The heuristic time stepping method (Yeh, 1987; Celia and Binning, 1992; Simunek and van Genuchten, 1994; Rathfelder and Abriola, 1994) is the most commonly used approach to adaptive time-step solutions to the Richards equation, which empirically adjust the step size according to the number of iterations required for convergence of the non-linear solver. SEEP/W also adopted a modified version of such scheme, which is based on the average number of iterations required in previous time-steps (GEO-SLOPE, 2004). The algorithm can be described as below:

- if $(N^i_{iter} < N_{min})$, then $\Delta t^{i+1} = \min(\Delta t^i \times F_{increase}, \Delta t_{max})$

if the iteration convergence is fast, increase the step size;

- if $(N^i_{iter} > N_{max})$, then $\Delta t^{i+1} = \max(\Delta t^i \times F_{decrease}, \Delta t_{min})$

  if the iteration convergence is slow, decrease the step size;

- else, $\Delta t^{i+1} = \Delta t^i$

  if the iteration convergence is moderate, retain the current step size.

where

N^i_{iter} = the number of iterations required by the nonlinear solver to converge for time-step i;

N_{min} = a lower iteration limit;

N_{max} = a upper iteration limit;

$F_{increase}$ = a time-step acceleration factor;

$F_{decrease}$ = a time-step deceleration factor;

Δt_{min} = the minimum allowable time-step size;

Δt_{max} = the maximum allowable time-step size.

The advantage of this empirical approach is that it is cheap to implement into existing fixed time-step programs. However, several *a-priori* arbitrary parameters need to be specified either by the code or the user. Little theoretical guidance is available in the selection of optimal parameter values.

4.3 Automatic Temporal Adaptive Method

The automatic temporal adaptive method was firstly proposed by Sloan and Abbo (1999) for quality-controlled time stepping for elasto-plastic consolidation analysis in geomechanics. Then, Kavetski et al. (2001) and Kavetski et al. (2002) applied the principles of this adaptive scheme to the solution of Richards equation. Their studies showed that this automatic algorithm led to a consistent and efficient selection of time-steps, improving the performance of the nonlinear solvers.

The algorithm uses a numerical estimate of the local temporal truncation error and selects the stepsize for the next time-step based on the value of this error estimate to constrain the temporal error near a user-prescribed tolerance. Based upon the solution of a first-order backward Euler scheme, a solution of the second-order Thomas-Gladwell approximation (Thomas and Gladwell, 1988) can be obtained at virtually no extra cost. Thus, the local truncation error can be monitored by comparing these two solutions of adjacent order of accuracy.

4.3.1 Error Estimator

In the following, the automatic adaptive time stepping algorithm is presented for the pressure-based form of Richards equation. The application to the transformed form is straightforward.

Recall that the Galerkin finite element form of the Richards equation can be expressed as:

$$[M]\{h\},t + [K]\{h\} + [K]\{z\} = \{Q\} \tag{4.1}$$

Applying the first-order backward Euler scheme leads to the following equation:

$$(\Delta t\,[K] + [M])\,\{h_n\} = \Delta t\,\{Q_n\} + [M]\,\{h_{n-1}\} - \Delta t\,[K]\,\{z\} \tag{4.2}$$

and the derivative is

$$\dot{h}_n = \frac{h_n - h_{n-1}}{\Delta t} \tag{4.3}$$

It is found that the accuracy of the above approximation can be raised to second-order by averaging the derivative estimates, which can be shown to correspond to a member of the Thomas and Gladwell integration family (Thomas and Gladwell, 1988):

$$h_n^{\mathrm{TG}} = h_{n-1} + \frac{1}{2}\,\Delta t\left(\dot{h}_{n-1} + \dot{h}_n\right) \tag{4.4}$$

while the original first-order backward Euler solution gives:

$$h_n^{\mathrm{BE}} = h_{n-1} + \Delta t \cdot \dot{h}_n \tag{4.5}$$

A measure of the absolute local truncation error of the backward Euler approximation (4.4) can then be estimated by the difference between (4.4) and (4.5):

$$e_n = \frac{1}{2}\,\Delta t\left|\dot{h}_{n-1} - \dot{h}_n\right| \tag{4.6}$$

It is noted that when applied to the transformed form of Richards equation, the error estimation is still in terms of the pressure head in the following studies. This is firstly for the convenience of comparing the performances of different adaptive schemes in transformed or non-transformed form with same error tolerances. Also, the value of transformed head is dependent directly on the transformation parameter. A small change of the parameter may produce a significantly different transformed head values. Thus, adopting an

error estimation in terms of the transformed head may increase the sensitivity of the transformation parameter on the performance, which is not well appreciated.

4.3.2 Stepsize Adaption

An error test takes place following the above estimation of the local truncation error. In order to simulate the flows in both saturated and unsaturated cases (where the pressure head may approach zero), a mixed absolute-relative error test is recommended. The time-step is accepted if

$$\max\left(e_n^i - \tau_R \left|h_n^i\right| - \tau_A\right) < 0 \tag{4.7}$$

where τ_R and τ_A are absolute and relative error tolerance respectively; and i is the spatial node index. The node with the largest mixed error is then stored as $iCrit$ to be used for the stepsize adaption.

If the current time-step size is accepted, the stepsize for the next time-step is calculated as

$$\Delta t_{n+1} = \Delta t_n \times \min\left(s\sqrt{\frac{\tau_R \left|h_n^{iCrit}\right| + \tau_A}{\max\left(e_n^{iCrit}, EPS\right)}}, r_{\max}\right) \tag{4.8}$$

and, if the current time-step is rejected, it is re-calculated with a reduced stepsize as

$$\Delta\widetilde{t}_n = \Delta t_n \times \max\left(s\sqrt{\frac{\tau_R \left|h_n^{iCrit}\right| + \tau_A}{\max\left(e_n^{iCrit}, EPS\right)}}, r_{\min}\right) \tag{4.9}$$

where the multiplier constraints $r_{\max}$ and $r_{\min}$, the safety factor s and the machine constant EPS are introduced to increase the robustness of the algorithm by guarding against spuriously large or small stepsize changes, since the error measure (4.6) is not exact and may contain numerical noise. Typical values

for these factors are recommended (Kavetski et al., 2001, 2002) as $r_{\max} = 4.0$, $r_{\min} = 0.1$, $s = 0.9$, and $EPS = 10^{-10}$. Kavetski et al. (2001, 2002) have shown that the performance of this automatic adaptive scheme is robust with respect to moderate changes in these parameters.

4.3.3 Other Implementation Details

The treatment of intermediate output time levels is an important issue from the practical point of view. Usually, the user would like to monitor the time-evolution of the solution for several fixed times within the simulation. Although it is not particularly important theoretically, treatment of such intermediate output time could have substantial implications on the computational performance of the algorithms. Shampine (1994) proposed an efficient "look-ahead" technique and adopted by Kavetski et al. (2001, 2002), which is shown to be able to avoid undesirable abrupt changes in time-step size, given by

- Check whether t_{output} can be reached in a single time-step Δt, i.e., $t_{\text{current}} + \Delta t \geq t_{\text{output}}$;
    - Yes $\Rightarrow$ truncate Δt to produce output at t_{output}: $\Delta t = t_{\text{output}} - t_{\text{current}}$. Perform the time-step;
    - No $\Rightarrow$ check whether t_{output} can be reached in two steps Δt, i.e., $t_{\text{current}} + 2 \cdot \Delta t \geq t_{\text{output}}$;
        - Yes $\Rightarrow$ equalize the time-steps, i.e., $\Delta t = (t_{\text{output}} - t_{\text{current}})/2$. Perform the time-step;

◇ No ⇒ proceed with unchanged time-step Δt.

The oscillation problem is another issue that needs to be considered. Since the time-step size is now not constant during the whole simulation, the minimum time-step criteria is obviously not applicable. Thus, the lumped mass scheme is adopted here to curb undesirable oscillations.

If the nonlinear iteration fails to converge in one time-step, i.e., the maximum number of iterations is reached without convergence, it is recommended to reduce the current stepsize by half and repeat the time-step (GEO-SLOPE, 2004). A small number of allowable iterations to reach convergence is preferred compared to a large one, because if the iteration gets stuck on any time-step, it will reach the maximum allowable iterations more quickly. It is a trade-off between repeating a time-step and allowing more iterations per time-step.

4.4 Numerical Studies

4.4.1 Problem Descriptions

The same one-dimensional infiltration problem from Chapter 3 is adopted here to study the performance of different approaches, while the geometry of the finite element mesh and boundary conditions are shown schematically in Figure 3.3. In the following analysis, a typical sandy clay loam soil (Case A) is adopted as the porous medium. The nonlinear soil hydraulic characteristics are presented in Figures 3.4 and 3.5.

The analysis in this Chapter focuses on temporal errors, since spatial errors

arise due to the finite element discretization and are unrelated to the time stepping scheme. Therefore, all solutions below are obtained using an identical and relatively dense spatial mesh with 100 linear elements of uniform size. The error measure used in the following study is calculated by comparing the approximate and an "exact-in-time" solution at a series of specified output times, where the "exact-in-time" solution is evaluated numerically by using the same spatial mesh and a very small time-step size of 0.05 s. This procedure isolates the temporal errors and facilitates the assessment of time accuracy.

In order to simplify the error analysis, pure absolute error requirements are enforced by setting $\tau_R = 0$ in the automatic adaptive scheme. The error norm is defined as

$$\| \epsilon \|_2 = \left[\frac{1}{nn} \sum_{i=1}^{nn} \left| \widehat{h^i} - h^i \right|^2 \right]^{1/2} \tag{4.10}$$

where $\widehat{h^i}$ is the "exact-in-time" solution. Run time is obtained by executing the code (compiled using Microsoft Fortran^{TM} PowerStation 4.0) on an Intel Core Duo 2, 2.4 GHz machine. For the Picard iterative procedures, the relative tolerance is set to be 0.001 percent. A transformation parameter value of -1.4 m^{-1} is adopted for all schemes with the TUR1 method.

4.4.2 Performance of Fixed Time-step Schemes

The performance of fixed time-step schemes are studied with no under-relaxation (hereafter referred to as UR0), UR2 and TUR1 method respectively. Figure 4.1 shows the temporal accuracy of the stepsize-fixed UR0, UR2 and TUR1 scheme with time-step size Δt ranging from 1000 s to 50 s. It can be seen that for fixed time-

step schemes, significant errors are observed at the beginning of the simulations, although the accuracy improves with elapsed time. The large discretization errors appearing at the beginning of the simulations may be explained in part by the highly nonlinear behavior of the solution at the initial time periods, where an abrupt change of the boundary condition is applied at $t = 0$. For example, Figure 4.2 shows the calculated derivatives of pressure heads with different time-step sizes for different times. It can be seen that the changes of pressure heads are quite nonlinear during the whole simulation as severe changes are found at the initial parts and milder at the later parts. If a big time-step size ($\Delta t = 200$ s) is adopted, the derivative of pressure heads will be highly underpredicted at the initial part of the simulation compared to a more accurate value from a smaller time-step size ($\Delta t = 1$ s), which can be seen from Figure 4.2. Thus, big temporal discretization errors will be incurred at the initial parts. This is because the backward Euler method which is used in the temporal discretization procedure assumes a linear change of pressure heads in one time-step. Therefore, if accurate intermediate results are required for the early part of the simulation, the user may be forced to run the entire analysis with fine time-step size which is controlled by a short segment of the temporal domain with pronounced nonlinearity. The errors decrease as time elapses because the nonlinearity weakens. Thus, the effort expended in using such fine time-steps is wasted for most parts of the simulations.

Comparison of the computational efficiency for fixed time-step UR0, UR2 and TUR1 schemes is given in Table 4.1 and Figure 4.3. The effects of under-relaxation and transformation are shown. It can be seen that with the same time step sizes, UR2 gets exactly the same solutions as UR0, while UR2 uses less iterations

than UR0 because of the effect of under-relaxation. The superiority of TUR1 method in efficiency over UR2 method is also demonstrated as shown in Chapter 3. It can be seen that TUR1 method can get more accurate solutions with less run time than UR0 and UR2 methods. For example, with a same time-step size of 500 s, TUR1 method generates a solution with maximum temporal error of 0.217 m at a cost of 446 iterations, while UR2 method uses 70% more run time (758 iterations) to achieve a solution with maximum temporal error of 0.318 m.

4.4.3 Performance of Heuristic Temporal Adaptive Schemes

In this section, several sets of typical values of the empirical parameters are adopted to illustrate the performance of the heuristic temporal adaptive schemes, which are given in Table 4.2. Figure 4.4 shows the temporal accuracy of the heuristic temporal adaptive UR0 (HUR0), UR2 (HUR2) and TUR1 (HTUR1) schemes with these adaptive parameters. It can be seen that the heuristic scheme is capable of producing solutions with more or less uniform error profiles throughout the entire simulation. And with more stringent adaptive parameters (Run 1 to Run 4), more accurate solutions are obtained. These results may be explained by Figure 4.6, which shows the time-step sequences selected by the heuristic schemes. It shows that the heuristic temporal adaptive schemes can select a meaningful time-step size variation: the beginning of the simulation with high nonlinearity is performed using relatively fine step sizes. When the nonlinear character of the infiltration front is reduced as time passes, the time-step increases correspondingly.

Table 4.3 and Figure 4.5 show the computational efficiency of the heuristic

temporal adaptive schemes without under-relaxation (HUR0) and combined with UR2 (HUR2) and TUR1 (HTUR1) methods. Compared with the fixed time-step schemes shown in Table 4.1, heuristic schemes outperform fixed time-step schemes for all of the UR0, UR2 and TUR1 methods at a comparable level of accuracy. For example, when an accuracy requirement on the maximum L_2 error of 0.1 m is applied, fixed time-step UR0 method needs to adopt a small time-step size of 50 s, which requires 3412 iterations and 11.58 s of run time; while the heuristic adaptive scheme requires 2105 iterations and total run time of 7.42 s. Fixed time-step UR2 method requires 2572 iterations and 9.16 s of run time with the time-step size of 50 s; while the heuristic adaptive UR2 method requires 1748 iterations and total run time of 6.34 s. Fixed time-step TUR1 method also needs the time-step size of 50 s to satisfy the accuracy requirement, but with less iterations (2275) and total run time (8.11 s) than fixed time-step UR0 and UR2 methods; while the heuristic adaptive TUR1 method appears to be the most efficient as it only takes 441 iterations and 1.61 s to get a solution with required accuracy.

It also can be seen from Table 4.3 and Figure 4.5 that the heuristic adaptive scheme alone does not guarantee an efficient solution. Actually, the heuristic adaptive UR2 method is slightly more efficient than the heuristic adaptive scheme alone without under-relaxation. While it becomes the most efficient when the heuristic adaptive scheme is combined with the TUR1 method.

Furthermore, it can be seen from Table 4.3 that with the same set of adaptive parameters, the heuristic adaptive TUR1 (HTUR1) method usually results in a smaller number of time-steps than HUR0 and HUR2 methods. Thus, temporal errors from the adaptive HTUR1 method may be bigger than those from adaptive

HUR0 and HUR2 methods with the same set of adaptive parameters. This is because the TUR1 method always use less iterations to reach a stable solution in a given time-step than UR0 and UR2 methods. Therefore, in the heuristic adaptive procedure, HTUR1 method tends to invoke much more times of step increasing operations. Time-step size selected by HTUR1 then becomes much bigger than HUR0 and HUR2 which takes much more iterations per time-step. For cases when a comparable number of time-steps are adopted, TUR1 with the heuristic adaptive scheme can achieve solutions with the same or slightly higher accuracy as UR2, but spends less run time, which makes it a more efficient approach. For example, HUR2 method takes 299 time-steps to get a solution with maximum error of 0.059 m for Run 2 case shown in Table 4.2. With the same set of adaptive parameters, HTUR1 only takes 95 time-steps. But the solutions obtained are less accurate with a higher maximum error of 0.078 m. When a set of more stringent adaptive parameters of Run 3 is adopted, HTUR1 can produce solutions with approximately the same accuracy as HUR2 with Run 2 parameters. However, it takes only half the run time (3.64 s) than that of HUR2 (6.34 s).

However, in the heuristic temporal adaptive schemes, there is little indication of the relationship between those adaptive parameters and actual numerical accuracy of the solutions. The iteration tolerance also interacts strongly with the iteration limits (N_{max} and N_{min}), because a small iteration tolerance means more iterations in a time-step. Thus, it is difficult to select appropriate parameter values for different problems. Moreover, it is less clear how to adjust those parameters if a different nonlinear solver is employed, such as the Newton-Raphson scheme instead of the Picard solver. In practice, the efficiency of such schemes becomes dependent on

the ability of the user to determine the optimal heuristic time stepping parameters.

4.4.4 Performance of Automatic Temporal Adaptive Method

In this section, performance of the automatic temporal adaptive method is studied with four different absolute error tolerances, which are given as 0.5 m, 0.1 m, 0.05 m and 0.01 m. Figure 4.7 shows the temporal accuracy of the automatic temporal adaptive scheme without under-relaxation (AUR0) and combined with UR2 (AUR2) and TUR1 (ATUR1) methods with these tolerances. It can be seen that the automatic scheme is also able to produce solutions with more or less uniform error profiles throughout the entire simulation, similar to the heuristic adaptive schemes. This may be explained by Figure 4.9, which shows the time step sequences selected by the automatic adaptive schemes. It shows a similar pattern in the time step variations to the heuristic temporal adaptive schemes: relatively fine step sizes are adopted at the beginning part of the simulation with high nonlinearity due to abrupt forcing. Then larger time-steps are selected to maintain an uniform error profile in the subsequent portion where the nonlinearity diminishes .

Table 4.4 and Figure 4.8 show the computational efficiency of the automatic temporal adaptive schemes without under-relaxation (AUR0) and combined with UR2 (AUR2) and TUR1 (ATUR1) methods. Comparing with the heuristic adaptive schemes shown in Table 4.3, it is found that the automatic adaptive schemes are quantitatively as efficient as the heuristic adaptive schemes. For example, AUR2 method requires around 100 time-steps to obtain a maximum error of about 0.17

m for both adaptive schemes. ATUR1 method also obtains a same maximum error of about 0.075 m at a similiar cost of around 100 time-steps for these two adaptive schemes.

Although the heuristic adaptive scheme is quantitatively as efficient as the automatic adaptive scheme, the latter scheme outperforms the former scheme in the way that it ensures a direct proportionality between the actual error and the prescribed tolerance, which can be seen from Figure 4.10. This relationship between the actual errors and the tolerance is critical for the success of an adaptive scheme (Shampine, 1994). Figure 4.10 shows that the maximum L_2 error is proportional to the square root of the tolerance for the automatic adaptive UR2 (AUR2) method. This result is consistent with the mathematical formulation derived by Kavetski (2002). On the other hand, the automatic adaptive TUR1 (ATUR1) method also can get a linear proportionality between the error and the tolerance, but the factor is different. This difference may be explained by the effect of transformation parameter as a fixed parameter value is adopted for the entire simulation. Previous studies have shown that the optimal transformation parameter value is sensitive to the element size and time step size, although near optimal solutions can be obtained by using the proposed method to choose a fixed value for this transformation parameter. The time step size changes over several orders of magnitude in the automatic adaptive schemes. Thus, additional errors may be introduced and the proportion factor is correspondingly changed. Nevertheless, these schemes are reliable in the sense that the temporal discretization error can be reduced in response to the reduction of the user prescribed tolerance.

It also can be seen from Table 4.4 and Figure 4.8 that the automatic adaptive

scheme alone (AUR0) does not guarantee an efficient solution. Although it is found that with a same error tolerance, automatic adaptive UR0, UR2 and TUR1 methods select almost the same number of time-steps, the adoption of under-relaxation and transformation can dramatically improve the convergence in one time step, which means less total iterations and run time are needed. The solutions from TUR1 are also found to be more accurate than those from UR0 and UR2. Overall, the automatic adaptive TUR1 (ATUR1) scheme seems to be the most efficient.

4.5 Concluding Remarks

In this chapter, the UR2 under-relaxation approach and the proposed TUR1 combination approach are studied with three different time stepping schemes, which can be listed as the fixed time step scheme, the heuristic temporal adaptive scheme, and the automatic temporal adaptive scheme. Several conclusions can be made based on a series of numerical studies:

- Temporal adaptive schemes presented in this chapter are superior to the fixed time step scheme in terms of the ability to control temporal errors. Both adaptive schemes are able to produce solutions with more or less uniform error profiles throughout the entire simulation, while the fixed time stepping scheme generates significant errors when highly nonlinear behavior of the solution is encountered, which is usually caused by abrupt changes of the boundary condition.

- Comparison between the heuristic and automatic temporal adaptive schemes shows that the latter outperforms the former scheme in the way that it ensures a direct proportionality between the actual error and the prescribed tolerance, which is critical for the success of an adaptive scheme. On the contrary, relationship between the heuristic adaptive parameters and the actual numerical accuracy of solutions is hard to identify. Hence, the efficiency of such scheme becomes uncertain as it is dependent on the ability of the user to determine optimal heuristic time stepping parameters for different scenarios.

- Neither the heuristic adaptive scheme nor the automatic adaptive scheme alone without under-relaxation and transformation gives an efficient solution. The adoption of under-relaxation and transformation can dramatically improve the convergence in one time step, which means less total iterations and run time are needed.

- The superiority of proposed TUR1 approach over UR2 approach is verified when combined with different time stepping schemes in terms of efficiency that it takes less run time to produce solutions satisfying the requirements in accuracy. In addition, the combination of TUR1 method and the automatic adaptive error control scheme provides the most efficient solution in a way that the temporal error is constrained proportionally to a user prescribed tolerance at minimal computational cost.

In conclusion, the combination of proposed TUR1 approach and the automatic adaptive scheme (ATUR1) can be a robust numerical method for practical

unsaturated flow simulations, as it provides the most efficient solution at minimal computational cost; its performance is robust with moderate changes of several parameters introduced. It is conceptually and computationally simple which can be easily incorporated into existing software codes based on the backward Euler scheme.

Table 4.1: Computational efficiency of the fixed time schemes

Approaches	Time step (s)	Maximum L_2 error (m)	Number of time-steps	Total iterations	Runtime (s)
UR0	1000	0.456	50	829	2.72
	500	0.318	100	1058	3.52
	250	0.190	200	1417	4.73
	100	0.113	500	2265	7.66
	50	0.063	1000	3412	11.58
UR2	1000	0.456	50	672	2.26
	500	0.318	100	758	2.58
	250	0.190	200	1274	4.39
	100	0.113	500	2140	7.40
	50	0.063	1000	2572	9.16
TUR1	1000	0.269	50	276	0.95
	500	0.217	100	446	1.56
	250	0.172	200	714	2.55
	100	0.118	500	1550	5.48
	50	0.083	1000	2275	8.11

Table 4.2: Time stepping parameters of the heuristic temporal adaptive schemes

	Run 1	Run 2	Run 3	Run 4
Δt_0 (s)	100	10	5	1
N_{min}	6	5	4	3
N_{max}	12	10	8	6
$F_{increase}$	1.5	1.2	1.1	1.1
$F_{decrease}$	0.95	0.95	0.9	0.9

Table 4.3: Computational efficiency of the heuristic temporal adaptive schemes

Approaches		Maximum L_2 error (m)	Number of time-steps	Total iterations	Runtime (s)
HUR0	Run 1	0.159	101	1079	3.78
	Run 2	0.057	401	2105	7.42
	Run 3	0.019	920	3693	13.55
	Run 4	0.011	1594	4744	16.95
HUR2	Run 1	0.172	92	734	2.64
	Run 2	0.059	299	1748	6.34
	Run 3	0.017	933	3676	13.34
	Run 4	0.016	984	3851	14.00
HTUR1	Run 1	0.154	44	264	0.95
	Run 2	0.078	95	441	1.61
	Run 3	0.054	260	991	3.64
	Run 4	0.018	987	2922	10.70

Table 4.4: Computational efficiency of the automatic temporal adaptive schemes

Approaches	τ_A (m)	Maximum L_2 error (m)	Number of time-steps	Total iterations	Runtime (s)
AUR0	0.5	0.170	112	1224	4.19
	0.1	0.073	268	1788	6.11
	0.05	0.054	380	2227	7.61
	0.01	0.023	925	3498	12.59
AUR2	0.5	0.170	111	925	3.39
	0.1	0.073	268	1604	5.73
	0.05	0.054	380	1964	7.00
	0.01	0.023	925	3496	12.56
ATUR1	0.5	0.075	113	530	1.92
	0.1	0.054	263	1024	3.68
	0.05	0.042	375	1246	4.53
	0.01	0.022	835	2480	8.99

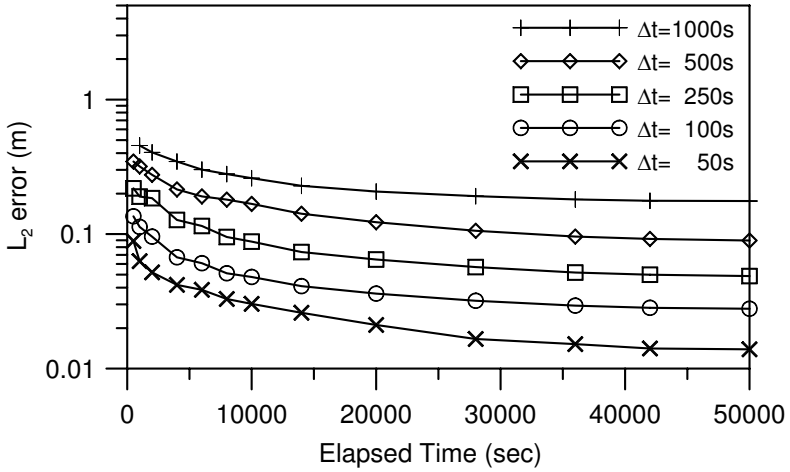

(a) UR0 (no under-relaxation)

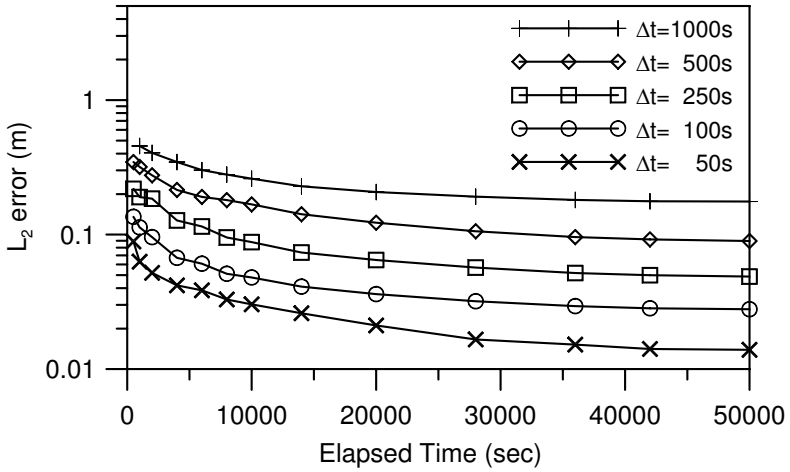

(b) UR2

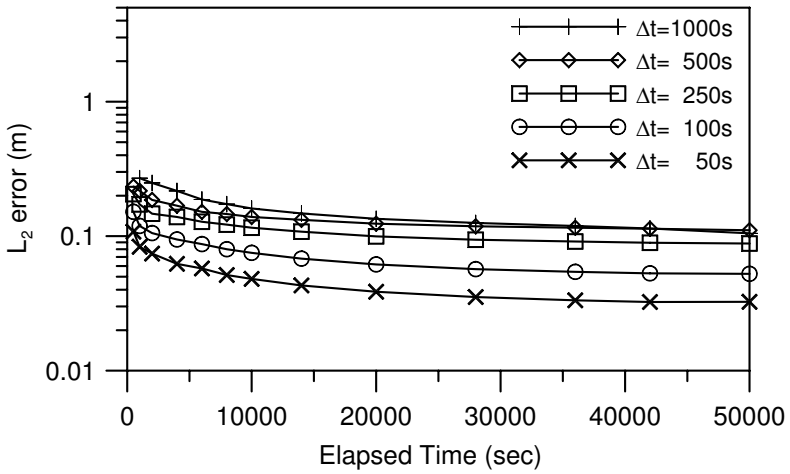

(c) TUR1

Figure 4.1: Temporal accuracy of the fixed time step schemes

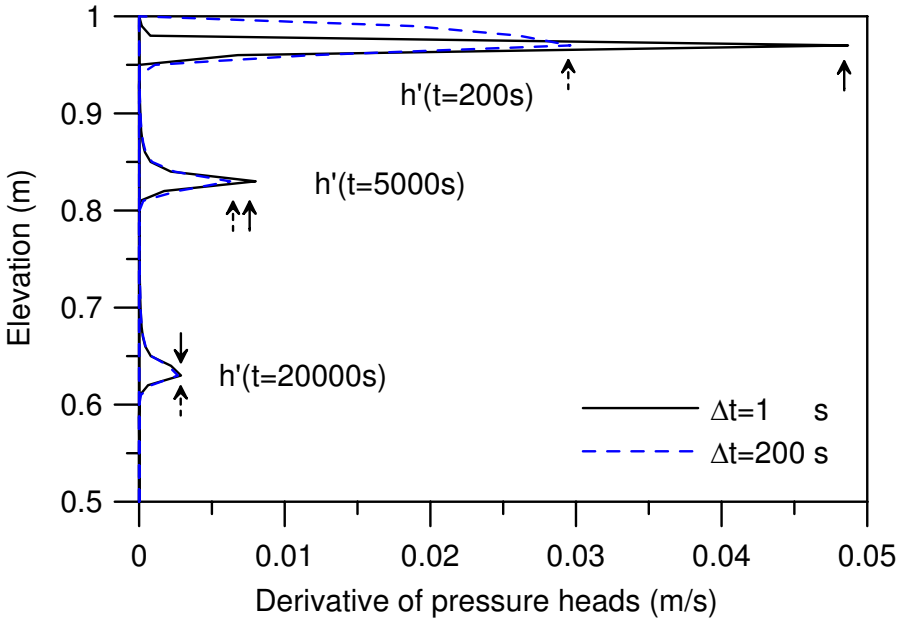

Figure 4.2: Derivative of pressure heads in different times of the fixed time step scheme with different time step sizes

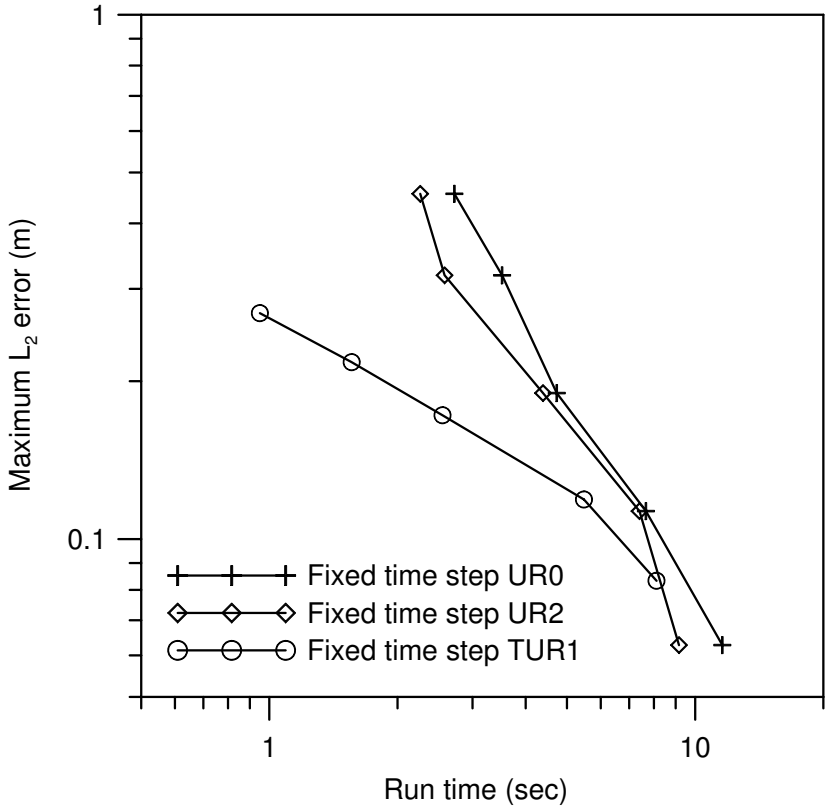

Figure 4.3: Efficiency comparison of the fixed time step schemes

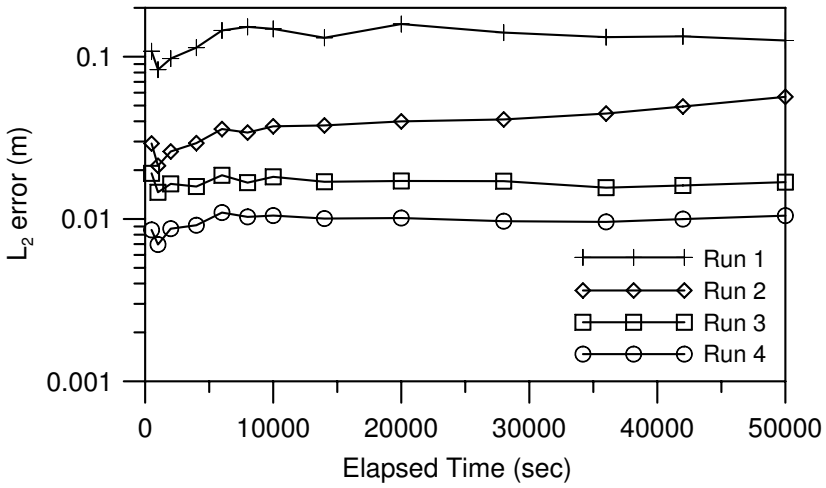

(a) HUR0 (no under-relaxation)

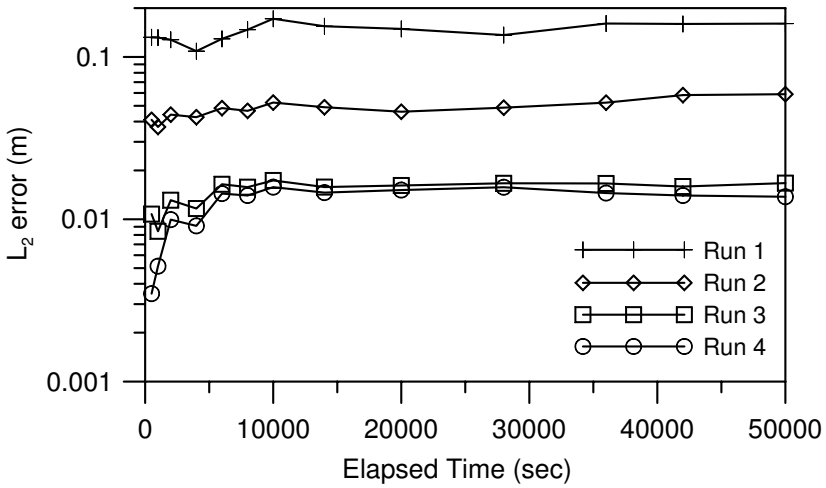

(b) HUR2

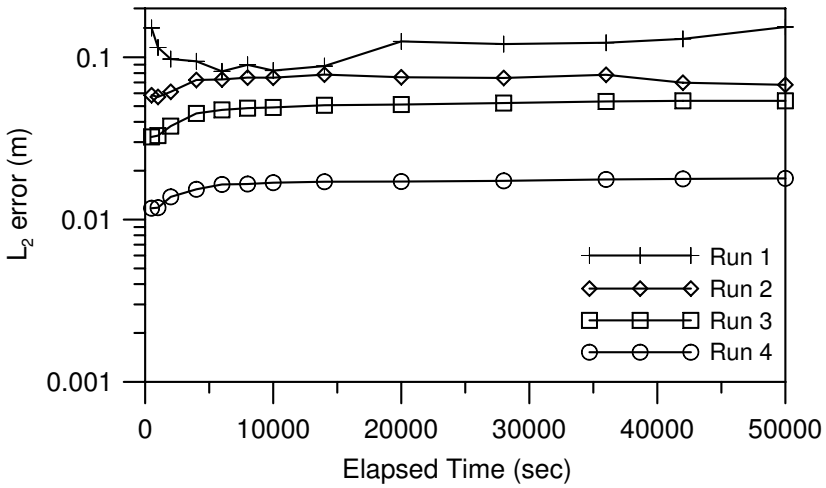

(c) HTUR1

Figure 4.4: Temporal accuracy of the heuristic temporal adaptive schemes

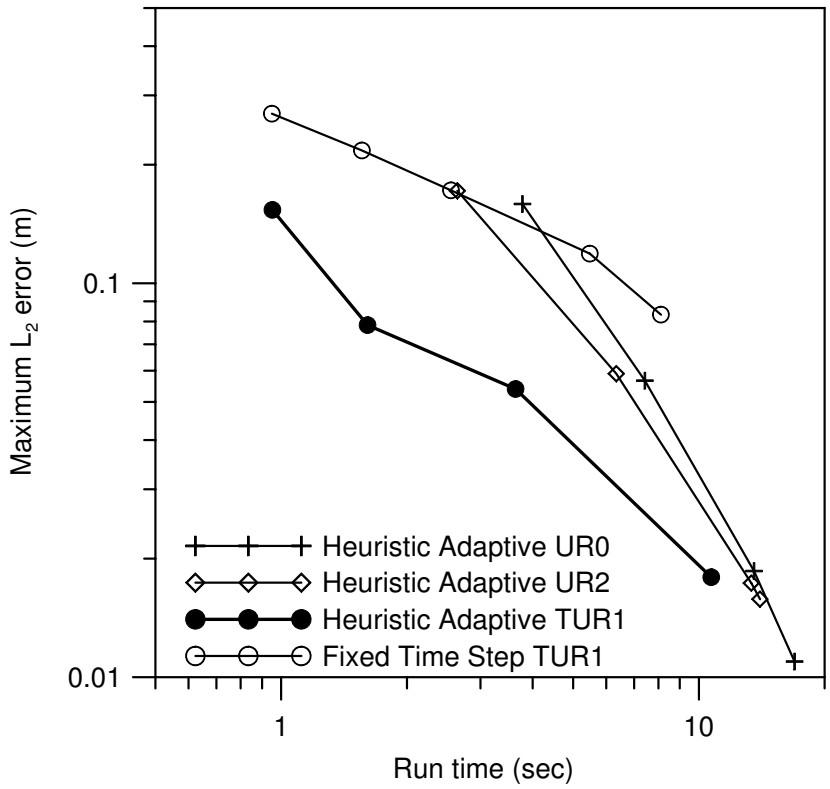

Figure 4.5: Efficiency comparison of the heuristic temporal adaptive schemes

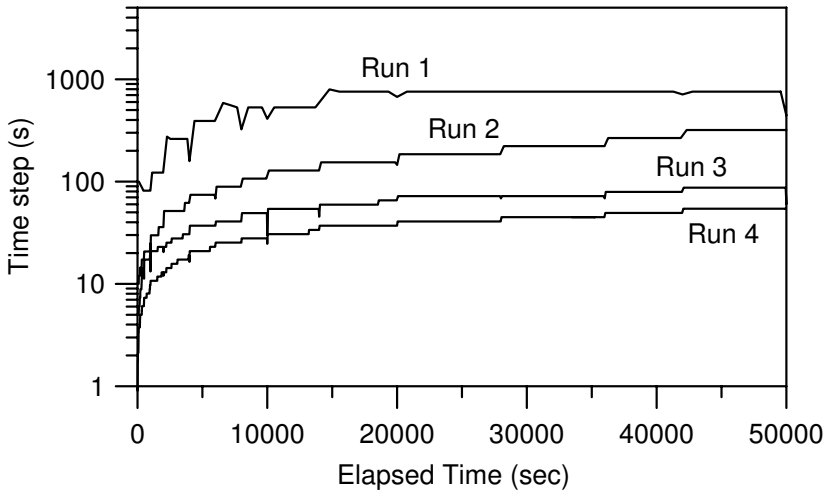

(a) HUR0 (no under-relaxation)

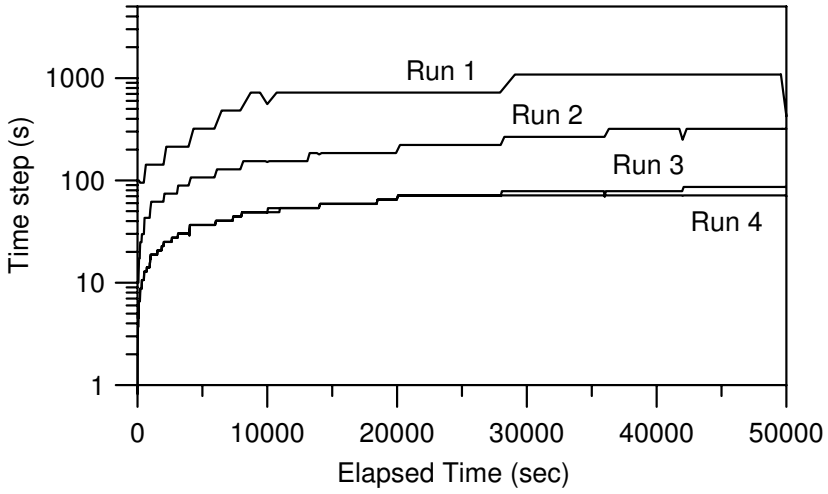

(b) HUR2

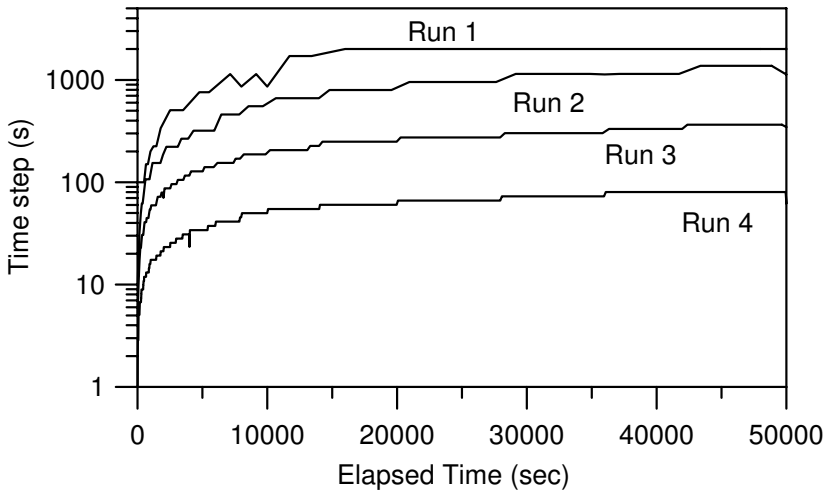

(c) HTUR1

Figure 4.6: Time step size variation given by the heuristic temporal adaptive schemes

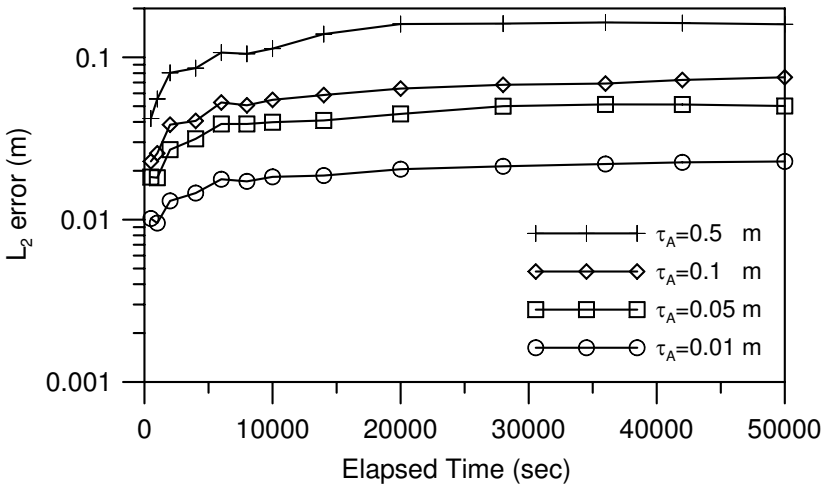

(a) AUR0 (no under-relaxation)

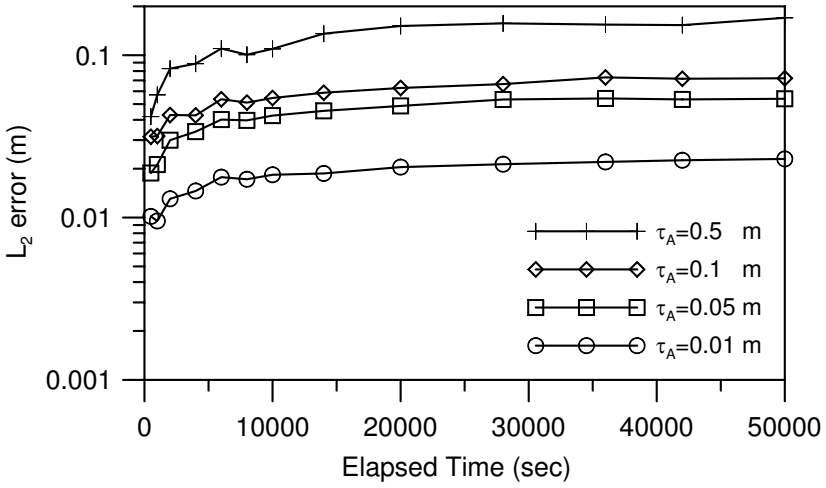

(b) AUR2

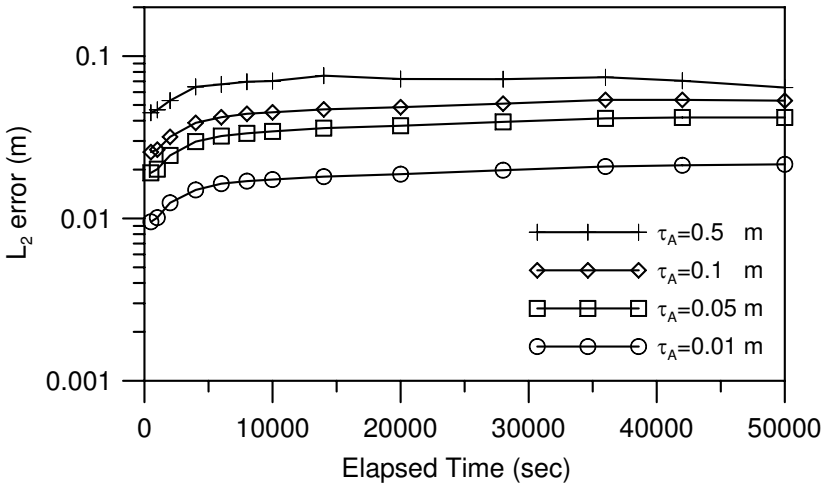

(c) ATUR1

Figure 4.7: Temporal accuracy of the automatic temporal adaptive schemes

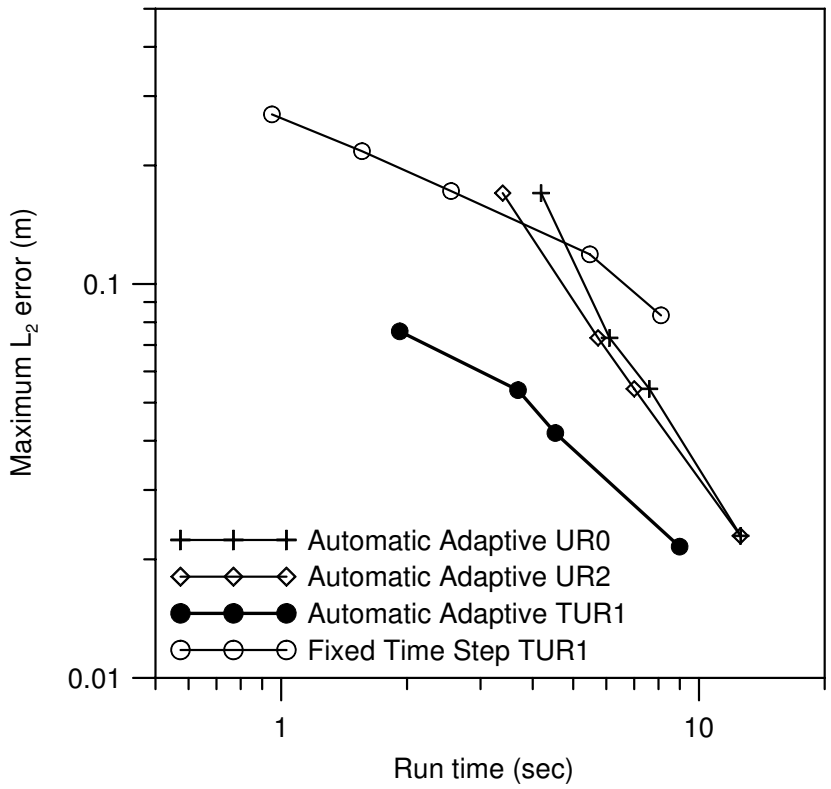

Figure 4.8: Efficiency comparison of the automatic temporal adaptive schemes

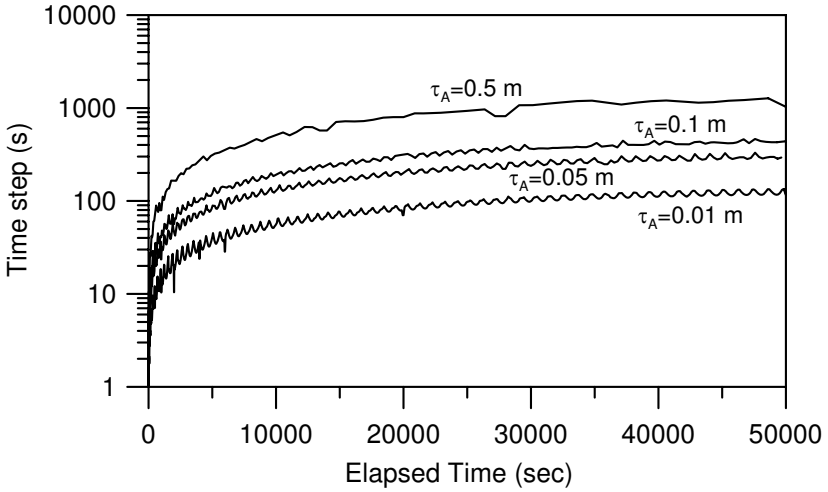

(a) AUR0 (no under-relaxation)

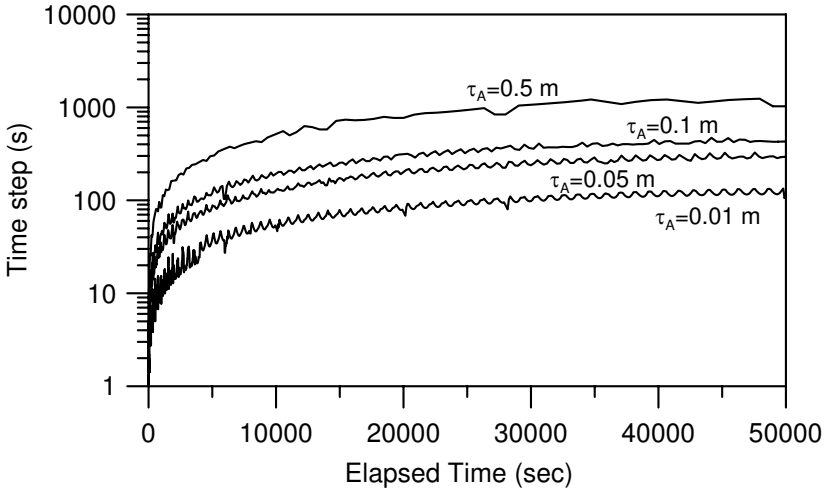

(b) AUR2

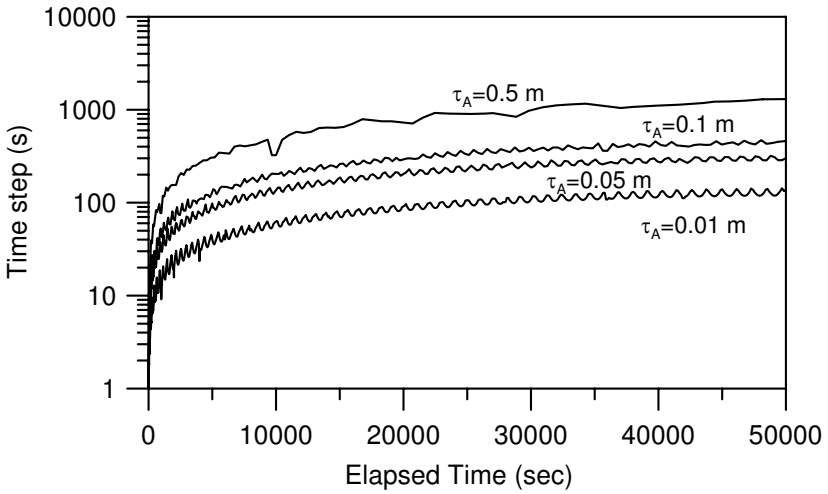

(c) ATUR1

Figure 4.9: Time step size variation given by the automatic temporal adaptive schemes

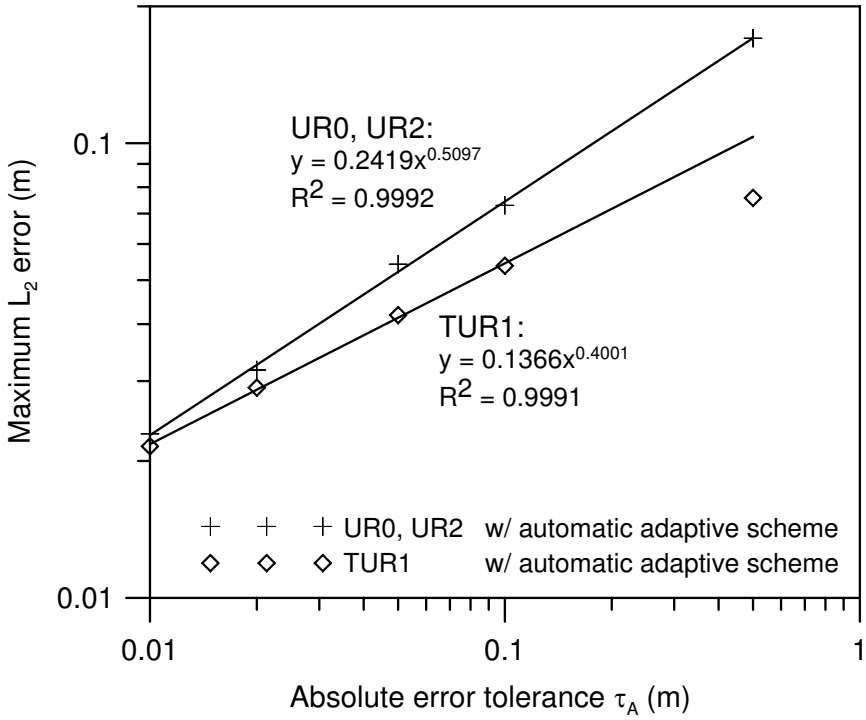

Figure 4.10: Relationship between the solution error and the prescribed tolerance

Chapter 5

Benchmark Studies for Unsaturated Flow Problems

5.1 Introduction

In Chapter 3 and Chapter 4, a combination approach TUR1 consisting of the RFT transformation method and a typical under-relaxation technique is proposed to solve the highly nonlinear unsaturated seepage flow problem. Detailed numerical investigation on a simple one-dimensional problem shows that such combination appears to be more superior than previous approaches without transformation in the sense that a more accurate solution can be obtained much more quickly using a practically reasonable spatial and temporal discretization. The superiority of the TUR1 method can be further identified and improved when combined with an automatic time stepping scheme with an embedded temporal error control. It shows that this ATUR1 method provides the most efficient solution in a way that the temporal error can be constrained proportionally to a user prescribed tolerance at minimal computational cost.

In this chapter, more realistic benchmarking examples are presented to show the robustness and efficiency of proposed TUR1 and ATUR1 methods.

5.2 One-dimensional Infiltration Problems

In this section, the performance of the proposed TUR1 method is studied using the same one-dimensional infiltration problem in Chapter 3, but with a variety of different soil types. The input parameters are given in Table 5.1, including constitutive parameters, spatial and temporal domains, initial and boundary conditions, spatial and temporal discretizations, and the transformation parameter values used in the simulations. The material properties in Problem A-D correspond to the average values for the soil textural group of sand, loamy sand, loam and clay loam, respectively, according to the estimation of Carsel and Parrish (1988) from a large number of soils. For each problem, two mesh sizes and three time-step sizes are simulated to study the effect of spatial and temporal discretization.

A set of simulations was conducted to compare the performance of proposed TUR1 method and UR1, UR2 method without transformation. Table 5.2 to Table 5.5 show the results of these simulations for four test problems, with one dense mesh and one coarse mesh, and three different time-step sizes. Based on this set of simulations, the following observations can be made:

1. TUR1 method generally leads to more accurate solutions than UR1 and UR2 approaches without transformation, as shown by the smaller L_2 errors;

2. TUR1 method is generally more robust than UR1 and UR2 approaches without transformation. It is shown that TUR1 is able to converge for all test cases, while both UR1 and UR2 failed to converge in several of the simulations;

3. for more uniform soil types ($n > 2.0$), TUR1 might take more CPU run time than UR1 and UR2, however the solutions were much more accurate. In terms of the overall performance , it still showed comparable or more efficiency.

5.3 Two-dimensional Infiltration Problems

In this section, the performance of proposed TUR1 and ATUR1 method is evaluated using two-dimensional infiltration problems with very dry and variably saturated conditions in heterogeneous soils.

5.3.1 Forsyth et al.'s Problem

An infiltration problem in a large caisson consisting of heterogeneous soils at dry initial conditions has been studied by Forsyth et al. (1995) and Diersch and Perrochet (1999). Figure 5.1 shows the schematic view of this 2D problem. The spatial discretization is 89 $\times$ 20 quadrilateral 4-noded elements (1890 nodes in total) as the same in Forsyth et al. (1995). The initial pressure head for all nodes is set to be -7.34 m. Four different soils are used for different zones of the domain. The material properties are listed in Table 5.6. The whole simulation time is 30 days.

Following the proposed criteria discussed previously, the optimal transformation parameter values for these four soils are different. Here, we choose the smallest value for the whole simulation, which is -2.0 m^{-1}.

In the following simulation, three different time-step sizes (86400 s; 22800 s;

8640 s) are adopted for the fixed time-step schemes (UR1, UR2 and TUR1). Three different tolerances (Case 1: $\tau_R = 1.0$, $\tau_A = 1.0$; Case 2: $\tau_R = 0.5$, $\tau_A = 0.5$; Case 3: $\tau_R = 0.1$, $\tau_A = 0.1$) are adopted for the automatic adaptive time-step scheme (ATUR1).

Table 5.7 shows the performance of the fixed time-step schemes (UR1, UR2 and TUR1). While the UR1 and UR2 methods failed for all cases, the TUR1 method achieved convergent results. Figure 5.2 shows the saturation contour results at 30 days of TUR1 with these 3 time-step sizes. Here, the saturation is defined as

$$S = \frac{\theta}{\theta_s}. \tag{5.1}$$

It can be seen that the most different part among these solutions occurs along the left-bottom edge. The wetting front is found to be predicted slightly ahead for larger time-steps. Compared with the solution of TUR1 with a very small time-step size (86.4 s), it shows that the solution with a time-step size of 8640 s has already converged.

Figure 5.3 shows the saturation contour results at 30 days of ATUR1. The same observation can be made that if loose tolerances are adopted in adaptive scheme, which usually means bigger time steps in simulations, substantial errors are found along the left-bottom edge as the depth of the wetting front is overpredicted. It also shows that the solution with case 3 tolerances can be seen as a converged solution. Table 5.8 shows the performance of ATUR1 approach. The robustness and efficiency of ATUR1 method are clearly shown.

For comparison, Figure 5.4 shows the result of Forsyth et al. (1995) using a variable substitution method. The results of TUR1 and ATUR1 are in general

agreement, but there are significant differences in the details. A more diffusive wetting front is found in Forsyth et al.'s result. However, it is found that very small number of time steps were used in their simulation (29 iterations in total), which may be not enough to get a correct solution. Diersch and Perrochet (1999) also noticed this problem. As shown in Figure 5.5, they found that Forsyth et al.'s solutions agreed quite well with their results of the "low-cost" TBFN method which also adopted a small number of time steps (15 time steps). The PCOSN method provided a much steeper saturation front, as more time steps were used (199 time steps). This result from PCOSN agrees well with solutions of TUR1 and ATUR1 as shown in Figure 5.2 and Figure 5.3. This example clearly illustrates that more emphasis should be put on the choice of appropriate time-step size or adaptive control parameters, and a convergence study is necessary as a seemingly accurate solution can be far from correct when dealing with a highly nonlinear unsaturated flow problem.

5.3.2 Kirkland et al.'s Problem 1

Kirkland et al. (1992) presented a challenging two-dimensional infiltration problem involving strictly unsaturated conditions. As shown in Figure 5.6, the whole domain is divided into nine alternating blocks of clay and sand, which generates a complex problem geometry. All boundaries are impermeable except where the infiltration is imposed. The material properties are listed in Table 5.9. The simulation is run with a very high initial negative pressure head of -500 m, which simulates a dry initial condition. As demonstrated in their study, a spatial discretization of 0.05

m was judged to be adequate for the problem presented, thus the element size is chosen to be 0.05 m $\times$ 0.05 m. The whole simulation time is 12.5 days.

Following the criteria discussed perviously, the transformation parameter for this problem is chosen to be equal to the smaller optimal value for these two soils, which is -1.0 m^{-1}.

In the following simulation, three different time-step sizes (3600 s; 1200 s; 600 s) are adopted for the fixed time-step schemes (UR1, UR2 and TUR1). Three different tolerances (Case 1: $\tau_R = 0.5$, $\tau_A = 5.0$; Case 2: $\tau_R = 0.1$, $\tau_A = 1.0$; Case 3: $\tau_R = 0.01$, $\tau_A = 0.1$) are adopted for the automatic adaptive time-step scheme (ATUR1).

Table 5.10 shows the performance of the fixed time-step schemes (UR1, UR2 and TUR1). While the UR1 and UR2 methods failed for all cases, the TUR1 method produces stable results when the time-step size is reduced to 1200 s and 600 s. Figure 5.8 shows the pressure head contour results at 12.5 days of TUR1 with these 2 time-step sizes. Slight differences are found between these two results and the dense time-step solution with a time-step size of 60 s. A comparison between these contours and Kirkland et al.'s results shown in Figure 5.7 reveals a good agreement, which verifies the correctness of these solutions.

Figure 5.9 shows the pressure head contour results at 12.5 days of ATUR1 method. These results are found to be indistinguishable with the dense time-step solution. It shows that the tolerances of Case 1 is enough to get correct solutions. Table 5.11 shows the computational efforts of ATUR1 approach. It can be seen that the adaptive ATUR1 method is more efficient than the fixed time-step TUR1

method, as it takes only 441 s to get acceptable results compared to 830 s using the TUR1 method. Actually, a closer examination of the iteration procedures of TUR1 method reveals that small time-step sizes are needed only for several time steps in the very beginning of the simulation due to convergence requirement. And this time-step size may be unnecessarily small for the rest of the simulation.

5.3.3 Kirkland et al.'s Problem 2

Kirkland et al. (1992) presents another two-dimensional infiltration problem of a developing perched water table surrounded by very dry unsaturated conditions. It is a good example to show the performances of the proposed TUR1 and ATUR1 methods in problems with both unsaturated and saturated zones. As shown in Figure 5.10, a 3 m $\times$ 2 m region of sand is surrounded by clay on both sides and underneath with a 1 m layer of sand below the clay. All boundaries are impermeable except where the infiltration is imposed. The material properties are listed in Table 5.9. The simulation is also run with a very high initial negative pressure head of -500 m, which simulates a dry initial condition. As demonstrated in their study, a spatial discretization of 0.05 m was judged to be adequate for the problem presented, thus the element size is also chosen to be 0.05 $\times$ 0.05 m. The whole simulation time is 1 day.

Following the criteria discussed perviously, the transformation parameter for this problem is chosen to be equal to the smaller optimal value for these two soils, which is -1.0 m^{-1}.

In the following simulation, three different time-step sizes (120 s; 60 s; 30 s) are

adopted for the fixed time-step schemes (UR1, UR2 and TUR1). Three different tolerances (Case 1: $\tau_R = 0.5$, $\tau_A = 5.0$; Case 2: $\tau_R = 0.1$, $\tau_A = 1.0$; Case 3: $\tau_R = 0.01$, $\tau_A = 0.1$) are adopted for the automatic adaptive time-step scheme (ATUR1).

Table 5.12 shows the performance of the fixed time-step schemes (UR1, UR2 and TUR1). Similar to the previous two examples, while the UR1 and UR2 methods failed for all cases, the TUR1 method produces stable results for these three time-step sizes. Figure 5.12 shows the pressure head contour results at 1 day of TUR1 with these three time-step sizes and also with a dense time-step of 10 s. It is found that the result with time-step size of 120 s shows some differences when compared with the dense time-step solution, while the other two with smaller time steps show good agreement. A comparison between these contours and Kirkland et al.'s results shown in Figure 5.11 reveals an acceptable agreement, which verifies the correctness of these solutions. However, it is worth noting that Kirkland et al.'s results appear to be more diffuse than the present solutions, which can be seen from the relatively larger intervals between the contours of pressure head 0 m and -400 m in Figure 5.11 compared with those in Figure 5.12. This could be the effect of the proposed transformation method as the sharpness of the wetting front can be alleviated, thus a more accurate solution can be obtained by using the same spatial discretization. The higher sharpness of the present solutions can also be identified in comparison with Diersch and Perrochet's results, shown in Figure 5.14.

Figure 5.13 shows the pressure head contour results at 1 day of ATUR1 method. These results are found to be indistinguishable from the dense time-step

solution. It shows that the tolerances of Case 1 is enough to get correct solutions. Table 5.13 shows the computational efforts of ATUR1 approach. It can be seen that the adaptive ATUR1 method is more efficient than the fixed time-step TUR1 method, as it takes only 489 s to get acceptable results compared to 1369 s of TUR1 method with time-step size of 60 s.

5.4 Experimental Verification

In this section, a two-dimensional (2D) infiltration example (Vauclin et al., 1979) is analyzed to assess the performance of TUR1 on real 2D problems. The geometry and the boundary conditions are shown in Figure 5.15.

In this problem, a fine river sand of fairly regular grain-size distribution is used as the porous medium. To define the hydraulic properties, different constitutive relations from previous studies are used to interpolate the soil-water characteristic curve and the hydraulic conductivity function.

The soil-water characteristic curve is defined as

$$\theta = \theta_s \frac{\alpha}{\alpha + |h|^{\beta}} \tag{5.2}$$

in which

θ = volumetric water content;

$\theta_s = 0.30$ cm^3/cm^3, the saturated volumetric water contents;

$\alpha = 40000$;

$\beta = 2.90$.

The hydraulic conductivity function is defined as

$$K = K_s \frac{A}{A + |h|^B} \tag{5.3}$$

in which

K = the hydraulic conductivity;

K_s = 35 cm/hr, the saturated hydraulic conductivity;

$A = 2.99 \times 10^6$;

$B = 5.0$.

The nonlinear soil hydraulic characteristics for this chosen soil type are shown in Figures 5.16 and 5.17.

Following the proposed criteria discussed perviously, we choose an intermediate value of β to be 0.20 cm^{-1} as long as the K^* curve is still monotonic.

In the following studies, 8-noded quadrilateral elements are adopted. Ju and Kung (1997) found that such quadratic elements could cause oscillation with both consistent mass and lumped mass schemes. Thus, to curb potential oscillation problems, the minimum time-step criteria is adopted. To use the criteria in Table 3.1 to determine the minimum time-step, the slope m_w of the soil-water characteristic curve and the permeability value k of the soil have to be established. As discussed before, they are derived from the initial dry state of the soil, and the critical values for both parameters correspond to a point where the matric suction is the highest. For this problem, and with the initial condition described, λ which equals to the product of m_w and γ_w is computed to be 0.000674 cm^{-1}, and k has a value of 0.0166 cm/hr.

Two reasonable element sizes of 10 cm $\times$ 10 cm and 5 cm $\times$ 5 cm are used.

The more stringent second criterion in Table 3.1 is adopted and, according to this formula, the minimum time-step to curb oscillation is 0.20 hr and 0.05 hr, respectively.

Table 5.14 shows that because of the convergence deficiency of UR2, it fails to get stable solution for both element sizes and corresponding oscillation-free time steps. On the other hand, UR1 and TUR1 can get stable solutions with these two reasonable element sizes. A comparison between experimental and numerical results is shown in Figures 5.18 to 5.21. It is showed that with reasonable element sizes, big errors were observed in the solutions of UR1 which makes it unacceptable from the practical view. On the contrary, TUR1 can get more accurate solutions than UR1. The accuracy is good enough to be used in the computation of other important design variables, such as the factor of safety of an embankment slope against translational and/or rotational failure.

5.5 Concluding Remarks

In this chapter, a number of two-dimensional examples are analyzed, using the improved numerical methods presented in previous chapters. These examples are chosen from the literature, with homogeneous or heterogenous materials. The robustness and efficiency of the proposed TUR1 and ATUR1 methods are demonstrated against traditional and alternative solution strategies. It is showed that these improved approaches are robust in complex problems with both very dry and variably saturated condition in homogenous or heterogeneous soils. The TUR1 method with the automatic time stepping scheme appears to be more efficient

than the fixed time-step schemes as acceptable results can be obtained using the least computational cost.

Table 5.1: One-dimensional infiltration problems

Variable		Problem A	Problem B	Problem C	Problem D
Medium Properties					
θ_r		0.045	0.057	0.078	0.095
θ_s		0.430	0.410	0.430	0.410
a	m^{-1}	14.5	12.4	3.60	1.90
n		2.680	2.280	1.560	1.310
K_s	md^{-1}	7.128	3.502	0.250	0.062
β	m^{-1}	-1.5	-3	-4.5	-3
Boundary Conditions					
$h(z, t = 0)$	m	-8	-8	-8	-8
$h(z = 1, t)$	m	0	0	0	0
$h(z = 0, t)$	m	-8	-8	-8	-8
Calculation Domain					
z	m	[0, 5.0]	[0, 5.0]	[0, 5.0]	[0, 5.0]
t	d	[0, 0.12]	[0, 0.225]	[0, 2.25]	[0, 5]
Discretizations					
Δz	m	0.0125	0.0125	0.0125	0.0125
		0.1	0.1	0.1	0.1
Δt	d	1.0×10^{-4}	1.5×10^{-4}	3.0×10^{-3}	2.0×10^{-3}
		3.0×10^{-4}	5.0×10^{-4}	9.0×10^{-3}	6.94×10^{-3}
		1.0×10^{-3}	1.5×10^{-3}	3.0×10^{-2}	2.0×10^{-2}

Table 5.2: Results of one-dimensional infiltration problem A

Δz (m)	Δt (d)	Approaches	L_2 error (m)	Run time (s)
0.0125	1.0×10^{-4}	UR1	5.86	18.03
		UR2	5.85	18.06
		TUR1	2.52	42.76
	3.0×10^{-4}	UR1	5.86	9.72
		UR2	5.85	9.97
		TUR1	2.25	20.33
	1.0×10^{-3}	UR1	5.88	3.32
		UR2	5.70	5.86
		TUR1	3.36	11.50
0.1	1.0×10^{-4}	UR1	5.92	2.08
		UR2	5.92	2.06
		TUR1	2.74	4.73
	3.0×10^{-4}	UR1	5.92	0.7
		UR2	5.92	0.7
		TUR1	2.74	2.01
	1.0×10^{-3}	UR1	5.92	0.22
		UR2	5.92	0.22
		TUR1	2.90	0.83

Table 5.3: Results of one-dimensional infiltration problem B

Δz (m)	Δt (d)	Approaches	L_2 error (m)	Run time (s)
0.0125	1.5×10^{-4}	UR1	Fail	
		UR2	Fail	
		TUR1	0.83	52.63
	5.0×10^{-4}	UR1	4.97	12.54
		UR2	Fail	
		TUR1	0.97	23.63
	1.5×10^{-3}	UR1	Fail	
		UR2	Fail	
		TUR1	1.43	15.08
0.1	1.5×10^{-4}	UR1	5.33	2.52
		UR2	5.33	2.50
		TUR1	0.71	5.84
	5.0×10^{-4}	UR1	5.33	0.77
		UR2	5.33	0.77
		TUR1	0.88	2.12
	1.5×10^{-3}	UR1	5.33	0.52
		UR2	5.33	0.52
		TUR1	1.11	0.95

Notes: "Fail" means "does not converge in 1000 iterations".

Table 5.4: Results of one-dimensional infiltration problem C

Δz (m)	Δt (d)	Approaches	L_2 error (m)	Run time (s)
0.0125	3.0×10^{-3}	UR1	0.79	25.67
		UR2	0.73	47.49
		TUR1	0.11	32.10
	9.0×10^{-3}	UR1	Fail	
		UR2	0.79	34.72
		TUR1	0.37	16.36
	3.0×10^{-2}	UR1	3.78	2.91
		UR2	Fail	
		TUR1	0.43	6.81
0.1	3.0×10^{-3}	UR1	2.00	3.00
		UR2	1.96	3.50
		TUR1	0.17	3.37
	9.0×10^{-3}	UR1	2.23	1.86
		UR2	1.94	2.61
		TUR1	0.11	1.50
	3.0×10^{-2}	UR1	Fail	
		UR2	Fail	
		TUR1	0.13	0.65

Notes: "Fail" means "does not converge in 1000 iterations".

Table 5.5: Results of one-dimensional infiltration problem D

Δz (m)	Δt (d)	Approaches	L_2 error (m)	Run time (s)
0.0125	2.0×10^{-3}	UR1	1.01	55.29
		UR2	1.00	55.48
		TUR1	0.40	62.74
	6.94×10^{-3}	UR1	0.36	23.53
		UR2	1.68	32.25
		TUR1	0.39	27.04
	2.0×10^{-2}	UR1	1.33	11.91
		UR2	1.29	19.22
		TUR1	0.28	13.19
0.1	2.0×10^{-3}	UR1	1.86	7.98
		UR2	1.86	7.98
		TUR1	0.44	8.56
	6.94×10^{-3}	UR1	1.89	2.60
		UR2	1.87	2.98
		TUR1	0.48	2.84
	2.0×10^{-2}	UR1	Fail	
		UR2	1.88	2.29
		TUR1	0.63	1.37

Notes: "Fail" means "does not converge in 1000 iterations".

Table 5.6: Soil properties for Forsyth et al.'s problem

Variable		Zone 1	Zone 2	Zone 3	Zone 4
θ_r		0.102	0.0985	0.0859	0.0859
θ_s		0.368	0.351	0.325	0.325
a	m^{-1}	3.34	3.63	3.45	3.45
n		1.982	1.632	1.573	1.573
K_s	ms^{-1}	9.153×10^{-5}	5.445×10^{-5}	4.805×10^{-5}	4.805×10^{-4}

Table 5.7: Performances of fixed time-step approaches for Forsyth et al.'s problem

Approaches	Δt (s)	Total Runtime (s)
UR1	86400	Fail
	28800	Fail
	8640	Fail
UR2	86400	Fail
	28800	Fail
	8640	Fail
TUR1	86400	20.87
	28800	46.16
	8640	118.04

Notes: "Fail" means "does not converge in 1000 iterations".

Table 5.8: Performances of adaptive approaches for Forsyth et al.'s problem

Approaches	Cases	$\tau_A(m)$	τ_R	Total Runtime (s)
ATUR1	Case 1	1	1	28.84
	Case 2	0.5	0.5	35.83
	Case 3	0.1	0.1	74.19

Table 5.9: Soil properties for Kirkland et al.'s problem

Variable		Sand	Clay
θ_r		0.0286	0.1060
θ_s		0.3658	0.4686
a	m^{-1}	2.80	1.04
n		2.239	1.3954
K_s	ms^{-1}	6.262×10^{-5}	1.516×10^{-6}

Table 5.10: Performances of the fixed time-step approaches for Kirkland et al.'s problem 1

Approaches	Δt (s)	Total Runtime (s)
UR1	3600	Fail
	1200	Fail
	600	Fail
UR2	3600	Fail
	1200	Fail
	600	Fail
TUR1	3600	Fail
	1200	829.28
	600	1469.42

Notes: "Fail" means "does not converge in 1000 iterations".

Table 5.11: Performances of the adaptive approaches for Kirkland et al.'s problem 1

Approaches	Cases	$\tau_A(m)$	τ_R	Total Runtime (s)
ATUR1	Case 1	5.0	0.5	441.17
	Case 2	1.0	0.1	667.44
	Case 3	0.1	0.01	1237.29

Table 5.12: Performances of the fixed time step approaches for Kirkland et al.'s problem 2

Approaches	Δt (s)	Total Runtime (s)
UR1	120	Fail
	60	Fail
	30	Fail
UR2	120	Fail
	60	Fail
	30	Fail
TUR1	120	855.22
	60	1369.24
	30	2596.93

Notes: "Fail" means "does not converge in 1000 iterations".

Table 5.13: Performances of the adaptive approaches for Kirkland et al.'s problem 2

Approaches	Cases	$\tau_A(m)$	τ_R	Total Runtime (s)
ATUR1	Case 1	5.0	0.5	489.48
	Case 2	1.0	0.1	771.80
	Case 3	0.1	0.01	1592.14

Table 5.14: Results of two-dimensional infiltration problems (elapased time 2 hr)

Approaches	Element size (cm)	Time-step (hr)	Total Iterations
UR1	10 × 10	0.20	165
	5 × 5	0.05	532
UR2	10 × 10	0.20	Fail
	5 × 5	0.05	Fail
TUR1	10 × 10	0.20	89
	5 × 5	0.05	850

Notes: "Fail" means "does not converge in 1000 iterations".

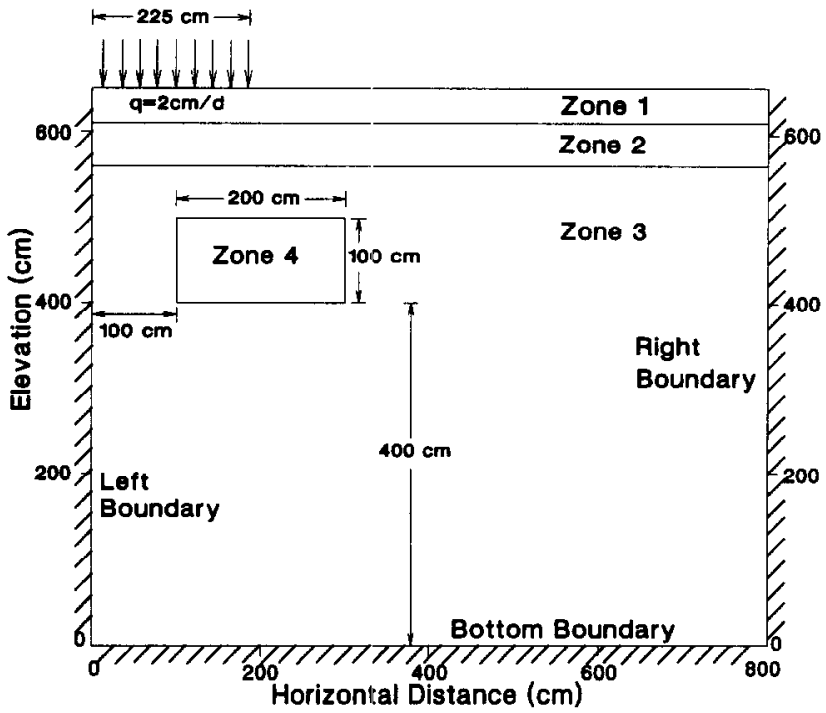

Figure 5.1: Forsyth et al.'s infiltration problem (Forsyth et al., 1995)

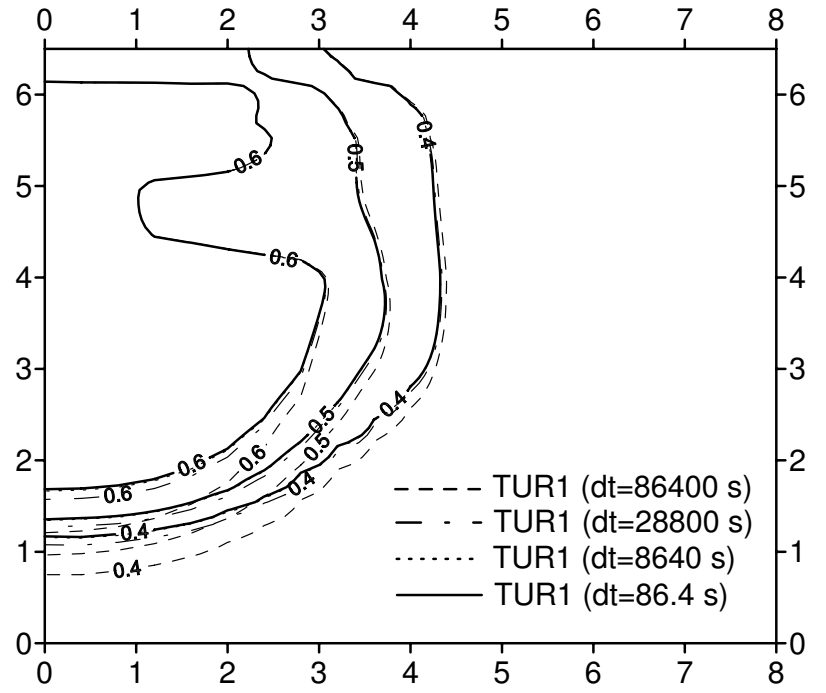

Figure 5.2: Saturation contours of TUR1 method for Forsyth et al.'s problem (dimensions in meter)

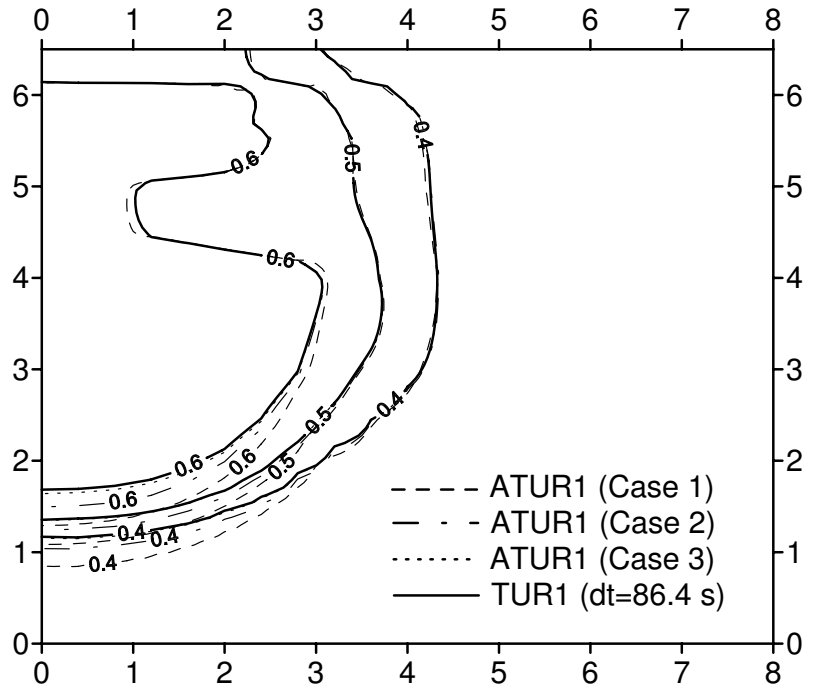

Figure 5.3: Saturation contours of ATUR1 method for Forsyth et al.'s problem (dimensions in meter)

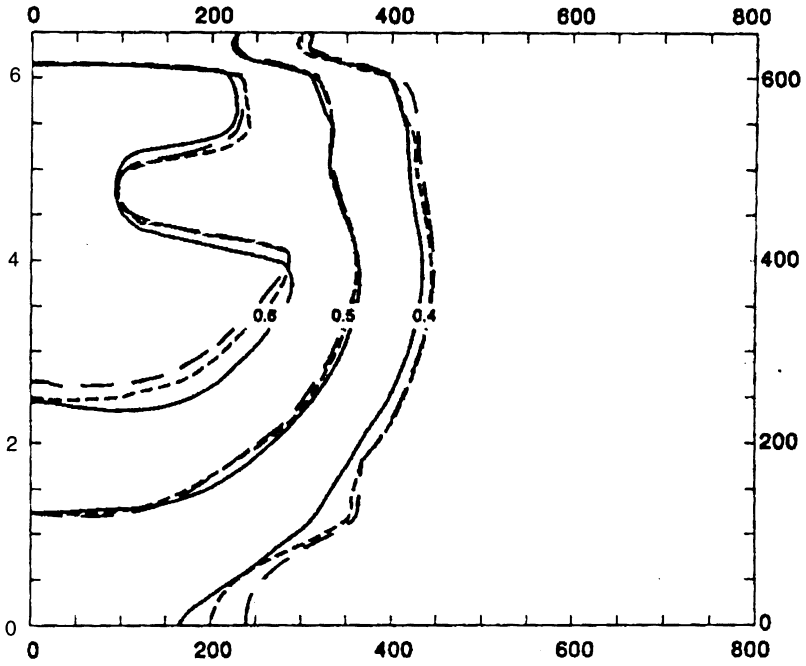

Figure 5.4: Saturation contours of Forsyth et al.'s results (Forsyth et al., 1995)

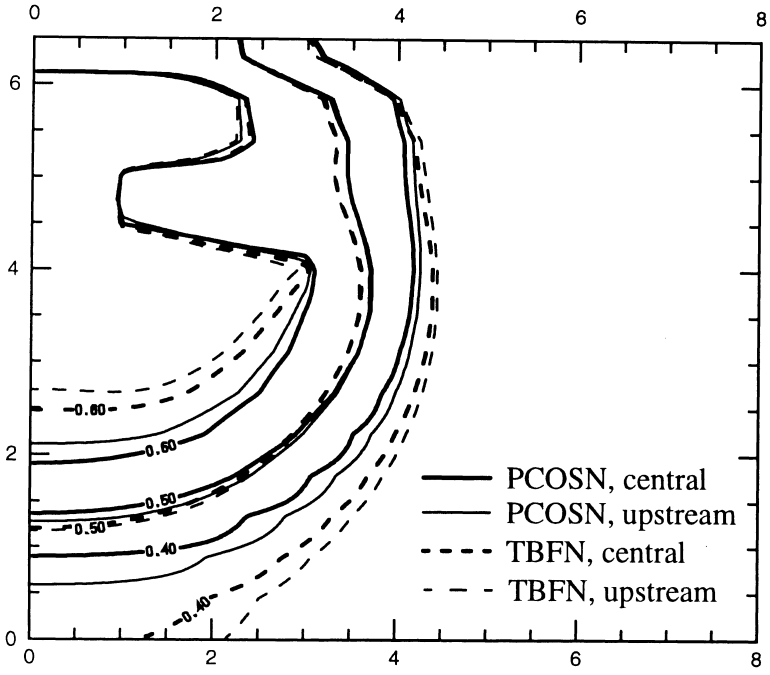

Figure 5.5: Saturation contours of Diersch and Perrochet's results (Diersch and Perrochet, 1999)

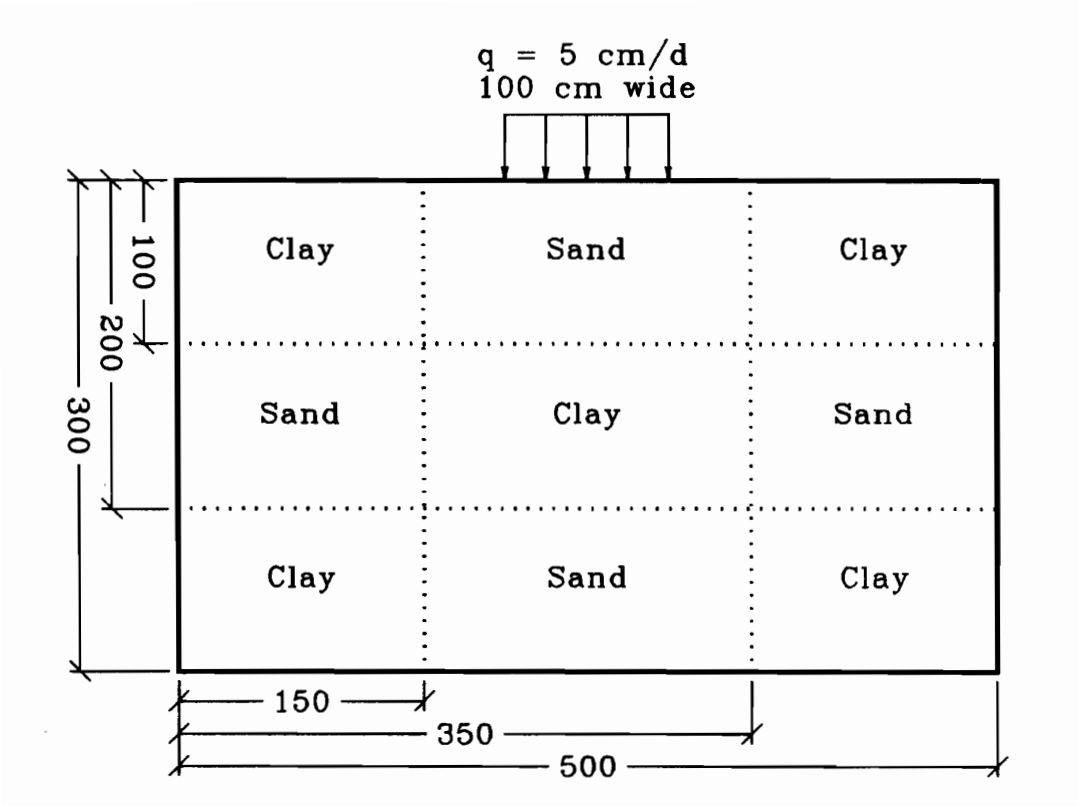

Figure 5.6: Kirkland et al.'s infiltration problem 1 (Kirkland et al., 1992)

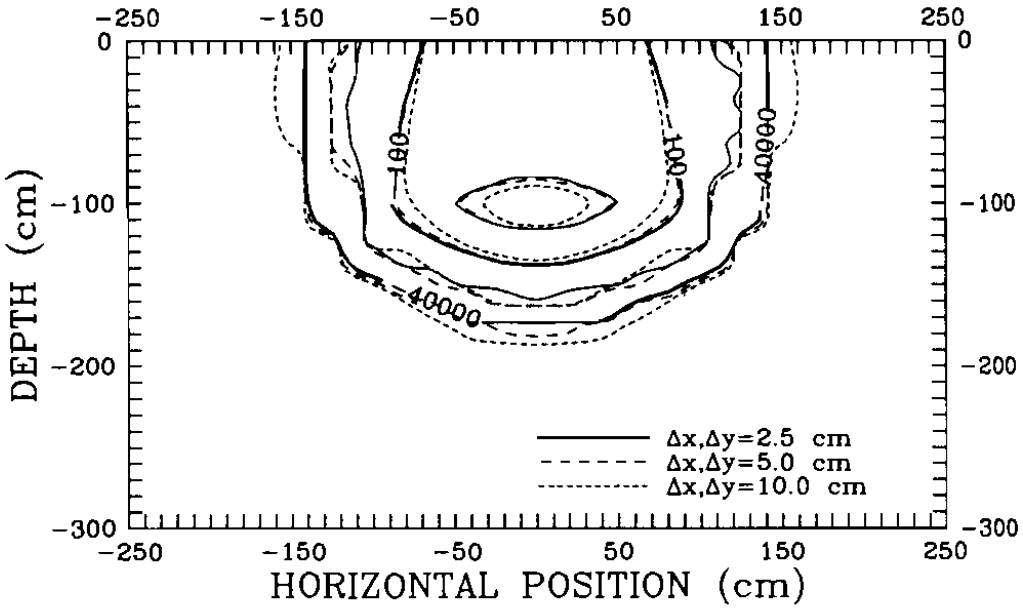

Figure 5.7: Pressure head contours of Kirkland et al.'s results (Kirkland et al., 1992)

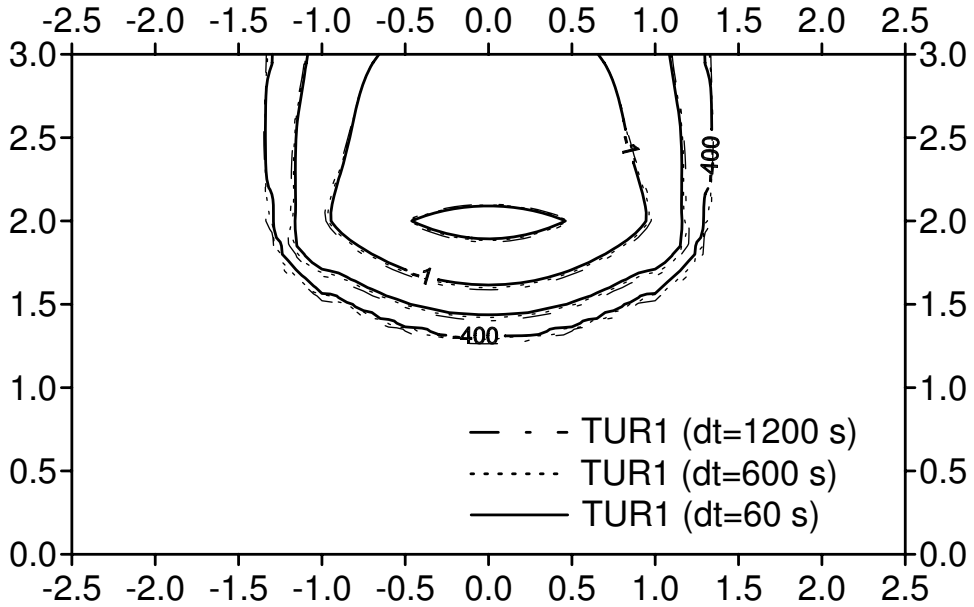

Figure 5.8: Pressure head contours of TUR1 method for Kirkland et al.'s infiltration problem 1 (dimensions in meter)

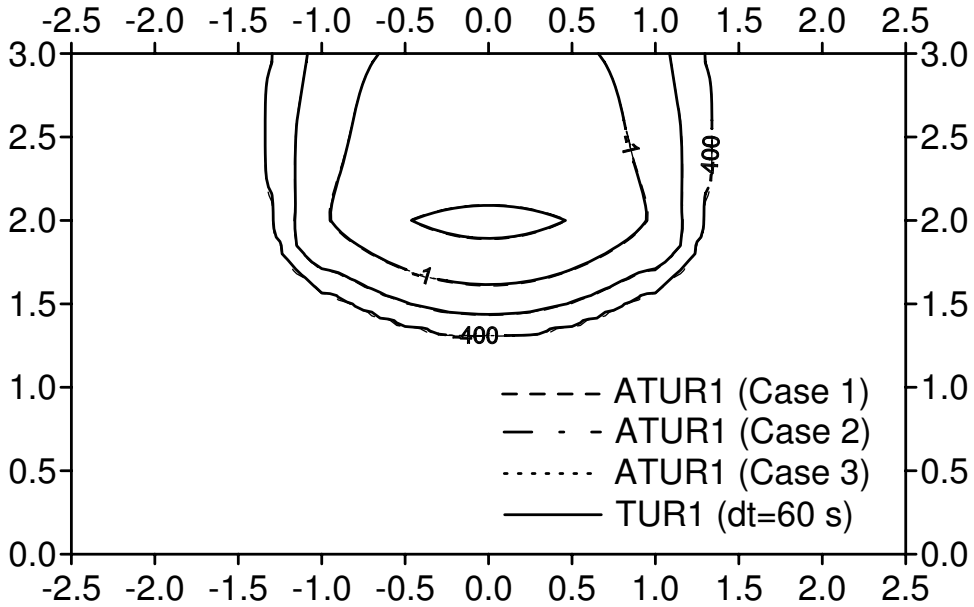

Figure 5.9: Pressure head contours of ATUR1 method for Kirkland et al.'s infiltration problem 1 (dimensions in meter)

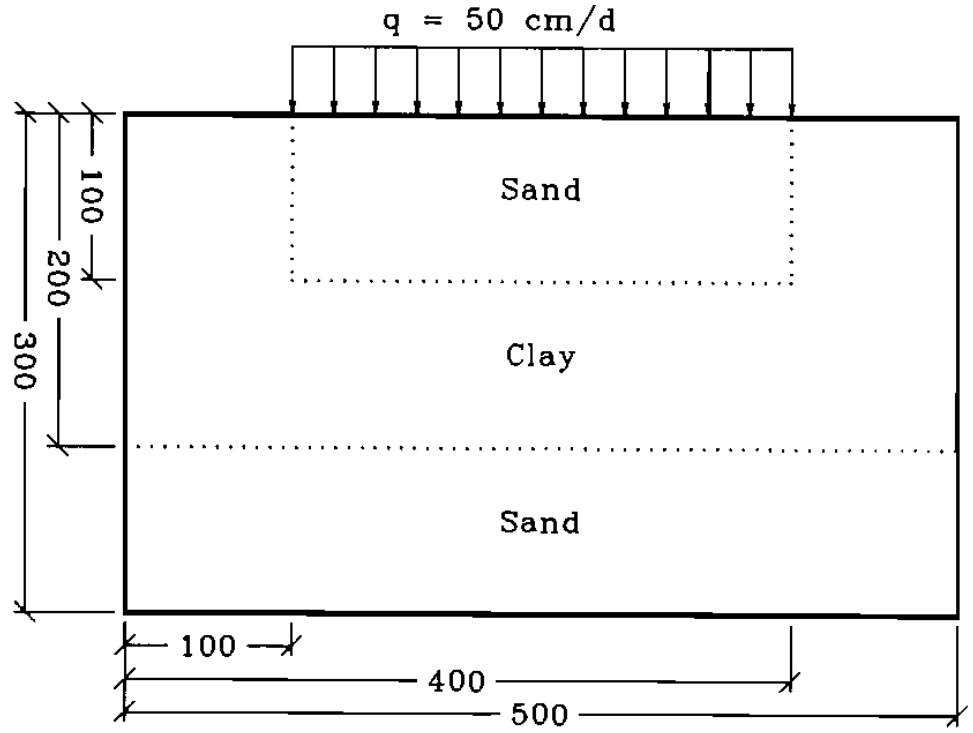

Figure 5.10: Kirkland et al.'s infiltration problem 2 (Kirkland et al., 1992)

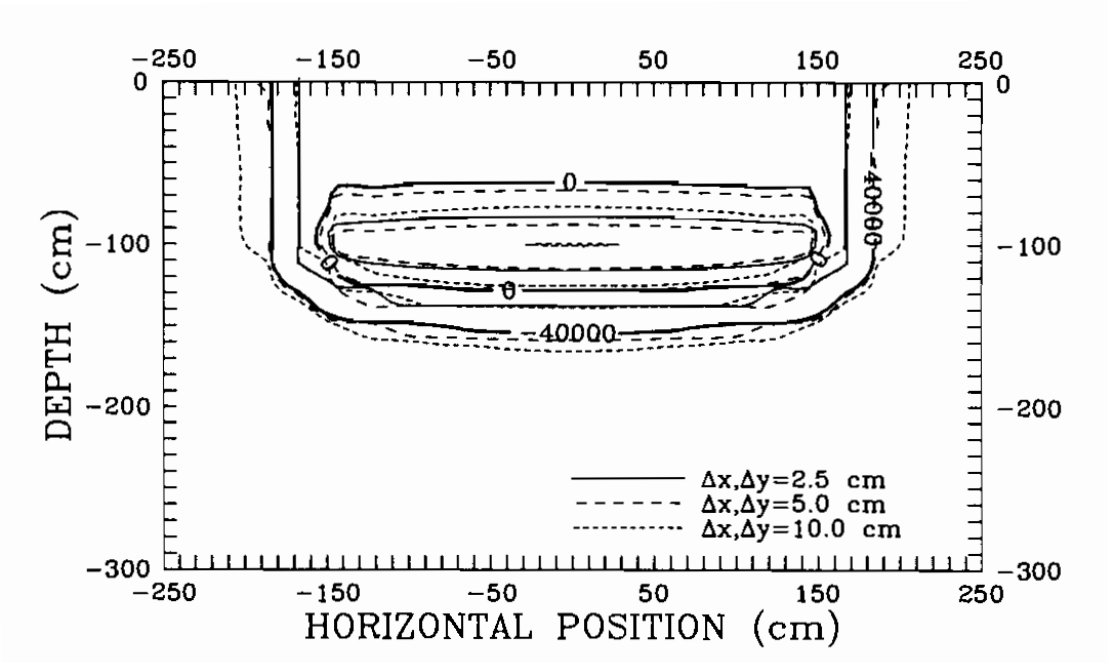

Figure 5.11: Pressure head contours of Kirkland et al.'s results (Kirkland et al., 1992)

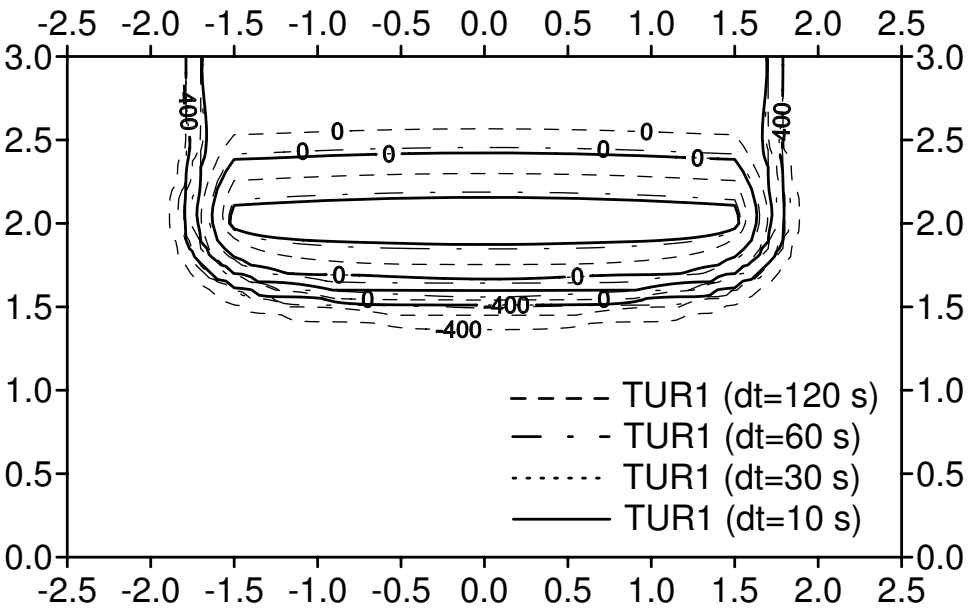

Figure 5.12: Pressure head contours of TUR1 method for Kirkland et al.'s infiltration problem 2 (dimensions in meter)

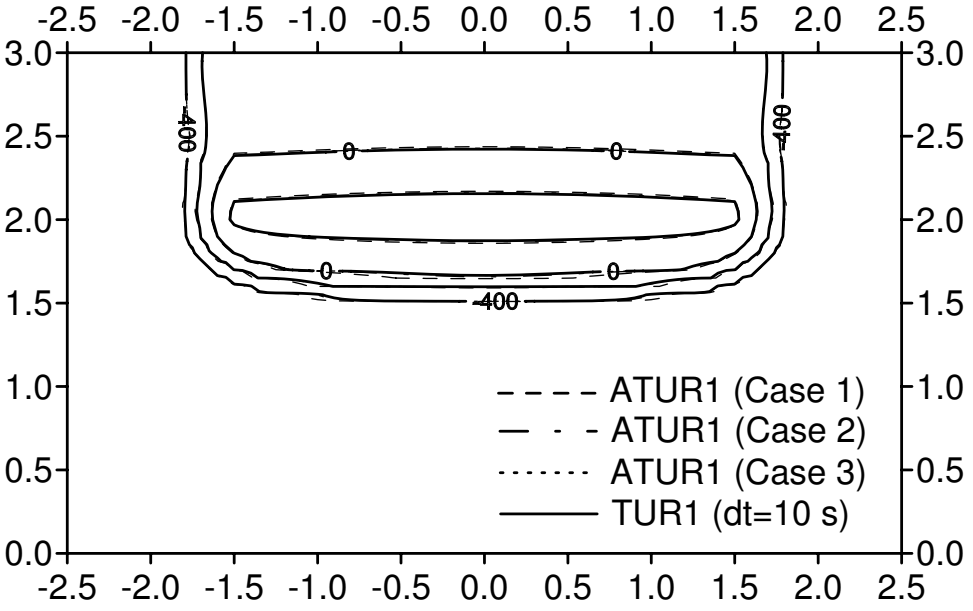

Figure 5.13: Pressure head contours of ATUR1 method for Kirkland et al.'s infiltration problem 2 (dimensions in meter)

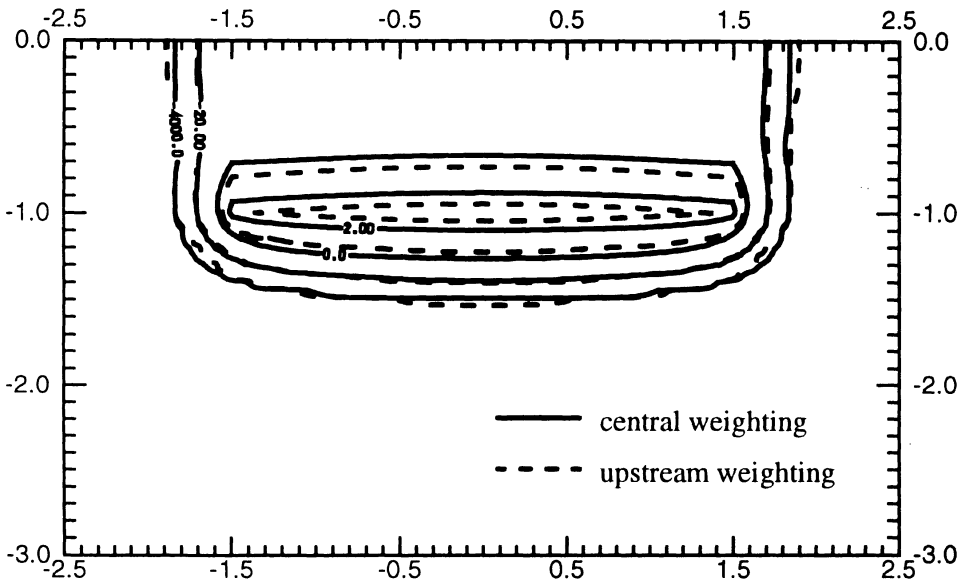

Figure 5.14: Pressure head contours of Diersch and Perrochet's results (Diersch and Perrochet, 1999)

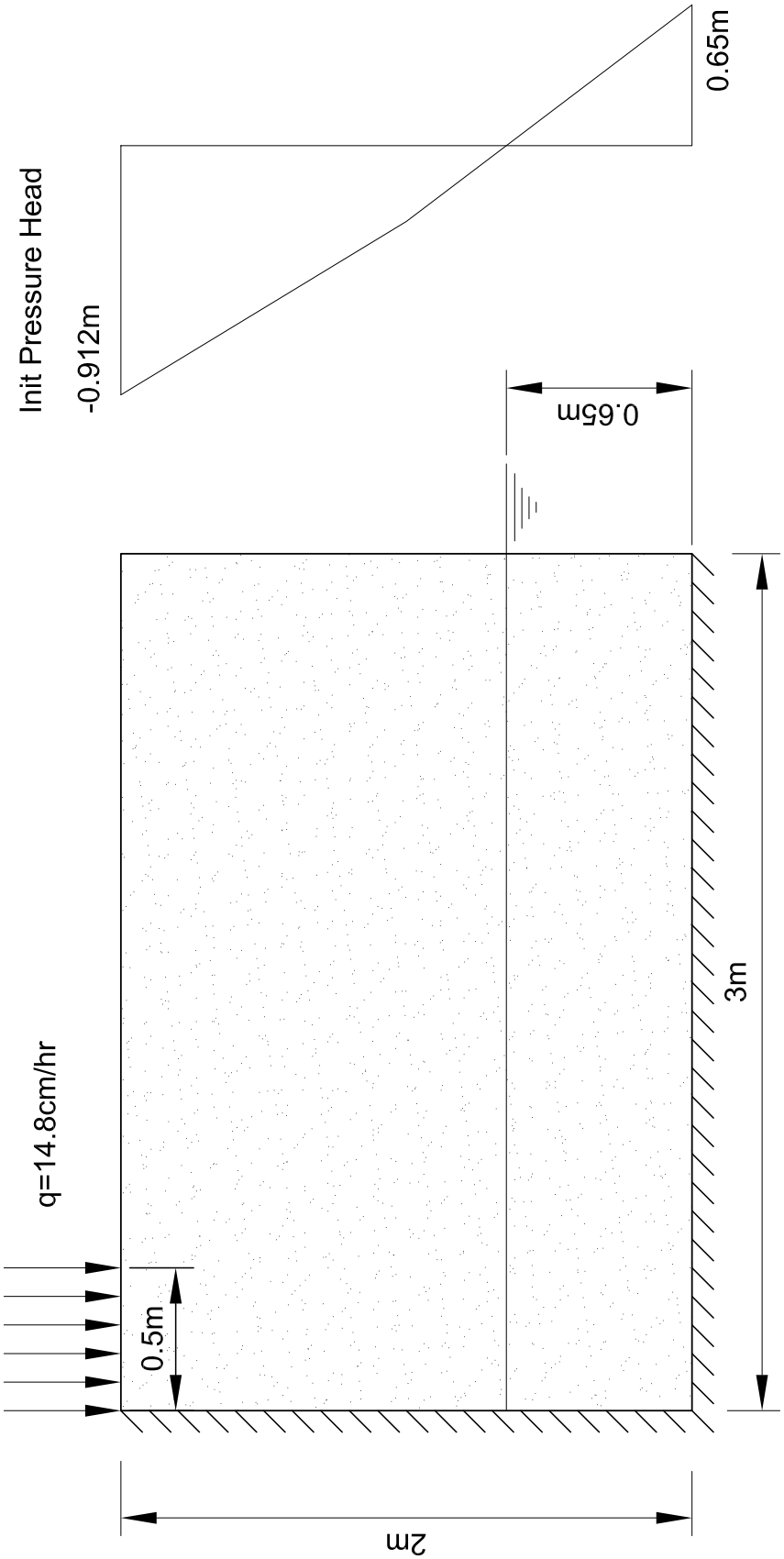

Figure 5.15: Geometry of Two-dimensional infiltration experiment

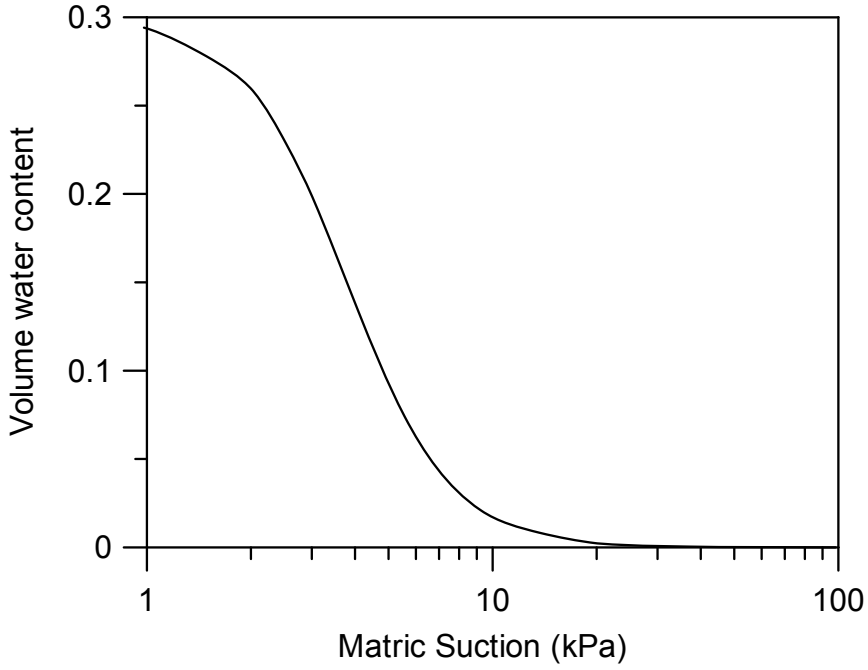

Figure 5.16: Soil-water characteristic curve for two-dimensional infiltration problem

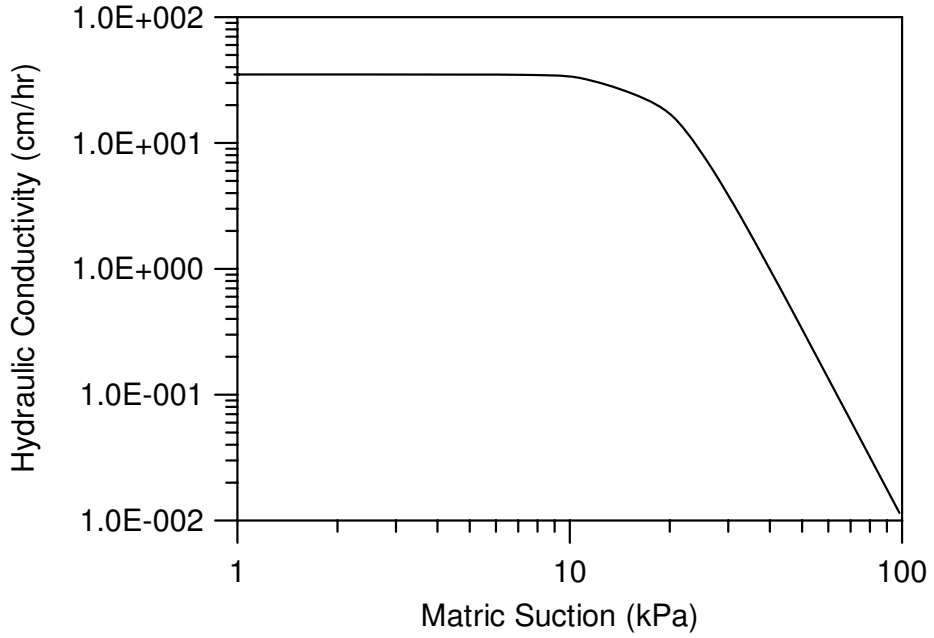

Figure 5.17: Conductivity function for two-dimensional infiltration problem

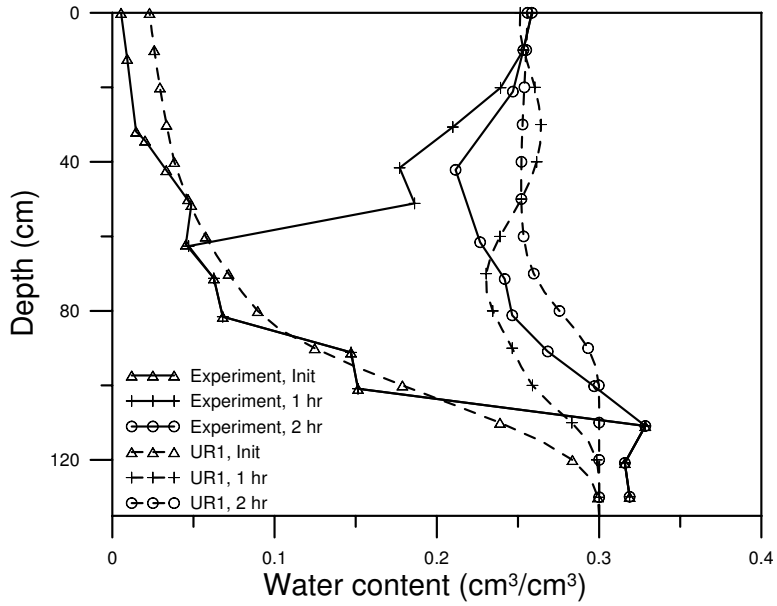

(a) x = 20 cm

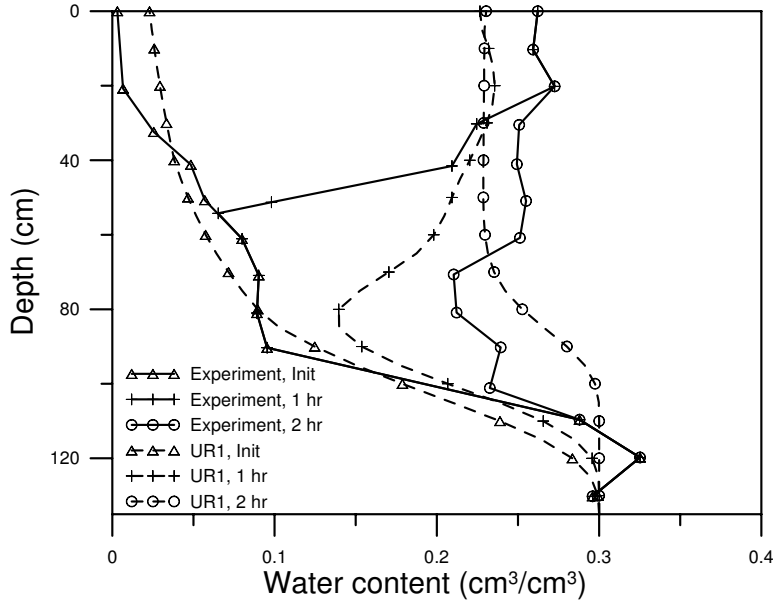

(b) x = 50 cm

Figure 5.18: Water content profiles measured and computed from UR1 with element size of 10 cm × 10 cm at different section for different times

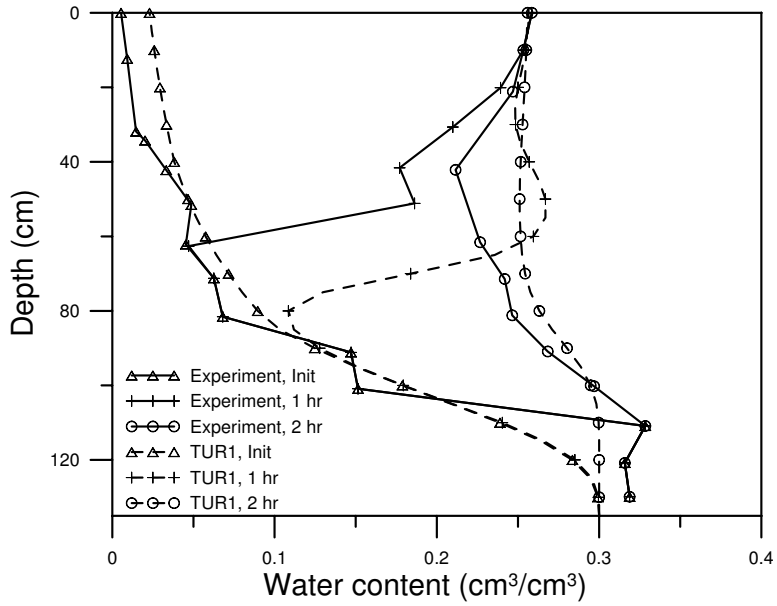

(a) x = 20 cm

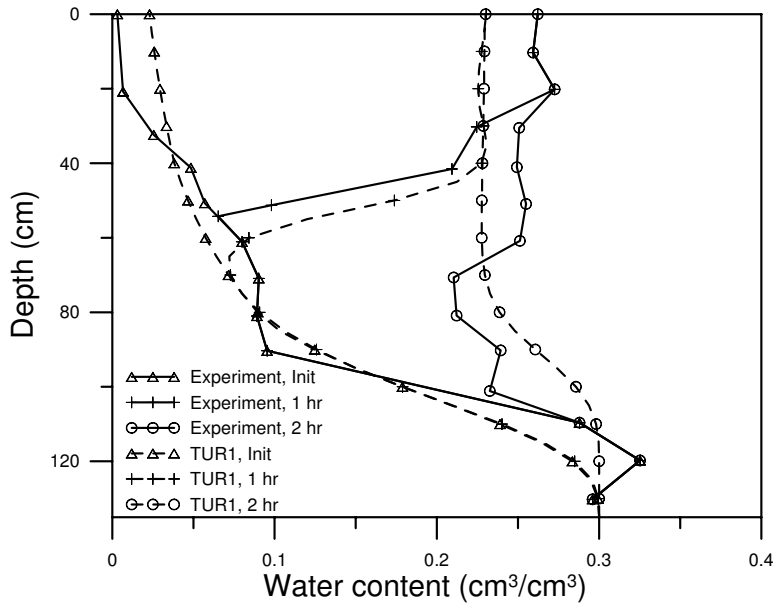

(b) x = 50 cm

Figure 5.19: Water content profiles measured and computed from TUR1 with element size of 10 cm × 10 cm at different section for different times

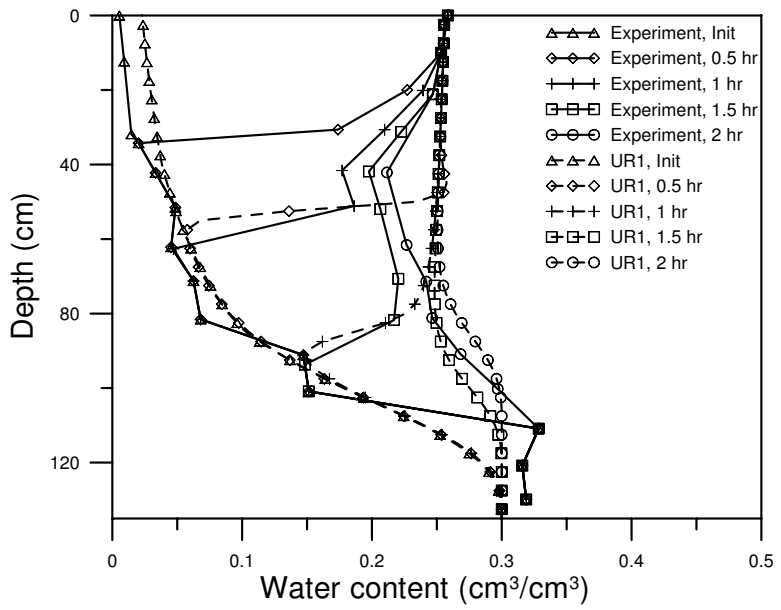

(a) x = 20 cm

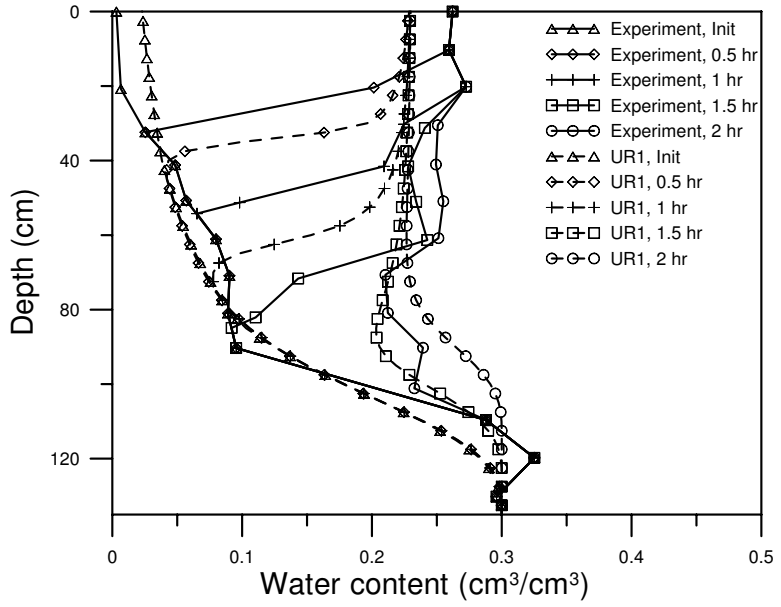

(b) x = 50 cm

Figure 5.20: Water content profiles measured and computed from UR1 with element size of 5 cm × 5 cm at different section for different times

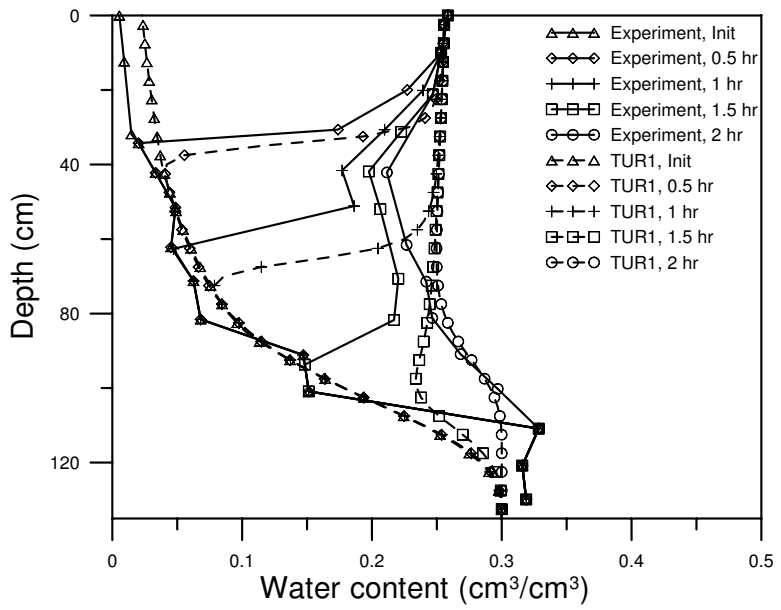

(a) x = 20 cm

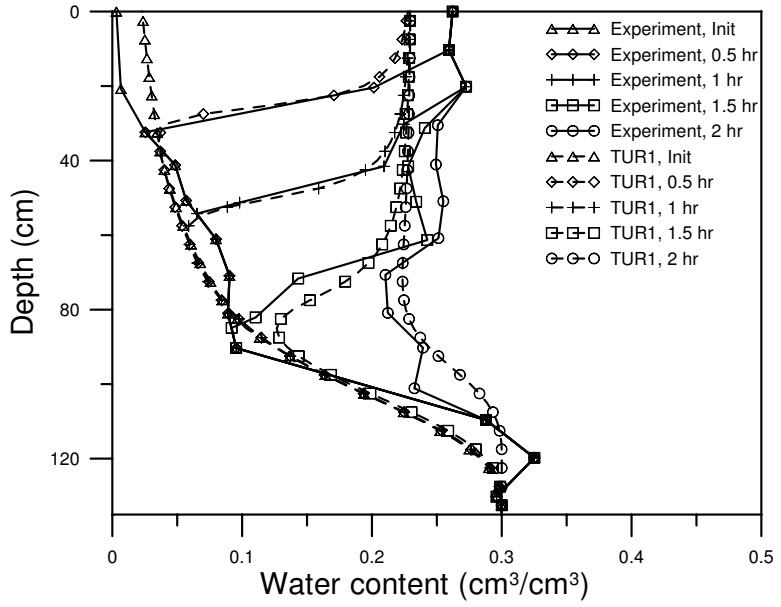

(b) x = 50 cm

Figure 5.21: Water content profiles measured and computed from TUR1 with element size of 5 cm × 5 cm at different section for different times

Chapter 6

Slope Stability Analysis due to Rainfall Infiltration

6.1 Introduction

Shallow failures of slopes due to rainfall infiltration are quite usual in tropical countries such as Singapore. During the rainfall, a wetting front goes deeper into the slope, which results in a gradual increase of the water content and a decrease of the matric suction, which is recognized to contribute towards the stability of unsaturated soil slopes. The loss of suction causes a decrease in shear strength of the soil on the potential failure surface and finally triggers the failure (Rahardjo et al., 1995; Ng and Shi, 1998). Thus, the accurate prediction of the propagating wetting front arising from rainfall infiltration into the unsaturated soil is of considerable importance to slope stability analysis, especially when unusual heavy and prolonged rainfall becomes more frequent due to the global climate changes.

Due to the limitations often exhibited by analytical solutions, to obtain realistic representations of the ground water condition under a transient rainfall situation, numerical methods such as finite element method are often necessary for such unsaturated flow simulations. Many commercial finite element packages are available

for such analyses. Among them, SEEP/W, developed by Geoslope (2004) is one of the most popular programs among engineers (e.g., Rahardjo et al., 2001; Tsaparas, 2002). It is observed in passing that the Green-Ampt and similar simplified models are popular in soil sciences (Green and Ampt, 1911; Cho and Lee, 2002; Kim et al., 2004), but there are fundamental difficulties in these models.

However, as the soil hydraulic properties are highly nonlinear, it has been shown in previous studies that numerical problems like oscillation and slow convergence rate exist in such unsaturated flow analysis. These results can lead to errors in the calculation of slope stability analysis. For example, Karthikeyan (2000) has shown that the oscillation of calculated pressure head around the wetting fronts can leads to serious discrepancy in the computed factor of safety. In view of the fact that results from seepage analyses are often imported directly into slope stability analyses by practicing engineers, it is thus important to investigate and highlight the influence of such numerical errors on the computed factor of safety of the slope.

6.2 Slow Convergence

Previous studies have already shown that slow convergence problem existed in unsaturated seepage analysis using SEEP/W. It is found that the calculated pressure heads converged to a correct solution very slowly with progressive refinement of the element size and time-step. However, in the literature, the effect of different mesh sizes and time-step sizes is not well emphasized and systematic convergence studies are quite rare. Usually, coarse meshes and big time-steps were used in their studies. For example, Rahardjo et al. (2001) used only 424 triangular or quadrilat-

eral elements in a slope stability analysis with the slope height of 35m and width of around 60m. Few of the studies discussed whether the solutions generated with such meshes and time-steps were accurate or not. For slope stability problems in unsaturated residual soils, errors made in the position of the wetting front could seriously affect the location of the failure surface and the eventual factor of safety. Thus, the correctness of numerical solutions obtained using reasonable spatial and temporal discretization schemes based on limited convergence studies is of direct practical concern.

In the following, numerical simulations are carried out to show the effects of different mesh sizes on the calculated pore-water pressure response during rainfall infiltration in a slope and also the influence on the calculation of slope stability. A 10m high slope at an inclination of 26.6° (inclination 2H:1V) is adopted in this study, which is shown in Figure 6.1. The soil properties are defined in Table 6.1. The four parameter van Genuchten model is used here to define the soil-water characteristic curve. The Mualem model is used to define the conductivity function. For the initial condition, a constant negative pressure head of -8 m is defined for the whole domain. To define the boundary condition, a zero pressure head is imposed at the slope surface. This type of boundary condition represents a rainfall greater than the saturated permeability of the soil with the non-infiltrating water taken as runoff. To avoid the oscillation problem, 4-noded quadrilateral element is adopted.

Two different meshes are compared in the following study, as a coarse one with mesh size of 0.5 × 0.5 m (2400 elements) and a dense one of mesh of 0.1 × 0.1 m (60000 elements). The time-step size is chosen to be the same in each case as 3600 sec. It is worth noting that a coarser mesh means less number of degrees of

freedom (2541 DOFs for coarse mesh vs. 60701 DOFs for dense mesh). This results in a smaller set of FEM equation to solve, which further implies fewer operations required for the direct matrix solver in each iteration, as it is reported that for large 2D and 3D problems involving matrices with significant bandwidth, the number of operations required for the direct matrix solver will approach $O(N^3)$ (Press et al., 1986), where N is the number of DOFs. For the specific problem studied here, it is observed that the solution of linear system grows with $N^{1.3}$ because the global matrix is relatively sparse. Therefore, the penalty on total run time becomes significantly heavier for denser mesh, which can be seen from the results of runtime in Table 6.2.

The result of pore-water pressure profiles at the crest of the slope from SEEP/W with different mesh sizes is shown in Figure 6.2. It clearly shows that with a coarse mesh of 0.5 $\times$ 0.5 m, elevations of the wetting fronts are largely over predicted compared to the dense mesh of 0.1 $\times$ 0.1 m. And this overprediction has serious influence on the slope stability calculations, which can be seen in Table 6.2 and Figure 6.4. For example, after 48 hours of rainfall, the wetting front reaches to the elevation of 18.2m with the dense mesh, compared to 19.0m with the coarse mesh. The corresponding factors of safety (FOS) are 1.137 for the dense mesh and 2.295 for the coarse mesh. The FOS for coarse mesh is significantly unconservative!

Note that the "coarse" mesh - 0.5 $\times$ 0.5 m - is already fine for most analyses undertaken by practising engineers. Hence, the error in the prediction of the wetting front is not artificially produced by the choice of an unrealistically coarse mesh. In fact, given that the mesh used by most engineers can be coarser than that shown in Figure 6.1, the error can be viewed as an optimistic estimate.

It also can be seen from Figure 6.2 and Figure 6.3 that with the same coarse mesh, the TUR1 method proposed in Chapter 3 generates much more accurate results than SEEP/W which adopts the UR1 under-relaxation technique. Actually, the calculated depths of wetting fronts from TUR1 are quite close to the dense mesh solution from SEEP/W. This is also true for the calculation of FOS of the slope, which can be seen in Table 6.2 and Figure 6.4. It clearly shows that with a "reasonable" mesh, TUR1 method can generate approximately correct solutions for unsaturated seepage flow problem, and hence more accurate computation of the factor of safety of the slope. A minor disadvantage of TUR1 is that it may requires a few more iterations per time-step to get a stable solution, thus more runtime than UR1 with the same mesh (Table 6.2). But considering the accuracy and efficiency of solutions, the superiority of TUR1 is obvious.

6.3 Positive Pore-water Pressure

In previous studies on numerical simulation of slope stability under rainfall condition, some authors have shown that positive pore-water pressure could develop above the infiltration front in highly permeable soils due to their hydraulic characteristics. For example, in the numerical flow simulation of Tsaparas (2002), positive pore-water pressures behind the wetting front were observed to develop to a value of around 15 kPa at the crest of the slope during a 16-hours heavy rainfall with rainfall intensity of 15 mm/hour for a highly permeable soil with saturated permeability of 1×10^{-4} m/s, which is shown in Figure 6.5. Collins and Znidarcic (2004) also showed that positive pore-water pressure developed in a one-

dimensional infiltration analysis for coarse soils (Figure 6.6). They explained that this positive pore-water pressure development was due to the low permeability of the unsaturated soil as a high gradient was needed to push water into such soils.

However, if homogenous soil is adopted in the infiltration analysis, such positive pore-water pressures could be artificial and doubtful. For example, for the one-dimensional simulation of Collins and Znidarcic (2004), Figure 6.6 shows their pressure head results with such positive water pressure profiles. A, B and C are three points chosen from the pressure head curve for time of 1.8 hr. It clearly shows that these three points are all in the saturated zone. Thus, the water content in the region from point A to C is constant as the saturated water content, and the permeability in this region is also constant as the saturated permeability. The seepage flow in this region is then a simple saturated flow problem. From Darcy's flow law, the flow rate between the points A and B, B and C can be calculated as

$$q_{AB} = K \cdot \frac{H_A - H_B}{z_A - z_B} = K_s \cdot \left\{ \frac{h_A - h_B}{z_A - z_B} + 1 \right\} \tag{6.1a}$$

and

$$q_{BC} = K \cdot \frac{H_B - H_C}{z_B - z_C} = K_s \cdot \left\{ \frac{h_B - h_C}{z_B - z_C} + 1 \right\} \tag{6.1b}$$

where H is the total head; h is the pressure head; and z is the elevation.

However, it can be easily seen from the figure that

$$\frac{h_A - h_B}{z_A - z_B} \neq \frac{h_B - h_C}{z_B - z_C} \tag{6.2a}$$

because

$$\frac{h_A - h_B}{z_A - z_B} \quad < \quad 0 \tag{6.2b}$$

and

$$\frac{h_B - h_C}{z_B - z_C} > 0 \tag{6.2c}$$

thus,

$$q_{AB} \neq q_{BC} \tag{6.3}$$

which obviously contradicts the mass conservative law.

In the following, numerical simulations are carried out using SEEP/W with two different mesh sizes and also TUR1 to show the possible causes of such artificial positive pore-water pressure response during rainfall infiltration and also its influence on the calculation of slope stability. The same slope example in Section 6.2 is adopted. The only change of the parameter is the saturated permeability of the soil. A higher value of 1.0×10^{-5} m/s is chosen here, which is 10 times the previous value.

The result of pore-water pressure profiles at the crest of the slope from SEEP/W with a mesh size of 0.5 m and a time-step size of 360 s is shown in Figure 6.7. Positive pore-water pressures can be observed to develop above the wetting front with the values around 0.5 m. And the maximum positive pressure value increases slowly with time. L'Heureux et al. (2006) also noticed this kind of numerical errors and they demonstrated that it is because inappropriate time stepping scheme was adopted in the simulations with SEEP/W. The adaptive time stepping option called "*nodal heads*" is suggested to be adopted, which scans every node individually in the whole mesh to see if the allowable percent head changes is upheld. The second option, called "*vector norm*", considers all heads simultaneously. This approach usually leads to bigger time-steps and thus is faster for large

mesh problems. However, positive pressure values are shown behind the infiltration front with this scheme. It implies that such numerical errors may be removed by using smaller time-steps. But even with a very small time-step size of 3.6 s, such artificial positive pressures still can be observed in Figure 6.8 with the same mesh, which shows that time-step size is not the only reason.

On the other hand, results with the dense mesh of 0.1 m and time-step size of 360 s are shown in Figure 6.9. No positive values can be found above the wetting fronts. Also, the results from the TUR1 method with the coarse mesh of 0.5 m and time-step size of 360 s, shown in Figure 6.10, do not show apparent positive pressures. These results suggest that this kind of numerical error would be a consequence of the high nonlinearities in the solutions, both spatially and temporally. As such nonlinearities can be reduced by either using a denser mesh or adopting the transformation method, more accurate results then can be obtained by these two options. However, considering the superiority of TUR1 method in efficiency, it is obviously a more attractive choice.

Besides the numerical error appearing as artificial positive pore-water pressures, the results in Figures 6.7, 6.9 and 6.10 also show the problem of slow convergence of wetting fronts when inappropriate mesh size or time-steps are adopted in simulations with SEEP/W. Section 6.2 has already showed the negative effects of such underprediction of depth of wetting fronts on the slope stability analysis. In the following, the effect of the artificial positive pressures behind the infiltration fronts on the calculation of slope stability is studied separately from the slow convergence problem. Figure 6.11 shows artificial pore-water pressure profile results at the crest of the slope, which are modified from the results of SEEP/W with mesh

size of 0.5 m and time-step size of 360 s, shown in Figure 6.7, by simply cutting off all the positive pressures above the wetting fronts to zero. Thus, for a given rainfall time, the pressure head distributions in these two figures are of the same depth, and the only difference is with or without positive values behind the wetting fronts. Slope stability calculation results with these two pore-water pressure profiles are given in Table 6.3. Much smaller FOS values are obtained for solutions with such artificial positive pressures than those without them, even if the depth of the wetting fronts are the same. The differences in FOS values between these two profiles can be as high as 20%.

Some field investigations on slopes under rainfall conditions also revealed that positive pore-water pressures can develop in the top layer of the slope (Tsaparas, 2002; Matsushi, 2006). However, this phenomenon should not be confused with the numerical errors discussed above. In fact, such positive water pressures develop because soils in the top layer of the slope are usually much more permeable than those in the lower layers, which could be due to the presence of grass roots or surficial weathering. During the rainfall, the infiltration front reaches the bottom of the top layer quickly, but then it is difficult to infiltrate further deeper due to the much lower permeability of soils at larger depth. Thus, the rainfall water accumulates in the top layer of the slope, which forms a saturated zone with positive pore-water pressures. The above discussion implies that in order to carry out more realistic simulations of field cases, more accurate soil parameters for the whole domain should be adopted.

6.4 Concluding Remarks

Accurate simulation of the rainfall-induced infiltration into unsaturated soils is of considerable importance to slope stability analysis. When rainfall water infiltrates the unsaturated soils, the negative pore-water pressures start to increase. The loss of such negative pore-water pressures decreases the shear strength of the soils along the potential failure surface. However, due to the high nonlinearity appeared in unsaturated hydraulic properties of soils, numerical problems such as oscillated wetting fronts, overprediction of the infiltration and artificial positive pore-water pressures above the infiltration fronts exist in such unsaturated seepage flow analysis. In this chapter, two typical numerical errors which are sometimes not well emphasized in the literature were studied. Numerical results show that such numerical errors could be a result of inappropriate mesh size or time-step size adopted in simulations. These errors in unsaturated flow analysis, including the overprediction of the wetting fronts and artificial positive pore-water pressure values above the infiltration fronts, have serious influence on the slope stability calculations. Furthermore, as the nonlinearity of solutions can be reduced by either using a denser mesh and smaller time-steps or adopting the transformation method, more accurate results can be produced by these two options. However, considering the superiority of TUR1 method in efficiency, it is obviously a more attractive choice.

Table 6.1: Summary of soil properties

Hydraulic parameters	θ_s	θ_r	a (m^{-1})	n	K_s (ms^{-1})
	0.363	0.186	1.000	1.53	1.0×10^{-6}
Strength parameters	Saturated unit weight (kN/m^3)	Unsaturated unit weight (kN/m^3)	c' (kN/m^3)	ϕ' (°)	ϕ^b (°)
	20	19	1	25	25
Notes:	*θ_s, θ_r, a, n, K_s are hydraulic parameters in van Genuchten and Mualem models;* *c', ϕ' are effective cohesion and effective angle of internal friction;* *ϕ^b is friction angle with respect to the matric suction.*				

Table 6.2: Results of slope safety factors and total runtime

Real time (hours)		Initial	12	24	36	48	60	72
Coarse mesh (SEEP/W)	Total runtime (seconds)	0	9	15	21	31	39	47
	Safety factor	2.768	2.726	2.704	2.675	2.295	1.856	1.023
Dense mesh (SEEP/W)	Total runtime (seconds)	0	368	848	1668	3448	5200	7080
	Safety factor	2.768	2.727	1.874	1.149	1.137	1.095	1.074
Coarse mesh (TUR1)	Total runtime (seconds)	0	10	20	31	42	53	64
	Safety factor	2.768	2.658	2.213	1.273	1.126	1.125	1.086

Table 6.3: Results of slope safety factors w/ or w/o the artificial positive pressures

Real time (hours)	6	8	10	12
Safety factors w/ artificial positive pressures	2.139	0.960	0.968	0.944
Safety factors w/o artificial positive pressures	2.188	1.171	1.171	1.123

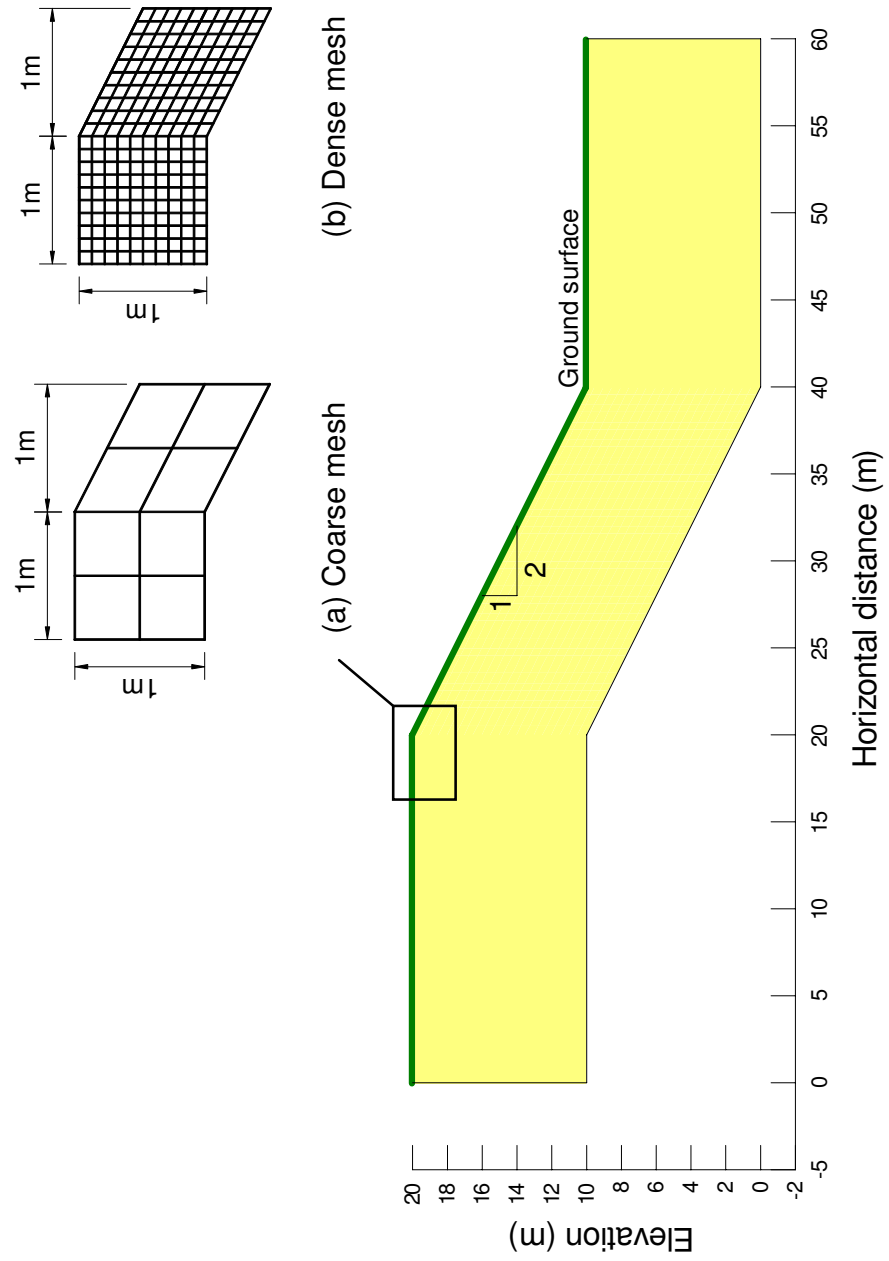

Figure 6.1: Geometry and finite element mesh of the slope used for stability analysis

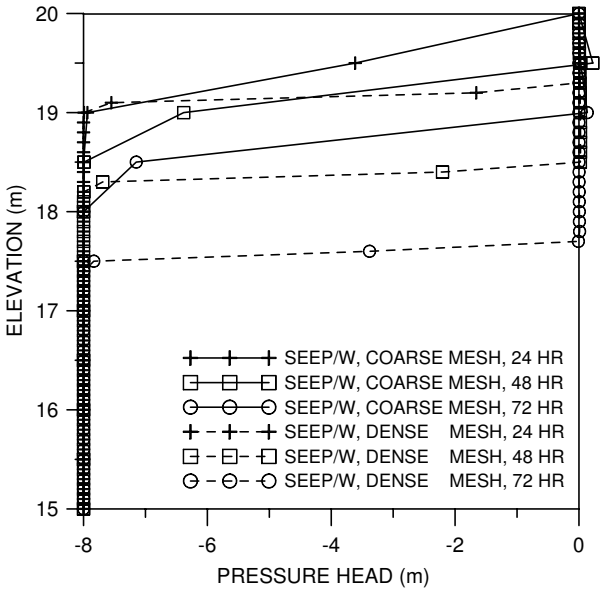

Figure 6.2: Pore-water pressure profiles at the crest of the slope from SEEP/W with different mesh sizes

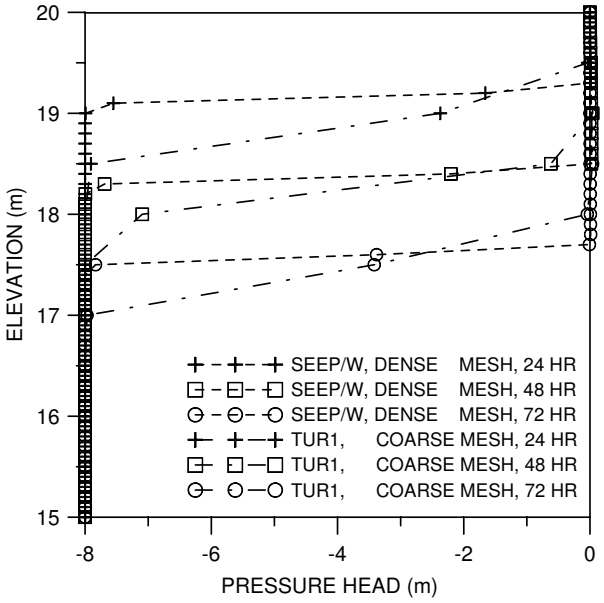

Figure 6.3: Pore-water pressure profiles at the crest of the slope from SEEP/W and TUR1 with different mesh sizes

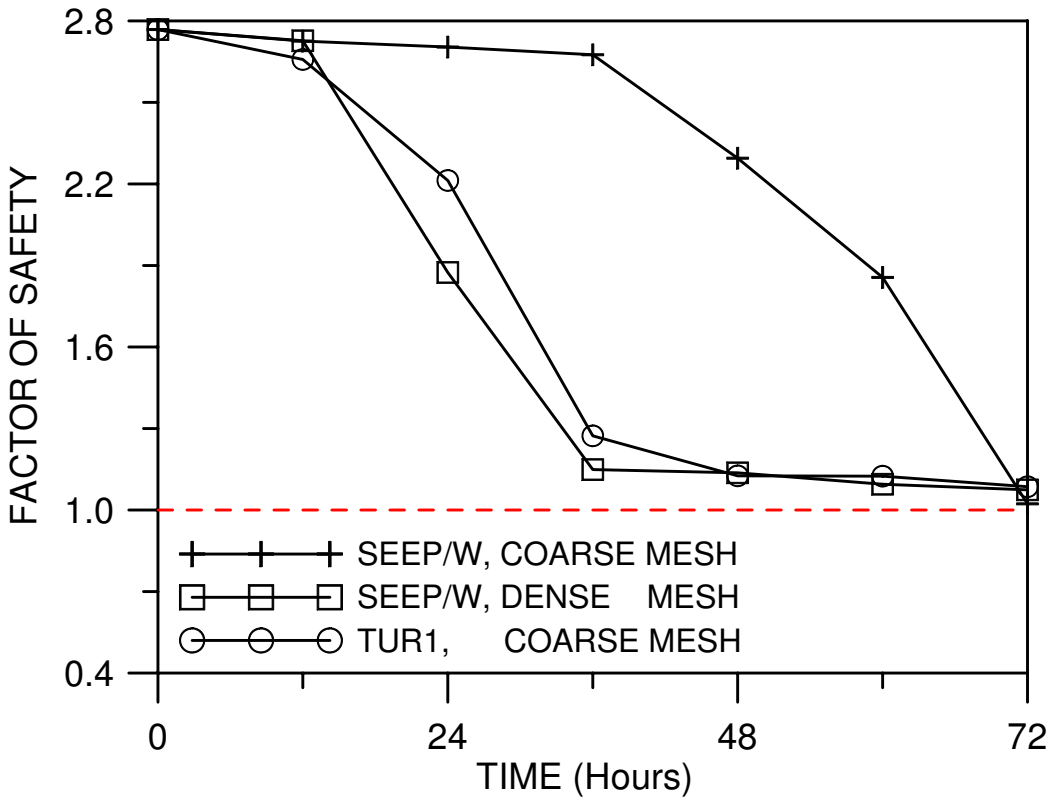

Figure 6.4: Change of slope factor of safety with time

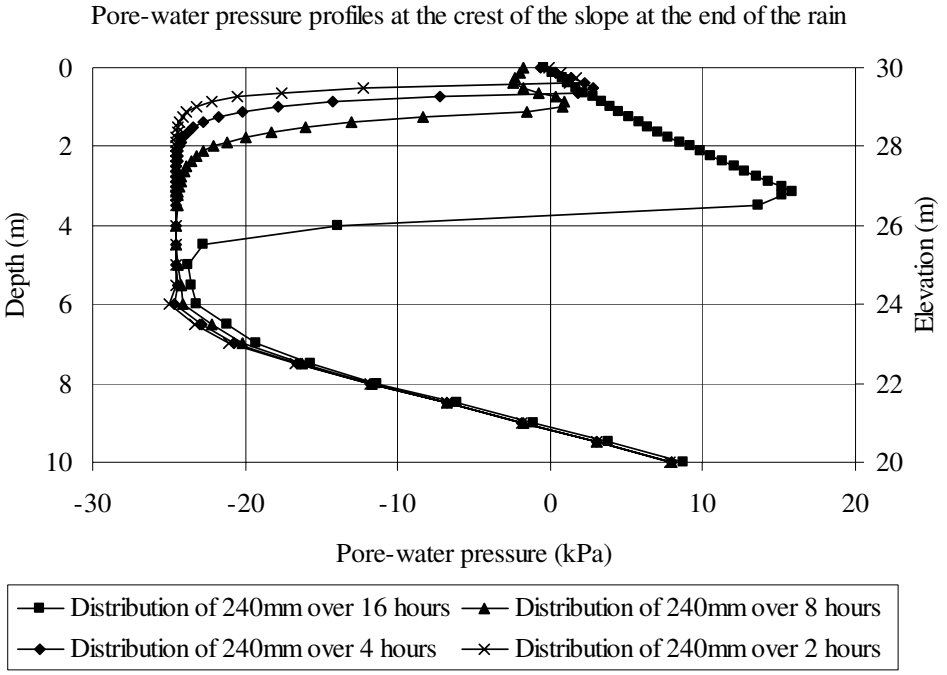

Figure 6.5: Pore-water pressure profiles at the crest of the slopes at the end of the rain (Tsaparas, 2002)

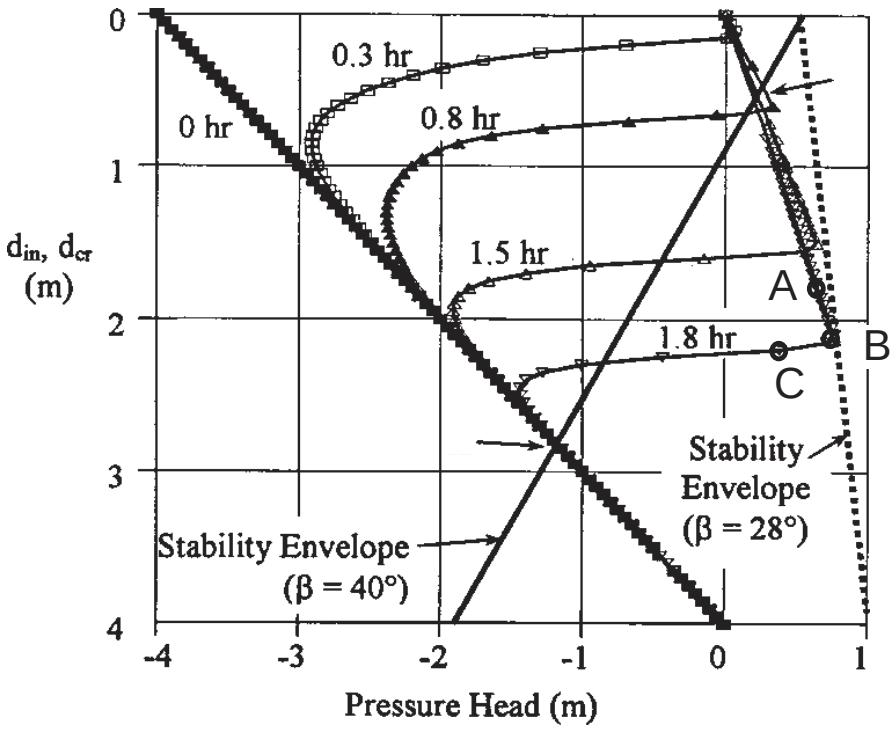

Figure 6.6: Infiltration results for coarse grain soil (Collins and Znidarcic, 2004)

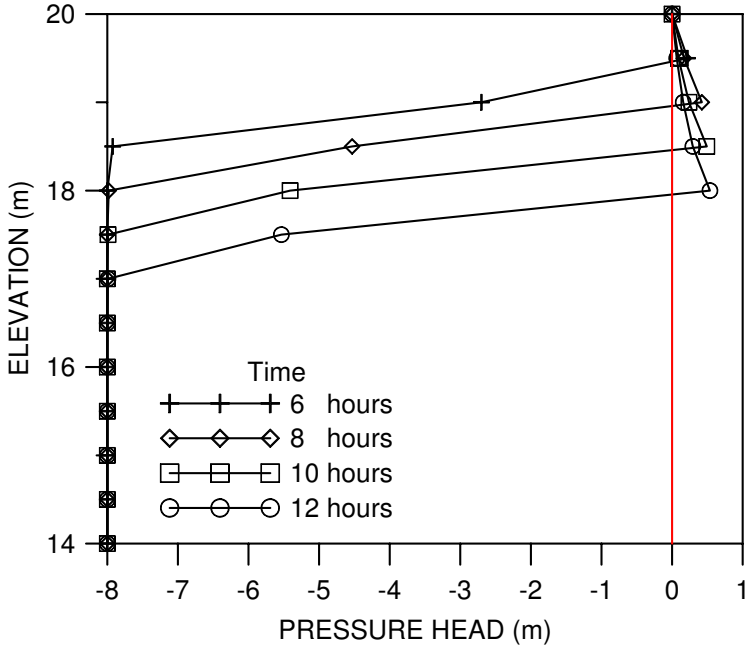

Figure 6.7: Pore-water pressure profiles at the crest of the slope from SEEP/W with mesh size of 0.5 m and time-step size of 360s

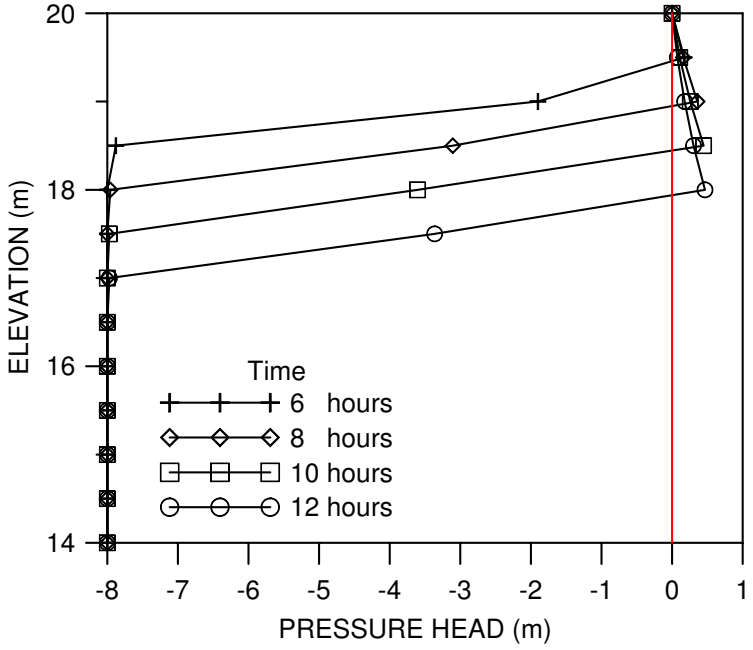

Figure 6.8: Pore-water pressure profiles at the crest of the slope from SEEP/W with mesh size of 0.5 m and time-step size of 3.6s

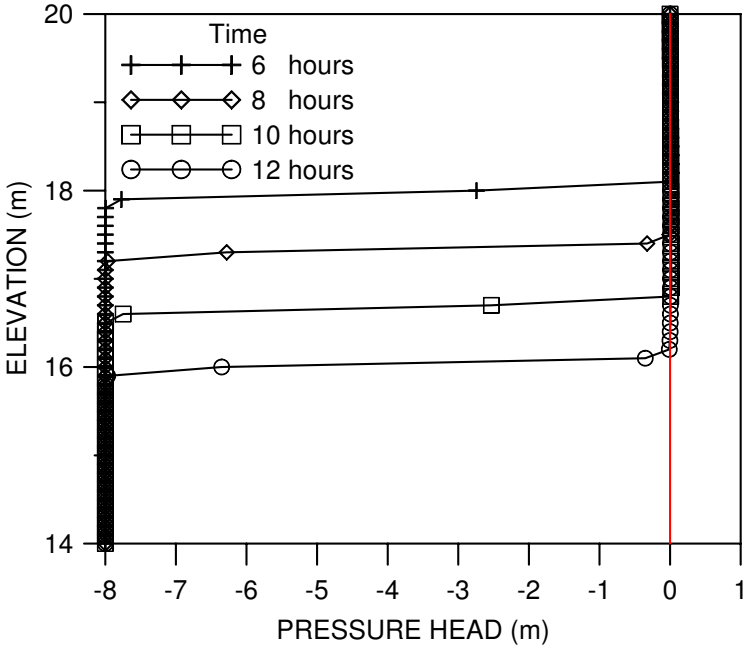

Figure 6.9: Pore-water pressure profiles at the crest of the slope from SEEP/W with mesh size of 0.1 m and time-step size of 360s

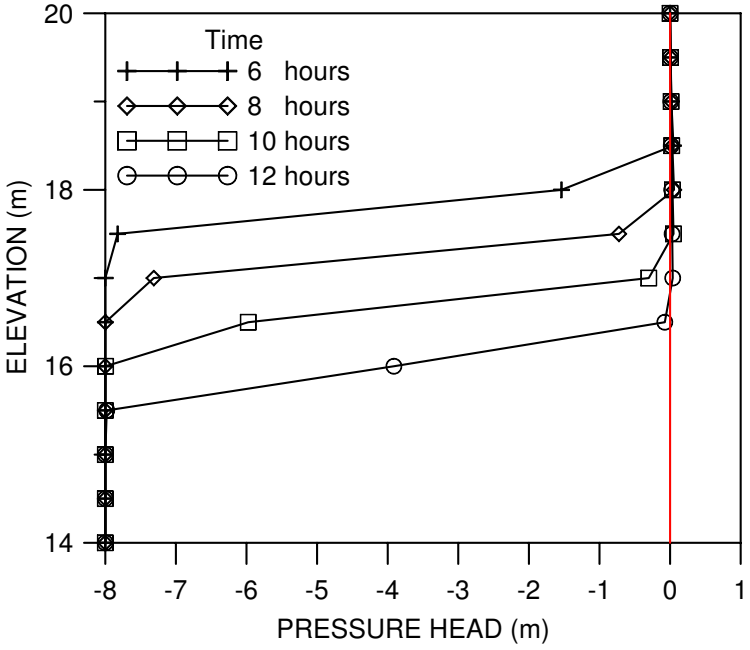

Figure 6.10: Pore-water pressure profiles at the crest of the slope from TUR1 with mesh size of 0.5 m and time-step size of 360s

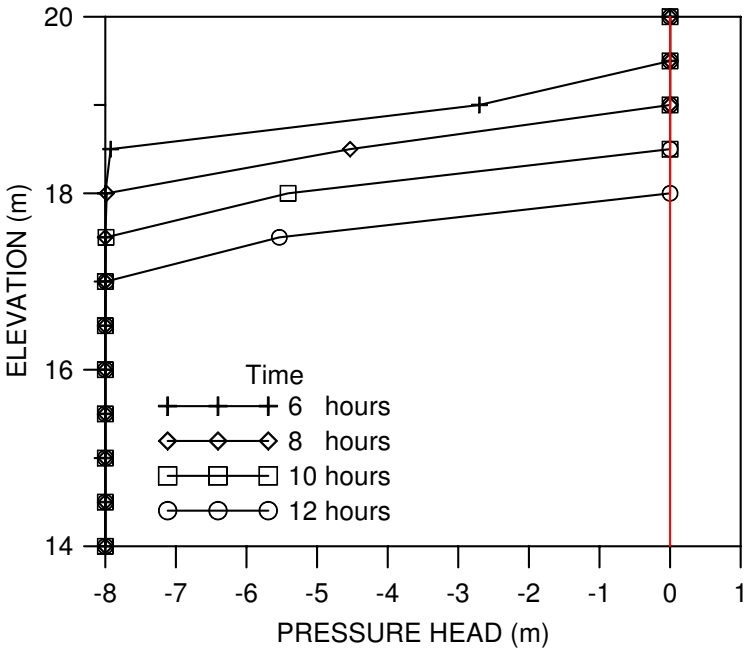

Figure 6.11: Artificial pore-water pressure profiles at the crest of the slope modified from Figure 6.7 by removing the positive values

Chapter 7

Conclusions

7.1 Summary and Conclusions

Shallow slope failures in residual soils are common in many tropical countries, which are usually related to intense rainfall. Under such external hydraulic conditions, seepage of water can cause a gradual loss of matric suction in an unsaturated soil slope, which has an adverse influence on the soil strength and therefore the stability of the slope. In order to obtain realistic representations of the slope condition under such situation, numerical modeling of groundwater flow is often necessary. However, in view of the limitation of computational resources, it is often impossible to use very refined element sizes and small time-step sizes in simulations. This often brings numerical difficulties, such as oscillation, slow convergence rate, in the solution process with popular numerical approaches, due to the strong nonlinearity often exhibited by the soil hydraulic functions. These numerical difficulties affect the accuracy of calculated pore-water pressure profiles, leading to errors in the subsequent computation of slope stability. The developments of robust and efficient numerical schemes are therefore of practical importance, which are expected to be able to achieve a more realistic solution using a practically reasonable spatial and

temporal discretization eventually.

The chief goal of this research is to develop robust numerical methods for solving the highly nonlinear partial differential equation describing unsaturated flow in porous media. The key focus of this research is to develop methods that are **practical**, i.e. reasonably easy to implement into existing computing codes and easy to use, minimizing the number of ad-hoc parameters that need "expert" judgement, be able to solve a broad range of soil hydraulic properties, be accurate and robust, and be suitable for running on an ordinary PC. A review of the literature showed that transformation methods for Richards equation such as RFT transform can lead to a more robust and efficient numerical approximation than traditional approaches. Therefore, a combination approach of RFT transformation method and UR1 under relaxation technique was proposed to solve the finite element formulation of h-based form of Richards equation. A detailed study was then implemented to look into its performance. Numerical studies showed that this combination method outperforms previous numerical schemes in the sense that it can use larger time-steps and mesh sizes to produce acceptable results and also converge to a stable solution quickly in each time-step. Furthermore, the superiority of proposed TUR1 approach was also identified when combined with different time stepping schemes in terms of efficiency that it takes less run time to produce solutions satisfying the requirements in accuracy. In addition, the combination of TUR1 method and the automatic time stepping scheme with embedded error control provides the most efficient and robust solution in a way that the temporal error can be constrained proportionally to a user prescribed tolerance at minimal computational cost.

In more detail, some useful concluding remarks can be summarized as follows:

1. A new combination approach of RFT transformation method (Pan and Wierenga, 1995) and a typical under relaxation technique was applied to solve the finite element formulation of the h-based form of Richards equation. A detailed investigation was then implemented to look into its effect on the slow convergence problems. In addition, the minimum time-step criterion presented by Karthikeyan et al. (2001) or the lumped-mass formulation was applied to suppress oscillations so that the convergence issue can be studied without being encumbered by extraneous complications. Comparison of this proposed combination approach (TUR1) and two under relaxation techniques without transformation (UR1 and UR2) were carried out. From the aspect of convergence to a correct solution with progressive refinement of the element size and time-step, numerical results showed the superiority of TUR1 over UR1 and UR2. UR1 is able to reach a stable solution very rapidly in each time-step, but requires significantly more refinement of the time-step to arrive at a solution of acceptable accuracy. At the same time, to suppress oscillation, element size needs to be correspondingly reduced, thus imposing even greater demands on computational resources. Adopting UR2 would mean that a large time-step, which permits a much coarser mesh under the Thomas and Zhou (1997) criterion for oscillation control, can produce reasonably accurate results, but at a price that within each time-step, many more iterations are needed and even diverge instead of converging to a stable solution when dealing with soils with highly nonlinear hydraulic properties. On the other hand, TUR1 has the advantages of both UR1 and UR2. Firstly, like UR2, TUR1 can use a larger time-step to produce acceptable results and

thus a correspondingly coarser mesh to suppress oscillation. Secondly, like UR1, TUR1 converges to a stable solution quickly in each time-step. Above all, TUR1 appears superior to UR1 and UR2 in the sense that a more realistic solution can be obtained using a practically reasonable spatial and temporal discretization eventually.

2. It was showed that the minimum time-step criteria (Thomas and Zhou, 1997) can be applied to the transformed flow equation by using the original λ and K to curb the oscillations. However, when steep soil parameter curves are encountered, the minimum oscillation-free time-step is sometimes too large in comparison to hourly or daily varieties in rainfall intensity. In this case, the lumped mass formulation could be an alternative choice. However, it is not applicable to quadratic/cubic elements to curb oscillations.

3. The transformation methods often involve arbitrary parameters. Selecting parameter values is then important to determine the efficiency of the method. Pan and Wierenga (1995) recommended a practical way to choose the parameter value in RFT transform. But they did not explore it rigorously. Williams et al. (2000) showed that the optimal transform parameters depend upon media properties, boundary conditions and spatial and temporal discretization. For the proposed combination method, numerical studies showed that choosing an intermediate value which equals to half of the biggest β value allowed for the transformed K^* curve to be still monotonic for the transformation parameter in the TUR1 method is a reasonable choice to produce near optimal results.

4. The proposed TUR1 method appeared to be a more practical choice than existing methods such as UR1, UR2 and a transformation method alone, because it can produce accurate solutions with reasonable computing costs; only one ad-hoc parameter is introduced and a robust recommendation on the choice of such parameter value is given; and finally it is workable for difficult problems with highly nonlinear soil hydraulic parameters. However, TUR1 would also break down when the soil hydraulic property curves are rather steep and a relatively large time-step is used.

5. Two temporally adaptive schemes were investigated and they were found to be superior to the fixed time-step scheme in terms of the ability to control temporal errors. Both adaptive schemes are able to produce solutions with more or less uniform error profiles throughout the entire simulation, while the fixed time stepping scheme generates significant errors when highly nonlinear behavior of the solution is encountered, which is usually caused by abrupt changes of the boundary condition.

6. Comparison between the heuristic and automatic temporally adaptive schemes showed that the latter outperforms the former scheme in the way that it ensures a direct proportionality between the actual error and the prescribed tolerance, which is critical for the success of an adaptive scheme. On the contrary, the relationship between the adaptive parameters and the actual numerical accuracy of solutions is hard to identify. Hence, the efficiency of such scheme becomes uncertain as it is dependent on the ability of the users to determine optimal heuristic time stepping parameters for different scenarios.

7. The superiority of the proposed TUR1 approach over the UR2 approach was verified when combined with different time stepping schemes in terms of efficiency that it takes less run time to produce solutions satisfying the requirements in accuracy. In addition, the combination of TUR1 method and the automatic adaptive error control scheme was found to provide the most efficient solution in a way that the temporal error is constrained proportionally to a user prescribed tolerance at minimal computational cost.

8. The combination of proposed TUR1 approach and the automatic adaptive scheme was shown to be a robust numerical method for practical unsaturated flow simulations, as it provides the most efficient solution at minimal computational cost; its performance is rather robust with moderate changes of several parameters introduced; and it is conceptually and computationally simple which can be easily incorporated into existing software codes based on the backward Euler scheme.

9. A number of multi-dimensional examples with both homogeneous or heterogenous materials were analyzed to show the robustness and efficiency of the proposed TUR1 and ATUR1 methods against traditional and alternative solution strategies. It was shown that these improved approaches are robust in complex problems with both very dry and variably saturated condition in homogenous or heterogeneous soils. And the TUR1 method with the automatic time stepping scheme appears to be more efficient than the fixed time-step schemes as acceptable results can be obtained using the least computational cost.

10. In the last, two typical numerical errors appearing in the simulation of rainfall infiltration problems which are sometimes not well emphasized in the literature were studied. Numerical results showed that such numerical errors could be a result of inappropriate mesh size or time-step size adopted in simulations. These errors in unsaturated flow analysis, including the overprediction of the wetting fronts and artificial positive pore-water pressure values above the infiltration fronts, have serious influence on the slope stability calculations. Furthermore, as the nonlinearity of solutions can be reduced by either using a denser mesh and smaller time-steps or adopting the transformation method, more accurate results can be produced by these two options. However, considering the superiority of TUR1 method in efficiency, it is obviously a more attractive and practical choice.

7.2 Recommendation for Future Study

To give a closure to this thesis, some suggestions of future work can be given:

1. Linearizing the nonlinear Richards equation by adopting the Newton-Raphson or Picard method always produces a system of linear equations that need to be solved. The traditional way to solve such linear system is to employ direct solution methods or its variants which are based on the classical Gaussian elimination scheme. These direct methods can lead to the exact solution in the absence of round-off errors. However, especially for large sparse linear systems arising from multi-dimensional problems, direct solution methods may incur a large number of floating point operations (additions,

subtractions and multiplications), which makes it significantly expensive to solve such a large linear system. On the contrary, iterative solution methods are more attractive for such large scale linear equations because only matrix-vector products and inner-products are required in the iteration process. Preconditioned Krylov subspace iterative methods, such as Bi-CG or GMRES, are commonly used in the simulation of unsaturated flow problems (Tocci et al., 1998; Jones and Woodward, 2001; GEO-SLOPE, 2004). The performance of proposed TUR1 approach is worth further study when combined with these iterative solution methods.

2. An examination of the spatial pressure head profiles in the above infiltration simulation cases shows that usually only a small part of the nodes are located in the region with highly nonlinear infiltration front. The remaining spatial nodes contribute little to accuracy, but bring much computational load. Therefore, spatially adaptive approaches appear attractive, especially when used together with the temporally adaptive approaches discussed in Chapter 4, although computational limitations are found in existing adaptive mesh techniques. Further studies are still needed to overcome those difficulties and to make spatial adaptive schemes more practical for engineering simulations. Specifically, meshfree methods such as the radial point interpolation method (RPIM) might be used as a more flexible tool for such spatial adaptive procedures.

References

Allen, M.B. and Murphy, C.L. A finite element collocation method for variable saturated flow in two space dimensions. Water Resour. Res., **22**:1537-1542. 1986.

Au, S.W.C. Rainfall and slope failure in Hong Kong. Engineering Geology, **36**:141-147. 1993.

Averjanov, S.F. About permeability of subsurface soils in case of incomplete saturation. In Eng. Coll., Vol.7, as quoted by P. Ya palubarinova, The theory of ground water movement. 1950.

Babajimopoulos, C. Revisiting the Douglas-Jones method for modelling unsaturated flow in a cultivated soil. Environmental Modelling & Software, **15**:303-312. 2000.

Babajimopoulos, C. A Douglas-Jones predictor-corrector program for simulating one-dimensional unsaturated flow in soil. Groundwater, **29**(2):267-270. 1991.

Baker, D.L. Applying higher order DIRK time steps to the 'modified Picard' method. Groundwater, **33**(2):259-263. 1995.

Bergamaschi, L. and Putti, M. Mixed finte elements and Newton-type linearizations for solution of Richards' equation. Int. J. Numer. Meth. Engng., **45**:1025-1046. 1999.

Bern, M.W., Flaherty J.E. and Luskin M. (ed.) Grid generation and adaptive algorithms. The Institute for Mathematics and its Applications. Vol. 113. New York: Springer-Verlag. 1999.

Bishop, A.W. The principle of effective stress. Technisk Ukeblad 106, No.**39**:859-863. 1959.

Bixler, N.E. An improved time integrator for finite element analysis. Communications Appl. Num. Meths., **5**:69-78. 1989.

Bouloutas, E.T. Improved numerical approximations for flow and transport in the unsaturated zone. Ph.D Thesis. Massachusetts Institute of Technology, Cambridge. 1989.

Brand E.W. Landslides in Southeast Asia: a state of the art report. In Proceedings of the 4th International Symposium on Landslides, Toronto, Canada, Vol. **1**:377-384. 1984.

Brandt, A., Bresler, E., Diner, N., Ben-Asher, L., Heller, J. and Goldberg, D. Infiltration from a trickle source, I, Mathematical models. Soil. Sci. Soc. Am. J., **35**:675-689. 1971.

Brooks, R.H. and Corey, A.T. Hydraulic properties of porous medium. Hydrology paper No.3. Civil Engrg. Dept., Colorada State Uni., Fort Collins, Colo. 1964.

Brutsaert, W.F. A functional iteration technique for solving Richards equation applied to two dimensional infiltration problems. Water Resour. Res., **7**:1583-1596. 1971.

Burdine, N.T. Relative permeability calculation size distribution data. Pet. Trans. Am. Inst. Min. Metal. Pet. Eng., **198**:71-78. 1953.

Celia, M.A., Ahuja, L.R. and Pinder, G.F. Orthogonal collocation and alternating-direction procedures for unsaturated flow problems. Adv. in Water Resour., **10**:178-187. 1987.

Celia, M.A. and Binning P. A mass conservative numerical solution for two-phase flow in porous media with application to unsaturated flow. Water Resour. Res., **28**(10):2819-2828. 1992.

Celia, M.A., Bouloutas, E. and Zarba, R.L. A general mass-conservative numerical solution for the unsaturated flow equation. Water Resour. Res., **26**(7):1483-1496. 1990.

Chatterjea, K. Observations on the fluvia and slope processes in Singapore and their impact on the urban environment. Ph.D Thesis, National University of Singapore. 1989.

Childs, E.C. and Collis-George, G.N. The permeability of porous materials. In Proc. Roy. Soc. London, Ser. A201, 392-405. 1950.

Cho, S.E. and Lee, S.R. Evaluation of surficial stability for homogeneous slopes considering rainfall characteristics. J. Geotech. Geoenviron. Engrg., **128**:756-763. 2002.

Chong, P.C. Numerical problems in transient seepage analysis for unsaturated soils. M.Eng Thesis, National University of Singapore. 2001.

Collins, B.D. and Znidarcic, D. Stability analyses of rainfall induced landslides. J. Geotech. Geoenviron. Engrg., **130**(4):362-372. 2004.

Cooley, R.L. Some new procedures for numerical solution of variably saturated flow problems. Water Resour. Res., **19**:1271-1285. 1983.

Dane, J.H. and Mathis, F.H. An adaptive finite difference scheme for the one-dimensional water flow equation. Soil Sci. Soc. Am. J., **45**:1048-1054. 1981.

Diersch, H.-J.G. Finite element modelling of recirculating density-driven saltwater intrusion processes in groundwater. Adv. Water Resour., **11**:25-43. 1988.

Diersch, H.-J.G. and Perrochet, P. On the primary variable switching technique for simulating unsaturated-saturated flows. Adv. in Water Resour., **23**:271-301. 1999.

Forsyth, P.A., Wu, Y.S. and Pruess, K. Robust numerical methods for saturated-unsaturated flow with dry initial conditions in heterogeneous media. Adv. in Water Resour., **18**:25-38. 1995.

Fredlund, D.G. and Rahardjo, H. Soil mechanics for unsaturated soils: John Wiley & Sons, Inc., 517. 1993.

Fredlund, D.G. and Xing, A. Equations for the soil water charactersitic curve. Can. Geotech. J., **31**:521-532. 1994.

Fredlund, D.G., Morgenstern, N.R. and Widger, R.A. The shear strength of unsaturated soils. Can. Geotech. J., **15**(3):313-321. 1978.

Fredlund, D.G., Xing, A. and Huang, S.Y. Predicting the permeability function for unsaturated soils using the soil water characteristic curve. Can. Geotech. J., **31**:533-546. 1994.

Freeze, R.A. Three-dimensional transient, saturated-unsaturated flow in a groundwater basin. Water Resour. Res., **7**:347-366. 1971.

Gardner, W.R. Some steady state solutions of the unsaturated moisture flow equation with application to evaporation from a water table. Soil. Sci., **85**(4):228-232. 1958.

Geo-slope. SEEP/W Engineering Book: Seepage Modeling with SEEP/W. Geo-Slope International Ltd., Calgary, Alta. 2004.

Green, W.H. and Ampt, G.A. Studies onsoil physics, part I: The flow of air and water through soils. J. Agric. Sci., **4**(1):1-24. 1911.

Gresho, P.M., Lee, R.L. and Sani, R.L. On the time-dependent solution of the incompressible Navier-Stokes equations in two and three dimensions. Preprint UCRL-83282, Lawrence Livermore Lab., University of California, 1979.

Griffiths, D.V. and Lu, N. Unsaturated slope stability analysis with steady infiltration or evaporation using elasto-plastic finite elements. Int. J. Numer. Anal. Meth. Geomech., **29**:249-267. 2005.

Guarracino, L. and Quintana, F. A third-order accurate time scheme for variably saturated groundwater flow modelling. Commun. Numer. Meth. Engng., **20**:379-389. 2004.

Hao X., Zhang R. and Kravchenko A. A mass-conservative switching method for simulating saturated-unsaturated flow. Journal of Hydrology, **311**:254-265. 2005.

Haverkamp, R., Vauclin, M., Touma, J., Wierenga, P.J. and Vachaud G. A comparison of numerical simulation models for one-dimensional infiltration. Soil Sci. Am. J., **41**:285-294. 1977.

Haverkamp, R. and Vauclin, M. A note on estimating finite difference inter-block hydraulic conductivity values for transient unsaturated flow problem. Water Resour. Res., **15**(1):181-187. 1979.

Hill, R.G., Porro, I., Hudson, D.B. and Wierenga, P.J. Modeling one-dimensional infiltration into very dry soils I: Model development and evaluation. Water Resour. Res., **25**:1259-1269. 1989.

Hornung, U. and Messing W. A predictor-corrector alternating-direction implicit method for two-dimensional unsteady saturated-unsaturated flow in porous media. Journal of Hydrology, **47**:317-323. 1980.

Horton, R.E. The role of infiltration in the hydrologic cycle. Trans. Am. Geophys. Union, **14**:446-460. 1933.

Huyakorn, P.S. and Pinder, G.F. Computational methods in subsurface flow: Academic Press, San Diego, Calif. 1983.

Jones, J.E. and Woodward, C.S. NewtonCKrylov-multigrid solvers for large-scale, highly heterogeneous, variably saturated flow problems. Adv. in Water Resour., **24**(7):763-774. 2001.

Ju, S.H. and Kung K.J.S. Mass types, element orders and solution schemes for the Richards equation. Computers and Geosciences, **23**(2):175-187. 1997.

Karthikeyan, M. Unsaturated seepage and slope stability analysis. M.Eng Thesis, National University of Singapore. 2000.

Karthikeyan, M., Tan, T.S. and Phoon, K.K. Numerical oscillation in seepage analysis of unsaturated soils. Can. Geotech. J., **38**:639-651. 2001.

Kavetski, D. Temporal integration in numerical models of unsaturated fluid flow: automatic time-stepping for Richards equation. Research report 230.11.2002. The University of Newcastle. 2002.

Kavetski, D., Binning, P. and Sloan, S.W. Adaptive time stepping and error control in a mass conservative numerical solution of the mixed form of Richards equation. Adv. in Water Resour., **24**:595-605. 2001.

Kavetski, D., Binning, P. and Sloan, S.W. Adaptive backward Euler time stepping with truncation error control for numerical modelling of unsaturated fluid flow. Int. J. Numer. Meth. Engng., **53**:1301-1322. 2002.

Kim, J., Jeong, S., Park, S. and Sharma, J. Influence of rainfall-induced wetting on the stability of slopes in weathered soils. Engineering Geology, **75**:251-262. 2004.

Kirkland, M.R., Hills, R.G. and Wierenga, P.J. Algorithms for solving Richards' equation for variably saturated soils. Water Resour. Res., **28**(8):2049-2058. 1992.

Lehmann, F. and Ackerer, PH. Comparison of iterative methods for improved solutions of the fluid flow equation in partially saturated porous media. Transp. in Porous Media, **31**:275-292. 1998.

Leij, F.J., Russell, W.B. and Lesch, S.M. Closed-form expressions for water retention and conductivity data. Groundwater, **35**(5):848-858. 1996.

Leong, E.C. and Rahardjo, H. Review of soil water characteristic curve equations. J. Geotech. Geoenviron. Engrg., **123**(12):1106-1117. 1997a.

Leong, E.C. and Rahardjo, H. permeability functions for unsaturated soils. J. Geotech. Geoenviron. Engrg., **123**(12):1118-1126. 1997b.

L'Heureux, J.S., Høeg, K. and Høydal, Ø.A. Numerical analyses and field case study of slope subjected to rainfall. In Unsaturated Soils 2006, Proceedings of the 4th International Conference on Unsaturated Soils, Carefree, AZ, USA, Vol. **2**:2279-2290. 2006.

Lumb, P. Slope failures in Hong Kong. Quarterly Journal of Engineering Geology. **8**:31-65. 1975.

Mansell, R.S., Ma, L., Ahuja, L.R. and Bloom, S.A. Adaptive grid refinement in numerical models for water flow and chemical transport in soil: a review. Vadose Zone Journal, **1**:222-238. 2002.

Matsushi, Y. Triggering mechanisms and rainfall thresholds of shallow landslides on soil-mantled hillslopes with permeable and impermeable bedrocks. Ph.D Thesis, University of Tsukuba. 2006.

Miller, C.T., Williams, G.A., Kelley, C.T. and Tocci, M.D. Robust solution of Richards equation for non-uniform porous media. Water Resour. Res., **34**(10):2599-2610. 1998.

Milly, P.C.D. A mass-conservative procedure for time-stepping in models of unsaturated flow. Adv. in Water Resour., **8**:32-36. 1985.

Mualem, Y. A new model for predicting the hydraulic conductivity of unsaturated porous media. Water Resour. Res., **12**:513-522. 1976a.

Mualem, Y. Hysterical models for prediction of the hydraulic conductivity of unsaturated porous media. Water Resour. Res., **12**:1248-1254. 1976b.

Mualem, Y. Hydraulic conductivity of unsaturated porous media: generalized macroscopic approach. Water Resour. Res., **14**:324-334. 1978.

Mualem, Y. Hydraulic conductivity of unsaturated soils: prediction and formulas. Methods of analysis: Part 1, Physical and Mineralogy methods, 2nd ed. Agronomy, ed. by Klute, A. Am. Soc. Agronomy, Inc. and Soil Sci. Am., Inc., Madison, Wis., USA, 799-823. 1986.

Neuman, S.P. Saturated-unsaturated seepage by finite elements. J. Hydraul. Div. Am. Soc. Civ. Engrg., **99**(HY12):2233-2250. 1973.

Ng, C.W.W. and Shi, Q. A numerical investigation of the stability of unsurated soil slopes subjected to transient seepage. Computers and Geotechnics, **22**(1):1-28. 1998.

Oden, J.T. and Demkowicz, L. Advances in adaptive improvements. In State of the art surveys in computational mechanics, ed by A.K. Noor, 441-467. New York: Am. Soc. Mechanical Engineers. 1987.

Pan, L., Warrick, A.W. and Wierenga, P.J. Finite element methods for modeling water flow in variably saturated porous media: Numerical oscillation and mass-distributed schemes. Water Resour. Res., **32**(6):1883-1889. 1996.

Pan, L. and Wierenga, P.J. A transformed pressure head-based approach to solve Richards' equation for variably saturated soils. Water Resour. Res., **31**(4):925-931. 1995.

Paniconi, C., Aldama, A.A. and Wood, E.F. Numerical evaluation of iterative and noniterative methods for the solution of the nonlinear Richards equation. Water Resour. Res., **27**(6):1147-1163. 1991.

Paniconi, C. and Putti, M. A comparison of Picard and Newton iteration in the numerical solution of multidimensional variably saturated flow problems. Water Resour. Res., **30**(12):3357-3374. 1994.

Philip, J.R. Numerical solution of equations of the diffusion type with diffusivity concentration-dependtent:2. Aust. J. Phys., **10**:29-42. 1957a.

Philip, J.R. The theory of infiltration:1. The infilatration equation and its solution. Soil Sci., **83**:345-347. 1957b.

Pitts, J. An investigation of slope stability on the NTI campus, Singapore. Applied Research project RPI/83, Nanyang Technological Institute, Singapore. 1985.

Press, W.H., Flannery, B.P., Teukolsky, S.A. and Vetterling, W.T. Numerical recipes. Cambridge University Press, Cambridge, U.K. 1986.

Rahardjo, H. and Leong, E.C. Soil water characteristic curves and flux boundary problems, Unsaturated Soil Engineering - Geotechnical Special Publication no-68, ASCE, 88-112. 1997.

Rahardjo, H., Lim, T.T., Chang, M.F. and Fredlund, D.G. Shear strength characteristics of a residual soil. Can. Geotech. J., **32**:60-77. 1995.

Rahardjo. H., Leong, E.C., Casmo, J.M. and Tang S.K. Assessment of rainfall effects on stability of residual soil slopes. In Proceedings of 2nd Int. Conf. on Unsaturated Soils, Beijing, China, Vol.**1**:280-285. 1998.

Rahardjo, H., Li, X.W., Toll, D.G., and Leong, E.C. The effect of antecedent rainfall on slope stability. Geotech. and Geological Engrg., **19**:371-399. 2001.

Rathfelder K. and Abriola, L.M. Mass conservative numerical solutions of the head-based Richards equation. Water Resour. Res., **30**(9):2579-2586. 1994.

Ross, P.J. Efficient numerical methods for infiltration using Richards' equation. Water Resour. Res., **26**(2):279-290. 1990.

Ross, P.J. and Bristow, K.L. Simulating water movement in layered and gradational soils using the Kirchhoff transform. Soil Sci. Soc. Am. J., **54**:1519-1524. 1990.

Sandhu, R.S., Liu H. and Singh, K.J. Numerical performance of some finite element schemes for analysis of seepage in porous elastic media. Int. J. Numer. Anal. Meth. Geomech., **1**:177-194. 1977.

Samani, Z.A., Walker, W.R., Jeppson, R.W. and Willardson, L.S. Numerical solution for unsteady two-dimensional infiltration in irrigation furrows. Trans. ASAE, **28**:1186-1190. 1985.

Segerlind, L.J. Applied finite element analysis. 2nd Edition, New York, Wiley. 1984.

Serrano, S.E. Modeling infiltration with approximate solutions to Richard's equation. J. Hydrologic Engrg., **9**(5):421-432. 2004.

Shampine, L.F. Numerical solution of ordinary differential equations. London: Chapman & Hall. 1994.

Simunek, J. and van Genuchten M.T. The CHAIN-2D code for simulating the two-dimensional movement of water, heat and multiple solutes in variably-saturated porous meida. Technical report 136, US Salinity Laborotary, USDA/ARS, Riverside, CA. 1994.

Sloan, S.W. and Abbo A.J. Biot consolidation analysis with automatic time stepping and error control. Part I: theory and implementation. Int. J. Numer. Anal. Methods. Geomech., **23**:467-492. 1999.

Smith, I.M. and Griffiths, D.V. Programming the finite element method, 3rd edition. John Wiley & Sons. 1998.

SoilVision. Help file for SoilVision Office software. SoilVision Systems Ltd. 2003.

Srivastava, R. and Yeh, J. T.-C. Analytical solutions for one-dimensional transient infiltration toward the water table in homogeneous and layered soils. Water Resour. Res., **27**:753-762. 1991.

Tan, T.S., Phoon, K.K. and Chong, P.C. Numerical study of finite element method based solutions for propagation of wetting fronts in unsaturated soil. J. Geotech. and Geoenvir. Engrg., **130**(3):254-263. 2004.

Thomas, R.M. and Gladwell, I. Variable-order variable-step algorithms for second-order systems. Part I: The methods. Int. J. Numer. Meth. Engng., **26**:39-53. 1988.

Thomas, H.R. and Zhou, Z. Minimum time-step size for diffusion problem in FEM analysis. Int. J. Num. Methods Engrg., **40**:3865-3880. 1997.

Tocci M.D., Kelly C.T. and Miller C.T. Accurate and economical solution of the pressure-head form of Richards' equation by the method of lines. Adv. in Water Resour., **20**(1):1-14. 1997.

Tocci, M.D., Kelley, C.T., Miller C.T. and Kees, C.E. Inexact Newton methods and the method of lines for solving Richards' equation in two space dimensions. Computational Geosciences, **2**(4):291-310. 1998.

Toll, D.G. Rainfall-induced landslides in Singapore. Geotechnical Engineering, **149**(4):211-216. 2001.

Tsaparas, I. Field Measurements and Numerical Modelling of Infiltration and Matric Suctions within Slopes. Ph.D Thesis, University of Durham. 2002.

van Genuchten, M.T. A close-form equation for predicting the hydraulic conductivity of unsaturated soils. Soil Sci. J., **44**(5):892-898. 1980.

van Genuchten, M.T. A comparison of numerical solutions of the one-dimensional unsaturated-saturated flow and mass transport equations. Adv. in Water Resour., **5**:47-55. 1982.

Vauclin, M., Khanji, D. and Vachaud, G. Experimental and numerical study of a transient, two-dimensional unsaturated-saturated water table recharge problem. Water Resour. Res., **15**:1089-1101. 1979.

Vermeer, P.A. and Verruijt, A. Accuracy conditions for consoliation by finite elements. Int. J. Numer. Anal. Meth. Geomech., **5**:1-14. 1981.

Warrick, A.W. and Amoozegar-Fard, A. Infiltration and drainage calculations using spatially scaled hydraulic properties. Water Resour. Res., **15**:1116-1120. 1979.

Warrick, A.W., Lomen, D.O. and Yates, S.R. A generalized solution to infiltration. Soil Sci. Soc. Am. J., **49**:34-38. 1985.

Williams, G.A. and Miller, C.T. An evaluation of temporally adaptive transformation approaches for solving Richards' equation. Adv. in Water Resour., **22**(8):831-840. 1999.

Williams, G.A., Miller, C.T. and Kelley, C.T. Transformation approaches for simulating flow in variably saturated porous media. Water Resour. Res., **36**(4):923-934. 2000.

Wolle C.M. and Hachichi, W. Rain-induced landslides in southeastern Brazil. In Proceedings of the 12th International Conf. on Soil mechanics and Foundation Engineering, Rio de janeiro, 1639-1642. 1989.

Wood, W.L. Practical time stepping schemes. Oxford: Oxford University Press. 1990.

Wu, Y.S. and Forsyth, P.A. On the selection of primary variables in numerical formulation for modeling multiphase flow in porous media. J. Contam. Hydrol.,**48**(3-4):277-304. 2001.

Yates, S.R., van Genuchten, M.T., Warrick, A.W. and Leij, F.J. Analysis of measured, predicted and estimated hydraulic conductivity using the RETC computer program. Soil Sci. Soc. Am. J., **56**:347-354. 1992.

Yeh, G.T. FEMWATER: A finite element model of water flow through saturated-unsaturatdd porous media - first revision. Oak Ridge National Laboratory, Oak Ridge, TN, ORNL-5567/R1 edition. 1987.

Youngs, E.G. Developments in the physics of infiltration. Soil Sci. Am. J., **59**:307-313. 1995.

Zienkiewicz, O.C. and Taylor, R.L. The finite element method, 5th Edtion. Oxford: Butterworth Heinemann. 2000.

Appendix A

Program Verification

A.1 Introduction

In Chapter 3, it was purported that the program HFE with UR1 generates essentially the same results as SEEP/W. In this chapter, the verification will be carried out with different cases. Close agreement between SEEP/W and HFE can be observed.

A.2 Modeling of One-dimensional Flow

A simple one-dimensional seepage problem (Figure A.1) is adopted here. The soil column is discretized using finite element method into ten 8-nodes quadrilateral elements with element size of 0.1 m. One time step level of 17000 sec is used to simulate the transient process. The boundary conditions are as followed:

Initial boundary condition: $h(z, 0) = -8$ m;

Transient boundary condition: $h(0, t) = -8$ m; and $h(1, t) = 0$ m.

Three cases are considered for the simulation.

A.2.1 Linear Soil-water Characteristic Curve and Nonlinear Hydraulic Conductivity Function

The slope of the soil-water characteristic curve, m_w is taken as 4.0×10^{-4} $\mathrm{m^2kN^{-1}}$. The hydraulic conductivity function is taken from Case A in Chapter 3. Figure A.2 shows that the results from HFE are almost identical to that of SEEP/W. The maximum difference is 6.0×10^{-6} m and the maximum relative difference is 1.3×10^{-6}.

A.2.2 Nonlinear Soil-water Characteristic Curve and Constant Hydraulic Conductivity Function

In this case, the soil-water characteristic curve is taken from Case A in Chapter 3. The constant hydraulic conductivity value, k is taken as 1.0×10^{-6} $\mathrm{ms^{-1}}$. Figure A.3 shows that the results from HFE are almost identical to that of SEEP/W. The maximum difference is 1.8×10^{-5} m; the maximum relative difference is 3.5×10^{-6}.

A.2.3 Nonlinear Soil-water Characteristic Curve and Nonlinear Hydraulic Conductivity Function

In this case, both the soil hydraulic relationships are nonlinear. They are taken from Case A in Chapter 3. Figure A.4 shows that the results from HFE are almost identical to that of SEEP/W. The maximum difference is 1.84×10^{-4} m; the maximum relative difference is 3.14×10^{-5}.

A.3 Modeling of Two-dimensional Flow

A two-dimensional infiltration problem is shown in Figure A.5. The soil geometry is 2 m high and 3 m wide. In the simulation, it is discretized using finite element method into 24 8-nodes quadrilateral elements with the element size of 0.5 m. The soil is assumed to be isotropic and the soil model of sandy clay loam of Case A in Chapter 3 is adopted.

Initially, the ground water table is 1.5 m below the surface. The initial pore-water pressure head is assumed to be linear with height. To simulate the infiltration problem, the pressure head at the infiltration surface is fixed to zero, and the total head at the vertical right hand side of 0.5 m high is maintained at 0.5 m.

In this case, 4 time steps of 22500 sec are used to simulate the transient process. Figure A.6, Figure A.7, Figure A.8, Figure A.9 show the contour of total head at Δt = 22500, 45000, 67500, 90000 sec, respectively. Again, close agreement can be observed between the results of SEEP/W and HFE.

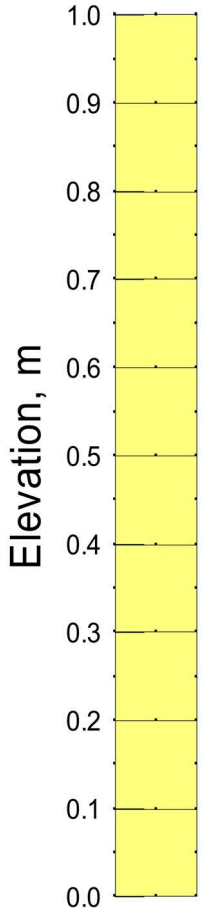

Figure A.1: Modeling of one-dimensional flow

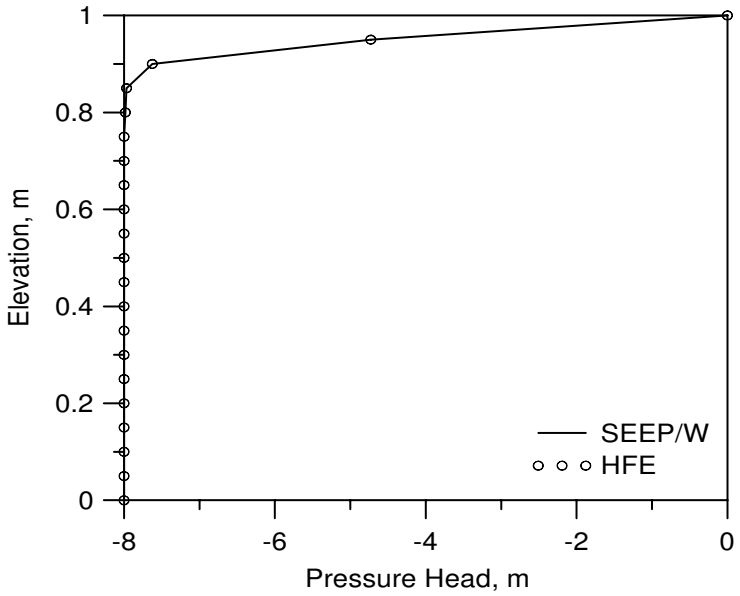

Figure A.2: Graph of elevation vs. pressure head for unsaturated transient flow with linear soil-water characteristic curve and nonlinear hydraulic conductivity function

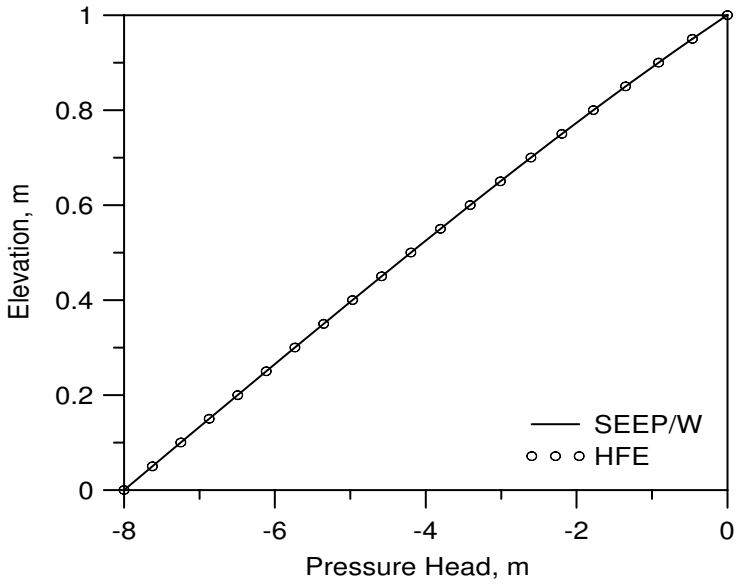

Figure A.3: Graph of elevation vs. pressure head for unsaturated transient flow with nonlinear soil-water characteristic curve and constant hydraulic conductivity function

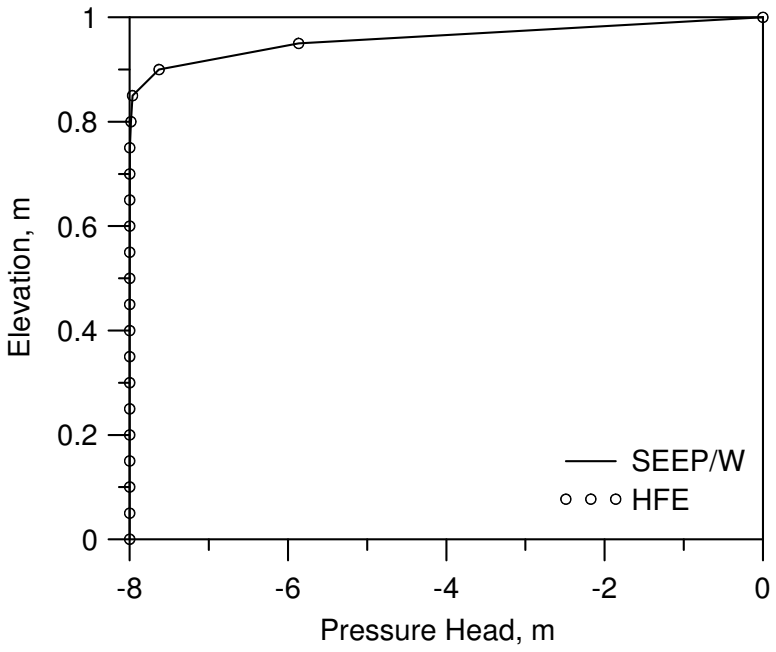

Figure A.4: Graph of elevation vs. pressure head for unsaturated transient flow with nonlinear soil-water characteristic curve and nonlinear hydraulic conductivity function

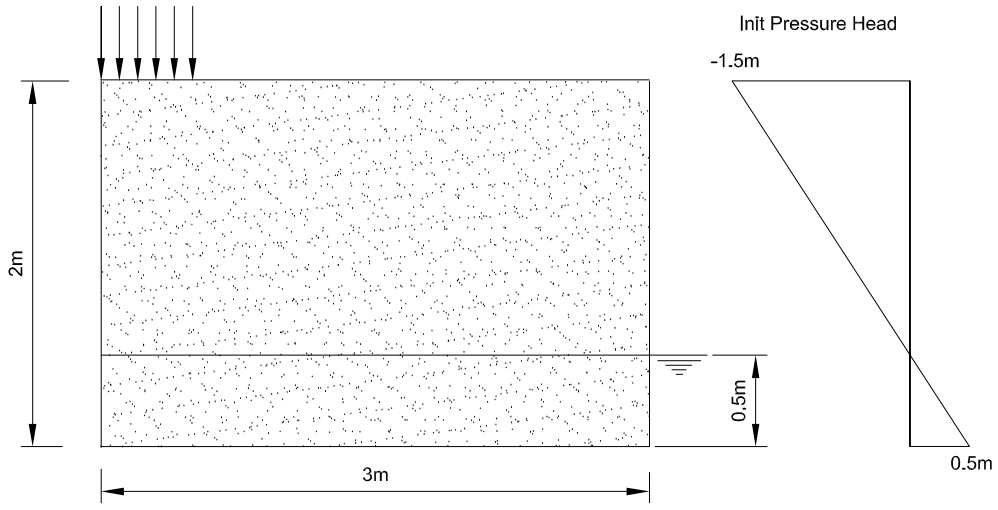

Figure A.5: Modeling of two-dimensional flow

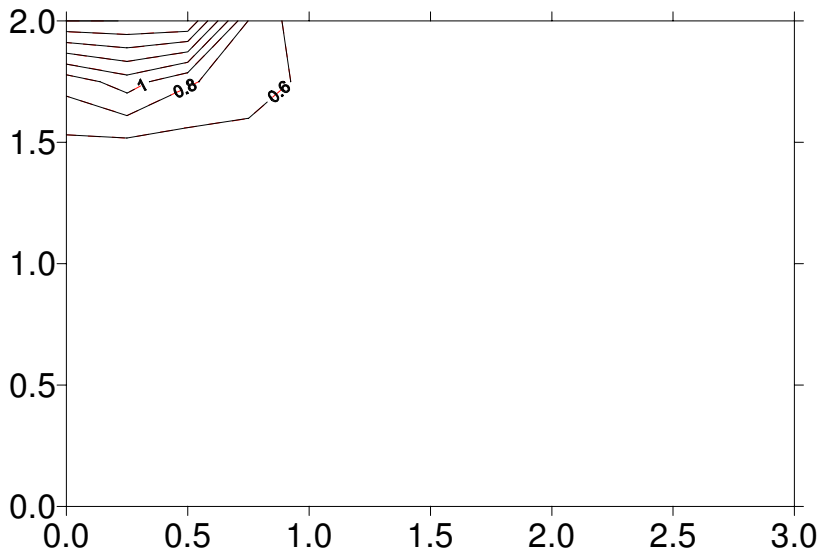

Figure A.6: Contour of total head of $\Delta t = 22500$ sec (solid line: SEEP/W; dash line: HFE)

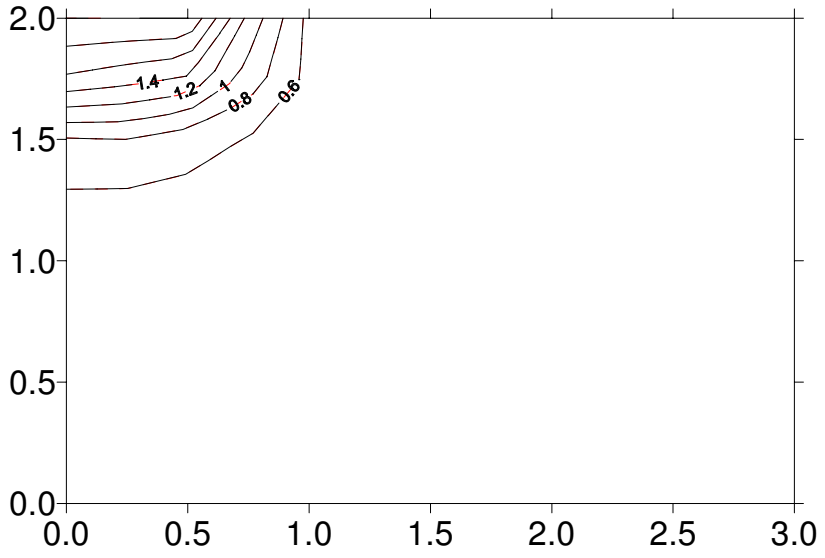

Figure A.7: Contour of total head of $\Delta t = 45000$ sec (solid line: SEEP/W; dash line: HFE)

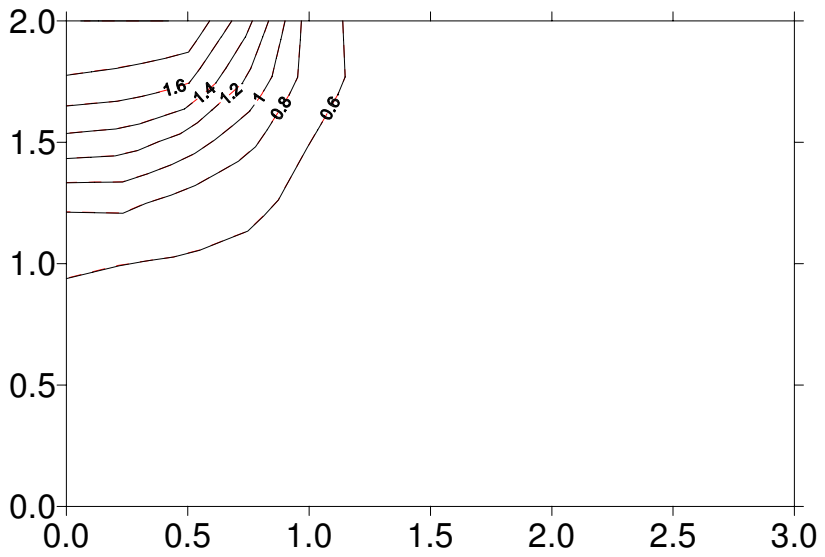

Figure A.8: Contour of total head of $\Delta t = 67500$ sec (solid line: SEEP/W; dash line: HFE)

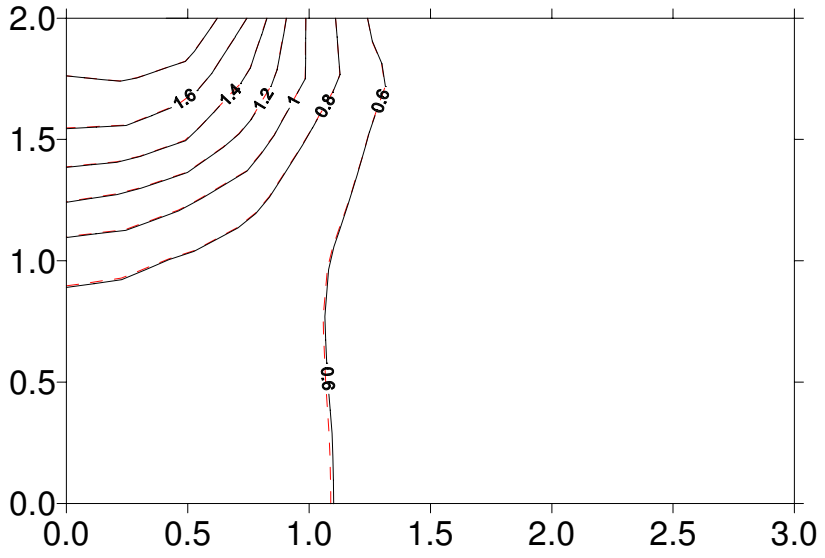

Figure A.9: Contour of total head of $\Delta t = 90000$ sec (solid line: SEEP/W; dash line: HFE)

Appendix B

Source Codes in FORTRAN 90

B.1 Introduction

The following FORTRAN 90 codes are modified partially from the book "Programming the finite element method" written by Smith and Griffiths (1998), and the program "richSolver7" written by Kavetski (2002).

B.2 Main Program

```
program THFELA
!-----------------------------------------------------
! Transient Unsaturated Flow Analysis using Richards Eqn
! general program for 2-D or 3-D analysis
!-----------------------------------------------------
use new_library
use geometry_lib
use unsat
use msflib
use portlib

implicit none

integer :: nels,neq,nband,nn,nr,nip,nodof,nod,ndof,i,k,iel,ndim,   &
           fixed_nodes,initial_nodes,timestep,nstep,count,MaxIter, &
           UR,loaded_nodes,no_total_head,np_types,npri,nres,stea,  &
           tran=1,nltyp
integer :: total,tt2,lumped,curTOut,nTOut,iCrit,DECtype,dtKeep,    &
           itMin,itMax,passNL=0,passEC,failprev,schtype=1
double precision :: det,perm,dtim,elapsedtime,diff,gammaw=9.807D0, &
                    tol,phg,phgi,phgf,thetagi,thetagf,norm,ethick
```

```
double precision :: theta0=0.D0,flux=0.D0,penalty=1.D20,cumumass,  &
                    temp,hEl,Lt,curT,preT,htmax,stepTolA,stepTolR, &
                    dtIni,q,dtIncF,dtRedF,trunErrA,safety,         &
                    qmin,qmax,NLtolA,NLtolR,stepTol,tt1
double precision :: beta,t_elev,pg,pgi,pgf,dhoverdp,ptmax
character(len=15) :: element
character(len=50) :: ctrl
logical :: status,ifmb=.false.
!----------------------Dynamic Arrays-----------------------------
double precision,allocatable :: bp(:),bk(:),elev(:),points(:,:),   &
    kay(:,:),coord(:,:),fun(:),jac(:,:),der(:,:),deriv(:,:),       &
    weights(:),kp(:,:), pm(:,:),funny(:,:),g_coord(:,:),value(:),  &
    h0(:),h1(:),LS(:),RS(:),trload(:),ph(:),mw(:),h2(:),havg(:),   &
    thetag(:),phi(:),phf(:),trload0(:),trload1(:),tothead_value(:),&
    flow_rate(:),nodal_flow_value(:),prop(:,:),PROP02(:,:)
double precision,allocatable :: p0(:),p1(:),p2(:),pavg(:),kg(:,:), &
    bg(:),p0t(:),p1t(:),ptt(:)
double precision,allocatable :: h0t(:),h1t(:),htt(:),TOut(:)
integer,allocatable :: nf(:,:),g(:),num(:),g_num(:,:),node(:),     &
    no(:),g_g(:,:),noln(:),nodal_flow_no(:),etype(:),elen(:),      &
    ltyp(:),enips(:,:)
!-----------------------input and initialisation------------------
status=changedirqq('D:\NR\Year2008\0117\THFELA\10cm')
IF(.not.status) stop 'WRONG DIRECTORY'
open (9  , file = 'FFEinitial.dat' , status = 'old' ,action ='read')
open (10 , file = 'FFEin.dat' ,      status = 'old' ,action ='read')

!read(10,*)stea,tran
READ(10,*)NELS,NN,NODOF,NOD,nip,NDIM,np_types,nltyp,ethick,lumped
read(10,*)dtIni,nstep,npri,nres
read(10,*)MaxIter,tol,UR,beta
ndof=nod*nodof

open(11,file='FFEout.txt',  status = 'replace', action ='write')
open(12,file='FFEcoord.txt',status = 'replace', action ='write')
open(13,file='FFEiter.txt', status = 'replace', action ='write')
open(14,file='FFEmb.txt',   status = 'replace', action ='write')
open(15,file='FFEadap.dat', status = 'old' ,    action ='read')

write(12,'(a,i5)')"number of elements = ",nels
write(12,'(a,i5)')"number of nodes = ",nn
allocate(nf(nodof,nn),points(nip,ndim),weights(nip),kay(ndim,ndim),&
     coord(nod,ndim), fun(nod), jac(ndim,ndim),g_coord(ndim,nn),   &
     der(ndim,nod), deriv(ndim,nod), pm(ndof,ndof),g_num(nod,nels),&
     kp(ndof,ndof), g(ndof),funny(1,nod),num(nod),g_g(ndof,nels),  &
     thetag(nip),mw(nip),prop(8,np_types),etype(nels),ltyp(nels),  &
     enips(2,5),PROP02(9,np_types),kg(ndof,ndof))
!read(10,*) PROP02      !READ PROP02:SWC,ALPHA,BETA,A,B,KX,KY,KZ,MV
```

```
read(10,*) prop         !READ PROP:swc,rwc,a,n,kx,ky,kz,mv
read(10,*) enips
etype=1
ltyp=1                                                  !!! 1D=5,2D=1
if (nltyp>1)    read(10,*) ltyp
READ(10,*) G_COORD
do k=1,nels
    read(10,*) etype(k),g_num(:,k)
end do

nf=1
read(10,*) nr
if (nr>0) read(10,*) (k,nf(:,k),i=1,nr)
call formnf(nf)
neq=maxval(nf)
!----loop the elements to find nband and store steering vectors----
nband = 0
elements_1: do iel = 1 , nels
    NUM=g_num(:,iel)
    call num_to_g (num,nf,g)
    g_g( : , iel ) = g
    if(nband<bandwidth(g)) nband = bandwidth(g)
end do elements_1
write(12,'(a)') "Global coordinates "
do k=1,nn
    write(12,'(a,i5,a,3e12.4)') "Node",k,"       ",g_coord(:,k)
end do
write(12,'(a)') "Global node numbers "
do k=1,nels
    write(12,'(a,i5,a,16i5)')"Element ",k,"        ",g_num(:,k)
end do
allocate(bp(neq*(nband+1)),bk(neq*(nband+1)),LS(neq*(nband+1)),    &
    RS(neq*(nband+1)),h0(0:neq),h1(0:neq),h2(0:neq),havg(0:neq),   &
    ph(0:neq),phi(0:neq),phf(0:neq),elev(0:neq),trload(0:neq),     &
    trload0(0:neq),trload1(0:neq),p0(0:neq),p1(0:neq),p2(0:neq),   &
    pavg(0:neq),bg(neq*(nband+1)),h0t(0:neq),h1t(0:neq),htt(0:neq),&
    p0t(0:neq),p1t(0:neq),ptt(0:neq))
write(12,'(2(a,i5))')                                              &
   "There are ",neq,"  equations and the half-bandwidth is ",nband
!------------- Obtaining Elevation Head For All Nodes---------------
elev=0.d0
do i=1, nn
    elev(i) = g_coord(ndim,i)
end do
!--------------------Specify Initial Nodal Values -----------------
read(9,*) initial_nodes
if (initial_nodes/=0) read(9,*) (k,h0(nf(:,k)),i=1,initial_nodes)
p0=0.d0
```

```
call h2p(h0,elev,p0,beta)
!-----Read Flow Rate Boundary Condition(if q>k, H=elevation)--------
no_total_head=0
trload0=0.d0
read(10,*) loaded_nodes
if (loaded_nodes /= 0) then
    allocate(noln(loaded_nodes),tothead_value(loaded_nodes),       &
             flow_rate(loaded_nodes),nodal_flow_no(loaded_nodes),  &
             nodal_flow_value(loaded_nodes),elen(loaded_nodes))    &
    noln=0
    tothead_value=0.d0
    read(10,*) (flow_rate(i), elen(i), nodal_flow_no(i),           &
               nodal_flow_value(i),i=1,loaded_nodes)
    do i=1, loaded_nodes
        !if (flow_rate(i) < PROP02(7,etype(elen(i)))) then
        if (flow_rate(i) < PROP(5,etype(elen(i)))) then
            trload0(nf(1,nodal_flow_no(i)))=nodal_flow_value(i)
        else
            no_total_head=no_total_head+1
            tothead_value(no_total_head)=elev(nodal_flow_no(i))
            noln(no_total_head)=nf(1, nodal_flow_no(i))
            call h2p1(tothead_value(i),elev(nodal_flow_no(i)),     &
                      tothead_value(i),beta)
        end if
    end do
end if
!-------------------------Read Total Head Fixity--------------------
read(10,*) fixed_nodes
if (fixed_nodes/=0) then
    allocate(node(fixed_nodes),no(fixed_nodes),value(fixed_nodes))
    read(10,*)(node(i),value(i),i=1,fixed_nodes)
    do i=1,fixed_nodes
        no(i)=nf(1,node(i))
        call h2p1(value(i),elev(node(i)),value(i),beta)
    end do
end if
!-------------------------Read Output Time--------------------------
read(10,*) nTOut
allocate(TOut(nTOut))
read(10,*) (TOut(i),i=1,nTOut)
Lt=TOut(nTOut)

!-------------------------
read(15,*) DECtype,stepTolA,stepTolR,NLtolA,NLtolR
read(15,*) safety,qmax,qmin
read(15,*) itMin,dtIncF
read(15,*) itMax,dtRedF
!====================================================================
```

```
IF (tran/=0) THEN
    !-------------------time stepping recursion---------------------
    total=0
    elapsedtime=timef()

    h2=h0
    h1=h0
    havg=h0

    WRITE(11,*) "Values at node:", nres
    WRITE(11,*) "   Time     Elev-Head    Total-Head   Pressure-Head"

    dtim=dtIni           !!!! no init cal
    preT=0.
    curTOut=1
    dtKeep=0
    count=0
    htt=0.d0
    timestep=1

    timesteps: do while(preT<Lt)

        !=====adjust the time step to avoid overshooting
        if (preT+dtim>=TOut(curTOut)) then
            if (DECtype/=3) dtIni=dtim
            dtim=TOut(curTOut)-preT
        else if (preT+dtim+dtim>TOut(curTOut)) then
            if (DECtype/=3) then
                dtIni=dtim
            else
                dtim=.5d0*(TOut(curTOut)-preT)
            end if
        end if

!       !=====initial guess for h
!       ! Method 1
!       h1=h0
!       ! Method 2
!       h1=h0+dtim*(h0t+.5d0*dtim*htt)
!       ! Method 3
!       !h1=h0+dtim*h0t

        !=====initial guess for p
        ! Method 1
        p1=p0
        ! Method 2
        !p1=p0+dtim*(p0t+.5d0*dtim*ptt)
        ! Method 3
```

```
!p1=p0+dtim*p0t

p2=p1
call unre(pavg,p0,p1,p2,UR)
call p2h(p1,elev,h1,beta)
h2=h1
call p2h(pavg,elev,havg,beta)

do  !iteration

    if (dtKeep==0) then
        curT=preT+dtim
    end if

    ph=havg-elev
    phi=h0-elev
    phf=h1-elev

    bk=0.d0
    bp=0.d0
    bg=0.d0

    do iel = 1 , nels

        call element_type(element,nip,nod,ltyp,enips,iel)
        ndof=nod*nodof
        deallocate (num,coord,g,points,weights,der,deriv,  &
                fun,kp,funny,mw,pm,kg)
        allocate (num(nod),coord(nod,ndim),g(ndof),mw(nip),&
               weights(nip),points(nip,ndim),der(ndim,nod),&
               deriv(ndim,nod),fun(nod),kp(ndof,ndof),     &
               funny(1,nod),pm(ndof,ndof),kg(ndof,ndof))
        call sample (element,points,weights)
        num = g_num(:,iel)
        coord = transpose( g_coord( : , num ))
        g = g_g( : , iel )

        kp=0.d0
        pm=0.d0
        kg=0.d0
        kay=0.d0

        if (lumped==1) then
            do i=1,ndof
                do k=1,ndof
                    if (i/=k) then
                        pm(i,i)=pm(i,i)+pm(i,k)
                        pm(i,k)=0.d0
```

```
                    end if
                end do
            end do
        end if

        call formkv(bk,kp,g,neq)
        call formkv(bp,pm,g,neq)
        call formkv(bg,kg,g,neq)
    end do

    !------------------factorise left hand side-------------
    LS=bk*dtim+bp
    !---total head fixity by flow rate boundary
    trload1=0.0
    if (no_total_head /= 0) then
        LS(noln)=LS(noln)+penalty
        trload1(noln)=LS(noln)*tothead_value  !(i)
    end if
    !--------Total Head Fixity-----------------------------
    trload=0.0
    if (fixed_nodes/=0) then
        LS(no)=LS(no)+penalty
        trload(no)=LS(no)*value                !(i)
    end if
    !-------------------------------------------------------
    call banred(LS,neq)
    call linmul(bp,p0,p1t)
    call linmul(bg,elev,p1)
    p1=p1t-dtim*p1+trload+trload1+trload0*dtim
    p1(0)=0.d0
    call bacsub(LS,p1)

    total=total+1
    count=count+1

    call p2h(p1,elev,h1,beta)
    call p2h(p2,elev,h2,beta)
    call control((h2-elev),(h1-elev),nn,nf,diff,norm)
    write(*,'(2f20.12,i7,e14.8)') curT,dtim,count,diff

    if (diff<=NLtolR) then
        passNL=1
    else
        passNL=0
    end if
!   passNL=1

    if (passNL==0) then
```

```
        if (mod(count,MaxIter)==0) then
            write(*,*) curT,' Iter cannot converge, &
                 decrease dt'
            write(13,*) curT,' Iter cannot converge &
                 in MaxIter, decrease dt'
            dtim=.5d0*dtim            !!!!
            dtKeep=0
            p1=p0
            p2=p1
            call p2h(p1,elev,h1,beta)
            h2=h1
            call unre(pavg,p0,p1,p2,UR)
            call p2h(pavg,elev,havg,beta)
            cycle
        else
            dtKeep=1
            call unre(pavg,p0,p1,p2,UR)
            call p2h(pavg,elev,havg,beta)
            p2=p1
            h2=h1
            cycle
        end if
    end if

    p1t=(p1-p0)/dtim
    h1t=(h1-h0)/dtim
    ptt=(p1t-p0t)/dtim
    htt=(h1t-h0t)/dtim

    select case(DECtype)
        case(0)
            q=1.d0
            count=0
            dtim=dtIni
            exit
        case(1)
            if (count<itMin) then
                q=dtIncF
            else if (count>itMax) then
                q=dtRedF
            else
                q=1.d0
            end if
            passEC=1
        case(3)
            call mixErrorTest(0.5d0*dtim*abs(h1t(1:)-h0t(1:)),&
                abs(h1(1:)-elev(1:)),nn,stepTolA,stepTolR,    &
                passEC,iCrit)
```

```
                trunErrA=.5d0*dtim*abs(h1t(iCrit)-h0t(iCrit))
                if (trunErrA>1.d-10) then
                    q=safety*sqrt((stepTolA +
                      stepTolR*abs(h1(iCrit)-elev(iCrit)))/trunErrA)
                else
                    q=qmax
                end if
        end select

        count=0

        if (timestep<=2) passEC=1  !no change Dt for the first two
        if (passEC==0) then
            !write(*,*) 'Step failed',dtim
            write(13,*) 'Step failed'
            failprev=1
            q=max(q,qmin)

            if (q>1.0) q=.9  !young add

            dtim=q*dtim
            dtKeep=0
            !p1=p0+dtim*(p0t+.5d0*dtim*ptt)
            p1=p0
            p2=p1
            call p2h(p1,elev,h1,beta)
            h2=h1
            call unre(pavg,p0,p1,p2,UR)
            call p2h(pavg,elev,havg,beta)
        else
            exit
        end if

    end do

    preT=curT
    timestep=timestep+1

    write(14,*) curT,dtim,trunErrA
    if (schtype==1) then
        p0=p1
        h0=h1
    else if (schtype==2) then
        p0=p0+.5d0*dtim*(p1t+p0t)
        call p2h(p0,elev,h0,beta)
    end if
    p0t=p1t
    h0t=h1t
```

```
        if (preT==TOut(curTOut)) then
            write(*,*) preT
            !write to file
            write(11,'(a,e12.4)') "For the time of", curT
            write(11,'(a)')" Node        X-Coord      Elev-Head    &
                Total-Head  Pressure-Head"
            do k=1,nn
                write(11,'(i5,5e15.7)') k,g_coord(:,k),h0(nf(1,k)),&
                   (h0(nf(1,k))-elev(k))
            end do
            curTOut=curTOut+1
            if (DECtype==0.or.DECtype==1) dtim=dtIni
        end if

        if (failprev==0) then
            q=min(q,qmax)
        else if (failprev==1) then
            q=min(q,1.d0)
            failprev=0
        end if
        dtim=q * dtim
        dtKeep=0

        if (dtim<1.d-20) then
            stop 'Time step size is too small!'
        end if

    end do timesteps

    elapsedtime=timef()
    write(11,'("*** Total iterations  :",i11)') total
    write(11,'("*** Under relaxation  :",i11)') UR
    write(11,'("*** Elapsed time      :",f16.4)') elapsedtime
    write(11,'("*** Adap tol(Rel&Abs) :",2e16.4)') stepTolR,stepTolA
    write(11,'("*** Transformation beta         :",f16.4)') beta
    2000 format('$$$ Transient Analysis ends at ',a,'.')
END IF

end program THFELA


!!!=================================================================
!!!=================================================================
subroutine mixErrorTest (absE, base, n, tolA, tolR, pass, iCrit)

implicit none
```

```
! Dummy variables:
! Input:
! n = physical and logical (dynamically allocated) dimension
! absE = properly defined absolute error vector
! tolA = absolute error tolerance
! tolR = relative error tolerance

integer, intent(in) :: n
double precision, dimension(n), intent(in) :: absE, base
double precision, intent(in) :: tolA, tolR

! output:
! pass = indicates whether convergence satisfied (1) or not (0)
! iCrit = coordinate of the worse offender in the mixed error sense

integer, intent(out) :: pass, iCrit

! Local variables
integer :: i ! loop counter
double precision :: curErr ! current worse mixed error
double precision :: ErrChar ! worse mixed error
double precision :: curAbs ! current absolute error
double precision :: absMax ! worse absolute error
double precision :: curRel ! current relative error
double precision :: relMax ! worse relative error
double precision :: scale ! implicit scale

!scale = tolA / tolR ! threshold absolute / relative

iCrit = 1
ErrChar = -1.d14 ! VERY negative number
absMax = 0.d0
relMax = 0.d0

if (maxval(abs(base))*tolR > tolA) then
    do i = 1, n
    ! employ relative test for critical points
        !if (abs(base(i))>=scale) then
        if (abs(base(i))*tolR>=tolA) then
    ! ignore Components below threshold
              curRel = abs(absE(i) / base(i))
              if (curRel > relMax) then
                  relMax = curRel
                  iCrit = i
              end if
         end if

    ! update infinity norm of the characteristic error vector
```

```
        curErr = abs(absE(i)) - abs(base(i)) * tolR
        if (curErr > ErrChar) ErrChar = curErr
    end do
else
    do i = 2, n
! employ absolute test for critical points
        curAbs = abs(absE(i))
        if (curAbs > absMax) then
            absMax = curAbs
            iCrit = i
        end if

! update infinity norm of the characteristic error vector
        curErr = abs(absE(i)) - abs(base(i)) * tolR
        if (curErr > ErrChar) ErrChar = curErr
    end do
end if

! Test error in mixed sense
if (ErrChar > 1*tolA) then
!if (ErrChar > tolA) then
    pass = 0 ! no good
else
    pass = 1 ! OK
end if

end subroutine mixErrorTest
```

B.3 New Subroutines for Module *new_library*

```
module new_library

!!!=================================================================
subroutine control(ph0,ph1,nn,nf,diff,ECnorm1)

double precision,intent(in):: ph0(0:),ph1(0:)
integer,intent(in)::nn,nf(:,:)
integer::i
double precision,intent(out)::diff,ECnorm1
double precision::add0,add1,ECnorm0

add0=0.0
ECnorm0=0.0
do 10 i=1,nn
    add0=add0+(abs(ph0(nf(1,i))))**2
10 continue
ECnorm0=sqrt(add0)+1.0
```

```
add1=0.0
ECnorm1=0.0
do 20 i=1,nn
    add1=add1+(abs(ph1(nf(1,i))))**2
20 continue
ECnorm1=sqrt(add1)+1.0

diff=abs((ECnorm1-ECnorm0)/ECnorm0*100.00)

return
end subroutine control

!!!=================================================================
subroutine element_type(element,nip,nod,ltyp,enips,iel)
integer, intent(in)::iel,ltyp(:),enips(:,:)
character(*), intent(out)::element ; integer, intent(out)::nip,nod
select case(ltyp(iel))
    case(1); element='quadrilateral'; nip=enips(1,1); nod=enips(2,1)
    case(2); element='triangle'     ; nip=enips(1,2); nod=enips(2,2)
    case(3); element='hexahedron'   ; nip=enips(1,3); nod=enips(2,3)
    case(4); element='tetrahedron'  ; nip=enips(1,4); nod=enips(2,4)
    case(5); element='line'         ; nip=enips(1,5); nod=enips(2,5)
end select
return
end subroutine

!-----------------------------------------------------------------
end module new_library
```

B.4 Module *unsat*

```
module unsat
contains
!--------- 4 parameter Van Genuchten (1980) model-------------------
!subroutine to get volumetric water content of unsaturated soil
!=================================================================
subroutine volwatcon(theta,swc,rwc,a,n,h)
implicit none
double precision,intent(in)::swc,rwc,a,n,h
double precision,intent(out)::theta
double precision::m

m=1.d0-(1.d0/n)
if(h<0.d0) then
   theta=rwc+(swc-rwc)/(1.d0+(a*abs(h))**n)**m
```

```
else
   theta = swc
end if
return
end subroutine volwatcon

!=====================================================================
!subroutine to get volumetric water content of unsaturated soil
!Vauclin et al. model
!=====================================================================
subroutine volwatcon02(theta,swc,alpha,beta,h)
implicit none
double precision,intent(in)::swc,alpha,beta,h
double precision,intent(out)::theta
if(h<0.d0) then
   theta = swc*alpha/(alpha+(abs(h))**beta)
else
   theta = swc
end if
return
end subroutine volwatcon02
!=====================================================================

!--------------- Mualem's Conductivity model (1976a)----------------
!subroutine to get hydraulic conductivity in unsaturated soil
!=====================================================================
subroutine hydrcond(k,swc,rwc,n,ks,theta)
implicit none
double precision,intent(in)::swc,rwc,n,ks,theta
double precision,intent(out)::k
double precision::m,nwc

m=1.d0-(1.d0/n)
if(theta<swc)then
   nwc=(theta-rwc)/(swc-rwc)
   k=ks*sqrt(nwc)*(1.d0-(1.d0-nwc**(1.d0/m))**m)**2.d0
else
   k=ks
end if
return
end subroutine hydrcond

!=====================================================================
!subroutine to get hydraulic conductivity in unsaturated soil
!Vauclin et al. model
!=====================================================================
subroutine hydrcond02(k,a,b,ks,h)
implicit none
```

```
double precision,intent(in)::a,b,ks,h
double precision,intent(out)::k
if(h<0.d0)then
    k=ks*a/(a+(abs(h))**b)
else
    k=ks
end if
return
end subroutine hydrcond02
!=====================================================================

!--------------- Secant (Chord) slope of swc curve------------------
!subroutine to get the mw of Soil Water Curve (SWC)
!given initial & final volumetric water contents
!=====================================================================
subroutine chordslope(cslope,theta1,wc2,h1,h2,mv)
implicit none
double precision,intent(in) :: theta1,wc2,h1,h2,mv
double precision,intent(out)::cslope
cslope=abs((wc2-theta1)/(h2-h1)/9.807d0)
return
end subroutine chordslope

!--------------- Tangent slope of swc curve-------------------------
!subroutine to get mw of SWC when h0 & h1 are similar
!given initial & final volumetric water contents
!=====================================================================
subroutine slope(mslope,swc,rwc,a,n,mv,h)
implicit none
double precision,intent(in) :: swc,rwc,a,n,mv,h
double precision,intent(out) :: mslope
double precision :: m
m=1.d0-1.d0/n
if (h<0.d0) then
   mslope=abs(a*n*m*(swc-rwc)*(a*abs(h))**(n-1.d0)/(1.d0+          &
      (a*abs(h))**n)**(m+1.d0)/9.807d0)
else
   mslope=mv
end if
return
end subroutine slope

!=====================================================================
!subroutine to get mw of SWC when h0 & h1 are similar
!given initial & final volumetric water contents
!Vauclin et al. model
!=====================================================================
subroutine slope02(mslope,swc,alpha,beta,mv,h)
```

```
implicit none
double precision,intent(in) :: swc,alpha,beta,mv,h
double precision,intent(out) :: mslope
if (h<0.d0) then
    mslope=swc*alpha*beta*(abs(h))**(beta-1.d0)/((alpha+          &
       (abs(h))**beta)**2.d0)/9.807d0
else
    mslope=mv
end if
return
end subroutine slope02

!---------------Under-relaxation techniques-----------------------
subroutine unre(havg,h0,h1,h2,UR)
implicit none
double precision,intent(in) :: h0(:),h1(:),h2(:)
double precision,intent(out) :: havg(:)
integer, intent(in) :: UR
             if (UR .eq. 1) then
              havg= (h0+h1)/2.d0
             else if (UR .eq. 2) then
              havg= (h1+h2)/2.d0
             else if (UR .eq. 0) then
              havg= h1
             !--add young, for test
             else if (UR .eq. 3) then
              havg=h1/2+(h0+h2)/4
             !--add end
             end if
return
end subroutine unre

!=====================================================================
! pressure head to transformed head
!=====================================================================
subroutine h2p(h,elev,p,beta)
implicit none
double precision,intent(in) :: h(0:),elev(0:),beta
double precision,intent(out) :: p(0:)
integer :: nn,i

nn=ubound(h,1)
do i=0,nn
    if ((h(i)-elev(i))<0) then
        p(i)=(h(i)-elev(i))/(1+beta*(h(i)-elev(i)))
    else
        p(i)=h(i)-elev(i)
    end if
```

```
end do

return
end subroutine h2p

!=====================================================================
! pressure head to transformed head
!=====================================================================
subroutine h2p1(h,elev,p,beta)
implicit none
double precision,intent(in) :: h,elev,beta
double precision,intent(out) :: p

if ((h-elev)<0) then
    p=(h-elev)/(1+beta*(h-elev))
else
    p=h-elev
end if

return
end subroutine h2p1

!=====================================================================
! transformed head to pressure head
!=====================================================================
subroutine p2h(p,elev,h,beta)
implicit none
double precision,intent(in) :: p(0:),elev(0:),beta
double precision,intent(out) :: h(0:)
integer :: nn,i

nn=ubound(h,1)
do i=0,nn
    if (p(i)<0) then
        h(i)=p(i)/(1-beta*p(i))+elev(i)
    else
        h(i)=p(i)+elev(i)
    end if
end do

return
end subroutine p2h

!=====================================================================
! transformed head to pressure head
!=====================================================================
subroutine p2h1(p,elev,h,beta)
implicit none
```

```
double precision,intent(in) :: p,elev,beta
double precision,intent(out) :: h

if (p<0) then
    h=p/(1-beta*p)+elev
else
    h=p+elev
end if

return
end subroutine p2h1

!=====================================================================
end module unsat
```

Appendix C

Description of Input Files

C.1 File *FFEin.dat*

```
nels,nn,nodof,nod,nip,ndim,np_types,nltyp,ethick,lumped
750  806  1  4  4  2  2  1  1.0  1

dtIni,nstep,npri,nres
10.00   8640   8640    0

MaxIter,tol,UR,beta
200  0.001  1 -1.0

swc,rwc,a,n,kx,ky,kz,mv (soil parameters; two soils given)
0.4686  0.1060  1.04  1.3954  1.516D-6  1.516D-6  1.516D-6 1.D-25
0.3658  0.0286  2.80  2.2390  6.261D-5  6.261D-5  6.261D-5 1.D-25

element type (see subroutine ‘‘element_type’’ for details)
4 4 0 0 0 0 0 0 4 2

coordinates(ndim,nn)
0   0
0.1 0
0.2 0
...

soil_type(nels), elements(nod,nels)
2                1   27  28  2
2                2   28  29  3
1                3   29  30  4
1                4   30  31  5
...

fixed_nodes
0
```

```
(nodes with flux boundary)
total number of nodes with flux boundary
16

flux,no_elem,no_nodes,nodal_flux
5.7870E-06  726 781 2.8935E-07
5.7870E-06  727 783 2.8935E-07
...

(nodes with fixed head boundary)
total number of nodes with fixed head boundary
26

no_nodes,fixed_head
1   -500
2   -500
...

(time for output)
total number of output times
24

output_times (in second)
3600
7200
...
```

C.2 File *FFEinitial.dat*

```
nn (number of nodes)
806

nnodes,init_head
1   -500
2   -500
3   -500
...
```

C.3 File *FFEadap.dat*

```
adap_type,tolA,tolR,NLtolA,NLtolR
3   1.d0    1.d-1   0.d-4   1.d-3
```

```
(adap_type =0, fixed time step scheme
           =1, heuristic adaptive scheme
           =3, automatic adaptive scheme)

(additional parameters in automatic adaptive scheme)
safety,qmax,qmin
.9d0    4.0d0   .1d0

(parameters in heuristic adaptive scheme)
itMin,dtIncF
4   1.1d0

itMax,dtRedF
8   .95d0
```